

UNCLASSIFIED

AD NUMBER	
AD374200	
CLASSIFICATION CHANGES	
TO:	unclassified
FROM:	confidential
LIMITATION CHANGES	
TO:	Approved for public release, distribution unlimited
FROM:	Distribution authorized to U.S. Gov't. agencies and their contractors; Administrative/Operational Use; NOV 1965. Other requests shall be referred to Rocket Propulsion Lab., AFSC, Edwards AFB, CA.
AUTHORITY	
30 NOV 1977, Dodd 5200.10; AFRPL ltr, 7 May 1977	

THIS PAGE IS UNCLASSIFIED

AD 374200

~~CONFIDENTIAL~~

AFRPL-TR-65-209

(UNCLASSIFIED TITLE)

**DUAL-CHAMBER CONTROLLABLE SOLID
PROPELLANT ROCKET MOTOR**

**THIRD ANNUAL REPORT - FISCAL YEAR 1964
Volume II - Analytical Study**

November 1965

AFSC PROGRAM STRUCTURE NO. 7506
PROJECT NO. 3059, TASK NO. 305906

(PREPARED UNDER CONTRACT
AF 04(611)-9067 by
NORTHROP CAROLINA, INC.
Asheville, N.C.)

DDC
RECEIVED
JUL 25 1966
D

20060130056

**ROCKET PROPULSION LABORATORY
AIR FORCE SYSTEMS COMMAND
Edwards Air Force Base, California**

Best Available Copy

~~CONFIDENTIAL~~

Volume II

NC-5025-65

APR-21-10

Copy No. ~~1~~

(Unclassified Title)

DUAL-CHAMBER

CONTROLLABLE SOLID PROPELLANT ROCKET MOTOR (U)

THIRD ANNUAL REPORT - FISCAL YEAR 1964

Volume II - Analytical Study

Prepared under Contract AF 04(611)-9067

by

Northrop Carolina, Inc., Asheville, North Carolina
A Subsidiary of Northrop Corporation

November 1965

APPROVED BY:



B. L. Johnson
Program Manager

~~CONFIDENTIAL~~

NOTICES

This document contains information affecting the national defense of the United States within the meaning of the Espionage Laws (Title 18, U. S. C., sections 793 and 794). Transmission or revelation in any manner to an unauthorized person is prohibited by law.

When U. S. Government drawings, specifications, or other data are used for any purpose other than a definitely related government procurement operation, the government thereby incurs no responsibility nor any obligation whatsoever and the fact that the government may have formulated, furnished, or in any way supplied the said drawings, specifications, or other data is not to be regarded by implication or otherwise, as in any manner licensing the holder or any other person or corporation, or conveying any rights or permission to manufacture, use, or sell any patented invention that may in any way be related thereto.

This report is furnished under U. S. Government Contract No. AF 04(611)-9067, and shall not be released outside the Government (except to foreign Governments, subject to these same limitations), nor be disclosed, used, or duplicated, for procurement or manufacturing purposes, except as otherwise authorized by said contract, without the permission of Northrop Carolina, Inc. This legend shall be marked on any reproduction hereof in whole or in part.

DOWNGRADED AT 3 YEAR INTERVALS;
DECLASSIFIED AFTER 12 YEARS
DOD DIR 5200. 10

FOREWORD

This annual report for the continued development of a dual-chamber controllable solid propellant rocket motor (DCCSR) describes the progress during the third year of this program, which is sponsored by the Air Force Rocket Propulsion Laboratory, Edwards Air Force Base, California. The research and development efforts of the program are being performed by Northrop Carolina, Inc., a Subsidiary of Northrop Corporation, Asheville, North Carolina, under Air Force Contract AF 04(611)-9067. This report is presented in two volumes: Volume I - Research and Development Efforts, and Volume II - Analytical Study. This volume (Volume II) presents the results of a study to determine the effect of motor performance parameters and propellant characteristics on the mass fraction, burnout velocity, and motor envelope of the dual-chamber controllable solid propellant rocket motor.

NOTICE

Northrop Carolina, Inc., has been assigned a patent application by the U. S. Patent Office to cover the Controllable Solid Propellant Rocket Motor invention disclosed in this publication, and the Commissioner of Patents has issued a secrecy order thereon. This secrecy order requires that those who receive a disclosure of the subject matter be informed of the existence of the secrecy order and of the penalties for the violation thereof.

The recipient of this report is accordingly advised that this publication includes information which is now under a secrecy order. It is requested that he notify all persons who will have access to this material of the secrecy order.

Each secrecy order provides that any person who has received a disclosure of the subject matter covered by the secrecy order is

"in nowise to publish or disclose the invention or any material information with respect thereto, including hitherto unpublished details of the subject matter of said application, in any way to any persons not cognizant of the invention prior to the date of the order, including any employee of the principals, but to keep the same secret except by written permission first obtained of the Commissioner of Patents, under the penalties of 35 U. S. C. (1952) 182, 186"

Although the original secrecy order forbids disclosure of the material to persons not cognizant of the invention prior to the date of the order, a supplemental permit attached to each order does permit such disclosures to:

- "(a) Any officer or employee of any department, independent agency or bureau of the Government of the United States.
- (b) Any person designated specifically by the head of any department, independent agency or bureau of the Government of the United States, or by his duly authorized subordinate, as a proper individual to receive the disclosure of the above indicated application.

The principals under the secrecy are further authorized to disclose the subject matter of this application to the minimum necessary number of persons of known loyalty and discretion, employed by or working with the principals or their licensees and whose duties involve cooperation in the development, manufacture or use of the subject matter by or for the Government of the United States, provided such persons are advised of the issuance of the secrecy order. "

No other disclosures are authorized, without written permission from the Commissioner of Patents. Penalties for violation of a secrecy order, include a fine of up to \$10,000 or imprisonment for not more than two years or both.

It must be understood that the requirements of the secrecy order of the Commissioner of Patents are in addition to the usual security regulations which are in force with respect to classified materials in this report. The usual security regulations must still be observed notwithstanding anything set forth in the secrecy order. In the event that this report shall be declassified, the secrecy order remains in full force until it is specifically rescinded.

TABLE OF CONTENTS

	<u>Page</u>
FOREWORD	iii
<u>Section</u>	<u>Title</u>
I	INTRODUCTION
	1
1.	General
	1
2.	Purpose of Study
	2
3.	Scope
	2
4.	Method of Computation
	4
II	TECHNICAL APPROACH
	7
1.	Parameter Selection
	7
<u>a.</u>	General
	7
<u>b.</u>	Phase I Parameters
	7
<u>c.</u>	Phase II Parameters
	9
<u>d.</u>	Output Parameters
	11
2.	Internal Ballistics Subroutine
	12
3.	Grain Configuration Subroutine
	15
4.	Weight Subroutines
	17
<u>a.</u>	General
	17
<u>b.</u>	Chamber Weights
	21
<u>c.</u>	Valve and Power Supply Weights
	22
<u>d.</u>	Insulation Weights
	24
<u>e.</u>	Nozzle Weights
	24
<u>f.</u>	Subroutine Output Data
	25

TABLE OF CONTENTS (CONT'D)

<u>Section</u>	<u>Title</u>	<u>Page</u>
III	DISCUSSION OF RESULTS	27
1.	General	27
2.	Phase I	27
	<u>a.</u> General	27
	<u>b.</u> Specific Impulse	27
	<u>c.</u> Thrust Ratio	27
	<u>d.</u> Number of Starts	32
	<u>e.</u> Total Impulse and Minimum Thrust	32
3.	Phase II	40
	<u>a.</u> General	40
	<u>b.</u> Case Material	40
	<u>c.</u> Burning-Rate Constants	40
	<u>d.</u> Pressure Exponents	49
	<u>e.</u> Aft-to-Forward Weight Flow Ratio	49
IV	SUMMARY	55
	LIST OF REFERENCES	57
<u>Appendix</u>		
A	COMPUTER PROGRAMS	A-1
B	PRESENTATION OF DATA	B-1

LIST OF ILLUSTRATIONS

<u>Figure</u>	<u>Title</u>	<u>Page</u>
1	Computer Program Diagram, Showing Information Flow through Subroutines	5
2	Internal Ballistics Subroutine Logic Diagram . . .	13
3	Grain Configuration Subroutine Logic Diagram . . .	16
4	Typical Configurations Considered in Grain Configuration Subroutine	18
5	Weight Subroutine A Logic Diagram	19
6	Weight Subroutine B Logic Diagram	20
7	Effect of Specific Impulse on Mass Fraction	28
8	Effect of Specific Impulse on Delta Velocity	29
9	Effect of Thrust Ratio on Mass Fraction	30
10	Effect of Thrust Ratio on Delta Velocity	31
11	Effect of Number of Starts on Mass Fraction	33
12	Effect of Number of Starts on Delta Velocity	34
13	Mass Fraction as a Function of Total Impulse	35
14	Delta Velocity as a Function of Total Impulse	36
15	Mass Fraction Contour Map for a Thrust Ratio of 1 .	37
16	Mass Fraction Contour Map for a Thrust Ratio of 20 .	38
17	Motor Diameter as a Function of Minimum Thrust and Total Impulse	39
18	Motor Length as a Function of Minimum Thrust and Total Impulse	41
19	Motor Length as a Function of Minimum Thrust . . .	42
20	Effect of Case Material on Mass Fraction	43
21	Effect of Case Material on Delta Velocity	44

LIST OF ILLUSTRATIONS (CONT'D)

<u>Figure</u>	<u>Title</u>	<u>Page</u>
22	Mass Fraction as a Function of Thrust Ratio for Three Case Materials	45
23	Delta Velocity as a Function of Thrust Ratio for Three Case Materials	46
24	Effect of Burning-Rate Constants on Mass Fraction	47
25	Effect of Burning-Rate Constants on Delta Velocity	48
26	Effect of Burning-Rate Pressure Exponents on Mass Fraction	50
27	Effect of Burning-Rate Pressure Exponents on Delta Velocity	51
28	Effect of θ on Mass Fraction	52
29	Effect of θ on Delta Velocity	53
B-1	Mass Fraction versus Minimum Thrust for $I_{sp} = 265$ $Lb_f\text{-Sec}/Lb_m$ and 1 Start	B-4
B-2	Mass Fraction versus Minimum Thrust for $I_{sp} = 265$ $Lb_f\text{-Sec}/Lb_m$ and 10 Starts	B-5
B-3	Mass Fraction versus Minimum Thrust for $I_{sp} = 265$ $Lb_f\text{-Sec}/Lb_m$ and 20 Starts	B-6
B-4	Mass Fraction versus Minimum Thrust for $I_{sp} = 280$ $Lb_f\text{-Sec}/Lb_m$ and 1 Start	B-7
B-5	Mass Fraction versus Minimum Thrust for $I_{sp} = 280$ $Lb_f\text{-Sec}/Lb_m$ and 10 Starts	B-8
B-6	Mass Fraction versus Minimum Thrust for $I_{sp} = 280$ $Lb_f\text{-Sec}/Lb_m$ and 20 Starts	B-9
B-7	Mass Fraction versus Minimum Thrust for $I_{sp} = 300$ $Lb_f\text{-Sec}/Lb_m$ and 1 Start	B-10
B-8	Mass Fraction versus Minimum Thrust for $I_{sp} = 300$ $Lb_f\text{-Sec}/Lb_m$ and 10 Starts	B-11

LIST OF ILLUSTRATIONS (CONT'D)

<u>Figure</u>	<u>Title</u>	<u>Page</u>
B-9	Mass Fraction versus Minimum Thrust for $I_{sp} = 300$ $Lb_f\text{-Sec}/Lb_m$ and 20 Starts	B-12
B-10	Mass Fraction versus Total Impulse for 20-Sec Burn Time	B-13
B-11	Mass Fraction versus Total Impulse for 50-Sec Burn Time	B-14
B-12	Mass Fraction versus Total Impulse for 200-Sec Burn Time	B-15
B-13	Mass Fraction versus Total Impulse for 500-Sec Burn Time	B-16
B-14	Delta Velocity versus Minimum Thrust for $I_{sp} = 265$ $Lb_f\text{-Sec}/Lb_m$ and 1 Start	B-17
B-15	Delta Velocity versus Minimum Thrust for $I_{sp} = 265$ $Lb_f\text{-Sec}/Lb_m$ and 10 Starts	B-18
B-16	Delta Velocity versus Minimum Thrust for $I_{sp} = 265$ $Lb_f\text{-Sec}/Lb_m$ and 20 Starts	B-19
B-17	Delta Velocity versus Minimum Thrust for $I_{sp} = 280$ $Lb_f\text{-Sec}/Lb_m$ and 1 Start	B-20
B-18	Delta Velocity versus Minimum Thrust for $I_{sp} = 280$ $Lb_f\text{-Sec}/Lb_m$ and 10 Starts	B-21
B-19	Delta Velocity versus Minimum Thrust for $I_{sp} = 280$ $Lb_f\text{-Sec}/Lb_m$ and 20 Starts	B-22
B-20	Delta Velocity versus Minimum Thrust for $I_{sp} = 300$ $Lb_f\text{-Sec}/Lb_m$ and 1 Start	B-23
B-21	Delta Velocity versus Minimum Thrust for $I_{sp} = 300$ $Lb_f\text{-Sec}/Lb_m$ and 10 Starts	B-24
B-22	Delta Velocity versus Minimum Thrust for $I_{sp} = 300$ $Lb_f\text{-Sec}/Lb_m$ and 20 Starts	B-25

LIST OF ILLUSTRATIONS (CONT'D)

<u>Figure</u>	<u>Title</u>	<u>Page</u>
B-23	Delta Velocity versus Total Impulse for 20-Sec Burn Time	B-26
B-24	Delta Velocity versus Total Impulse for 50-Sec Burn Time	B-27
B-25	Delta Velocity versus Total Impulse for 200-Sec Burn Time	B-28
B-26	Delta Velocity versus Total Impulse for 500-Sec Burn Time	B-29
B-27	Length versus Minimum Thrust for $I_{sp} = 265 \text{ Lb}_f\text{-Sec/Lb}_m$	B-30
B-28	Length versus Minimum Thrust for $I_{sp} = 300 \text{ Lb}_f\text{-Sec/Lb}_m$	B-31
B-29	Diameter versus Minimum Thrust for $I_{sp} = 265 \text{ Lb}_f\text{-Sec/Lb}_m$	B-32
B-30	Diameter versus Minimum Thrust for $I_{sp} = 300 \text{ Lb}_f\text{-Sec/Lb}_m$	B-33
B-31	Mass Fraction versus Minimum Thrust at Thrust Ratio of 1	B-34
B-32	Mass Fraction versus Minimum Thrust at Thrust Ratio of 5	B-35
B-33	Mass Fraction versus Minimum Thrust at Thrust Ratio of 20	B-36
B-34	Delta Velocity versus Minimum Thrust at Thrust Ratio of 1	B-37
B-35	Delta Velocity versus Minimum Thrust at Thrust Ratio of 5	B-38
B-36	Delta Velocity versus Minimum Thrust at Thrust Ratio of 20	B-39

LIST OF ILLUSTRATIONS (CONT'D)

<u>Figure</u>	<u>Title</u>	<u>Page</u>
B-37	Mass Fraction versus Minimum Thrust for Aft Propellant Burning-Rate Constant of 0.0002	B-40
B-38	Mass Fraction versus Minimum Thrust for Aft Propellant Burning-Rate Constant of 0.0004	B-41
B-39	Mass Fraction versus Minimum Thrust for Aft Propellant Burning-Rate Constant of 0.0010	B-42
B-40	Delta Velocity versus Minimum Thrust for Aft Propellant Burning-Rate Constant of 0.0002	B-43
B-41	Delta Velocity versus Minimum Thrust for Aft Propellant Burning-Rate Constant of 0.0004	B-44
B-42	Delta Velocity versus Minimum Thrust for Aft Propellant Burning-Rate Constant of 0.0010	B-45
B-43	Length versus Aft Propellant Burning-Rate Constant for $F_{min} = 200 \text{ Lb}_f$	B-46
B-44	Length versus Aft Propellant Burning-Rate Constant for $F_{min} = 500 \text{ Lb}_f$	B-47
B-45	Length versus Aft Propellant Burning-Rate Constant for $F_{min} = 1000 \text{ Lb}_f$	B-48
B-46	Length versus Aft Propellant Burning-Rate Constant for $F_{min} = 5000 \text{ Lb}_f$	B-49
B-47	Diameter versus Aft Propellant Burning-Rate Constant for $F_{min} = 200 \text{ Lb}_f$	B-50
B-48	Diameter versus Aft Propellant Burning-Rate Constant for $F_{min} = 500 \text{ Lb}_f$	B-51
B-49	Diameter versus Aft Propellant Burning-Rate Constant for $F_{min} = 1000 \text{ Lb}_f$	B-52
B-50	Diameter versus Aft Propellant Burning-Rate Constant for $F_{min} = 5000 \text{ Lb}_f$	B-53

CONFIDENTIALLIST OF ILLUSTRATIONS (CONT'D)

<u>Figure</u>	<u>Title</u>	<u>Page</u>
B-51	Mass Fraction versus Thrust Ratio for Forward Propellant Burning-Rate Exponent of 0.6	B-54
B-52	Mass Fraction versus Thrust Ratio for Forward Propellant Burning-Rate Exponent of 0.8	B-55
B-53	Mass Fraction versus Thrust Ratio for Forward Propellant Burning-Rate Exponent of 0.9	B-56
B-54	Delta Velocity versus Thrust Ratio for Forward Propellant Burning-Rate Exponent of 0.6	B-57
B-55	Delta Velocity versus Thrust Ratio for Forward Propellant Burning-Rate Exponent of 0.8	B-58
B-56	Delta Velocity versus Thrust Ratio for Forward Propellant Burning-Rate Exponent of 0.9	B-59
B-57	Length versus Thrust Ratio for Forward Propellant Burning-Rate Exponent of 0.6	B-60
B-58	Length versus Thrust Ratio for Forward Propellant Burning-Rate Exponent of 0.8	B-61
B-59	Length versus Thrust Ratio for Forward Propellant Burning-Rate Exponent of 0.9	B-62
B-60	Diameter versus Thrust Ratio for Forward Propellant Burning-Rate Exponent of 0.6	B-63
B-61	Diameter versus Thrust Ratio for Forward Propellant Burning-Rate Exponent of 0.8	B-64
B-62	Diameter versus Thrust Ratio for Forward Propellant Burning-Rate Exponent of 0.9	B-65
B-63	Mass Fraction versus Minimum Thrust for Theta Values of 2, 3, and 4	B-66
B-64	Delta Velocity versus Minimum Thrust for Theta Values of 2, 3, and 4	B-67

CONFIDENTIAL

LIST OF ILLUSTRATIONS (CONT'D)

<u>Figure</u>	<u>Title</u>	<u>Page</u>
B-65	Length versus Minimum Thrust for Theta Values of 2, 3, and 4	B-68
B-66	Diameter versus Minimum Thrust for Theta Values of 2, 3, and 4	B-69

LIST OF TABLES

<u>Table</u>	<u>Title</u>	<u>Page</u>
I	Total Impulse and Thrust Ranges for Parametric Analysis	3
II	Parameters Investigated in Each Phase	8
III	Output Format of Weight Subroutine.	26

SECTION I - INTRODUCTION

1. GENERAL

Northrop Carolina, Inc., a subsidiary of Northrop Corporation, has been developing a dual-chamber controllable solid propellant rocket motor (DCCSR) under sponsorship of the Air Force Systems Command, Rocket Propulsion Laboratory, Edwards Air Force Base, California. This program, now in its third year, is funded under Contract AF 04(611)-9067. The progress of the program has been reported in quarterly and annual technical documentary reports (References 1 through 13). This volume presents the results of a separate parametric study conducted as part of the third year's effort.

The DCCSR concept is fully described and illustrated in Volume I. However, a brief description is given here to provide a better understanding of the information and data presented in this volume. The concept utilizes two propellant chambers separated by a throttle valve. The forward chamber contains a cool-burning fuel-rich propellant; the aft, an oxidizer-rich propellant. The fact that the forward-chamber combustion products are relatively cool burning (2800°F) permits state-of-the-art materials to be used on the aft chamber, where high-temperature combustion takes place. A multiple pyrogen ignition system is included as a part of the forward chamber. (Confidential)

Thrust is initiated by igniting the forward propellant with a single pyrogen. The relatively cool combustion products from the forward chamber are throttled through the control valve into the aft chamber where additional thermochemical reaction occurs, resulting in more energy release. The aft propellant will not burn without the heat supplied by the forward propellant. Throttleability is achieved by varying the forward-chamber pressure (and burning rate) by varying the position of the valve. The aft propellant actively supports combustion when the combustion gases from the forward propellant pass over it. (Confidential)

Thrust can be terminated at any time during the burning period by suddenly increasing the valve flow area, which produces a rarefaction wave that extinguishes combustion of the forward propellant. Since the aft propellant will not sustain combustion except at high chamber pressures and/or temperatures above 300°C without an external heat source, it too is extinguished. The on-off cycle operation can be repeated on command by reigniting the forward propellant using another pyrogen igniter of the multiple ignition system for each restart. (Confidential)

2. PURPOSE OF STUDY

This study was conducted in order to establish trends and optimum conditions of mass fraction, boost velocity, and motor envelope with variations in motor performance parameters and propellant characteristics for the dual-chamber controllable solid propellant rocket motor concept. It should be noted that the results presented herein do not necessarily represent optimum designs; rather, off-optimum as well as optimum conditions have been examined.

3. SCOPE

Five independent variables (motor performance parameters and propellant characteristics) were selected for this study: (1) total impulse, (2) minimum thrust, (3) thrust throttling range, (4) number of on-off cycles available, and (5) motor specific impulse. The first four variables define the capability of a throttleable stop-restart motor, and each directly affects mass fraction, boost velocity, and motor envelope. The fifth variable, which is a function of propellant composition, directly affects motor size and boost velocity.

The range of total impulse, minimum thrust, and thrust throttling range values included in this study are presented in Table I. Minimum thrust was varied from 1/500 to 1/20 of total impulse, that is, for maximum burn times of 20 to 500 sec. The thrust throttling ranges considered were 1 to 1, 5 to 1, and 20 to 1, and the number of on-off cycles used was 1, 10, 20, and 40. Vacuum specific impulse, at an expansion ratio of 20 to 1, was varied from 265 to 280 to 300 lb-sec/lb. It was felt that these ranges of independent variables would encompass those required in most applications of a DCCSR. (Confidential)

The analysis was divided into two phases. In Phase I, the independent variables listed above were investigated separately, with propellant properties and structural materials fixed. In Phase II, case

TABLE I - TOTAL IMPULSE AND THRUST RANGES
FOR PARAMETRIC ANALYSIS

Total Impulse (lb _f -sec)	Minimum Thrust (lb _f)	Maximum Thrust (lb _f)		
		Case 1	Case 2	Case 3
10,000	20	20	100	400
10,000	50	50	250	1,000
10,000	100	100	500	2,000
10,000	500	500	2,500	10,000
100,000	200	200	1,000	4,000
100,000	500	500	2,500	10,000
100,000	1,000	1,000	5,000	20,000
100,000	5,000	5,000	25,000	100,000
500,000	1,000	1,000	5,000	20,000
500,000	2,000	2,000	10,000	40,000
500,000	5,000	5,000	25,000	100,000
500,000	25,000	25,000	125,000	500,000
1,000,000	2,000	2,000	10,000	40,000
1,000,000	4,000	4,000	20,000	80,000
1,000,000	10,000	10,000	50,000	200,000
1,000,000	50,000	50,000	250,000	1,000,000

(Confidential)

material, propellant mixture ratio, burning-rate constants, and burning-rate pressure exponents were varied as follows:

1. The effect of three case materials (steel, titanium and fiberglass) was evaluated for (1) the four thrust levels in the 100,000-lb-sec motor, (2) the other impulse levels at a minimum thrust corresponding to 200-sec operating time, and (3) for throttling ratios of 1, 5, and 20.
2. The effect of aft-to-forward-chamber propellant mixture ratios (2 to 1, 3 to 1, and 4 to 1) was investigated over the total impulse and minimum thrust range at a constant throttling ratio of 5 to 1.
3. The effect of burning-rate constants was investigated for the four thrust levels in the 100,000-lb-sec motor at a throttling ratio of 5 to 1.
4. The effect of propellant burning-rate (pressure) exponent was evaluated at throttling ratios of 1 to 1, 5 to 1, and 20 to 1 at a minimum thrust of 500 lb_f in the 100,000-lb-sec motor. The burning-rate exponents evaluated were: (1) for the forward chamber, 0.6, 0.8, and 0.9; (2) for the aft chamber, 0.8, 1.0, and 1.1. (Confidential)

The range of variables and constants used in this study are listed in detail in Section II, paragraph 1.

4. METHOD OF COMPUTATION

This study was carried out by means of Northrop Carolina's IBM 1620 Data Processing System and an IBM 1622 Card Read Punch, which assured accurate and rapid processing of the required data. The data processing system's limited storage capacity (20,000 digits) necessitated the processing of data through four separate computer subroutines. These subroutines, prepared by Northrop Carolina, consisted of (1) a steady-state internal ballistics subroutine, (2) a grain configuration subroutine, and (3) two weight subroutines. The information flow through these subroutines is shown in Figure 1. A detailed description of the subroutines and the overall computer program is presented in Section II.

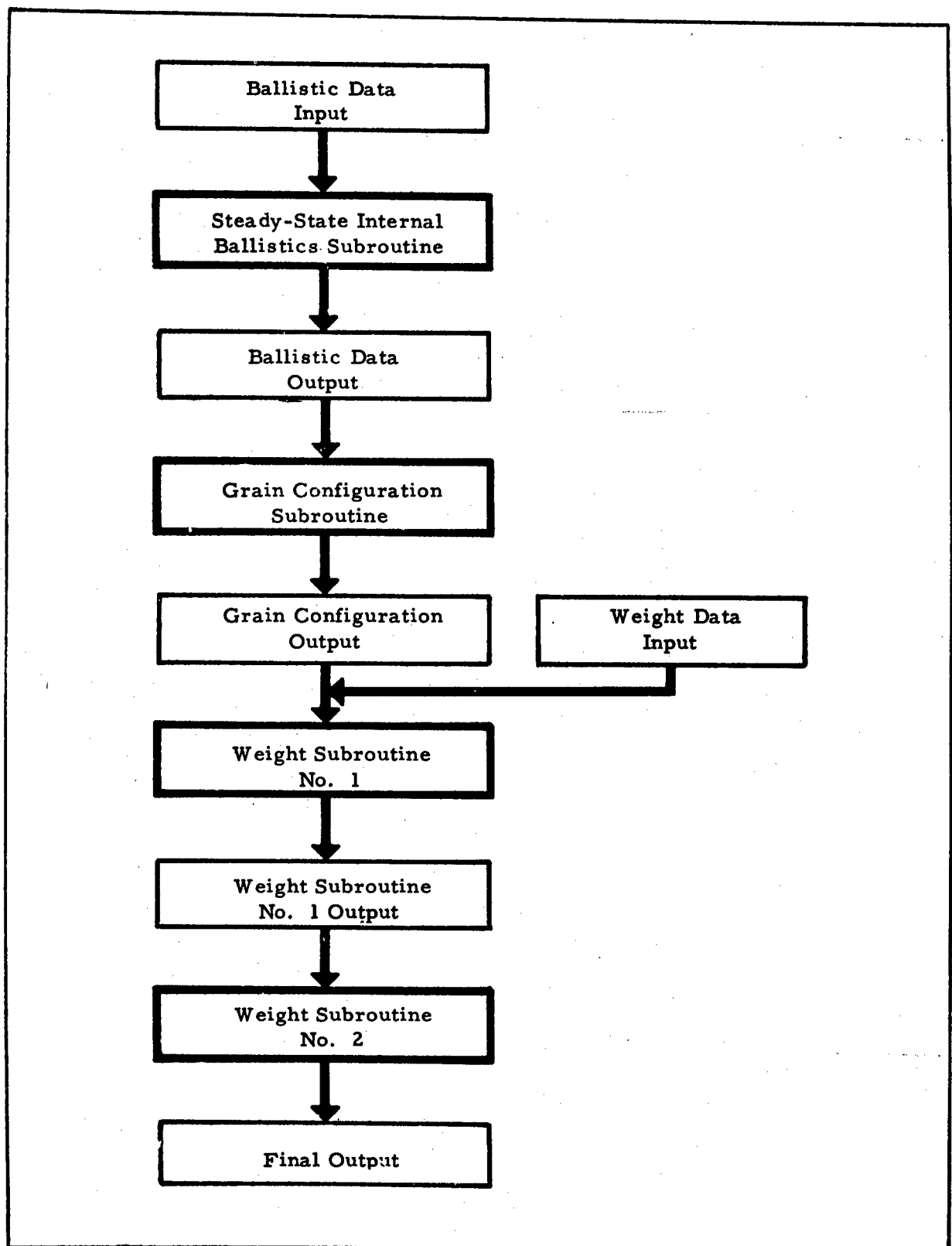


Figure 1 - Computer Program Diagram, Showing Information Flow through Subroutines

CONFIDENTIALSECTION II - TECHNICAL APPROACH1. **PARAMETER SELECTION**a. General

As mentioned in Section I, this parametric study was conducted in two phases. The effect of the major ballistic parameters was investigated in Phase I; the remaining, less significant parameters in Phase II. As a result, more computer runs were required for Phase I than for Phase II.

Table II summarizes the parameters investigated in each phase, showing which were varied and which held constant. Note that, as shown in Table II, Phase II was subdivided into Phases IIa through IId, depending on the parameters that were held constant, as follows:

<u>Phase</u>	<u>Variable</u>
II a	Case material
II b	Burning rate
II c	Propellant burning rate exponent
II d	O/F ratio, θ (theta)

The values and ranges of the parameters investigated in each phase are listed in paragraphs b and c, below, respectively.

b. Phase I Parameters

The values of the constants used in Phase I are listed below.

<u>Constant</u>	<u>Value</u>
Case material	Steel
O/F ratio, θ	3.0
Forward propellant density ($\text{lb}_m/\text{in.}^3$)	0.053
Aft propellant density ($\text{lb}_m/\text{in.}^3$)	0.070

THIS PAGE WAS BLACK REDACTED AND NOT FILMED

CONFIDENTIAL

TABLE II - PARAMETERS INVESTIGATED IN EACH PHASE*

Parameter	Phase				
	I	II a	II b	II c	II d
Total impulse, vacuum (lb_f -sec)	V	V	C	C	V
Specific impulse, vacuum (lb_f -sec/ lb_m)	V	C	C	C	C
Minimum thrust (lb_f)	V	V	V	C	V
Thrust ratio, maximum/minimum	V	V	C	V	C
Starts	V	C	C	C	C
Case material	C	V	C	C	C
Aft propellant rate constant (in./sec)	C	C	V	C	C
Forward propellant rate constant (in./sec)	C	C	V	C	C
Aft propellant burning-rate exponent	C	C	C	V	C
Forward propellant burning-rate exponent	C	C	C	V	C
O/F ratio, θ	C	C	C	C	V
Aft propellant density ($lb_m/in.^3$)	C	C	C	C	C
Forward propellant density ($lb_m/in.^3$)	C	C	C	C	C
Aft propellant flame temperature ($^{\circ}F$)	C	C	C	C	C
Forward propellant flame temperature ($^{\circ}F$)	C	C	C	C	C
Aft chamber C_d (sec^{-1})	C	C	C	C	C
Forward chamber C_d (sec^{-1})	C	C	C	C	C
Minimum aft chamber pressure (psia)	C	C	C	C	C
Minimum forward chamber pressure (psia)	C	C	C	C	C
Expansion ratio	C	C	C	C	C

* C and V denote constant and variable, respectively.

(Confidential)

<u>Constant</u>	<u>Value</u>
Forward propellant exponent, n	0.80
Aft propellant exponent, n	1.00
Forward propellant rate constant (in. /sec)	0.0008
Aft propellant rate constant (in. /sec)	0.0004
Forward propellant flame temperature ($^{\circ}\text{F}$)	2700
Aft propellant flame temperature ($^{\circ}\text{F}$)	5500
C_d , forward chamber (sec^{-1})	0.00765
C_d , aft chamber (sec^{-1})	0.00643
Minimum forward-chamber pressure (psia)	100.0
Minimum aft-chamber pressure (psia)	50.0
Expansion ratio	20.0

(Confidential)

The range of the variables used for Phase I are as follows:

<u>Variable</u>	<u>Range</u>
Total impulse ($\text{lb}_f\text{-sec}$)	10^4 to 10^6
Maximum/minimum thrust ratio	1, 5, 10
Minimum thrust (lb_f)	25 to 1,000
Specific impulse, vacuum ($\text{lb}_f\text{-sec/lb}$)	250, 280, 300
Starts	1, 10, 20

(Confidential)

c. Phase II Parameters

The less significant parameters (case material, burn rate, pressure exponent, and theta) were varied in Phase II. The range of these variables and the values of the constants used in each portion of Phase II are listed below.

Phase II a

Constants - Same as Phase I, except for the following:

Case Material	Listed below
Specific impulse, vacuum ($\text{lb}_f\text{-sec}/\text{lb}_m$)	280
Starts	20

Variables

Maximum/minimum thrust ratio	1, 5, 20
Case material	Steel, Fiberglass, Titanium
Total impulse ($\text{lb}_f\text{-sec}$)	10^4 to 10^6
Minimum thrust (lb_f)	50 to 5000

Phase II bConstants - Same as Phase I, except for the following:

Burn rate constants	Listed below
Specific impulse, vacuum ($\text{lb}_f\text{-sec}/\text{lb}_m$)	280
Starts	20
Maximum/minimum thrust ratio	5
Total impulse ($\text{lb}_f\text{-sec}$)	10^5

Variables

Aft propellant burn rate constant (in./sec)	0.0001 to 0.0010
Forward propellant burn rate constant (in./sec)	0.0002 to 0.0032
Minimum thrust	200 to 500

Phase II cConstants - Same as Phase I, except for the following:

Burn rate exponents	Listed below
Specific impulse, vacuum ($\text{lb}_f\text{-sec}/\text{lb}_m$)	280
Starts	20

Total impulse ($\text{lb}_f\text{-sec}$)	10^5
--	--------

Minimum thrust (lb_f)	500
----------------------------------	-----

Variables

Aft propellant exponent	0.8 to 1.1
-------------------------	------------

Forward propellant exponent	0.6 to 0.9
-----------------------------	------------

Maximum/minimum thrust ratio	1, 5, 20
------------------------------	----------

Phase II dConstants - Same as Phase I, except for the following:

Theta	Listed below
-------	--------------

Specific impulse, vacuum ($\text{lb}_f\text{-sec}/\text{lb}_m$)	280
--	-----

Starts	20
--------	----

Maximum/minimum thrust ratio	5
------------------------------	---

Variables

Theta	2.0 to 4.0
-------	------------

Total impulse ($\text{lb}_f\text{-sec}$)	10^4 to 10^6
--	------------------

Minimum thrust (lb_f)	50 to 5000
----------------------------------	------------

d. Output Parameters

(Confidential)

The parameters listed in c and d, above, were used as inputs to the computer program. The chief dependent variables calculated (computer outputs) were:

1. Mass fraction
2. Delta velocity, ideal (fps)
3. Total motor length (in.)
4. Total motor diameter (in.)
5. Grain design

For some computer runs, other values were calculated as data checks; however, they are not presented here.

2. INTERNAL BALLISTICS SUBROUTINE

The internal ballistics subroutine was prepared to calculate ballistic design and performance parameters for the DCCSR motor under steady-state operating conditions. This subroutine contains two principal options which permit the program to be used to design aft-chamber parameters and calculate performance for test motors (Option I) or to design motors to meet specified thrust and total impulse requirements (Option II). The general subroutine logic is shown in the diagram in Figure 2; the actual IBM 1620 computer subroutine listing is given in Appendix A.

The equations employed in this subroutine are conventional ballistic relationships which have been modified for dual-chamber motors, as outlined previously (Reference 1). The forward chamber, with choked flow at the valve, operates as a conventional rocket motor. Aft-chamber parameters are calculated as a function of the ratio of aft-to-forward mass flow, θ , which under steady-state conditions is defined as:

$$\theta = \frac{(\rho S a P^n)_{\text{aft}}}{(\rho S a P^n)_{\text{fwd}}} \quad (1)$$

where

- ρ = propellant density,
- S = burning area,
- a = burn-rate constant,
- P = operating pressure, and
- n = pressure exponent*

The aft-chamber surface area was calculated by rearranging this equation, as follows:

$$S_{\text{aft}} = \theta \frac{(\rho S a P_{\text{min}}^n)_{\text{fwd}}}{(\rho a P_{\text{min}}^n)_{\text{aft}}} \quad (2)$$

* Also referred to as burning-rate exponent herein.

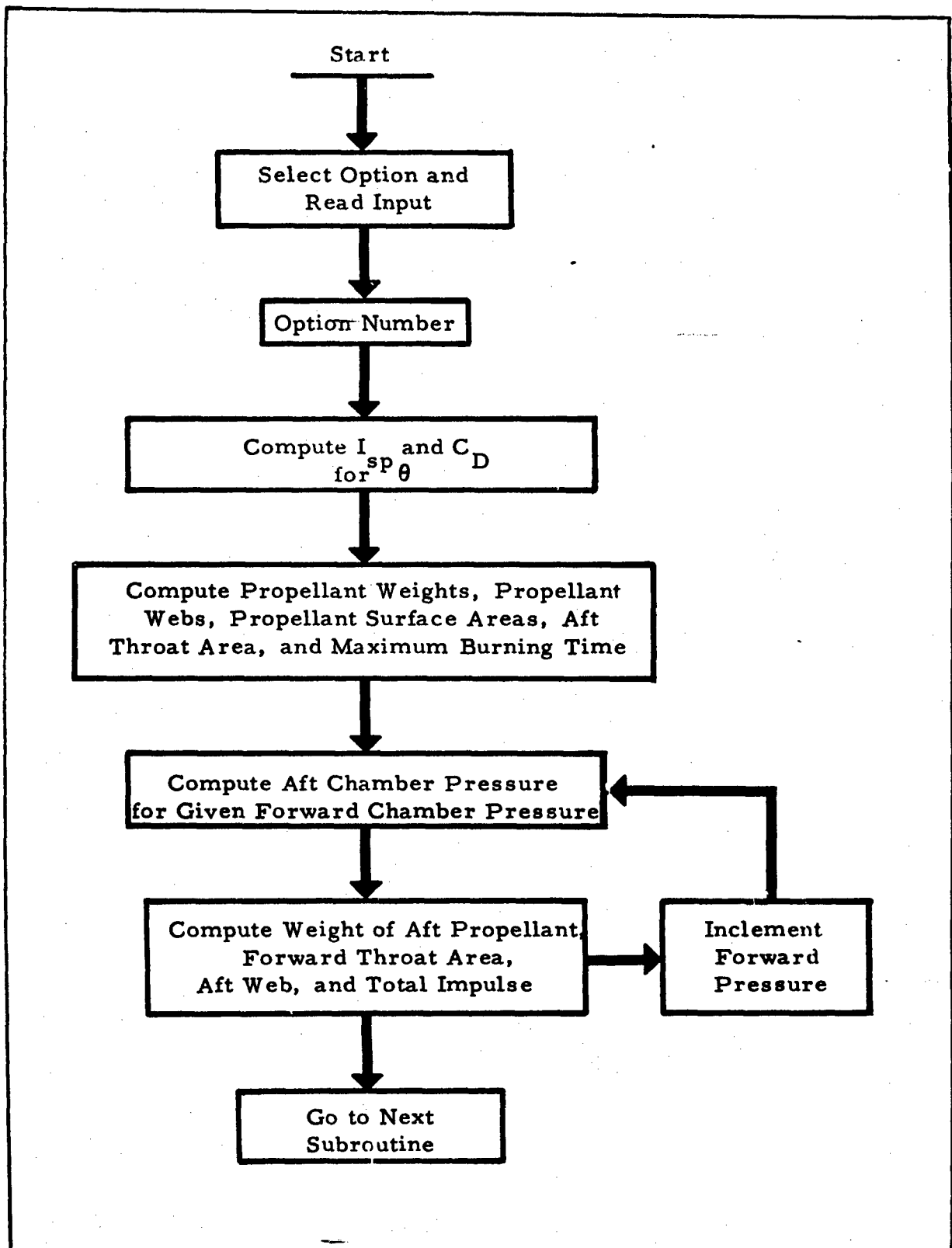


Figure 2 - Internal Ballistics Subroutine Logic Diagram

The over-all mass flow balance for the motor is

$$\dot{M}_{fwd} + \dot{M}_{aft} = \dot{M}_{tot} = (C_d P A_t)_{aft}, \quad (3)$$

where

C_d = discharge coefficient at aft nozzle, and
 A_t = aft nozzle throat area.

Hence,

$$(\rho S a P^n)_{fwd} + (\rho S a P^n)_{aft} = (C_d P A_t)_{aft}, \quad (4)$$

or

$$1 + \theta = \frac{(C_d P A_t)_{aft}}{(\rho S a P^n)_{fwd}}. \quad (5)$$

The aft-chamber throat area was calculated by rearranging Equation 5; that is,

$$A_{t,aft} = (1 + \theta) \frac{(\rho S a P_{min}^n)_{fwd}}{(C_d P_{min})_{aft}}. \quad (6)$$

Aft-chamber pressure was calculated as a function of forward-chamber pressure from Equation 4 by an iterative procedure. Initially, an estimate of aft-chamber pressure was substituted into the left side of Equation 4, and the aft-chamber pressure on the right side was calculated from

$$P_{aft} = \frac{(\rho S a P^n)_{fwd} + (\rho S a P_{est}^n)_{aft}}{(C_d A_t)_{aft}}.$$

The calculated pressure was then compared with the estimated pressure. If the two did not agree within 0.5 percent, another estimated pressure was obtained by

$$P_{est,n} = 2 P_{calc,(n-1)} - P_{est,(n-1)},$$

and the procedure repeated until convergence was achieved.

When the calculated pressure agreed with the estimated pressure within 0.5 percent, θ was calculated from Equation 1 and compared with the estimated θ from which $C_{d_{aft}}$ was obtained. If these did not agree within 0.5 percent, a new θ was estimated and aft-chamber pressure was calculated using a new $C_{d_{aft}}$. This procedure was repeated until convergence was achieved. Thrust was then calculated from the product of specific impulse at the final θ value and mass flow rate.

3. GRAIN CONFIGURATION SUBROUTINE

The grain configuration subroutine was prepared for determining the most suitable grain configurations for the DCCSR forward and aft chambers. The subroutine calculated the diameter, length, port area, and volumetric loading of the grains, but did not calculate the detailed grain design. The four basic grain types employed, in order of increasing mass flow requirements, were end burning, cylindrically (center) perforated, star, and wagon-wheel designs. These configurations were selected for either a cylindrical or spherical forward chamber and for a cylindrical aft chamber, either in tandem or around the outside of the forward chamber. The required input for this subroutine, supplied by the steady-state internal ballistics subroutine, consisted of forward- and aft-grain burning surface areas and web thicknesses, and aft-chamber throat area. The subroutine output provided the dimensions necessary for case and insulation design. The subroutine logic is shown in the diagram in Figure 3, while the actual computer subroutine listing is given in Appendix A.

The equations employed in this subroutine are general geometry equations that relate diameters to areas and volumes of both cylinders and spheres; the actual equations used are shown in the program listing for this subroutine in Appendix A. The subroutine initially established the forward-grain configuration and its dimensions, based on forward-grain surface area and web thickness inputs. First, a cylindrical end-burner design was assumed and the grain diameter calculated from the inputs. If the length-to-diameter ratio of this design was less than 0.5, the cylindrical end-burner design was rejected and a spherical end burner assumed. The program thus proceeded from designs with high web fractions to those with low web fractions until a design with a reasonable length-to-diameter ratio was obtained. The program then printed out the type of configuration, grain outside diameter, length, and volumetric loading. For cylindrical

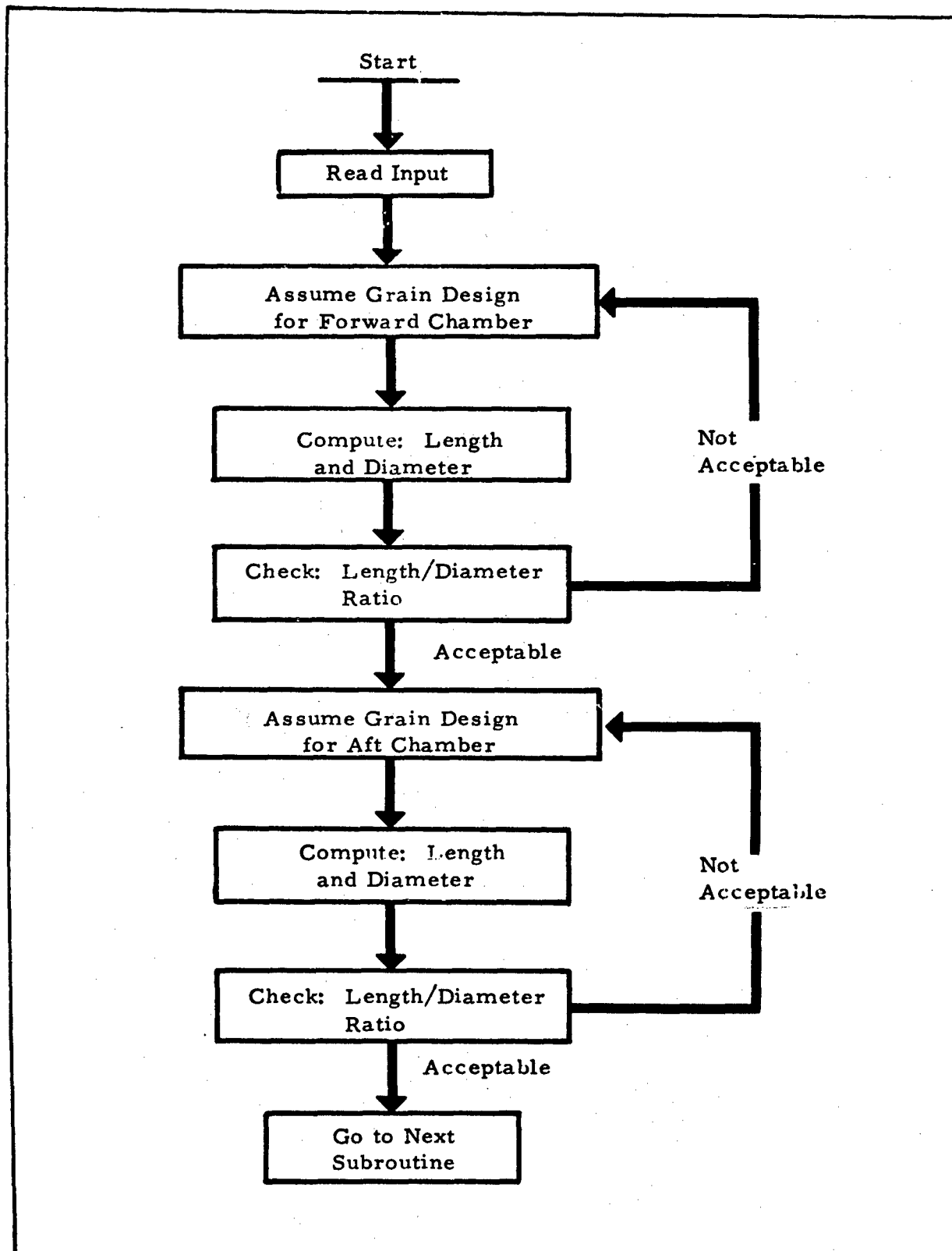


Figure 3 - Grain Configuration Subroutine Logic Diagram

center perforated and star designs, the program would, when feasible, give an alternate spherical forward-chamber design.

After the forward grain configuration was selected, the subroutine had the option of proceeding to another case or establishing the aft-grain configuration. The aft-grain program was similar to the forward one in that designs with increasing web-to-diameter ratios were considered until a design giving a reasonable length-to-diameter ratio was achieved. An attempt was made to design an aft grain with an outside diameter equal to that of the forward. If this diameter proved to be unsatisfactory, larger or smaller diameters were used. For forward-chamber designs with high length-to-diameter ratios, the aft-chamber subroutine considered the feasibility of placing the aft chamber around the forward chamber, rather than in tandem, to reduce the over-all length-to-diameter ratio for the dual-chamber system. Figure 4 shows some typical configurations for chambers in tandem and with one chamber inside the other.

The subroutine assumed that the surface-time history of the selected grain configuration was neutral. This assumption is true for end-burning grains and can be made approximately so for the star and wagon-wheel configurations. Although most of the cylindrically perforated designs would not be neutral, this can be corrected in a detailed design by using slotted-tube configurations of approximately the same diameter and length.

4. WEIGHT SUBROUTINES

a. General

As mentioned in Section I, the weight calculation subroutine was divided into two parts (A and B) to facilitate computation in Northrop-Carolina's IBM 1620 computer. The subroutine calculated the weight and dimensions of the forward and aft motor case, end closures, insulation, nozzle, igniters, and the control valve. The weights and dimensions were selectively calculated, depending on geometrical constraints such as the forward- and aft-chamber grain configurations and the materials used for each individual component. The generalized flow diagrams for the two weight subroutines are shown in Figures 5 and 6, respectively. The subroutine program listings are given in Appendix A.

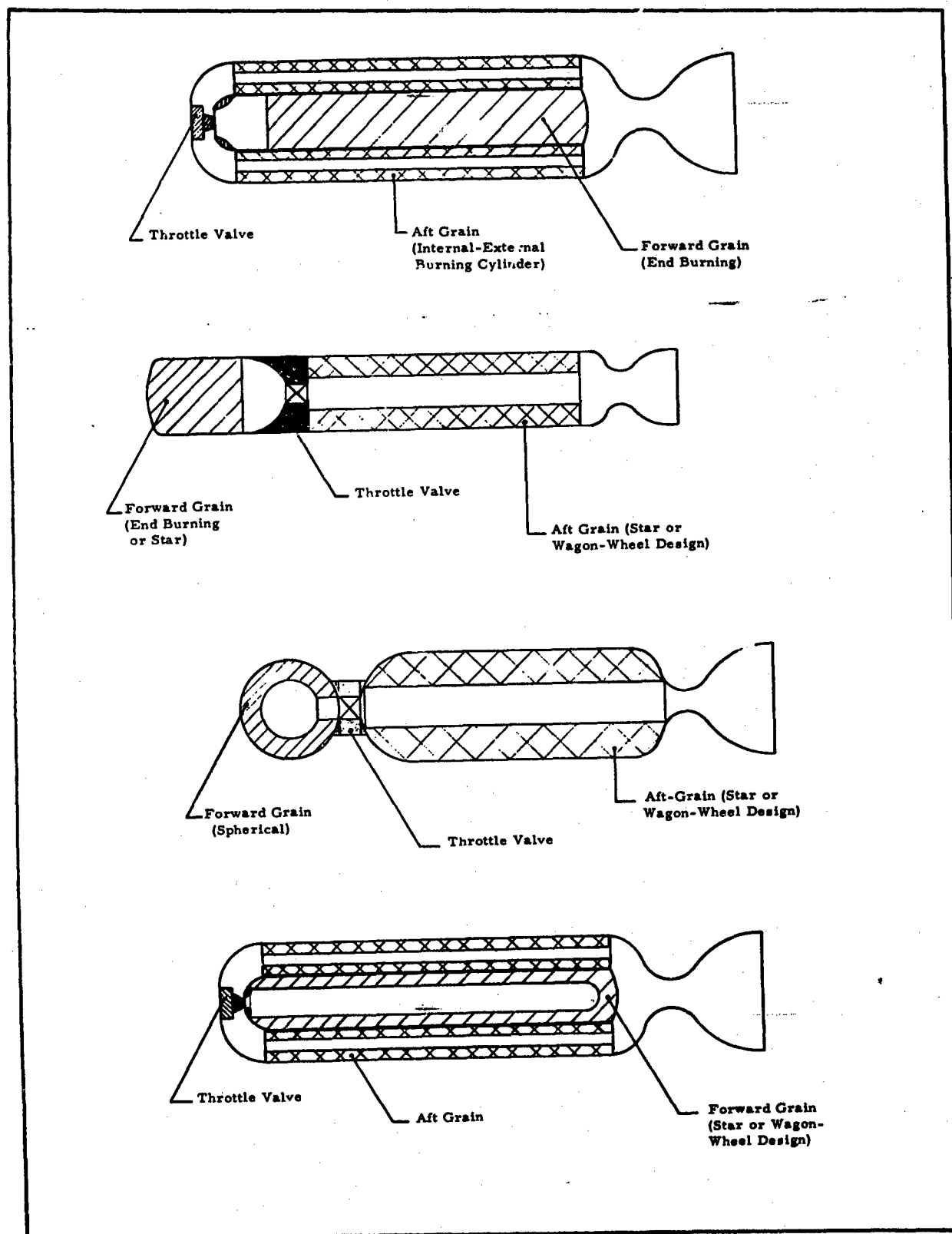


Figure 4 - Typical Configurations Considered in Grain Configuration Subroutine

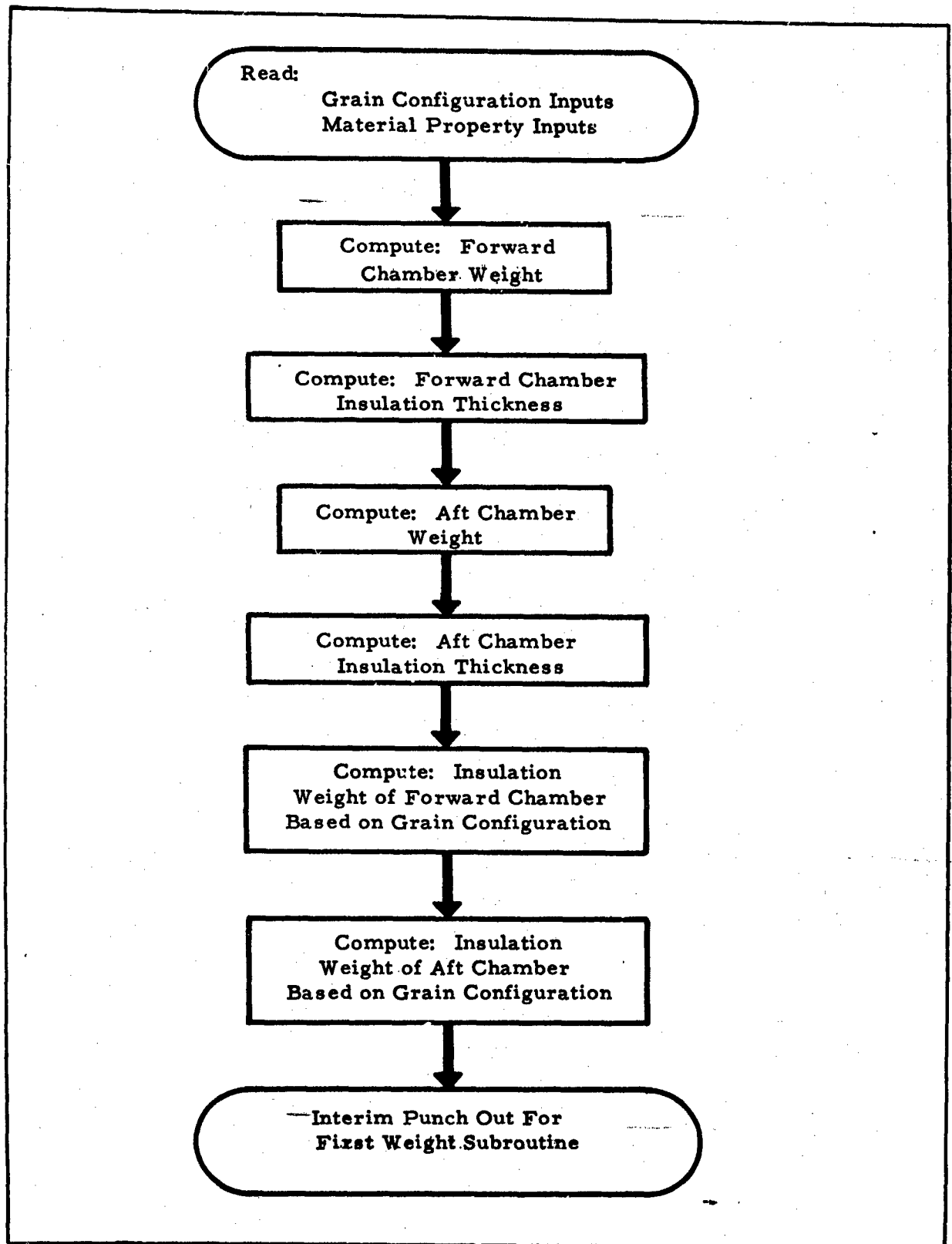


Figure 5 - Weight Subroutine A Logic Diagram

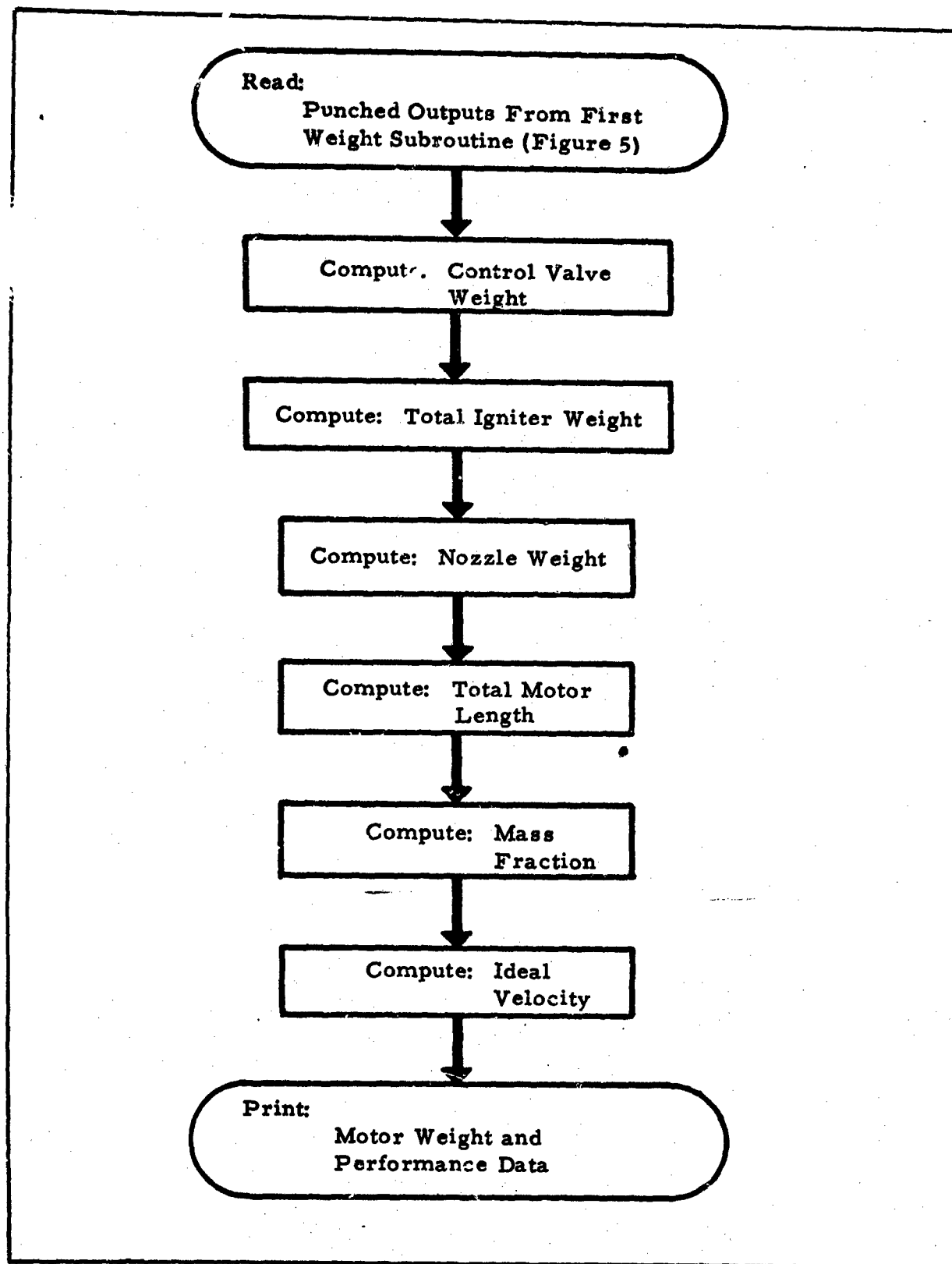


Figure 6 - Weight Subroutine B Logic Diagram

b. Chamber Weights

Chamber weights were calculated by multiplying the chamber surface area by the thickness of the particular section (based on the operating pressure times material density. The weight of the head closures was calculated from

$$W_{\text{ellipsoid}} = t_{\text{ell}} \rho \pi \left[R^2 + \left(\frac{b^2}{2e} \right) \left(\ln \frac{1+e}{1-e} \right) \right], \quad (7)$$

where

$$t_{\text{ell}} = \frac{PRSF}{\sqrt{2}\sigma}, \text{ and}$$

$$e = \frac{\sqrt{R^2 - b^2}}{R}.$$

The cylindrical chamber weight was calculated from

$$W_{\text{cyl}} = t_{\text{cyl}} \rho 2\pi R, \quad (8)$$

where

$$t_{\text{cyl}} = \frac{PRSF}{\sigma}.$$

The symbols used in Equations 7 and 8 are defined below:

$W_{\text{ellipsoid}}$	= total head closure weight (lb _m)
W_{cyl}	= total cylindrical chamber weight (lb _m)
t_{ell}	= thickness of head closure (in.)
t_{cyl}	= thickness of cylindrical chamber (in.)
ρ	= material density (lb _m /in. ³)
R	= major case radius (in.)
b	= minor ellipse radius (in.)
e	= ellipse eccentricity ratio
σ	= material yield strength (lb _f /in. ²)
SF	= safety factor
P	= operating pressure (psia)

c. Valve and Power Supply Weights

Valve and power supply weights were determined by a parametric derivation of each component's contribution to total control weight as a function of valve size. The weight equations used for each component are listed below:

<u>Component</u>	<u>Weight Equation</u>
Intermediate plate	$W = 0.00939 D_t^3 (\Delta P)^{\frac{1}{2}}$
Intermediate plate insulation	$W = 0.0025 D_t^2 t_b \quad (t_b \geq 9 \text{ sec})$ $W = 0.0225 D_t^2 \quad (t_b < 9 \text{ sec})$
Housing insulation	$W = 0.00233 D_t^2 t_b \quad (t_b \geq 9 \text{ sec})$ $W = 0.02097 D_t^2 \quad (t_b < 9 \text{ sec})$
Tube insulation	$W = 0.0053 D_t^2 t_b \quad (t_b \geq 9 \text{ sec})$ $W = 0.0476 D_t^2 \quad (t_b < 9 \text{ sec})$
Piston insulation	$W = 0.00162 D_t^2 t_b \quad (t_b \geq 9 \text{ sec})$ $W = 0.0146 D_t^2 \quad (t_b < 9 \text{ sec})$
Pintle	$W = 0.0282 D_t^3 \quad (D_t \geq 1.07$ and $L = f(D_t)$ $W = 0.0302 D_t^3 \quad (D_t < 1.07)$
Power pack	$W = 0.33 D_t^3$
Servo valves	$W = 0.59 D_t^3 + 0.9$
Piston	$W = 0.022 D_t^3 + 0.00676 D_t^3$ $(D_t \geq 2.67)$ $W = 0.0403 D_t^3 \quad (D_t < 2.67)$

<u>Component</u>	<u>Weight Equation</u>
End of piston	$W = 0.022 D_t^3 + 0.0000581 D_t^3 \sqrt{P}$ $(D_t \geq 0.68)$ $W = 0.22 D_t^3 + 0.0000294 D_t^3 \sqrt{P}$ $(D_t < 0.68)$
Cylinder	$W = 0.0297 D_t^3 \quad (D_t \geq 2.9)$ $W = 0.00792 D_t^3 + 0.027 D_t^3$ $(D_t < 2.9)$
Duct	$W = CD_t^3 = 0.00563 D_t^3$ $(D_t \geq 10.7)$ $W = CD_t^3 = 0.0602 D_t^3$ $(D_t < 10.7)$
Struts	$W = 0.000301 D_t^3 P^{\frac{2}{3}}$
Housing	$W = 0.0966 D_t^3 \quad (D_t \geq 2.38)$ $W = 0.0934 D_t^3 + 0.575 D_t^3$ $(D_t < 2.38)$

where

$$D_t = \sqrt{\frac{4 V_f}{\pi C}} \quad (\text{input}),$$

t_b = burn time,

ΔP = forward-chamber pressure - aft-chamber pressure (maximum),

C = constant input, and

V_f = final free volume of forward chamber.

d. Insulation Weights

Insulation weight was determined as a function of exposed insulation area, flame temperature, burning time, and insulation density, by means of the following equation:

$$W_{ins} = A_{ins} \rho t_{ins},$$

where

$$t_{ins} = 0.007 t_b \left(\frac{T_c + 460}{5806} \right)^4 + 0.05,$$

A_{ins} = exposed insulation surface area (in.²)

ρ = insulation density (lb_m/in.³)

t_b = maximum duration (sec), and

T_c = chamber flame temperature (°F).

e. Nozzle Weights

Nozzle weight was determined by the following empirically derived equation, which is dependent upon the yield strength of the material used in each component of the nozzle, flame temperature, expansion ratio, throat area, chamber pressure, maximum burn time, and propellant C*:

$$W_{noz} = \frac{(104 + 9.65\epsilon)(A_t)^{1.5}}{10^6} P_{c_{max}} + 1.53 (A_t)^{0.9} \\ + \left[\frac{0.00268 t_b \left(\frac{C^*}{32.2} \right)^{1.7} (P_{c_{max}})^{0.9} + 0.1}{10^6} \right] \times \\ (0.0865) (\epsilon - 4) A_t,$$

where

ϵ = expansion ratio,

A_t = throat area (in.²)

$P_{c_{max}}$ = maximum chamber pressure ($lb_f/in.^2$)
 t_b = maximum burn time (sec), and
 C^* = propellant characteristic velocity (fps).

f. Subroutine Output Data

Output data from these subroutines was very complete. An attempt was made to summarize all motor characteristics, dimensions, and weights in one tabulation, shown in Table III. Output data are coded by a line heading that increases from 100 to 1800.

TABLE III - OUTPUT FORMAT OF WEIGHT SUBROUTINE

	Strength/Density, Nozzle Structure Flame Temperature, Aft Chamber L/D Aft Chamber	Strength/Density, Nozzle Throat Flame Temperature, Forward Chamber L/D Forward Chamber	Strength/Density, Nozzle Exit Maximum Aft- Chamber Pressure Ellipse Ratio, Aft Chamber Propellant Weight, Aft Chamber Maximum Propellant Surface Area, Aft Grain	Strength/Density, Aft Chamber Maximum Forward- Chamber Pressure Ellipse Ratio, Forward Chamber Propellant Weight, Forward Chamber Maximum Propellant Surface Area, Forward Grain	Strength/Density, Forward Chamber Minimum Aft- Chamber Pressure Diameter, Aft Chamber Maximum Burn Time Insulation Density, Aft Chamber	Total Impulse
100						
200						
300						
400						
500						
600						
700						
800						
900						
1000						
1100						
1200						
1300						
1400						
1500						
1600						
1700						
1800						

SECTION III - DISCUSSION OF RESULTS

1. GENERAL

The over-all results of the parametric study are presented and discussed in this section. The data from the computer runs have been plotted in semi-logarithmic form to facilitate analysis. The data from these basic plots, which are presented sequentially in Appendix B by phase and variable, have been cross-plotted and presented in this section to highlight the trends observed.

This section is organized by study phase, with the effect of each independent variable discussed separately.

2. PHASE I

a. General

In Phase I, the effect of specific impulse, thrust ratio, number of starts, total impulse, and minimum thrust on mass fraction and delta velocity was studied. The effect of each of these variables is discussed below.

b. Specific Impulse

The effects of specific impulse on mass fraction and delta velocity, for a thrust ratio of 1 and 10 starts, are shown in Figures 7 and 8, respectively. As shown in Figure 7, mass fraction decreases slightly with increasing specific impulse. However, delta velocity increases as specific impulse is increased. Curves for higher thrust ratios and other than 10 starts are similar, but the mass fraction and delta velocity levels differ. (Confidential)

c. Thrust Ratio

In Figures 9 and 10, the effects of thrust ratio (that is, maximum thrust/minimum thrust) on mass fraction and delta velocity are shown, for 10 starts and a specific impulse of $280 \text{ lb}_f\text{-sec/lb}_m$. For thrust ratios up to 5, the penalty on

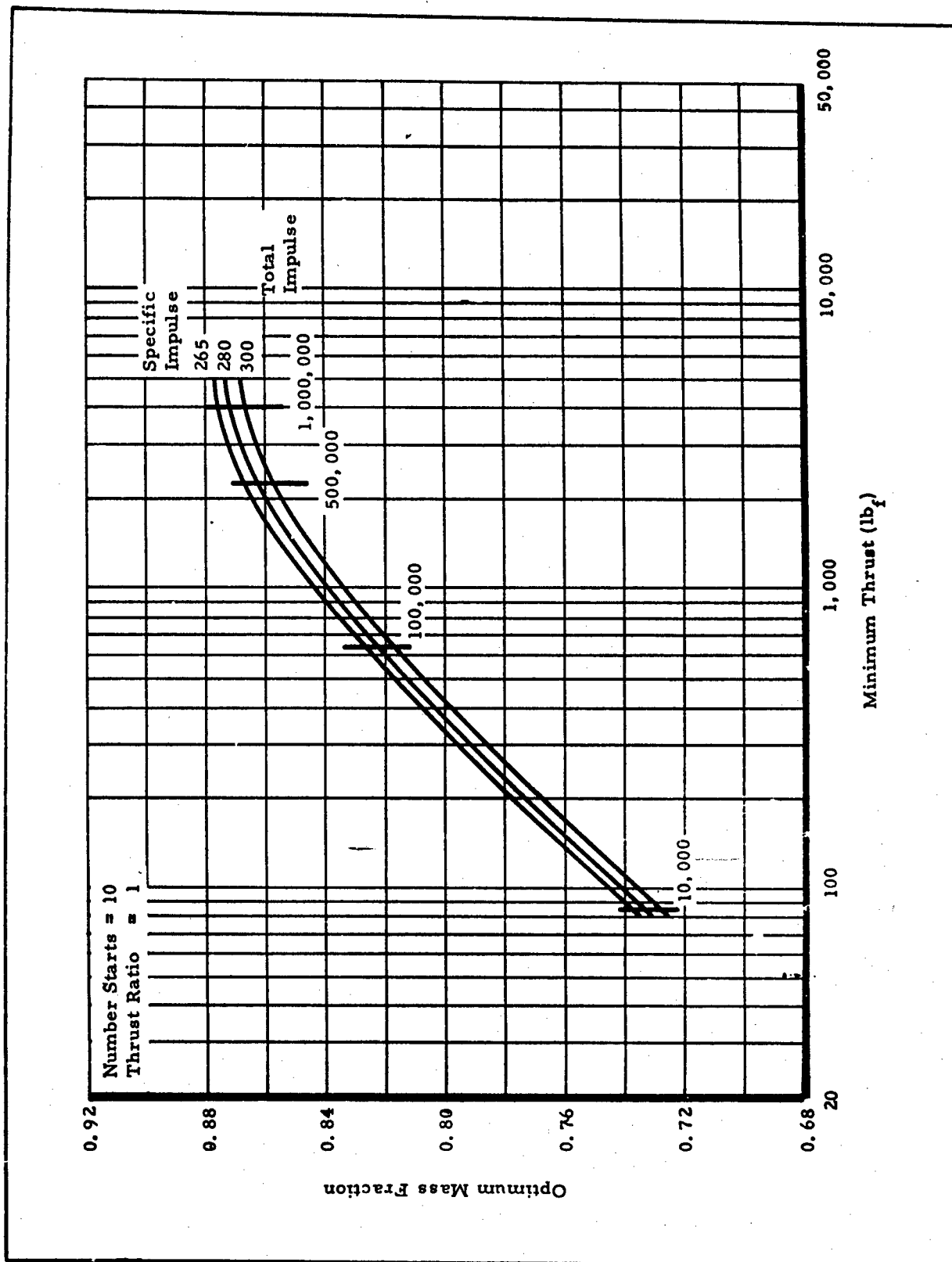


Figure 7 - Effect of Specific Impulse on Mass Fraction

CONFIDENTIAL

CONFIDENTIAL

AFRPL-TR-65-209, Vol II

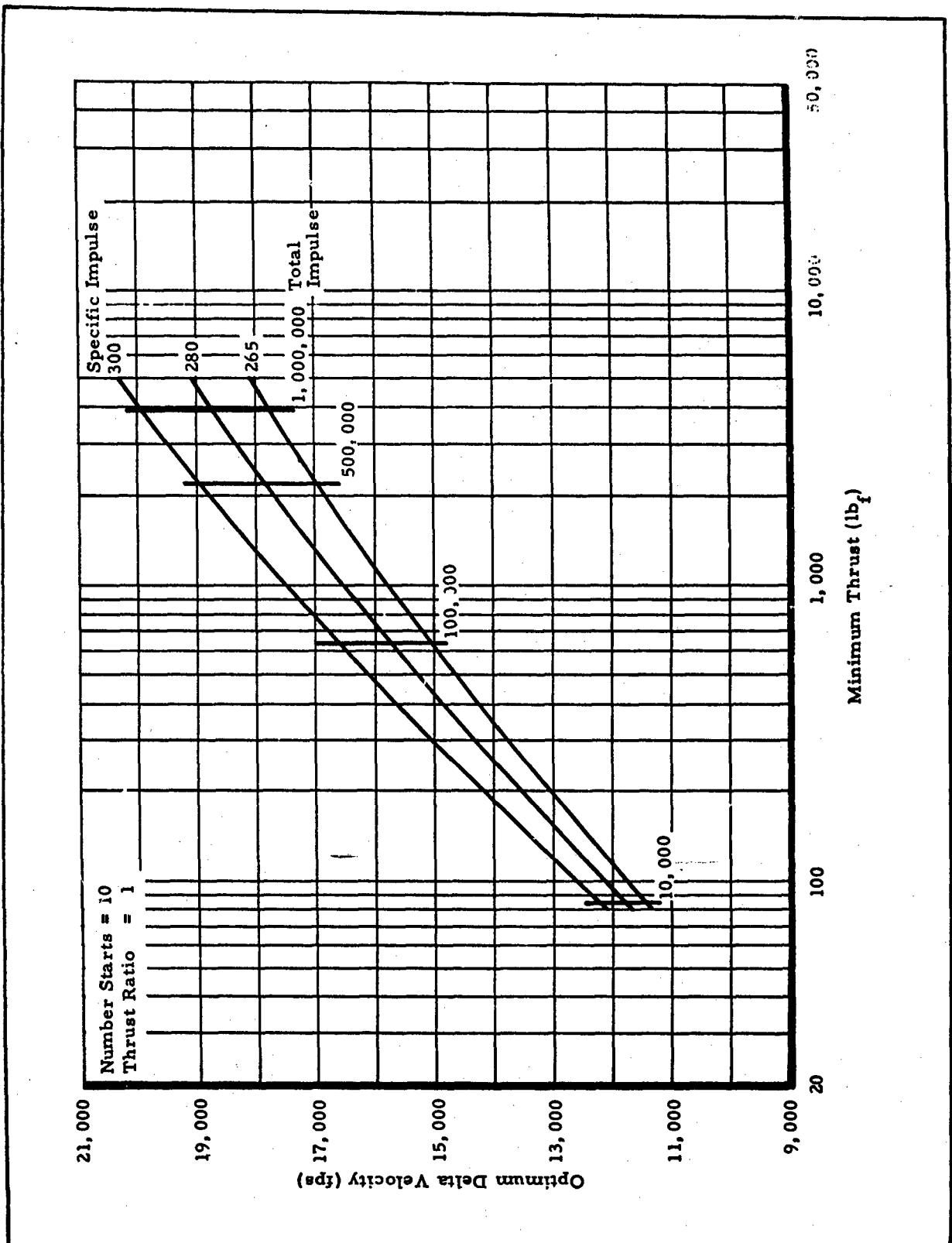


Figure 8 - Effect of Specific Impulse on Delta Velocity

CONFIDENTIAL

CONFIDENTIAL

AFRPL-TR-65-209, Vol. II

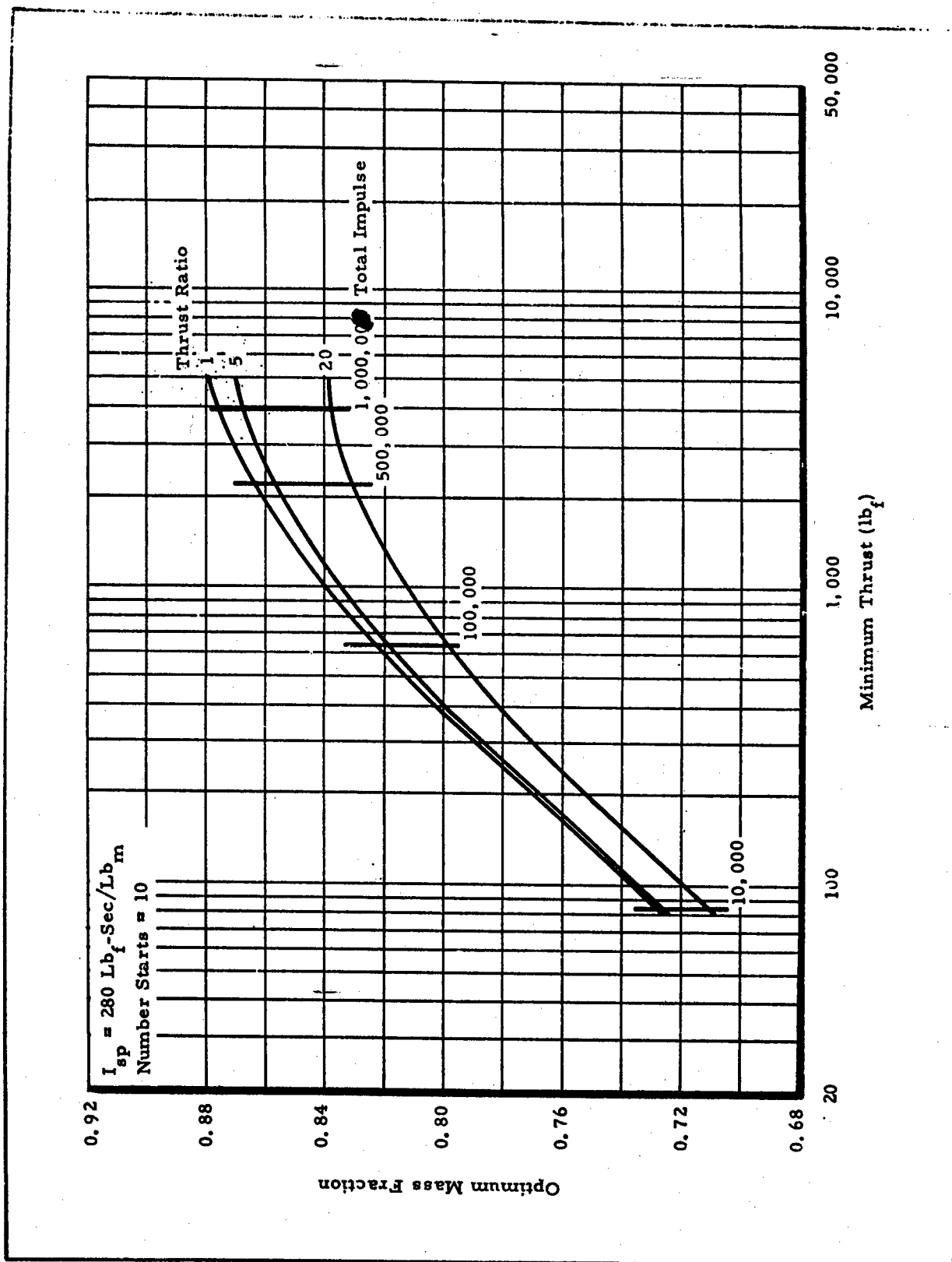


Figure 9 - Effect of Thrust Ratio on Mass Fraction

CONFIDENTIAL

CONFIDENTIAL

AFRPL-TR-65-209, Vol II

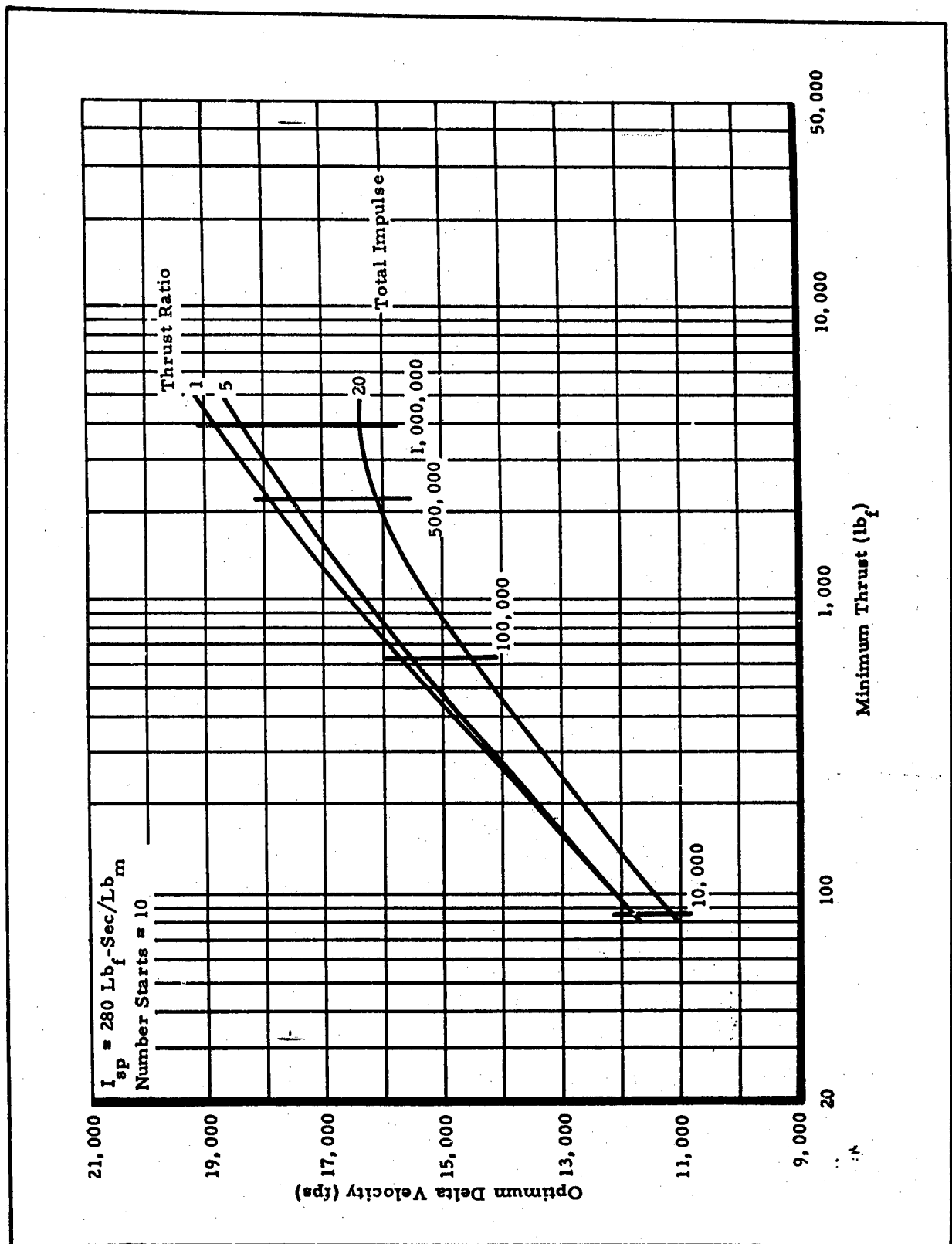


Figure 10 - Effect of Thrust Ratio on Delta Velocity

CONFIDENTIAL

mass fraction and delta velocity is small. This penalty becomes more pronounced, however, for a thrust ratio of 20, particularly for the larger motors. For example, the mass fraction is decreased 2.7 percent at a 20-to-1 thrust ratio for a 10,000-lb-sec motor, compared to a decrease of 4.5 percent for a 1,000,000-lb-sec motor. This penalty is due to the effect of the higher chamber pressure, required for the 20-to-1 thrust ratio, on case thickness, resulting in a greater weight penalty in the large-diameter (high total impulse) motors. However, the 20-to-1 throttling range imposes very little penalty over that of a stop-restart motor alone (thrust ratio of 1) at the lower total impulse levels. (Confidential)

d. Number of Starts

The effects of the number of starts, for a restartable motor, on mass fraction and delta velocity are shown in Figures 11 and 12, respectively. The differences represent the weight penalty imposed by the multiple pyrogen units for restart capability. The weight of a valve for termination was included for all motor designs, including the motor with one start. The mass fraction penalty for 20 starts, compared to one start, is 1.8 percent for the 10,000-lb-sec motors, and 1.2 percent for the 1,000,000-lb-sec motors. (Confidential)

e. Total Impulse and Minimum Thrust

The effects of total impulse on mass fraction and delta velocity are shown in Figures 13 and 14, respectively, for motors with thrust ratios of 1, 5, and 20 to 1. The mass fraction for each total impulse level corresponds to that at the optimum minimum thrust level, derived from Figure B-5. Figure 15 is a contour map of mass fraction as a function of total impulse and minimum thrust for a thrust ratio of one. A similar plot for a thrust ratio of 20 is given in Figure 16. The dotted constant mass fraction lines in Figures 15 and 16 are extrapolated values. These plots give the optimum minimum thrust levels corresponding to various total impulse level motors. (Confidential)

Figure 17 shows the effects of minimum thrust and total impulse on motor diameter. The dotted lines connect the values for constant total impulse designs, and the solid lines connect values for motor designs with similar grain configurations.

CONFIDENTIAL

AFRPL-TR-65-209, Vol II

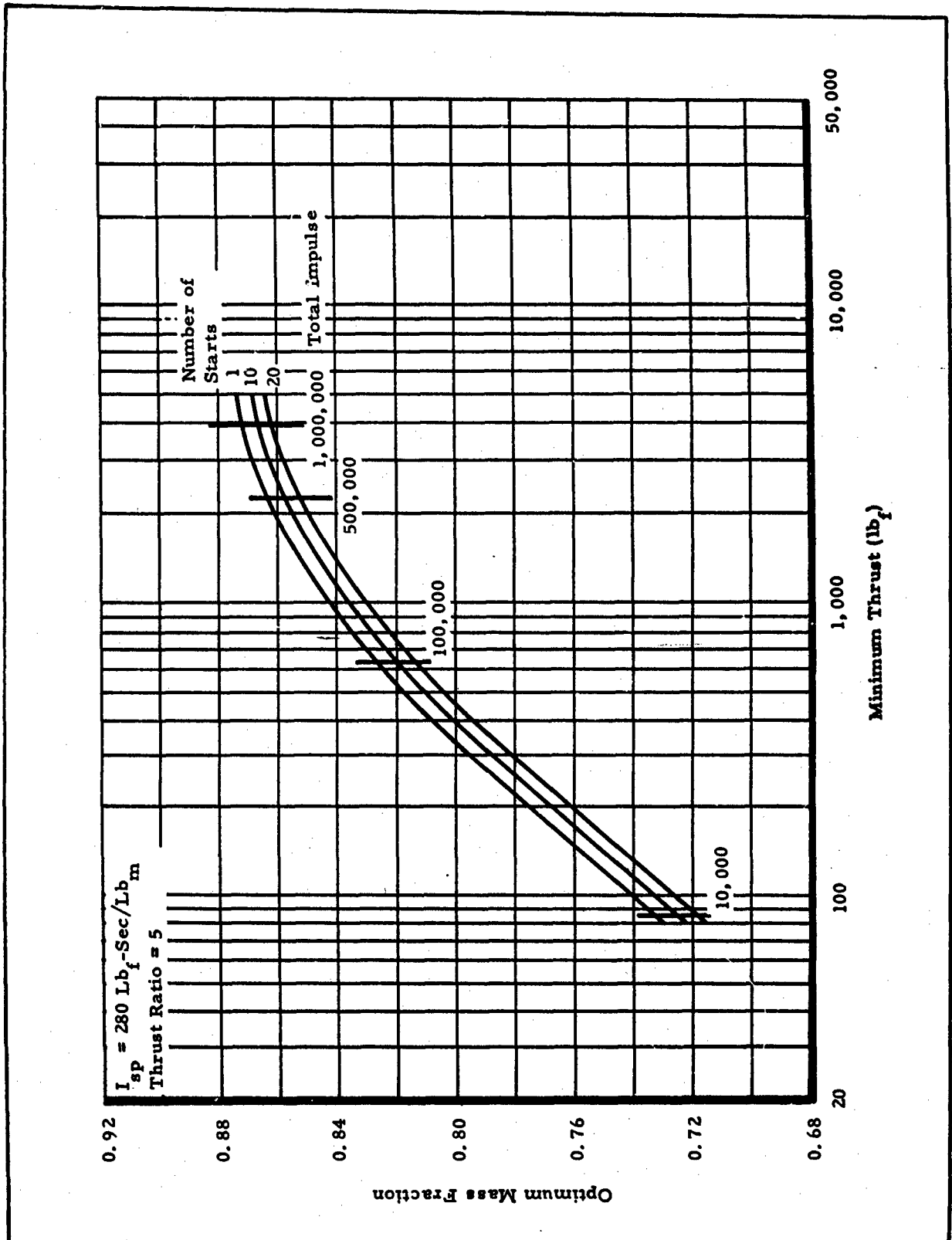


Figure 11 - Effect of Number of Starts on Mass Fraction

CONFIDENTIAL

CONFIDENTIAL

AFRPL-TR-65-209, Vol II

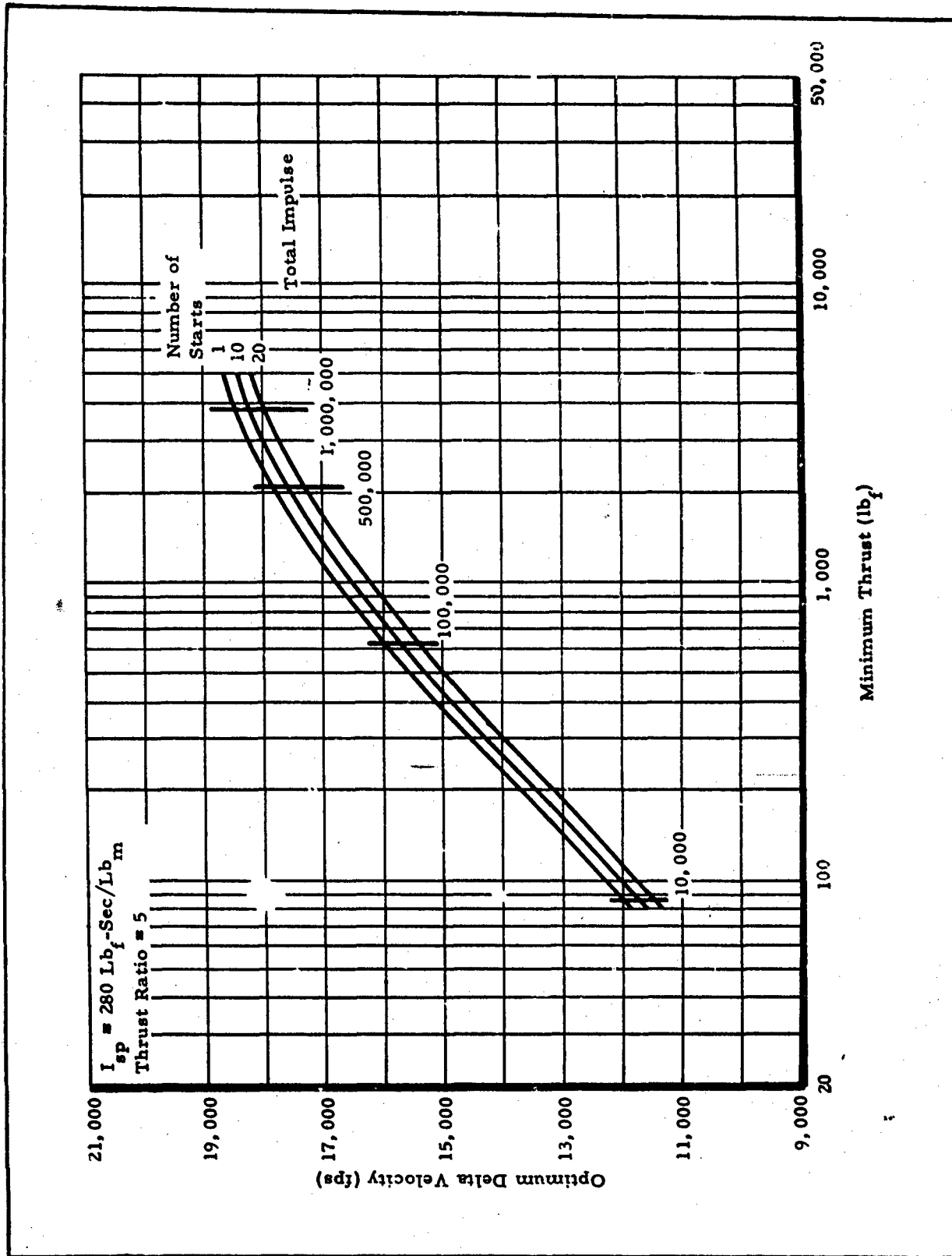


Figure 12 - Effect of Number of Starts on Delta Velocity

CONFIDENTIAL

CONFIDENTIAL

AFRPL-TR-65-209, Vol II

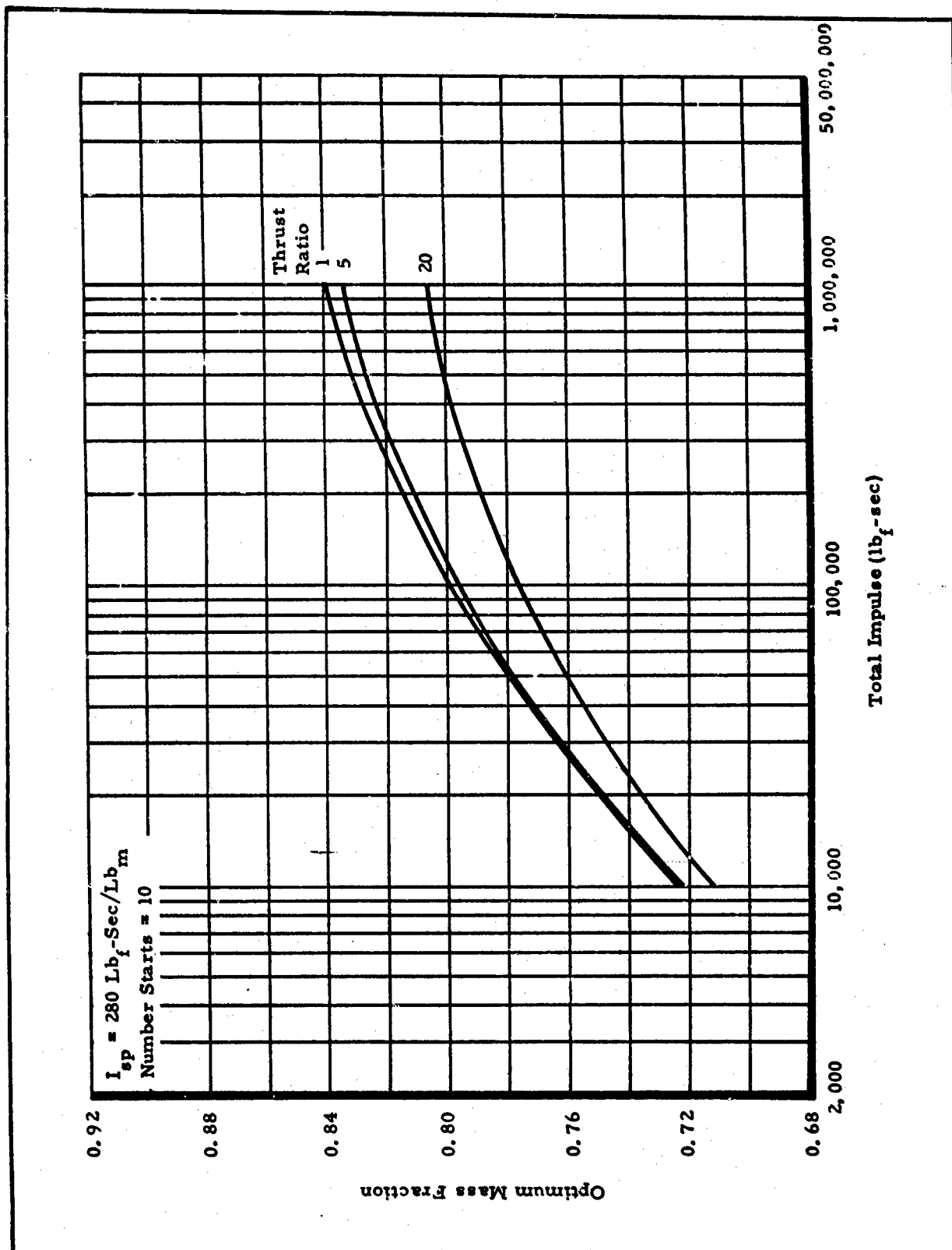


Figure 13 - Mass Fraction as a Function of Total Impulse

CONFIDENTIAL

CONFIDENTIAL

AFRPL-TR-65-209, Vol II

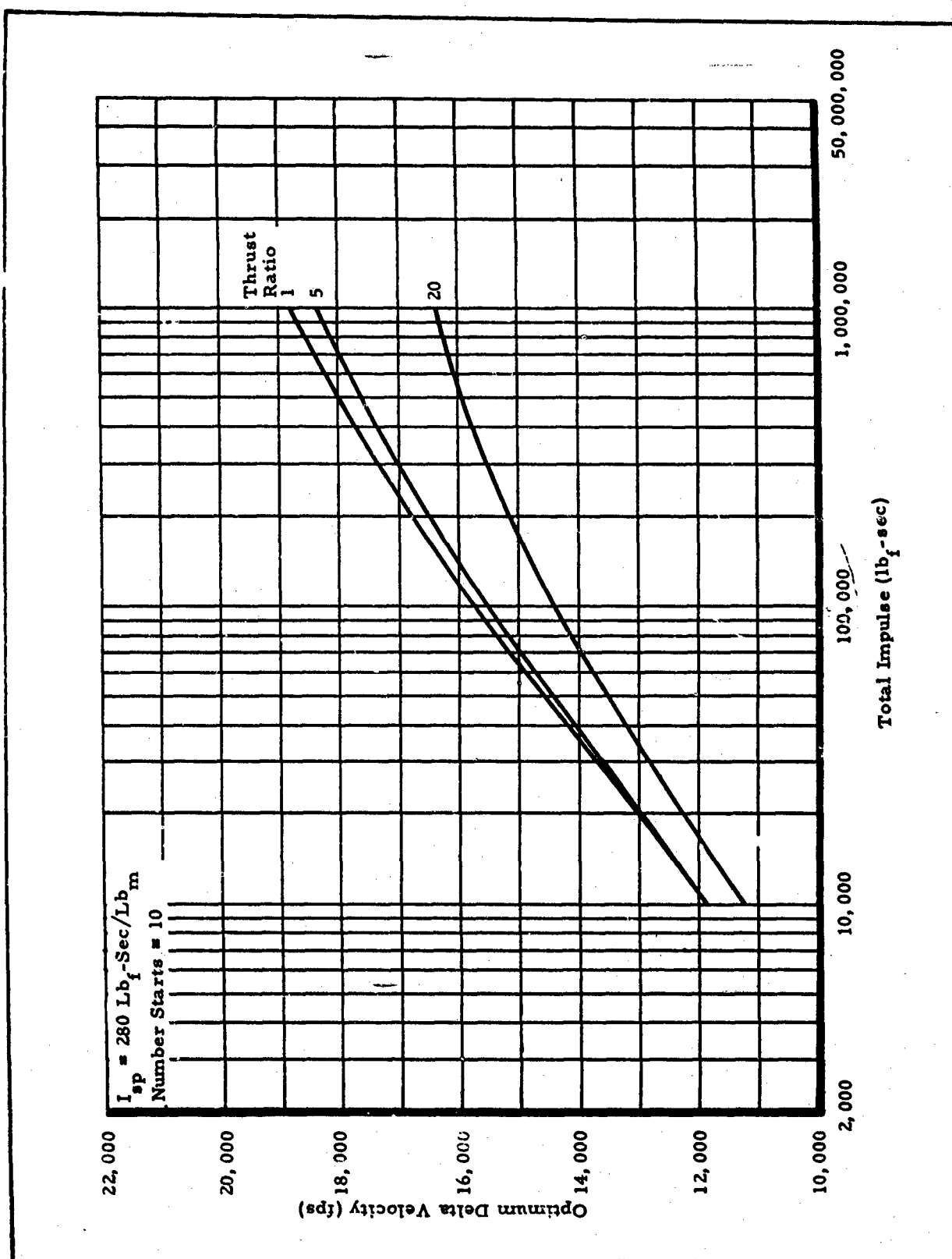


Figure 14 - Delta Velocity as a Function of Total Impulse

CONFIDENTIAL

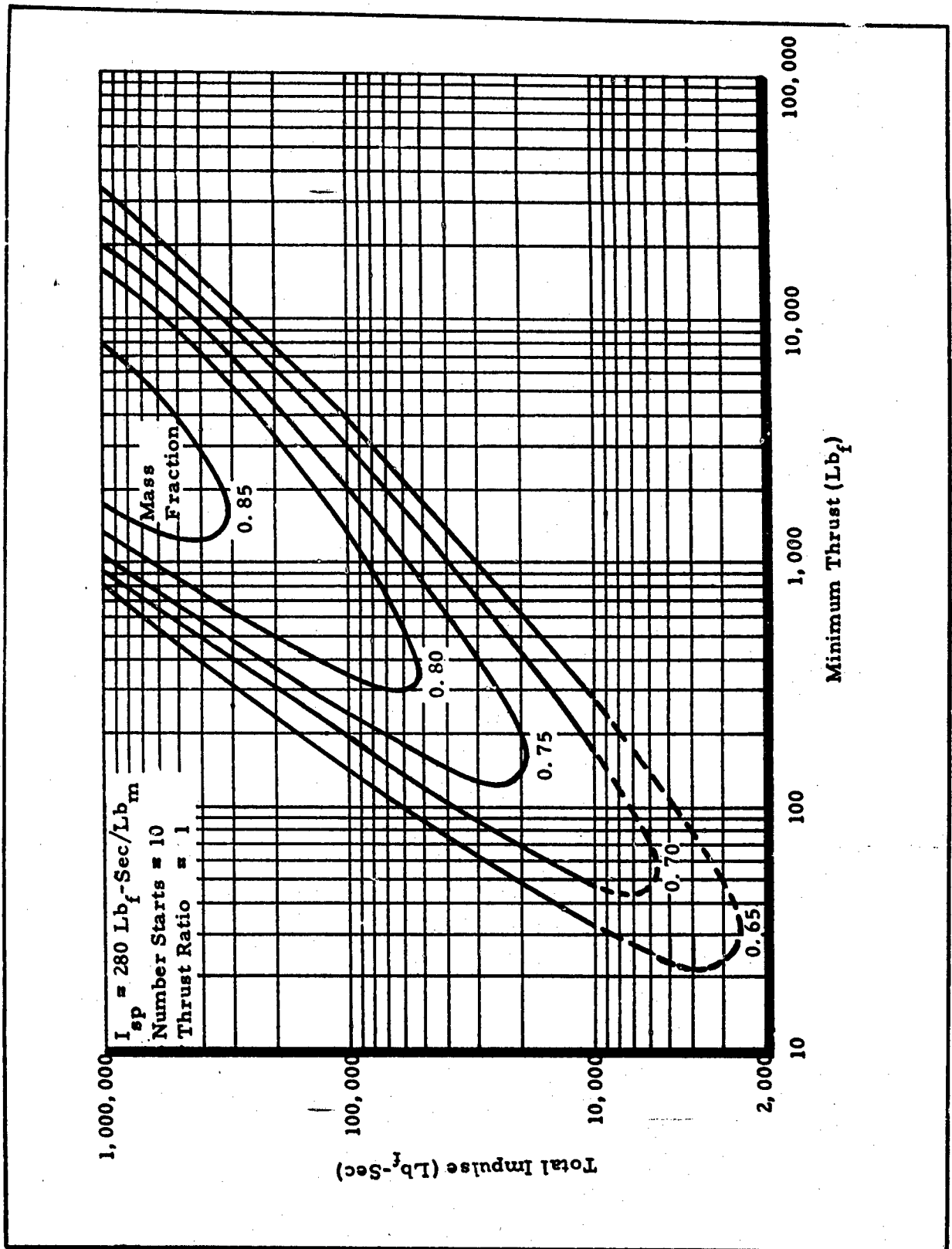


Figure 15 - Mass Fraction Contour Map for a Thrust Ratio of 1

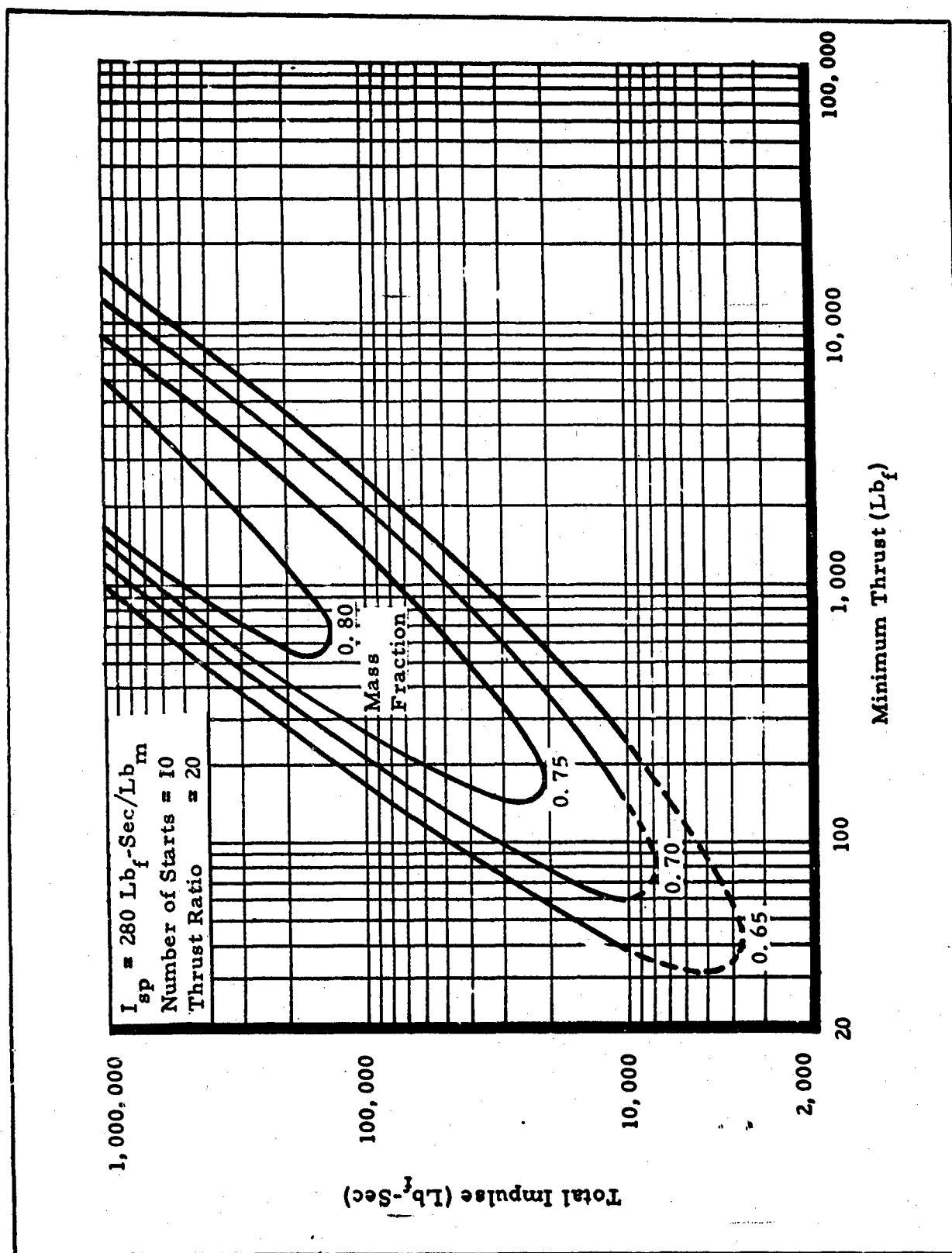


Figure 16 - Mass Fraction Contour Map for a Thrust Ratio of 20

CONFIDENTIAL

AFRPL-TR-65-209, Vol II

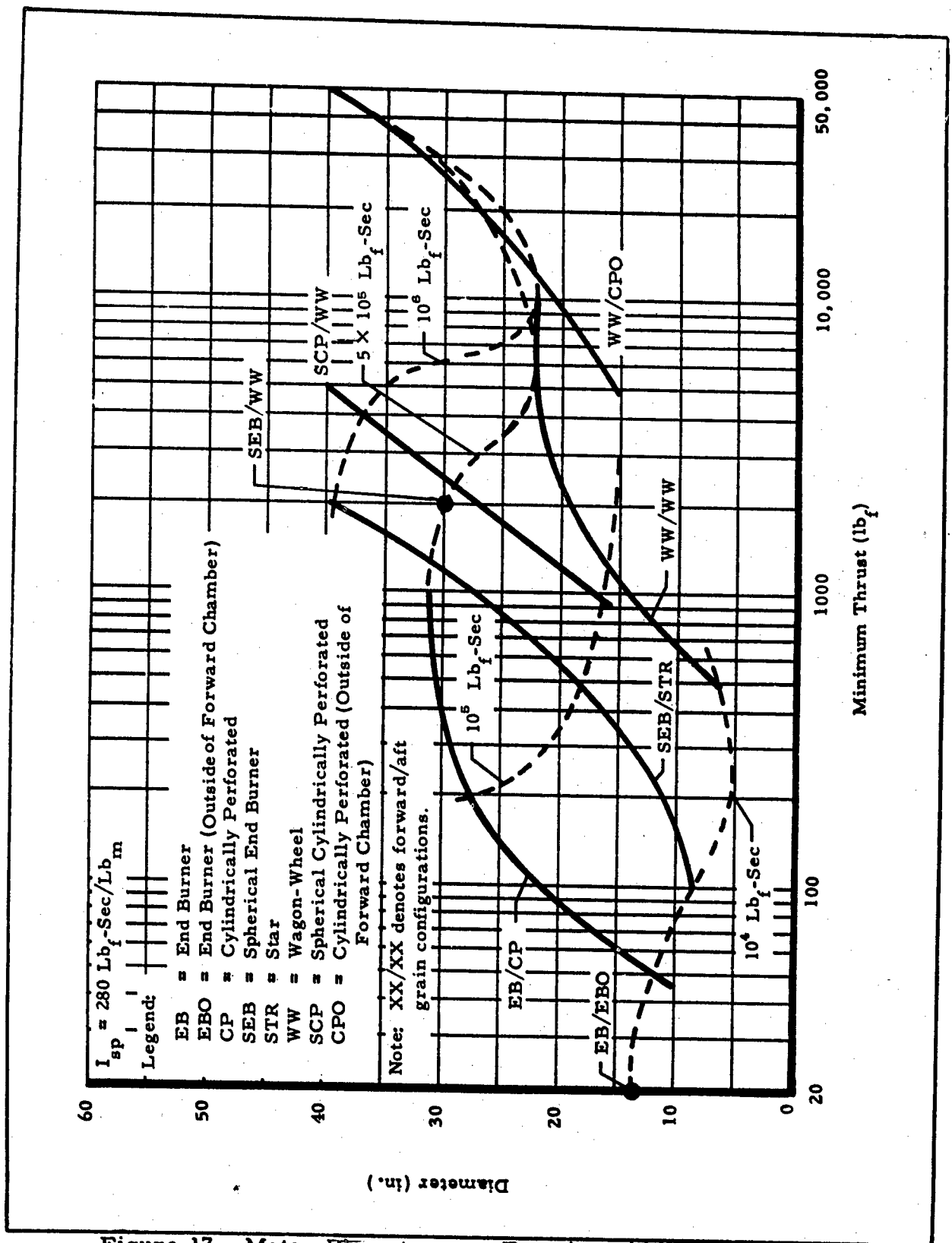


Figure 17 - Motor Diameter as a Function of Minimum Thrust and Total Impulse

CONFIDENTIAL

A minimum diameter is obtained for each total impulse level motor at different minimum thrust levels. Note that the optimum minimum thrust level increases with increasing total impulse.

In Figure 18, the effects of total impulse and minimum thrust on motor length are shown; the dotted lines connect designs with similar grain configurations. This graph shows that total impulse affects grain length much less than minimum thrust. This is also borne out in Figure 19 in which the band of motor length is plotted as a function of minimum thrust.

3. PHASE II

a. General

The results of Phase II, in which case material, burning rate constants, pressure exponents, and weight flow ratios were investigated, are presented in the following paragraphs.

b. Case Material

Three case materials, fiberglass, titanium, and steel, were investigated in Phase IIa. The effect of the mass fraction ratio of fiberglass to steel motors and titanium to steel motors as a function of minimum thrust is shown in Figure 20 for 100,000-lb-sec total impulse motors. The effect of delta velocity ratio for these same conditions is shown in Figure 21. The advantages of fiberglass and titanium over steel become more significant at the higher thrust levels. (Confidential)

The effects of case material on mass fraction and delta velocity as a function of thrust ratio are presented in Figures 22 and 23, respectively. As thrust ratio increases, which corresponds to higher chamber pressures, the effect of the three materials on mass fraction and delta velocity becomes more pronounced. (Confidential)

c. Burning-Rate Constants

The effects of forward- and aft-propellant burning-rate constants on optimum mass fraction and optimum delta velocity are shown in Figures 24 and 25, respectively, for 100,000-lb-sec motors. For this motor size the highest forward rate constant

CONFIDENTIAL

AFRPL-TR-65-209, Vol II

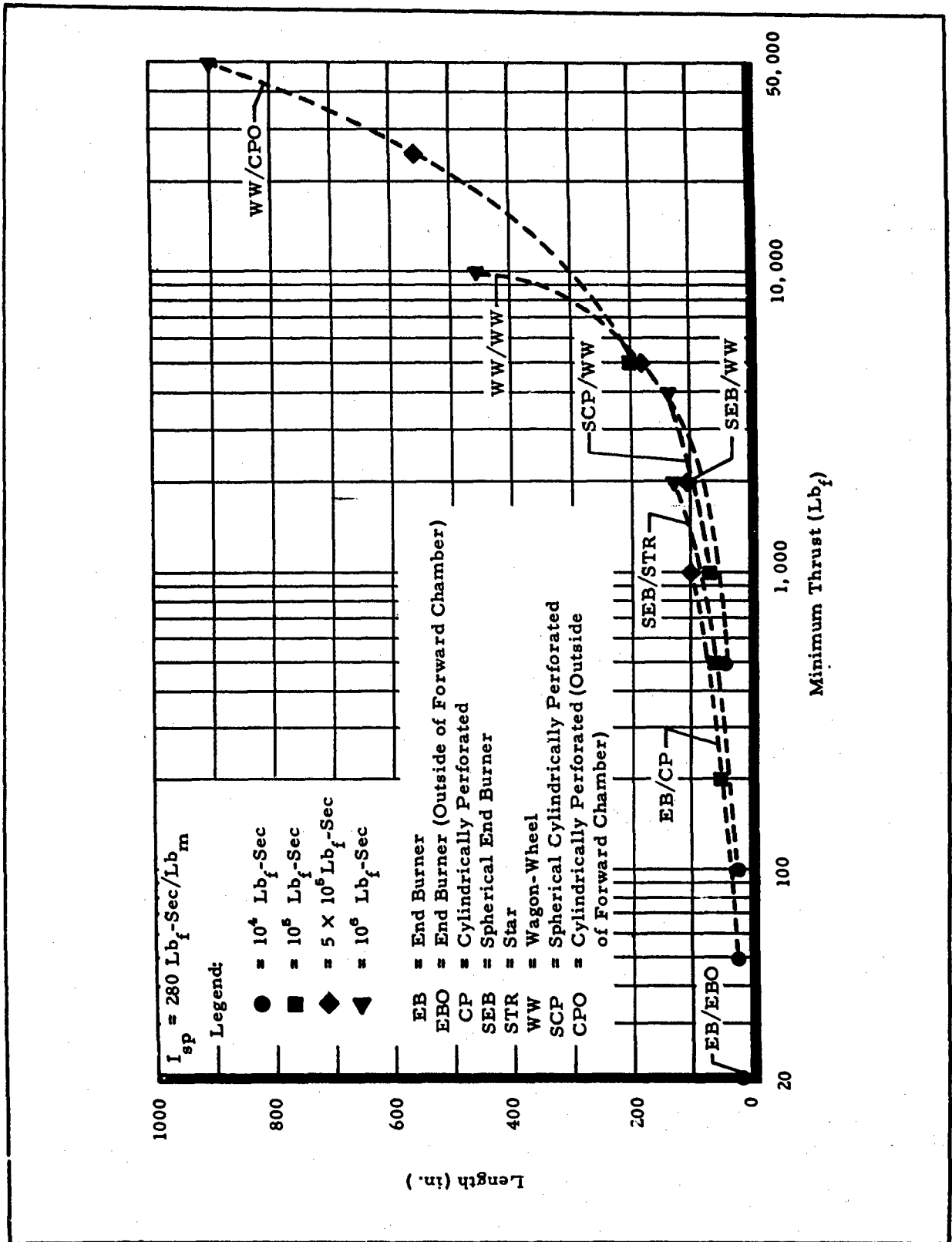


Figure 18 - Motor Length as a Function of Minimum Thrust and Total Impulse

CONFIDENTIAL

CONFIDENTIAL

AFRPL-TR-65-209, Vol II

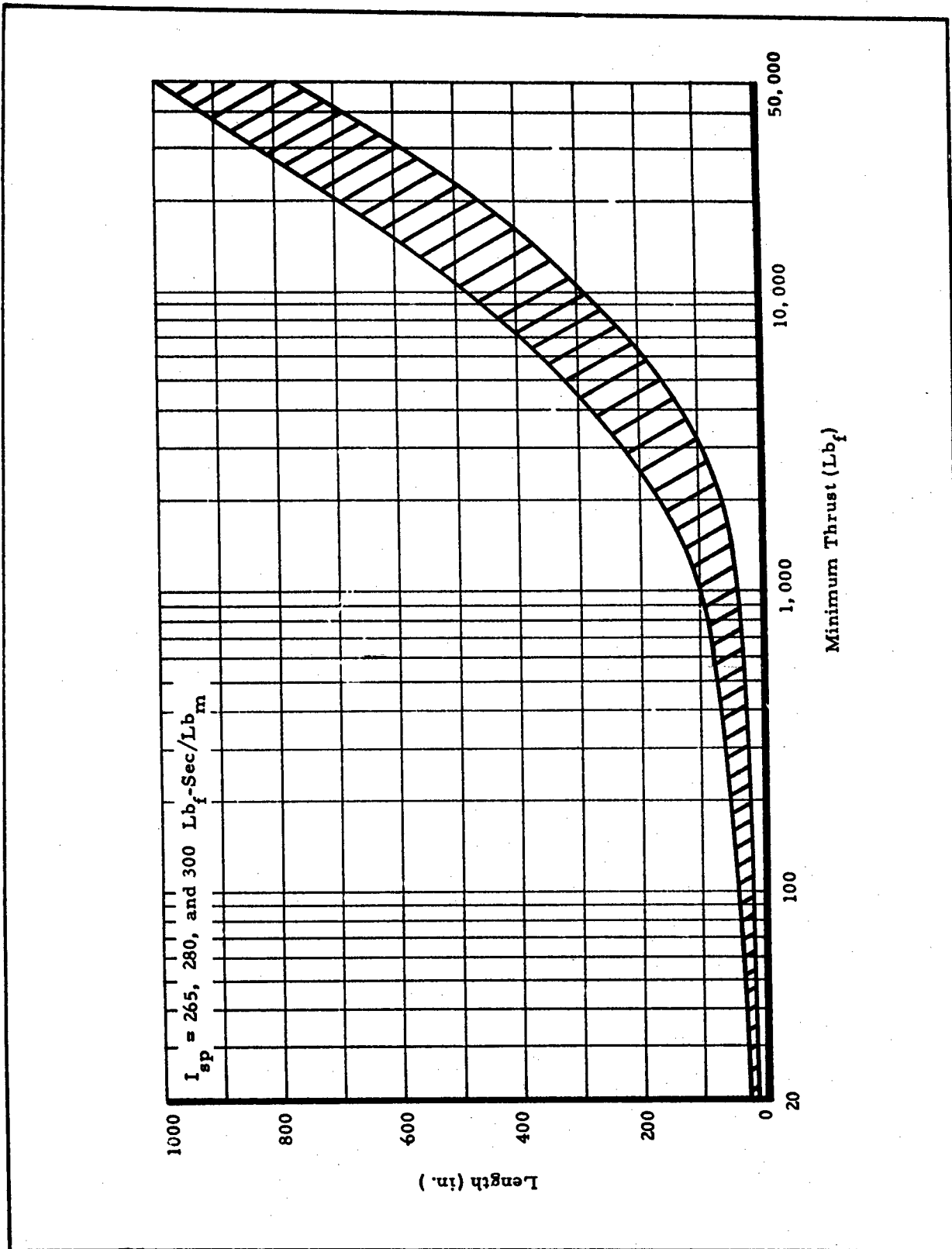


Figure 19 - Motor Length as a Function of Minimum Thrust

CONFIDENTIAL

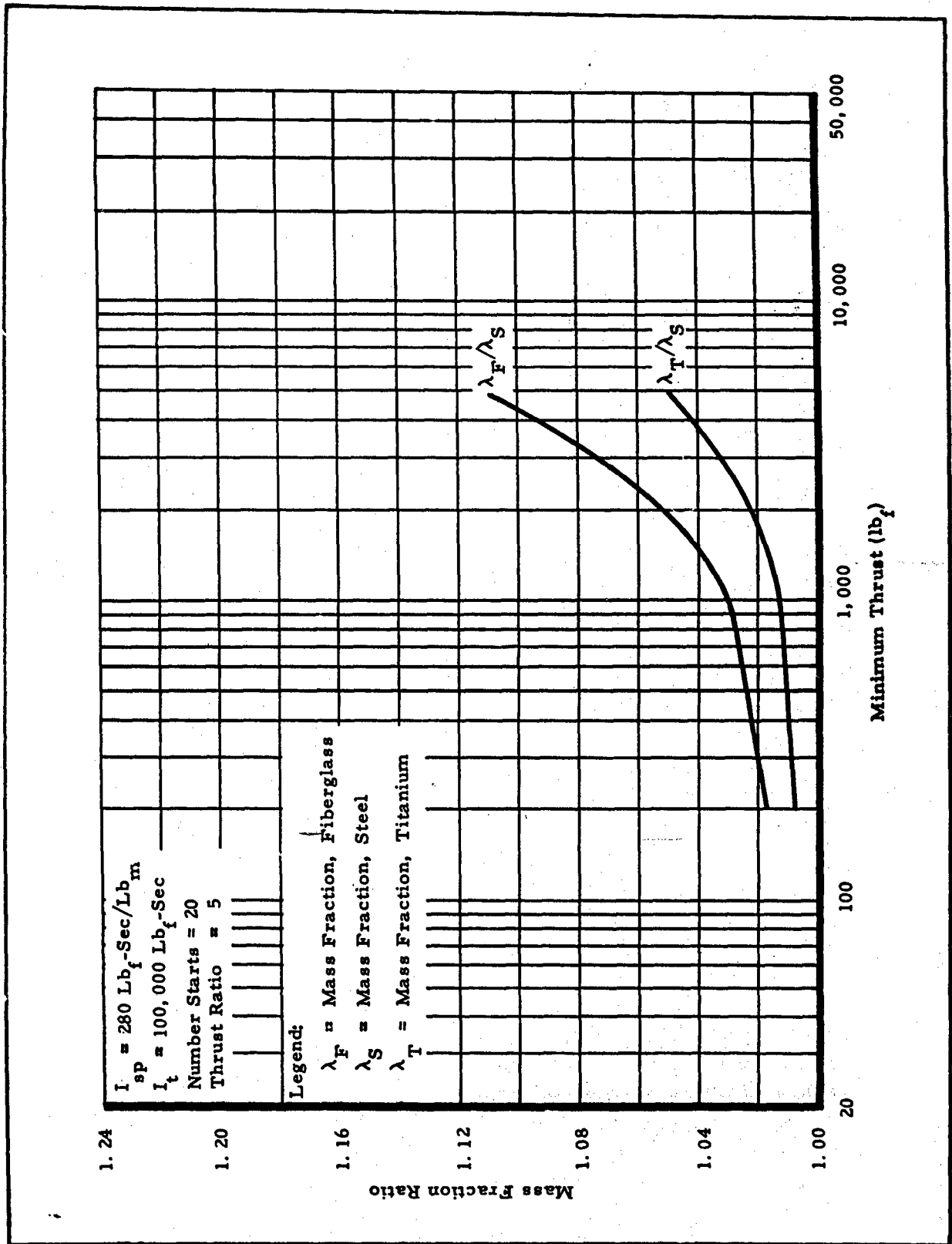


Figure 20 - Effect of Case Material on Mass Fraction

CONFIDENTIAL

AFRPL-TR-65-209, Vol II

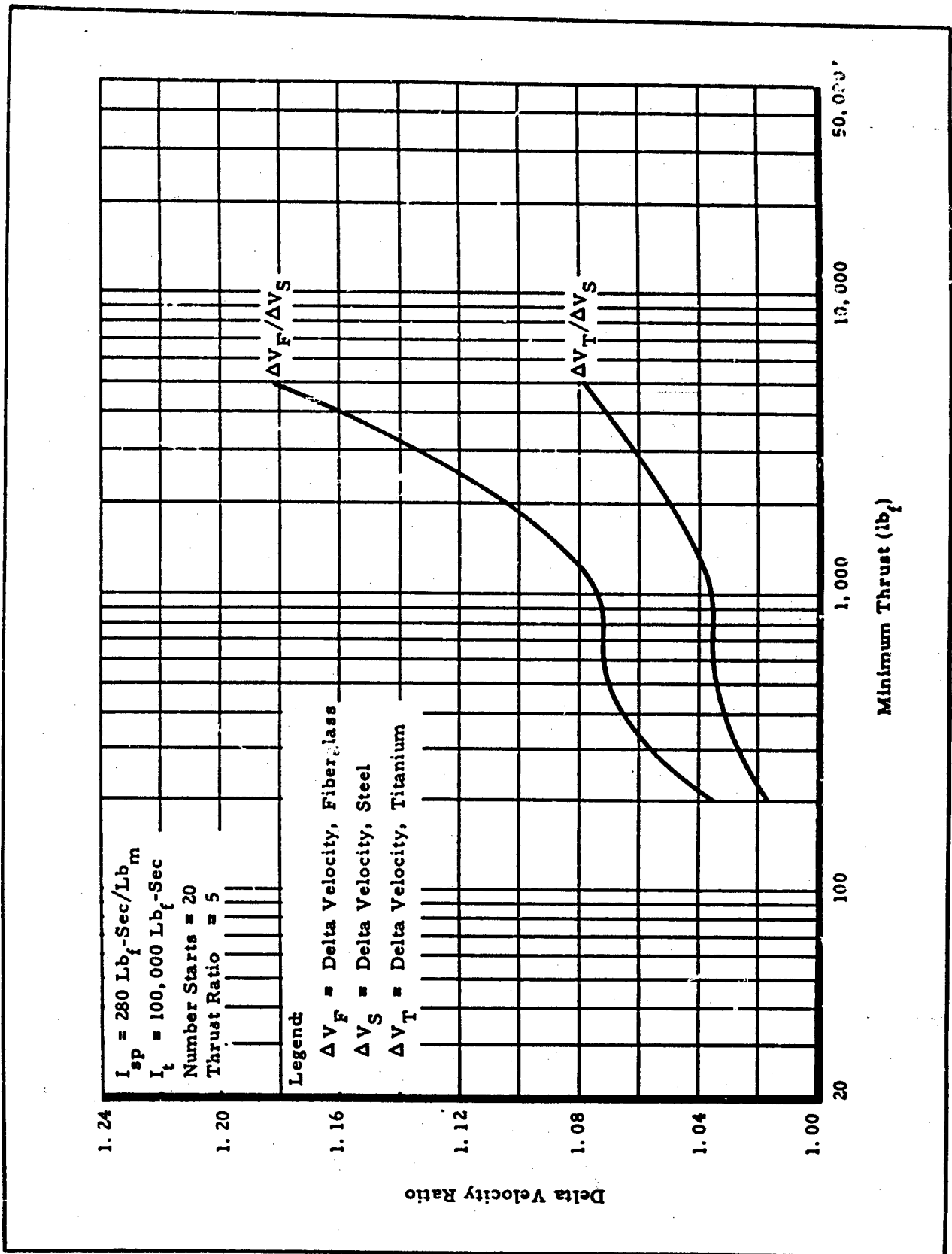


Figure 21 - Effect of Case Material on Delta Velocity

CONFIDENTIAL

CONFIDENTIAL

AFRPL-TR-65-209, Vol II

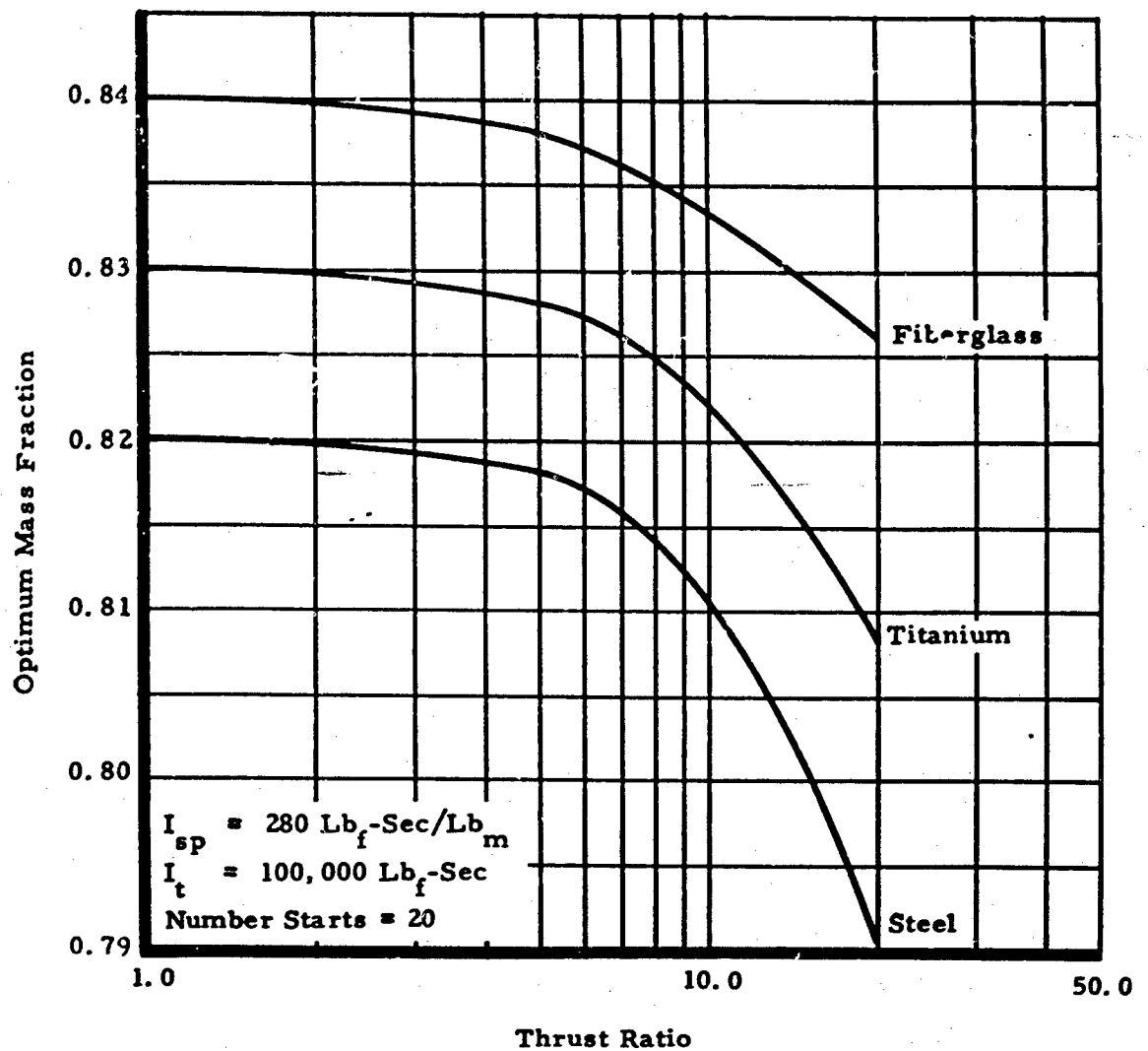


Figure 22 - Mass Fraction as a Function of Thrust Ratio
for Three Case Materials

CONFIDENTIAL

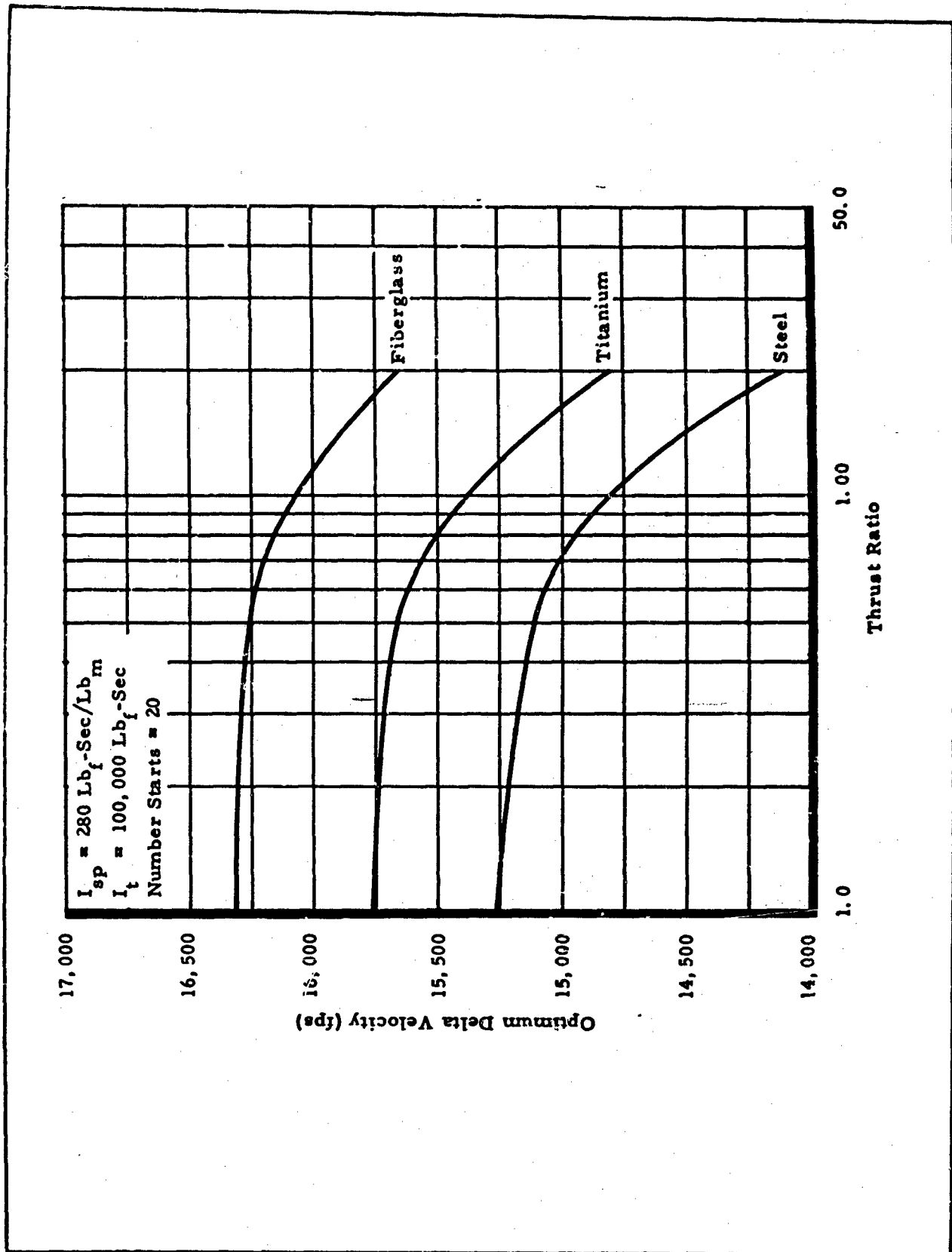


Figure 23 - Delta Velocity as a Function of Thrust Ratio for Three Case Materials

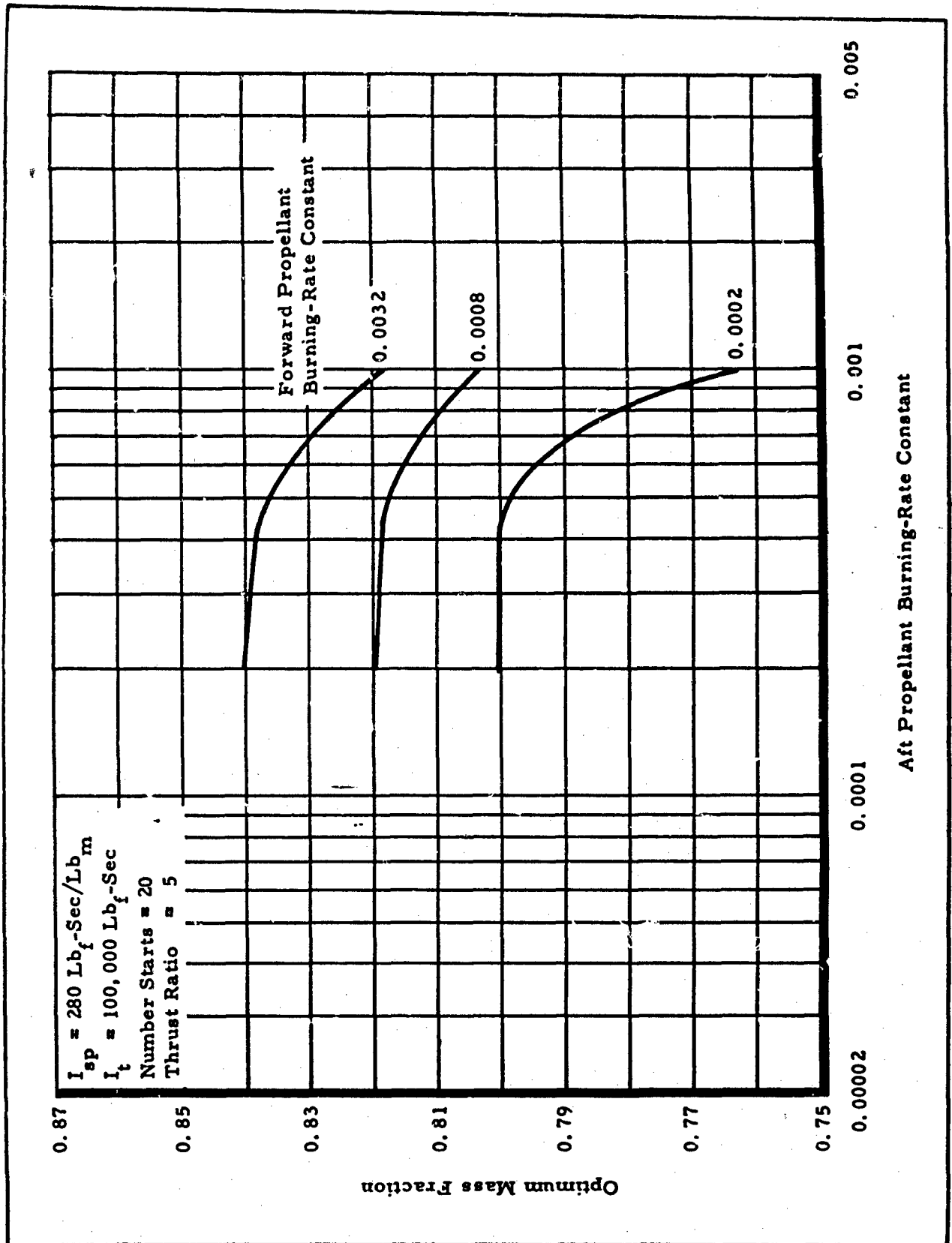


Figure 24 - Effect of Burning-Rate Constants on Mass Fraction

CONFIDENTIAL

AFRPL-TR-65-209, Vol II

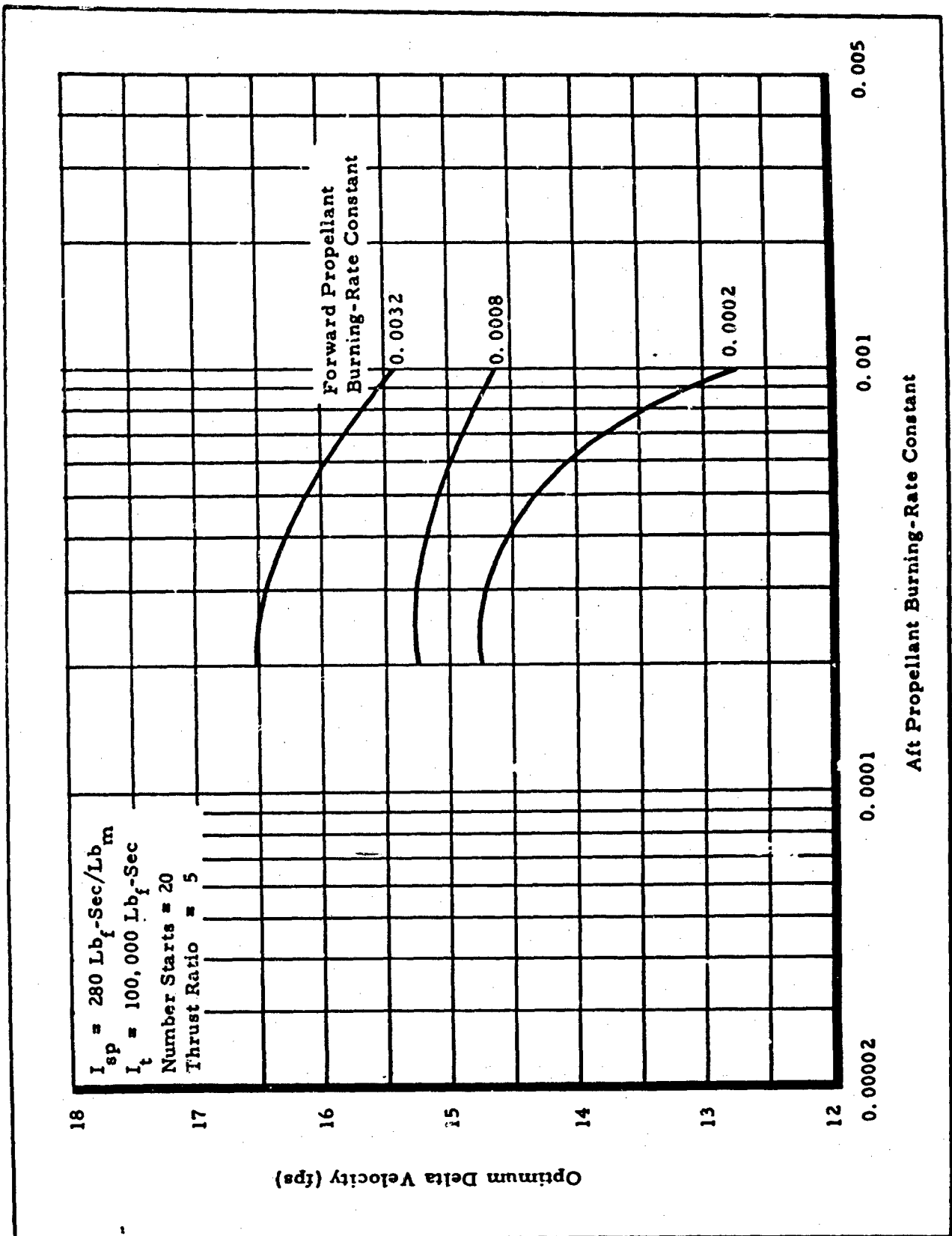


Figure 25 - Effect of Burning-Rate Constants on Delta Velocity

CONFIDENTIAL

and lowest aft rate constant investigated produced the highest mass fraction and boost velocity. These constants gave motor designs with smaller diameters than others, as shown in Appendix B. The higher forward rate constant permitted an end-burning forward-grain configuration to be used, while the lower aft rate constant allowed a star aft-grain configuration to be employed. These optimum mass fraction and delta velocity values were calculated at a minimum thrust of 500 lb. At lower minimum thrust values, lower forward rate constants were more advantageous. (Confidential)

d. Pressure Exponents

As expected, the higher burning-rate pressure exponents give higher mass fractions and boost velocities for throttleable motors, as shown in Figures 26 and 27. At a thrust ratio of 20, the effects of forward and aft exponents are very pronounced. For example, as the forward exponent increases from 0.60 to 0.90 and the aft exponent changes from 0.80 to 1.00 (Figure 26), mass fraction increases from 0.52 to 0.81. For a thrust ratio of 5 to 1, on the other hand, the effect of the exponents is very slight. (Confidential)

e. Aft-to-Forward Weight Flow Ratio

The effects of aft to forward weight flow ratio (θ) on mass fraction and delta velocity are shown in Figures 28 and 29, respectively. The higher θ values are advantageous because, at these conditions, the aft chamber operates at a lower pressure than the forward chamber and has a higher aft propellant density. A θ of 4 produces less than a 4-percent increase in mass fraction over a θ of 2, but provides a 7.5-percent increase in delta velocity. (Confidential)

CONFIDENTIAL

AFRPL-TR-65-209, Vol II

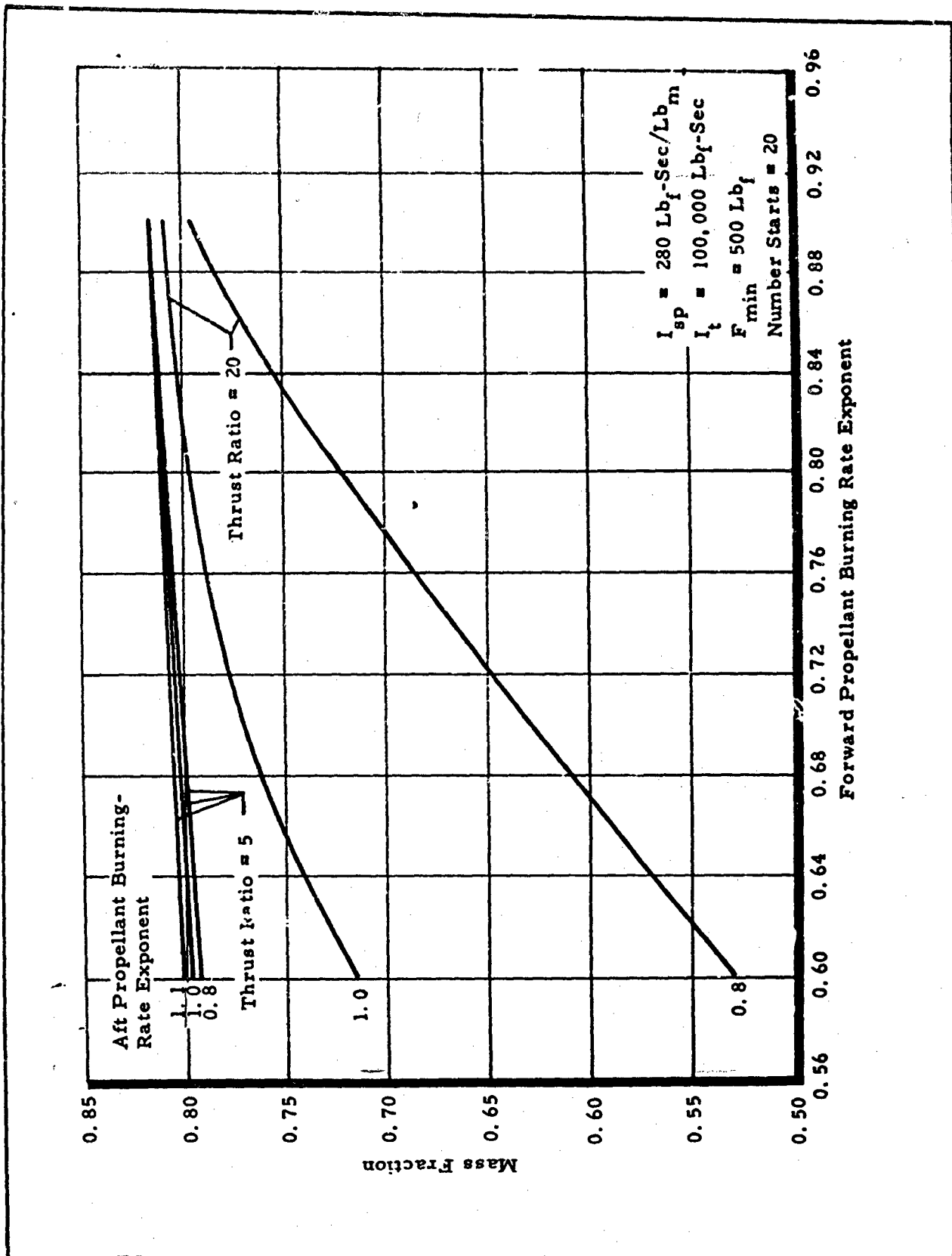


Figure 26 - Effect of Burning-Rate Pressure Exponents on Mass Fraction

CONFIDENTIAL

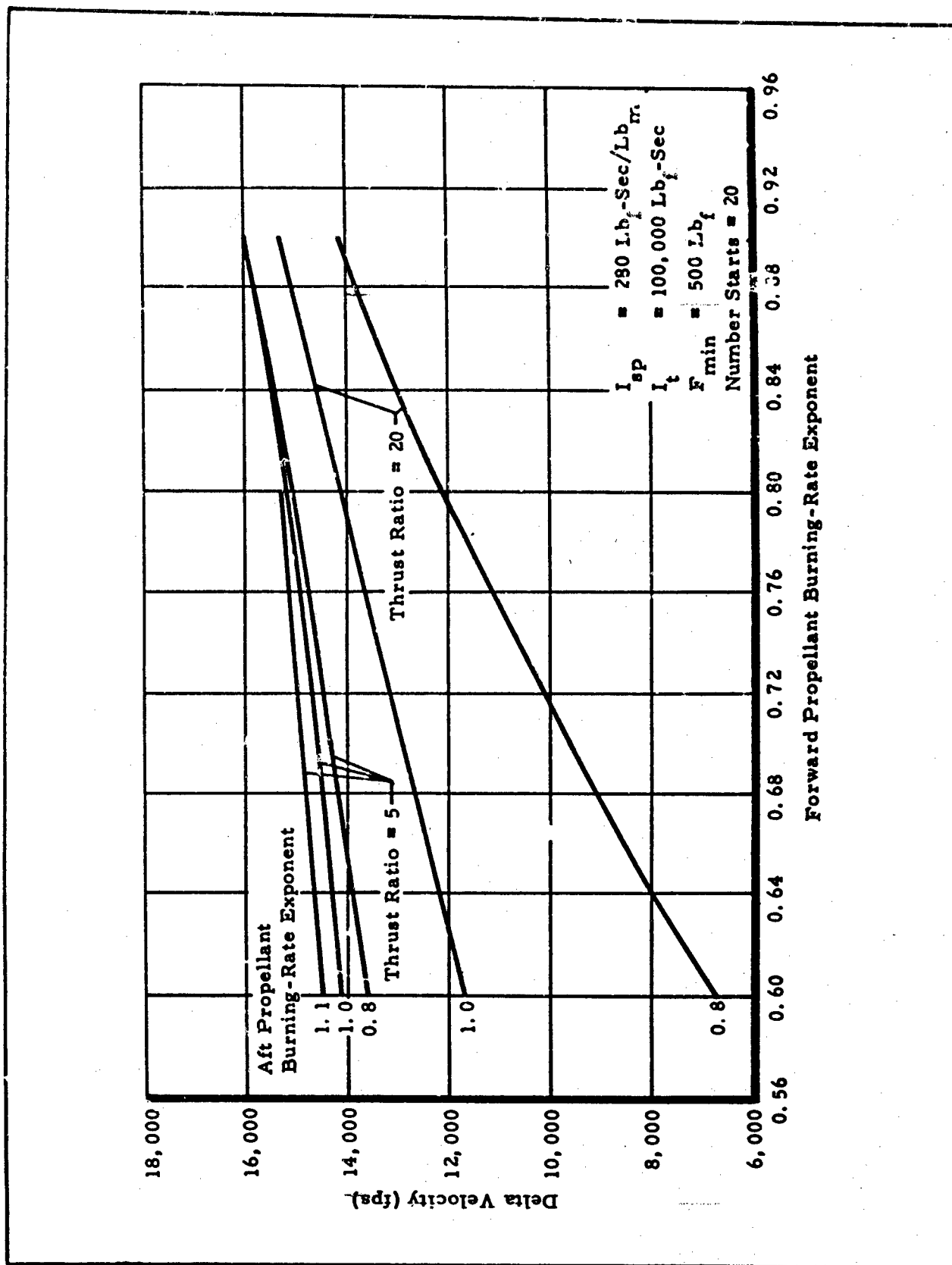


Figure 27 - Effect of Burning-Rate Pressure Exponents on Delta Velocity

CONFIDENTIAL

AFRPL-TR-65-209, Vol II

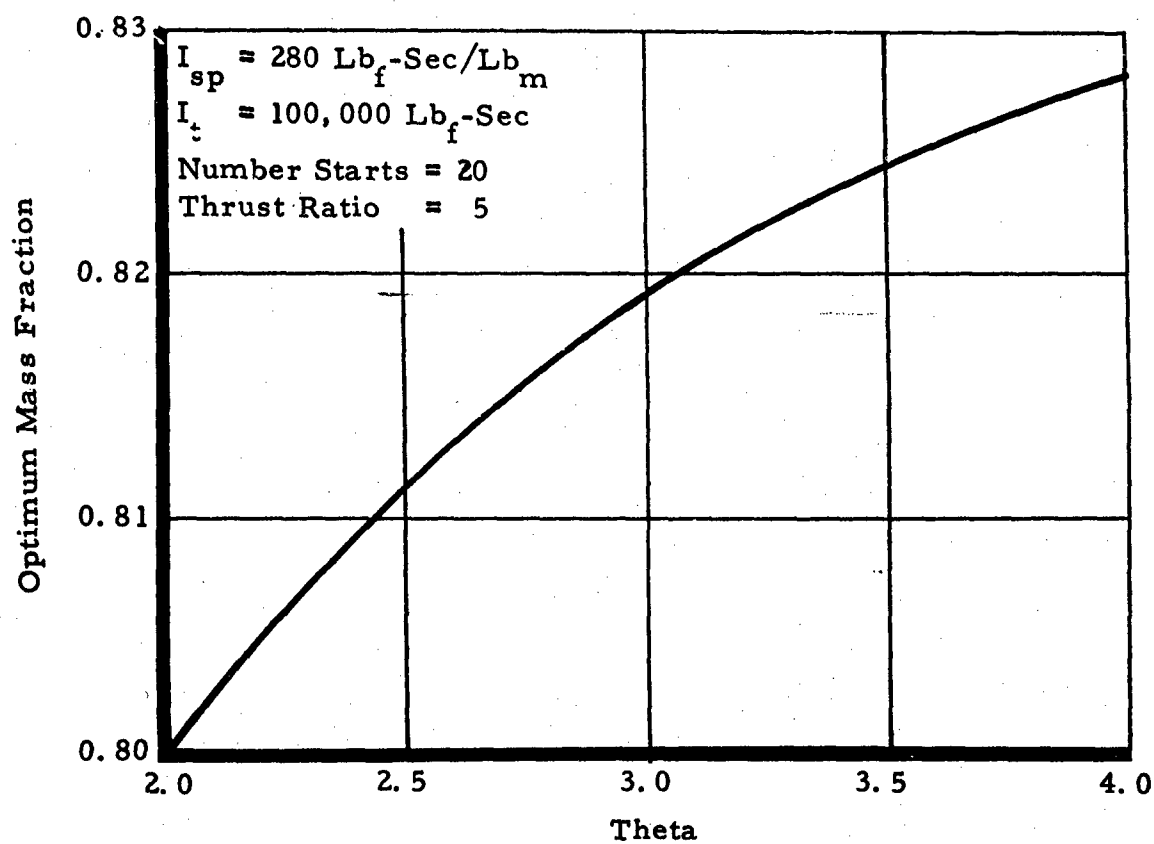


Figure 28 - Effect of θ on Mass Fraction

CONFIDENTIAL

CONFIDENTIAL

AFRPL-TR-65-209, Vol II

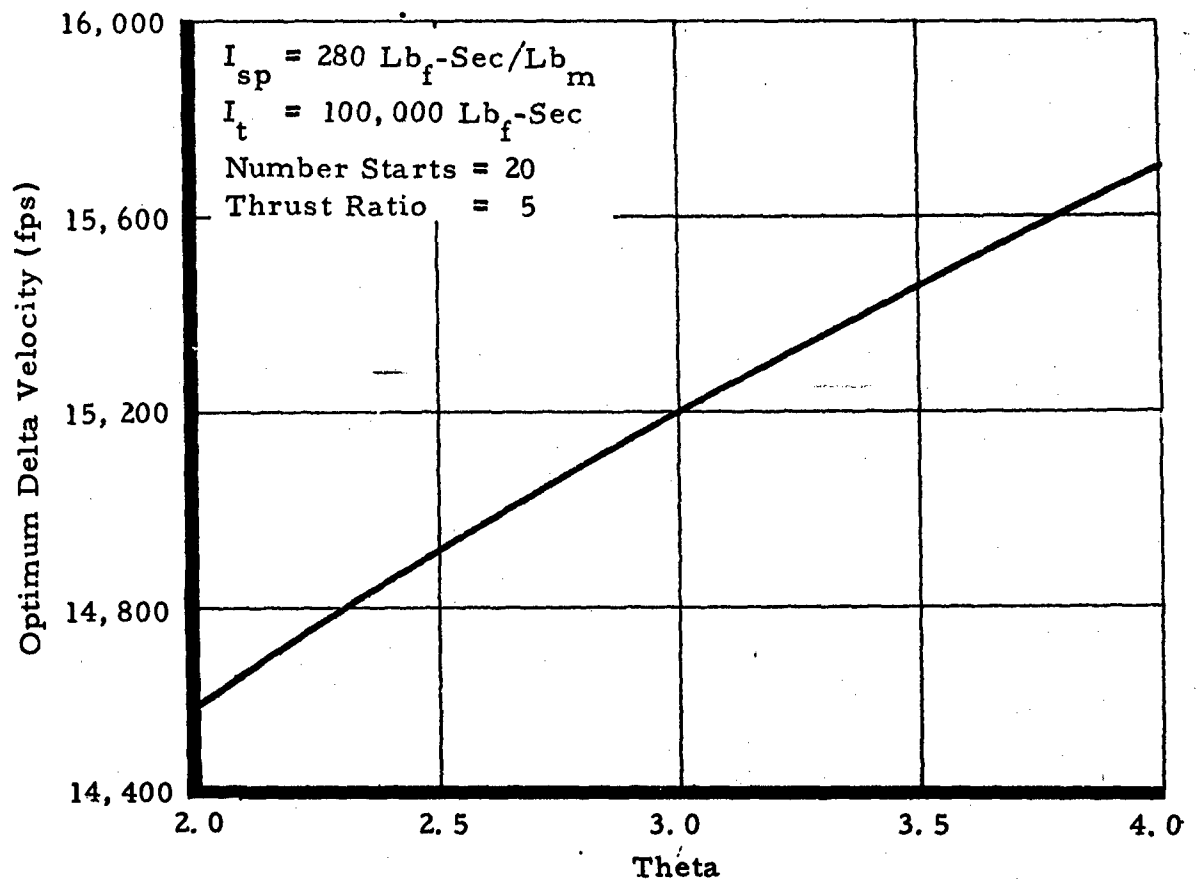


Figure 29 - Effect of θ on Delta Velocity

CONFIDENTIAL

SECTION IV - SUMMARY

Although the performance values for mass fraction, delta velocity, and envelope generated in this study are not intended to represent those that would be obtained from detailed designs, the values agree fairly well with those previously calculated in detail for individual motors.

It was found that, by increasing specific impulse, mass fraction is reduced but delta velocity and total motor weight are increased. For 10,000-lb-sec motors, an increase in specific impulse from 265 to 300 lb-sec/lb increased delta velocity by 7 percent, whereas for 1,000,000-lb-sec motors, the increase was 12 percent. (Confidential)

The mass fraction penalty imposed by a 20-to-1 thrust modulation was 2.5 percent for low-impulse (10,000 lb-sec), low-thrust (100 lb_f) motors. This penalty increased to above 4 percent as impulse increased to 1,000,000 lb-sec and thrust to 4,000 lb_f. These values were based on the characteristics of available propellants. Improved propellant pressure exponents would reduce the penalties. (Confidential)

For motors having stop-restart capability (that is, an on-off valve), the number of restarts available had little effect on mass fraction and delta velocity. The mass fraction penalty for additional igniters was less than 0.1 percent per restart.

At each impulse level, there was an optimum thrust range for throttleable motors which was close to the optimum thrust level for non-throttling motors. If the thrust was increased or decreased beyond this range, both mass fraction and delta velocity decreased.

Fiberglass and, to a lesser degree, titanium were found to be very advantageous for motor case materials, compared to steel, for motors with high thrust levels and high throttling requirements.

The highest forward propellant burning-rate constant and lowest aft propellant burning-rate constant investigated gave the highest mass fraction and delta velocity values for the 100,000-lb-sec motor size.

Mass fraction was more sensitive to forward and aft propellant pressure exponents than to any other propellant characteristics at high

throttling ratios. Aft propellant pressure exponent significantly affected mass fraction for motors with low forward exponents. However, with high forward exponents, the effect of the aft exponent was much less. Conversely, forward exponent change is less significant with high aft exponents. (Confidential)

Increasing the aft-to-forward grain weight flow ratio from 2 to 4, for the 100,000-lb-sec motor size, increased mass fraction from 0.80 to 0.83. (Confidential)

LIST OF REFERENCES

1. APR-7-1: Development of an Intermittent Operating Variable Thrust Solid Propellant Rocket Motor (U). (First Quarterly Report). Amcel Propulsion Company, Asheville, North Carolina, July 1962. (Confidential Report)
2. APR-7-2: Development of an Intermittent Operating Variable Thrust Solid Propellant Rocket Motor (U). (Second Quarterly Report). Amcel Propulsion Company, Asheville, North Carolina, October 1962. (Confidential Report)
3. APR-7-3: Development of an Intermittent Operating Variable Thrust Solid Propellant Rocket Motor (U). (Third Quarterly Report). Amcel Propulsion Company, Asheville, North Carolina, January 1963. (Confidential Report)
4. APR-7-4: Development of an Intermittent Operating Variable Thrust Solid Propellant Rocket Motor (U). (First Annual Report - Fiscal Year 1962). RPL-TDR-63-1061. Amcel Propulsion Company, Asheville, North Carolina, December 1963. (Confidential Report)
5. APR-21-1: Controllable Solid Propellant Rocket Motor (U). (First Quarterly Report). Amcel Propulsion Company, Asheville, North Carolina, June 1963. (Confidential Report)
6. APR-21-2: Controllable Solid Propellant Rocket Motor (U). (Second Quarterly Report). Amcel Propulsion Company, Asheville, North Carolina, September 1963. (Confidential Report)
7. APR-21-3: Controllable Solid Propellant Rocket Motor (U). (Third Quarterly Report). Amcel Propulsion Company, Asheville, North Carolina, December 1963. (Confidential Report)
8. APR-21-5: Dual-Chamber Controllable Solid Propellant Rocket Motor (U). (Fourth Quarterly Report). Amcel Propulsion Company, Asheville, North Carolina, May 1964. (Confidential Report)

LIST OF REFERENCES (CONT'D)

9. APR-21-6: Dual-Chamber Controllable Solid Propellant Rocket Motor (U). (Fifth Quarterly Report). Amcel Propulsion Company, Asheville, North Carolina, August 1964. (Confidential Report)
10. APR-21-7: Dual-Chamber Controllable Solid Propellant Rocket Motor (U). (Sixth Quarterly Report). Amcel Propulsion Company, Asheville, North Carolina, November 1964. (Confidential Report)
11. APR-21-8: Dual-Chamber Controllable Solid Propellant Rocket Motor (U). (Seventh Quarterly Report). Amcel Propulsion Company, Asheville, North Carolina, February 1965. (Confidential Report)
12. APR-21-9: Dual-Chamber Controllable Solid Propellant Rocket Motor (U). (Eighth Quarterly Report). Amcel Propulsion Company, Asheville, North Carolina, September 1965. (Confidential Report)
13. APR-21-4: Controllable Solid Propellant Rocket Motor (U). (Second Annual Report - Fiscal Year 1963). RPL-TDR-64-52. Amcel Propulsion Company, Asheville, North Carolina, September 1964. (Confidential)

APPENDIX A - COMPUTER PROGRAMS

A printout of the entire computer program is presented on the following pages. The program is arranged by subroutine in the sequence shown in Figure 1. The individual subroutines are shown in more detail in Figures 2, 3, 5, and 6, respectively.

AFRPL-TR-65-209, Vol II

```

-6600 C CSR STEADY STATE BALLISTIC PROGRAM, FOR PARAMETRIC STUDY
-6600 C DR. ALLEY M.K. OPPRECHT AUGUST 1964
-6600 C REVISION BY W. OSTERHOUT OCTOBER 1, 1964
-6600 C
-6600 C C(1) IS CODE 1 = CODE FOR OPERATION OF STEADY STATE PROGRAM
-6600 C C(2) IS CODE 2 = CODE FOR OPERATION OF GRAIN CONFIGURATION PROGRAM
-6600 C C(3) IS RHOF = FWD. PROP. DENSITY
-6600 C C(4) IS ALPF = FWD. PROP. BURN RATE CONSTANT
-6600 C C(5) IS ENPF = FWD. PROP. EXPONENT
-6600 C C(6) IS RHOA = AFT. PROP. DENSITY
-6600 C C(7) IS ALPA = AFT PROP. BURN RATE CONSTANT
-6600 C C(8) IS ENPA = AFT PROP. EXPONENT
-6600 C C(9) IS CDF = FWD. PROP. CD
-6600 C C(10) IS DELPF = DELTA FWD PRESSURE
-6600 C C(11) IS FMN = MINIMUM THRUST
-6600 C C(12) IS FMX = MAXIMUM THRUST
-6600 C C(13) IS PFMN = FWD CHAMBER MINIMUM PRESSURE
-6600 C C(14) IS THEPR = THETA PRIME
-6600 C C(15) IS PAMN = AFT CHAMBER MINIMUM PRESSURE
-6600 C C(16) IS XIPR = TOTAL IMPULSE AT THETA PRIME
-6600 C C(17) IS WF = FWD PROP WEIGHT
-6600 C C(18) IS ASF = FWD PROP AVERAGE SURFACE AREA
-6600 C C(19) IS PFMX = FWD CHAMBER MAXIMUM PRESSURE
-6600 C C(20) IS ASA = AFT PROP AVERAGE SURFACE AREA
-6600 C C(21) IS BLANK
-6600 C C(22) IS BLANK
-6600 C C(23) IS BLANK
-6600 C C(24) IS BLANK
-6600 C C(25) IS BLANK
-6600 C C(26) IS BLANK
-6600 C C(27) IS ATA = AFT THROAT AREA
-6600 C C(28) IS WEBF = FWD WEB THICKNESS
-6600 C C(29) IS WEBA = AFT WEB THICKNESS
-6600 C C(30) IS WA = AFT PROP WEIGHT
-6600 C C(31) IS TBMX = MAXIMUM WEB TIME
-6600 C C(32) IS PAMX = MAXIMUM AFT PRESSURE
-6600 C C(33) IS CD = CDD
-6600 C C(34) IS ATF = MAXIMUM OPERATING FWD THROAT AREA
-6600 C C(35) IS BLANK
-6600 18 FORMAT (11H THETA PRIME, F14.2)
-6652 19 FORMAT (11H AFT SURFACE, F14.2)
-6704 20 FORMAT (10H AFT THROAT, F16.3)
-6754 23 FORMAT (7H AFT WEB, F18.2)
-6798 24 FORMAT (13H AFT PROP. WT., F12.2)
-6854 25 FORMAT (11H FWD SURFACE, F14.2)
-6906 26 FORMAT (7H FWD WEB, F18.2)
-6950 27 FORMAT (13H FWD PROP. WT., F12.2)
-7006 28 FORMAT (12H MAX WEB TIME, F13.2)
-7060 51 FORMAT (7H FWD WEB, F18.2)
-7104 103 FORMAT (30H
-7198 30 FORMAT (/36H P FWD P AFT THETA THRUST)
-7300 31 FORMAT (/)
-7322 35 FORMAT (/13HPA GREATER PF)
-7378 43 FORMAT (F9.1, F9.1, F9.2, F9.1, F9.2, F9.0, F9.2, F9.4)
-7436 52 FORMAT (36X, 36H WT AFT IMPULSE WEB AFT AT FWD )
-7540 101 FORMAT (14)
-7562 102 FORMAT (3F20.10)

```

```

-7594 C
-7594 C SWITCH 1 OFF TO PUNCH C(1) THRU C(25)
-7594 C SWITCH 2 ON TO ACCEPT INPUT CHANGES ANYWHERE IN C(1) THRU C(25)
-7594 C SWITCH 3 ON STOPS ALL OUTPUT PRINTING EXCEPT SUMMARY LINE
-7594 C
-7594 DIMENSION THE(30),XISP(30),CD(30),C(35)
-7594 502 PRINT 21
-7594 READ 102
-7594 PRINT 103
-7594 PUNCH 103
-7594 KK=1
-7594 IF(SENSE SWITCH 2)512,510
-7594 510 PRINT 31
-7594 READ 101,N
-7594 DO 499 K=1,N
-7594 499 READ 102,THE(K),XISP(K),CD(K)
-7594 DO 501 J=1,35
-7594 READ 103,C(J)
-7594 IF(C(J))550,501,550
-7594 550 PRINT 103,C(J)
-7594 501 CONTINUE
-7594 GO TO 520
-7594 512 READ 103,X,HP
-7594 IF(X)511,520,511
-7594 511 PRINT 103,X,HP
-7594 C(HP)=X
-7594 GO TO 512
-7594 520 PRINT 31
-7594 S4=C(13)
-7594 S5=C(14)
-7594 S6=C(15)
-7594 HF=0
-7594 LL=C(1)
-7594 F1=C(11)
-7594 P1=C(13)
-7594 GO TO(10,11,21),LL
-7594 C 10=OPTION 1A
-7594 C 11=OPTION 1B
-7594 C 21=OPTION 11
-7594 10 C(20)=C(14)*C(3)*C(18)*C(4)*C(13)**C(5)/(C(6)*C(7)*C(15)**C(3))
-7594 GO TO 12
-7594 11 C(14)=C(6)*C(20)*C(7)*C(15)**C(8)/(C(3)*C(18)*C(4)*C(13)**C(5))
-7594 12 M=1
-7594 13 THE1=C(14)
-7594 K=1
-7594 14 IF(THE(K+1)-THE1)15,16,16
-7594 15 K=K+1
-7594 GO TO 14
-7594 16 RATIO=(THE1-THE(K))/(THE(K+1)-THE(K))
-7594 XISP0=XISP(K)+RATIO*(XISP(K+1)-XISP(K))
-7594 C(33)=CD(K)+RATIO*(CD(K+1)-CD(K))
-7594 GO TO(17,22,32),M
-7594 17 C(27)=(1.+C(14))*C(3)*C(18)*C(4)*C(13)**C(5)/(C(33)*C(15))
-7594 PRINT 19,C(14)
-7594 PRINT 19,C(20)
-7594 PRINT 20,C(27)
-7594 C(28)=C(17)/(C(3)*C(18))

```

```

-9832      PRINT 51,C(28)
-9906      GO TO 29
-9914      21 M=2
-9926      GO TO 13
-9934      22 C(17)=C(16)/(XISPO*(1.+C(14)))
-9994      C(30)=C(17)*C(14)
J0030      C(31)=C(16)/C(11)
J0066      C(28)=C(31)*(C(4)*C(13)**C(5))
J0126      C(29)=C(31)*(C(7)*C(15)**C(8))
J0136      C(18)=C(17)/(C(3)*C(28))
J0234      C(20)=C(30)/(C(6)*C(29))
J0282      C(27)=(1.+C(14))*C(3)*C(18)*C(4)*C(13)**C(5)/(C(33)*C(15))
J0450      PRINT 20,C(27)
J0474      PRINT 19,C(20)
J0498      PRINT 23,C(29)
J0522      PRINT 24,C(30)
J0546      PRINT 25,C(18)
J0570      PRINT 26,C(28)
J0594      PRINT 27,C(17)
J0618      PRINT 28,C(31)
J0642      29 PRINT 30
J0654      PRINT 52
J0666      PRINT 31
J0678      44 CON1=C(3)*C(18)*C(4)*C(13)**C(5)
J0774      32 CON3=C(6)*C(20)*C(7)*C(15)**C(8)
J0870      PACAL=(CON1+CON3)/(C(27)*C(33))
J0954      IF(PACAL-C(13))50,34,34
J1022      34 PRINT 35
J1034      GO TO 46
J1042      50 IF(PACAL-.998*C(15))49,36,48
J1134      48 IF(PACAL-1.002*C(15))36,36,49
J1226      49 C(15)=2.*PACAL-C(15)
J1274      GO TO 32
J1292      36 THECA=CON3/CON1
J1318      IF(THECA-.998*C(14))38,39,37
J1410      37 IF(THECA-1.002*C(14))39,39,38
J1502      38 C( )=0.5*(C(14)+THECA)
J1550      M=3
J1562      GO TO 13
J1570      39 F=XISPO*(CON1*(1.+THECA))
J1630      507 C(30)=C(17)*THECA
J1666      C(34)=CON1/(C(9)*C(13))
J1714      C(29)=C(28)*C(7)*PACAL**C(8)/(C(4)*C(13)**C(5))
J1858      XI=C(17)*(1.+THECA)*XISPO
J1918      GO TO(509,508),KK
J1994      509 GO TO(40,40,41),LL
J2074      C 40=OPTION I
J2074      C 41=OPTION II
J2074      40 IF(C(13)-C(19))42,42,46
J2142      41 IF(F-C(12))42,42,46
J2210      42 IF(SENSE SWITCH 3)513,514
J2230      514 PRINT 43,C(13),PACAL,THECA,F,C(30),XI,C(29),C(34)
J2338      513 IF(NF)1001,1002,1001
J2394      1002 S1=C(29)
J2406      S2=C(30)
J2418      S3=C(34)
J2430      NF=1

```

```

J2442 1001 F1=F
J2454 P1=PACAL
J2456 C(13)=C(13)+C(10)
J2502 GO TO 45
J2510 45 KK=2
J2522 C(32)=((C(12)-F1)/(F-F1))*(PACAL-P1)+P1
J2666 C(19)=(C(12)/XISPO)-C(6)*C(20)*C(7)*C(32)**C(3)
J2822 C(19)=(C(19)/(C(3)*C(18)*C(4)))*(1./C(5))
J2954 THECA=(C(6)*C(7)*C(20)*C(32)**C(8))/(C(3)*C(4)*C(18)*C(19)**C(5))
J3158 GO TO 507
J3166 508 PRINT 31
J3178 PRINT 43,C(19),C(32),THECA,C(12),C(30),X1,C(29),C(34)
J3286 C(29)=S1
J3298 C(30)=S2
J3310 C(34)=S3
J3322 C(13)=S4
J3334 C(14)=S5
J3346 C(15)=S6
J3358 506 PAUSE
J3370 IF(SENSE SWITCH 1)502,503
J3390 503 DO 504 J=1,35
J3402 504 PUNCH 102,C(J)
J3496 GO TO 502
J3494 END
PROCESSING COMPLETE
START

```

```

-6600 C GRAIN CONFIGURATION PROGRAM FOR CSR PARAMETRIC STUDY
-6600 C DR ALLEY H K OPPRECHT AUG 64
-6600 C REVISION BY W. OSTERHOUT
-6600 C DECEMBER 10, 1964
-6600 C PIDO FORTRAN PROGRAM
-6600 C C(18) IS FORWARD CHAMBER AVERAGE SURFACE, SQ IN ASF
-6600 C C(28) IS FORWARD CHAMBER WEB THICKNESS, IN WEDF
-6600 C C(27) IS AFT THROAT AREA, SQ IN ATA
-6600 C C(20) IS AFT AVERAGE SURFACE AREA, SQ IN ASA
-6600 C C(29) IS AFT WEB THICKNESS, IN WERA
-6600 1 FORMAT(30H ,F20.6,13)
-6694 2 FORMAT (F20.6)
-6716 3 FORMAT (/22H FWD GRAIN IS A CYL EB)
-6790 4 FORMAT(12H FWD PROP OD,F10.2)
-6844 5 FORMAT(13H FWD PROP LEN,F10.2)
-6900 6 FORMAT(13H FWD PROP L/D,F10.2)
-6956 7 FORMAT(/22H FWD GRAIN IS A SPH EB)
-7030 8 FORMAT(/22H FWD GRAIN IS A CYL CP)
-7104 9 FORMAT(18H FWD CHAM VOL LOAD,F10.4)
-7170 10 FORMAT(/22H FWD GRAIN IS A SPH CP)
-7244 11 FORMAT(/24H FWD GRAIN IS A CYL STAR)
-7322 12 FORMAT(/24H FWD GRAIN IS A SPH STAR)
-7400 13 FORMAT(/22H FWD GRAIN IS A CYL WW)
-7474 102 FORMAT(/19H AFT GRAIN IS AN EB)
-7542 103 FORMAT(14H AFT GRAIN DIA,F10.3)
-7600 104 FORMAT(14H AFT GRAIN LEN,F10.3)
-7658 105 FORMAT(19H AFT GRAIN VOL LOAD,F10.3)
-7726 106 FORMAT(15H AFT GRAIN PORT,F10.3)
-7736 107 FORMAT(/18H AFT GRAIN IS A CP)
-7852 103 FORMAT(25H AFT PORT TO THROAT RATIO,F10.3)
-7932 109 FORMAT(/20H AFT GRAIN IS A STAR)
-8002 110 FORMAT(/18H AFT GRAIN IS A WW)
-8068 111 FORMAT(/39H AFT GRAIN IS AN EB OUTSIDE OF FWD CHAM)
-8176 112 FORMAT(/39H AFT GRAIN IS A CP OUTSIDE OF FWD CHAM)
-8292 500 FORMAT (30H )
-8366 DIMENSION C(37)
-8366 C FORWARD CHAMBER CALCULATIONS OR PYROGEN CALCULATIONS
-8366 1002 READ 500,N
-8390 PUNCH 500,N
-8414 PRINT 500,N
-8438 CONTROL 102
-8450 DIAA=0.
-8462 XLODA=0.
-8474 CONTROL 102
-8486 DO 501 J=1,37
-8498 501 C(J)=0.
-8570 DO 21 K=1,35
-8582 21 READ 2,C(K)
-8656 J=1
-8678 L=1
-8690 DIAF=(C(18)/.7854)**.5

```

AFRPL-TR-65-209, Vol II

```

-3739      XLF=C(29)
-3750      XLDF=XLF/DIAF
-3775      IF(XLDF-.5)23,22,22
-3754      22 PRINT3
-3755      C(37)=2.
-3779      PRINT4,DIAF
-3902      PRINT5,XLF
-3926      PRINT6,XLDF
-3950      GO TO 45
-3953      23 IF(XLDF-.2)25,24,24
-3926      24 DIAF=((C(18)*C(28))/(.4199))**2*(1./2.)
-3956      VLF=.8
-3970      PRINT7
-3982      C(37)=3.
-3994      43 PRINT4,DIAF
-39213     PRINT9,VLF
-39242     XLDF=1.
-39254     GO TO 45
-39262     25 DIAF=C(28)/.35
-39298     M=1
-39310     26 DIAFS=DIAF*DIAF
-39346     VLF=(DIAFS-(DIAF-(2.*C(28))))**2./DIAFS
-39454     XLF=C(18)*C(28)/(.7854*VLF*DIAFS)
-39550     XLDF=XLF/DIAF
-39596     IF(XLDF-3.)29,27,27
-39654     27 GO TO (23,31),M
-39730     28 DIAF=C(28)/.3
-39766     M=2
-39778     GO TO 26
-39786     29 PRINT3
-39798     C(37)=1.
-39810     J=2
-39822     72 PRINT4,DIAF
-39846     PRINT5,XLF
-39870     PRINT6,XLDF
-39894     PRINT9,VLF
-39918     GO TO 45
-39926     31 DIAF=C(28)/.25
-39962     M=1
-39974     VLF=.85
-39998     32 XLF=(C(18)*C(28))/(.7854*VLF*DIAF*DIAF)
J0106     XLDF=XLF/DIAF
J0142     IF(XLDF-3.)35,33,33
J0210     33 GO TO (34,37),M
J0286     34 M=2
J0298     DIAF=C(28)/.2
J0334     VLF=.8
J0358     GO TO 32
J0366     35 PRINT11
J0378     C(37)=1.
J0390     J=3
J0402     GO TO 72
J0410     37 DIAF=C(28)/.15
J0446     38 XLF=C(18)*C(28)/(.7854*VLF*DIAF*DIAF)
J0554     XLDF=XLF/DIAF

```

```

J0590      IF(XLODF-3.)40,41,41
J0653      40 PRINT13
J0670      C(37)=1.
J0682      GO TO 72
J0690      41 GO TO (45,42,40),41
J0770      42 DIAF=C(28)/.1
J0806      M=3
J0818      VLF=.7
J0842      GO TO 38
J0850      C      AFT GRAIN DESIGN IF C(2)=1.
J0850      45 IF(C(2))51,73,51
J0906      73 GO TO (81,20),L
J0932      81 GO TO (20,502,502),J
J1062      502 DIAF=(C(18)*C(28)/.4186)**(1./3.)
J1182      VLF=.8
J1206      GO TO (20,74,77),J
J1286      74 IF(C(28)-.3*DIAF)75,75,20
J1378      75 PRINT 10
J1390      C(37)=1.
J1402      76 PRINT 4,DIAF
J1426      PRINT 9,VLF
J1450      XLODF=1.
J1462      L=2
J1474      IF(C(2))80,20,80
J1530      77 IF(C(28)-.2*DIAF)78,20,20
J1622      78 PRINT12
J1634      C(37)=1.
J1646      XLODF=1.
J1658      GO TO 76
J1666      51 CONTROL 102
J1678      CONTROL 102
J1690      80 IF(XLODF-3.)65,65,63
J1758      65 DIAA=((C(20)+2.*C(27))/.786)**.5
J1830      XLODA=C(29)/DIAA
J1866      IF(XLODA-.5)55,53,53
J1934      53 XLA=C(29)
J1946      APA=2.*C(27)
J1982      VLA=1.-APA/(DIAA*DIAA*.786)
J2066      PRINT102
J2078      C(36)=2.
J2090      54 PRINT103,DIAA
J2114      PRINT104,XLA
J2138      PRINT105,VLA
J2162      PRINT106,APA
J2186      GO TO 73
J2194      55 DIAA=DIAF
J2206      WFA=C(29)/DIAA
J2242      IF(WFA-.3)60,56,56
J2310      56 IF(WFA-.4)90,59,59
J2378      90 APA=(DIAA-2.*C(29))**2.*.786
J2462      IF(APA-2.*C(27))59,57,57
J2554      57 VLA=1.-APA/(DIAA*DIAA*.786)
J2638      XLA=C(29)*C(20)/(.786*DIAA*DIAA*VLA)
J2746      PTA=APA/C(27)
J2782      PRINT107

```


AFRPL-TR-65-209, Vol II

```

J2734      C(35)=1.
J2805      53 PRINT103,DIAA
J2830      PRINT104,XLA
J2854      PRINT105,VLA
J2878      PRINT108,PTA
J2902      GO TO 73
J2910      59 APA=2.*C(27)
J2946      DIAA=2.*C(29)+(APA/.786)**.5
J3042      VLA=1.-APA/(DIAA*DIAA*.786)
J3126      XLA=C(29)*C(20)/(.786*DIAA*DIAA*VLA)
J3234      PTA=2.0
J3246      PRINT107
J3258      C(36)=1.
J3270      GO TO 58
J3278      60 VLA=.85
J3302      69 APA=(1.-VLA)*DIAA*DIAA*.786
J3374      IF (APA-2.*C(27))70,71,71
J3466      70 VLA=VLA-.05
J3502      GO TO 69
J3510      71 XLA=C(20)*C(29)/(.786*DIAA*DIAA*VLA)
J3512      IF(VFA-.2)62,61,61
J3686      61 PRINT109
J3698      C(36)=1.
J3710      GO TO 54
J3718      62 PRINT110
J3730      C(36)=1.
J3742      GO TO 54
J3750      63 IF(C(29)-.6*XLF)64,66,66
J3842      64 IF(C(29)-.25*DIAF)68,65,65
J3934      66 APA=2.*C(27)
J3970      DIAA=.2+((C(20)+APA+.786*DIAF*DIAF)/.796)**.5
J4102      XLA=C(29)
J4114      VLA=C(20)/(C(20)+APA)
J4162      PRINT111
J4174      C(36)=3.
J4186      GO TO 54
J4194      68 APA=2.*C(27)
J4230      DIAA=2.*C(29)+((APA+.786*(2.*C(29)+DIAF+.2)**2.)/.786)**.5
J4398      CONI=.786*DIAA*DIAA-.786*(DIAF+.2)**2.-APA
J4542      VLA=CONI/(CONI+APA)
J4590      XLA=C(29)*C(20)/CONI
J4638      PRINT112
J4650      C(36)=4.
J4662      GO TO 54
J4670      C PUNCH OUTPUT UNLESS SENSE SWITCH 1 IS ON
J4670      20 IF(SENSE SWITCH 1)1002,1003
J4690      1003 C(22)=DIAF
J4702      C(23)=DIAA
J4714      C(24)=XL0DF
J4726      C(25)=XLA/DIAA
J4762      C(26)=C(2)
J4774      DO 1001 K=1,37
J4786      1001 PUNCH 1,C(K),K
J4882      PAUSE
J4894      GO TO 1002
J4902      END
PROCESSING COMPLETE
START

```

AFRPL-TR-65-209, Vol II

```

-6600 C   CSR COMBINED WEIGHTS ANALYSIS PROGRAM
-6600 C   PROGRAM 5017A 24 NOV 64 M A TODD
-6600     DIMENSION C(70)
-6600     DO 250 J=1,70
-6612     250 C(J)=0
-6708     10 READ 200,X,I
-6744     PUNCH 200,X,I
-6780     201 READ 200,X,I
-6816     IF(X-9999999.)204,17,17
-6884     204 C(I)=X
-6920     GO TO 201
-6928     17 MCAG=C(36)
-6964     RHOF = C(3)
-6976     ALPF = C(4)
-6988     ENPF = C(5)
-7000     RHOA=C(6)
-7012     ALPA=C(7)
-7024     ENPA=C(8)
-7036     PAMH=C(15)
-7048     XIPR = C(16)
-7060     WF=C(17)
-7072     ASF = C(18)
-7084     PFMX=C(19)
-7096     ASA=C(20)
-7108     DIAF=C(22)
-7120     DIAA=C(23)
-7132     CHBNU = C(26)+1.
-7168     ATA=C(27)
-7180     WA=C(30)
-7192     TBMX=C(31)
-7204     PAMX=C(32)
-7216     ATF=C(34)
-7228     MCFG=C(37)
-7264     ROCHF=C(38)
-7276     ERATA=C(39)
-7288     SDCHA=C(40)
-7300     ROCHA=C(41)
-7312     ROINF=C(42)
-7324     ROINA=C(43)
-7336     CD=C(44)
-7348     WMIG=C(45)
-7360     GSIG=C(46)
-7372     FLTP1=C(47)
-7384     CPF=C(48)
-7396     THCOF=C(49)
-7408     WMFG=C(50)
-7420     TEMF=C(51)
-7432     CONIG=C(52)
-7444     XMFIG=C(53)
-7456     ENIG=C(54)
-7468     SFIG=C(55)
-7480     SDNTH=C(56)
-7492     SDNST=C(57)
-7504     SDNXN=C(58)
-7516     EXPRI=C(59)

```

```

-7523      TEMA=C(50)
-7540      THCOA=C(52)
-7552      ERATE=C(53)
-7564      SDCHF=C(54)
-7576      PRCON=C(55)
-7588      CPA=C(56)
-7600      WMAG =C(57)
-7612      IF(C(25)-1.)31,31,32
-7680      31 ELODA=0.
-7592      ERATA=1.0000001
-7704      GO TO 33
-7712      32 ELODA=C(25)-(ERATA-1.)/2.
-7784      33 IF(C(24)-1.)34,34,35
-7852      34 ELODF=0.
-7864      ERATF=1.0000001
-7876      GO TO 39
-7884      35 ELODF=C(24)-(ERATF-1.)/2.
-7956      39 RDCHF=DIAF/2.
-7992      RDCHA=DIAA/2.
-8028      4 RAD=(1.-(1./ERATA)**2.):**.5
-8112      WCX = (RDCHA/ERATA)**2./2.*RAD)
-8184      IF(ERATA-2.5) 46,46,45
-8252      46 AFCL = (WCX*LOG((1.+RAD)/(1.-RAD))+RDCHA**2.)*3.14159
-8420      TFCL=(PAMX*RDCHA)/(1.414*SDCHA*ROCHA)
-8516      GO TO 47
-8524      45 TFCL=RDCHA*((3.*PAMX)/4.*SDCHA*ROCHA)**.5
-8620      AFCL = 3.14159*(RDCHA)**2.
-8652      47 IF(TFCL-.025)43,44,44
-8736      43 TFCL=.025
-8760      44 WFCL=AFCL*TFCL*ROCHA
-8808      ACYL = 12.566*RDCHA*RDCHA*ELODA
-8868      TCYL=(PAMX*RDCHA/SDCHA*ROCHA)
-8928      IF(TCYL-.025)41,42,42
-8996      41 TCYL=.025
-9020      42 WCYL=ACYL*TCYL*ROCHA
-9068      WACL=(AFCL-2.*ATA)*TFCL*ROCHA
-9152      WCHBT=WFCL+WACL+WCYL
-9200      TINS=.007*TBHX*(((TEMA+460.)/5806.):**.1)+.05
-9320      WINFC=AFCL*TINS*ROINA
-9368      VINAC=(AFCL-2.*ATA)*TINS*ROINA
-9452      WINCY=ACYL*TINS*ROINA
-9500      C
-9500      IF(CHBIII-2.)209,8,8
-9568      8 F AD=(1.-(1./ERATF)**2.):**.5
-9652      WFCX=((RDCHF/ERATF)**2./2.*F AD)
-9724      IF(ERATF-2.5) 460,460,450
-9792      460 FAFCL=(WFCX*LOG((1.+F AD)/(1.-F AD))+RDCHF**2.)*3.14159
-9960      FTFCL=(PFMX*RDCHF)/(1.414*SDCHF*ROCHF)
J0056      GO TO 470
J0064      450 FTFCL=RDCHF*((3.*PFMX)/4.*SDCHF*ROCHF)**.5
J0160      FAFCL = 3.14159*(RDCHF)**2.
J0208      470 IF(FTFCL-.025)430,440,440
J0276      430 FTFCL=.025
J0300      440 FWFCL=FAFCL*FTFCL*ROCHF
J0343      FACYL = 12.566*RDCHF*RDCHF*ELODF

```

AFRPL-TR-65-209, Vol II.

```

J0408      FTCYL=(PFMX*RDCHF)/(SDCHF*ROCHF)
J0492      IF(FTCYL-.025)410,420,420
J0560      410 FTCYL=.025
J0584      420 FWCYL=FACYL*FTCYL*ROCHF
J0632      FWACL=(FAFCL-2.*ATF)*FTFCL*ROCHF
J0716      FCHBT=FWFCL+FWACL+FWCYL
J0764      FTINS=.007*TBMX*((TEMF+460.)/5806.):**4.+.05
J0834      FINFC=FAFCL*FTINS*ROINF
J0932      FINAC=(FAFCL-2.*ATF)*FTINS*ROINF
J1016      FINCY=FACYL*FTINS*ROINF
J1064      C
J1064      GO TO(210,211,212),MCFG
J1144      C
J1144      210 FWD GRAIN IS A CYL OR SPH CP, STAR, WAGONWHEEL
J1144      FWINS=FINAC+FINFC
J1180      GO TO 209
J1188      C
J1188      211 FWD GRAIN IS A CYL END BURNER
J1188      FWINS=FINAC+(FINCY/2.)
J1236      GO TO 209
J1244      C
J1244      212 FWD GRAIN IS A SPH END BURNER
J1244      FWINS=FINAC+(FINFC/2.)
J1292      C
J1292      209 GO TO(205,206,207,208),MCAG
J1376      C
J1376      205 AFT GRAIN IS A CP, STAR, OR WAGONWHEEL
J1376      WINS=WINFC+WINAC
J1412      GO TO 100
J1420      C
J1420      206 AFT GRAIN IS AN END BURNER
J1420      WINS=WINAC+(WINCY/2.)
J1468      GO TO 100
J1476      C
J1476      207 AFT GRAIN IS AN END BURNER OUTSIDE OF FORWARD CHAMBER
J1476      WINS=WINFC+WINAC+(WINCY/2.)*FINAC+(FINCY/2.)
J1620      GO TO 100
J1628      C
J1628      208 AFT GRAIN IS A CP OUTSIDE OF FORWARD CHAMBER
J1628      WINS=WINFC+WINAC+FINAC+FINFC
J1688      100 WCASE=WCHBT+FCHBT
J1724      WINSL=WINS+FWINS
J1760      WIGT = 0.0
J1772      WIGP = 0.0
J1784      WIG = 0.0
J1796      C
J1796      PUNCH501,SDNST,SDNTH,SDNXN,SDCHA,SDCHF,XIPR
J1796      PUNCH 502,TEMA,TEMF,PAMX,PFMX,PAMN
J1952      PUNCH503,ÉLODA,ÉLODF,ERATA,ERATF,DIAA,DIAF
J2036      PUNCH 504,CHBNÜ,PRCON,WA,Wf,TBMX,EXPRN
J2120      PUNCH 505,ATA,ATF,ASA,ASF,ROINA,ROINF
J2204      PUNCH 506,FLTPI,WMAG,WMFG,ALPA,ALPF
J2276      PUNCH 507,SFIG,WMIG,ENIG,GSIG,CONIG,XMFIG
J2360      PUNCH 508,ENPA,ENPF,CPA,CPF,THCOA,THCOF
J2444      PUNCH 509,WIGT,WIGP,WIG,RHOA,RHOF,CD
J2528      PUNCH 510,WINSL,WINFC,WINAC,WINCY,WINS,MCFG
J2612      PUNCH 511,FINFC,FINAC,FINCY,FWINS
J2672      PUNCH 512,WCASE,WFCL,WACL,WCYL,WCHBT,MCAG
J2756      PUNCH 513,FWFCL,FWACL,FWCYL,FCHBT
J2816      PUNCH 514,TCYL,TINS,FTCYL,FTINS,ROCHA,ROCHF
J2900      200 FORMAT(30H
J2994      501 FORMAT(4H 100,6F11.0)

```

AFRPL-TR-65-209, Vol II

```
J3056 502 FORMAT(4H 200,6F11.4)
J3118 503 FORMAT(4H 300,6F11.5)
J3130 504 FORMAT(4H 400,6F11.3)
J3242 505 FORMAT(4H 500,6F11.3)
J3304 506 FORMAT(4H 600,6F11.5)
J3366 507 FORMAT(4H 700,6F11.4)
J3428 508 FORMAT(4H 800,6F11.8)
J3490 509 FORMAT(4H 900,6F11.5)
J3552 510 FORMAT(4H1000,5F11.3,111)
J3614 511 FORMAT(4H1100,6F11.3)
J3676 512 FORMAT(4H1200,5F11.3,111)
J3738 513 FORMAT(4H1300,6F11.3)
J3800 514 FORMAT(4H1400,6F11.4)
J3862 GO TO 10
J3970 END
PROCESSING COMPLETE
START
```

```

-6600 C CSR COMBINED WEIGHTS ANALYSIS PROGRAM
-6600 C PROGRAM 5017B 27 OCT 64 M A TODD
-6600 DIMENSION C(31)
-6600 10 DO 250 J=1,31
-6612 250 C(J)=0
-6703 READ 200,X
-6732 PRINT 200,X
-6756 READ 501,SDNST,SDNTH,SDNXN,SDCHA,SDCHF,XIPR
-6840 READ 502,TEMA,TEMF,PAMX,PFMX,PAMN
-6912 READ 503,EL0DA,EL0DF,ERATA,ERATF,DIAA,DIAF
-6996 READ 504,CHBNH,PRCON,WA,WF,TBMX,EXPRH
-7080 READ 505,ATA,ATF,ASA,ASF,ROINA,ROINF
-7164 READ 506,FLTPI,WMAG,WMFG,ALPA,ALPF
-7236 READ 507,SFIG,WMIG,ENIG,GSIG,CONIG,XMFIG
-7320 READ 508,ENPA,ENPF,CPA,CPF,THCOA,THCOF
-7404 READ 509,WIGT,WIGP,WIG,RHOA,RHOF,CD
-7488 READ 510,WINSL,WINFC,WINAC,WINCY,WINS,MCFG
-7572 READ 511,FINEC,FINAC,FINCY,FWINS
-7632 READ 512,WCASE,WFCCL,WACL,WCYL,WCHBT,MACG
-7716 READ 513,FWFCL,FWACL,FWCYL,FCHBT
-7776 READ 514,TCYL,TINS,FTCYL,FTINS,ROCHA,ROCHF
-7860 RDCHA = DIAA/2.
-7896 RDCHF = DIAF/2.
-7932 IF(CHBNH-2.)7,9,19
-8000 C VALVE WEIGHT CALCULATION
-8000 C VFREE=C(1),DTH1=C(2),DTH2=C(3),DTH3=C(4),PLINS=C(5)
-8000 C COVIN=C(6),TUBIN=C(7),PISIN=C(8),TOINS,C(9),PISTH=C(10)
-8000 C PINT=C(11),COVE=C(12),PIST=C(13),CYL=C(14),DUCT=C(15)
-8000 C STRUT=C(16),PLIN=C(17),POWPK=C(18),SERVO=C(19),VALVE=C(20)
-8000 19 C(1)=6.283*(RDCHF*...)*(EL0DF+2./(3.*ERATF))
-8120 5 C(2)=(ATF/.7856)**.5
-8168 C(3)=C(2)**2.
-8204 C(4)=C(2)**3.
-8240 IF(TBMX-9.)20,21,21
-8308 20 C(5)=.0225*C(3)
-8344 C(6)=.02097*C(3)
-8380 C(7)=.0476*C(3)
-8416 C(8)=.0146*C(3)
-8452 GO TO 22
-8460 21 C(5) =.0025*C(3)*TBMX
-8508 C(6) =.00233*C(3)*TBMX
-8556 C(7) =.0053*C(3)*TBMX
-8604 C(8) =.00162*C(3)*TBMX
-8652 22 C(9)=C(5)+C(6)+C(7)+C(8)
-8712 IF(C(2)-.68)23,24,24
-8790 23 C(10)=(.022*C(3))+(.0000294*C(3)*(PFMX**.5))
-8912 GO TO 25
-8920 24 C(10)=(.022*C(3))+(.0000581*C(4)*(PFMX**.5))
-9052 25 IF(C(2)-1.07)26,27,27
-9120 26 C(11)=.0302*C(3)
-9156 GO TO 28
-9164 27 C(11)=.0282*C(4)
-9200 28 IF(C(2)-2.38)29,30,30
-9268 29 C(12)=(.0931*C(3))+(.0575*C(4))
-9352 GO TO 31

```

AFRPL-TR-65-209, Vol II

```

-9360      30 C(12)=.0966*C(4)
-9396      31 IF(C(2)-2.67)32,33,33
-9454      32 C(13)=.0403*C(3)
-9500      GO TO 34
-9508      33 C(13)=(.022*C(3))+(.00676*C(4))
-9592      34 IF(C(2)-2.9)35,36,36
-9660      35 C(14)=(.00792*C(3))+(.027*C(4))
-9744      GO TO 37
-9752      36 C(14)=.0297*C(4)
-9788      37 IF(C(2)-1.07)38,39,39
-9856      38 C(15)=.0602*C(3)
-9892      GO TO 40
-9900      39 C(15)=.00563*C(4)
-9936      40 C(16)=(.000301*C(4))*(PFMX** .666))
J0020      C(17)=(.00939*C(4))*((PFMX-PAMX)**.5))
J0116      C(18)=.33*C(4)
J0152      C(19)=(.59*C(4))+.9
J0200      C(31)=C(9)+C(10)+C(11)+C(12)+C(13)+C(14)+C(15)+C(16)+C(17)
J0320      C(20)=C(31)+C(18)+C(19)
J0358      AS=ASF
J0380      RHO=RHO
J0392      TEM=TEM
J0404      ENP=ENPF
J0416      CP=CPF
J0428      ALP=ALPF
J0440      THCO=THCOF
J0452      WMG=WMFG
J0464      GO TO 100
J0472      C      7      100      IGNITER WEIGHT CALCULATION
J0472      7      PRINT 70
J0484      C(1)=6.283*(RDCHA**3.)*(ELODA+2./(3.*ERATA))
J0604      AS=ASA
J0616      RHO=RHOA
J0628      TEM=TEMA
J0640      ENP=ENPA
J0652      CP=CPA
J0664      ALP=ALPA
J0676      THCO=THCOA
J0688      WMG=WMAG
J0700      100      CON1=AS *RHO *TEM *18550./((C(1) *WM G)
J0808      CON2=(CON1*2.*THCO *ENP )/(CP *ALP *RHO )
J0928      PSTAR = (CONIG*CON2)**(1./(1.+ENP))
J1048      WIGP=(WMIG*PSTAR*C(1) )/(GSIG*FLTPI*18550.)*SFIG.
J1168      WIG=WIGP/XMFIG
J1204      WIGT=WIG*ENIG
J1240      C      NOZZLE WEIGHT CALCULATION
J1240      C      WNST=C(21),SDST=C(22),WNSTR=C(23),WNTH=C(24),SDTH=C(25)
J1240      C      WNHT=C(26),WNXI=C(27),SDXN=C(28),WNXIN=C(29),WNOZ=C(30)
J1240      C(21)=((104.+(9.65*EXPRN))*(ATA)**1.5)*PAMX/1000000.
J1360      C(22)=773000./SDNST
J1396      C(23)=C(21)*C(22)
J1432      C(24)=1.53*ATA** .9
J1480      C(25)=128900./SDNTH
J1516      C(26)=C(24)*C(25)
J1552      C(27)=.00219*ATA*(EXPRN-4.)*TBMX*(1./CD)**1.7*PAMX** .9/1000000.

```

AFRPL-TR-65-209, Vol II

```

J1769      C(28)=40000./SDMXN
J1704      C(29)=C(27)*C(29)
J1760      C(30)=C(23)+C(26)+C(29)
J1938      C  COMPONENT LENGTH CALCULATION
J1938      FWDLT=2.*RDCHF*((ELODF*ERATF+1.)/ERATF)
J1936      AFTLT=2.*RDCHA*((ELODA*ERATA+1.)/ERATA)
J2104      XNOLT=((ATA/3.14159)**.5*((EXPRN)**.5-1.))/3.153
J2224      C  MOTOR WEIGHT, MASS FRACTION, AND DELTA VELOCITY CALCULATION
J2224      WCHR=WCASE+WINSL
J2260      WINRT=(WCHR+C(20)+WIGT+C(30))*1.02
J2332      WPROP=WA+WF
J2368      XMFRG=(WA+WF)/(WPROP+WINRT)
J2452      DELV=(32.174)*(XIPR/WPROP)*LOG((WINRT+WPROP)/(WINRT))
J2572      WMTR=WINRT+WPROP
J2608      C  IF GRAIN CONFIG IS TANDEM ADD ALL LENGTHS. IF GRAIN CONFIG IS
J2608      C  PARALLEL CHECK FOR LONGER OF FWD AND AFT CHAMBERS AND ADD NOZZLE
J2608      IF(MCAG-3)300,301,301
J2676      300 RLGT=FWDLT+AFTLT+XNOLT
J2724      GO TO 304
J2732      301 IF(FWDLT-AFTLT)302,302,303
J2800      302 RLGT=AFTLT+XNOLT
J2836      GO TO 304
J2944      303 RLGT=FWDLT+XNOLT
J2880      304 IF(RDCHF-RDCHA)305,305,306
J2948      305 RDIA=2.*RDCHA+2.*TCYL+2.*TINS
J3080      GO TO 307
J3088      306 RDIA=2.*(RDCHF+FTCYL+FTINS)
J3148      307 ELODM=RLGT/RDIA
J3184      IF(SENSE SWITCH 1)309,309
J3204      309 IF(SENSE SWITCH 2)311,311
J3224      311 PRINT 511,C(1),CON1,PSTAR,FWDLT,AFTLT,XNOLT
J3308      310 PRINT501,SDNST,SDNTH,SDMXN,SDCHA,SDCHF,XIPR
J3332      PRINT 502,TEMA,TEMF,PAMX,PFMX,PAMH
J3464      PRINT503,ELODA,ELODF,ERATA,ERATF,DIAA,DIAF
J3548      PRINT 504,CHBNH,PRCON,WA,WF,TBMX,EXPRN
J3632      PRINT 505,ATA,ATF,ASA,ASF,ROINA,ROINF
J3716      PRINT 506,FLTPI,WMAG,WMFG,ALPA,ALPF
J3788      PRINT 507,SFIG,VMIG,ENIG,GSIG,CONIG,XMFIG
J3872      PRINT 508,ENPA,ENPF,CPA,CPF,THCOA,THCOF
J3956      PRINT 509,WIGT,WIGP,WIG,RHOA,RHOF,CD
J4040      PRINT 510,WINSL,WINF,WINAC,WINCY,WINS,HCFG
J4124      PRINT 511,FINF,FINAC,FINCY,FWINS
J4184      PRINT 512,WCASE,WFCL,WACL,WCYL,WCHBT,MCAG
J4268      PRINT 513,FWFCL,FWACL,FWCYL,FCHBT
J4328      PRINT 514,TCYL,TINS,FTCYL,FTINS,ROCHA,ROCHF
J4412      PRINT 515,C(20),C(9),C(10),C(13),C(11),C(12)
J4496      PRINT 516,C(19),C(18),C(17),C(16),C(15),C(14)
J4580      PRINT 517,C(30),C(23),C(26),C(29),EXPRN
J4652      309 PRINT 518,WMTR,RDIA,RLGT,XMFRG,DELV,ELODM
J4736      PUNCH 200,XMFRG,DELV,RLGT,RDIA
J4796      70 FORMAT(28H SINGLE CHAMBER MOTOR FOLLOWS)
J4876      200 FORMAT(30H ,F11.3,F11.0,2F11.2)
J4980      501 FORMAT(4H 100,6F11.0)
J5042      502 FORMAT(4H 200,6F11.4)
J5104      503 FORMAT(4H 300,6F11.5)

```


AFRPL-TR-65-209, Vol II

```
J5166 504 FORMAT(4H 400,6F11.3)
J5223 505 FORMAT(4H 500,6F11.3)
J5290 506 FORMAT(4H 600,6F11.5)
J5352 507 FORMAT(4H 700,6F11.4)
J5414 508 FORMAT(4H 800,6F11.8)
J5476 509 FORMAT(4H 900,6F11.5)
J5538 510 FORMAT(4H1000,5F11.3,111)
J5600 511 FORMAT(4H1100,6F11.3)
J5662 512 FORMAT(4H1200,5F11.3,111)
J5724 513 FORMAT(4H1300,6F11.3)
J5786 514 FORMAT(4H1400,6F11.4)
J5848 515 FORMAT(4H1500,6F11.4)
J5910 516 FORMAT(4H1600,6F11.4)
J5972 517 FORMAT(4H1700,6F11.4)
J6034 518 FORMAT(4H1800,6F11.4)
J6096 CONTROL 102
J6108 GO TO 10
J6116 END
PROCESSING COMPLETE
START
```

APPENDIX B - PRESENTATION OF DATA

A detailed presentation of data from this study is given herein in Figures B-1 through B-66. For ease of reference, the figures are presented by phase, and are arranged in sequence. Figures B-1 through B-30 present the results from Phase I; the remaining figures are for Phase II.

The plots for Phase I are presented in the following sequence:

- Mass fraction versus minimum thrust at an I_{sp} of 265 $\text{lb}_f\text{-sec}/\text{lb}_m$ for 1, 10, and 20 starts (Figures B-1, B-2, and B-3, respectively); at an I_{sp} of 280 $\text{lb}_f\text{-sec}/\text{lb}_m$ for 1, 10, and 20 starts (Figures B-4, B-5, and B-6, respectively); and at an I_{sp} of 300 $\text{lb}_f\text{-sec}/\text{lb}_m$ for 1, 10, and 20 starts (Figures B-7, B-8, and B-9). For each plot, curves are shown for total impulse values of 10^4 , 10^5 , and 10^6 $\text{lb}_f\text{-sec}$ at constant thrust ratios of 1, 5, and 20.
- Mass fraction versus total impulse for burn times of 20, 50, 200, and 500 sec (Figures B-10 through B-13, respectively). All curves are for 10 starts and constant specific impulse of 280 $\text{lb}_f\text{-sec}/\text{lb}_m$.
- Delta velocity versus minimum thrust at an I_{sp} of 265 $\text{lb}_f\text{-sec}/\text{lb}_m$ for 1, 10, and 20 starts (Figures B-14, B-15, and B-16, respectively); at an I_{sp} of 280 $\text{lb}_f\text{-sec}/\text{lb}_m$ for 1, 10, and 20 starts (Figures B-17, B-18, and B-19, respectively); and at an I_{sp} of 300 $\text{lb}_f\text{-sec}/\text{lb}_m$ for 1, 10, and 20 starts (Figures B-20, B-21, and B-22, respectively). For each plot, curves are shown for total impulse values of 10^4 , 10^5 , and 10^6 $\text{lb}_f\text{-sec}$ at constant thrust ratios of 1, 5, and 20.
- Delta velocity versus total impulse for burn times of 20, 50, 200, and 500 sec (Figures B-23 through B-26, respectively). All curves are for 10 starts and constant specific impulse of 280 $\text{lb}_f\text{-sec}/\text{lb}_m$.

- Length versus minimum thrust for I_{sp} of 265 and 300 $\text{lb}_f\text{-sec}/\text{lb}_m$ (Figures B-27 and B-28, respectively). Curves of constant configuration are shown on each plot.
- Diameter versus minimum thrust for I_{sp} of 265 and 300 $\text{lb}_f\text{-sec}/\text{lb}_m$ (Figures B-29 and B-30, respectively). Curves of constant configuration and constant total impulse values (10^4 , 10^5 , 5×10^5 , and 10^6 $\text{lb}_f\text{-sec}$) are shown on each plot.

(Confidential)

The plots for Phase II are arranged as follows:

- Mass fraction versus minimum thrust at thrust ratios of 1, 5, and 20 (Figures B-31, B-32, and B-33, respectively). Curves for three materials are shown on each plot.
- Delta velocity versus minimum thrust at thrust ratios of 1, 5, and 20 (Figures B-34, B-35, and B-36, respectively). Curves for three materials are shown on each plot.
- Mass fraction versus minimum thrust for aft propellant burning-rate constants of 0.0002, 0.0004, and 0.0010 (Figures B-37, B-38, and B-39, respectively). Curves for constant forward propellant burning rates of 0.002, 0.0008, and 0.0032 are shown on each plot.
- Delta velocity versus minimum thrust for aft propellant burning-rate constants of 0.0002, 0.0004, and 0.0010 (Figures B-40, B-41, and B-42, respectively). Curves for constant forward propellant burning rates of 0.0002, 0.0008, and 0.0032 are shown on each plot.
- Length versus aft propellant burning-rate constant at minimum thrust values of 200, 500, 1000, and 5000 lb_f (Figures B-43 through B-46, respectively). Curves for constant forward propellant burning rates of 0.0002, 0.0008, and 0.0032 are shown on each plot.
- Diameter versus aft propellant burning-rate constant at minimum thrust values of 200, 500, 1000, and 5000 lb_f (Figures B-47, through B-50, respectively). Curves for constant forward propellant burning rates of 0.0002, 0.0008, and 0.0032 are shown on each plot.

CONFIDENTIAL

- Mass fraction versus thrust ratio at forward propellant burning-rate exponents of 0.6, 0.8, and 0.9 (Figures B-51, B-52, and B-53, respectively). Curves for constant aft propellant burning rate exponents of 0.8, 1.0, and 1.1 are shown on each plot.
- Delta velocity versus thrust ratio at forward propellant burning-rate exponents of 0.6, 0.8, and 0.9 (Figures B-54, B-55, and B-56, respectively). Curves for constant aft propellant burning-rate exponents of 0.8, 1.0, and 1.1 are shown on each plot.
- Length versus thrust ratio at forward propellant burning-rate exponents of 0.6, 0.8, and 0.9 (Figures B-57, B-58, and B-59, respectively). Curves for constant aft propellant burning-rate exponents of 0.8, 1.0, and 1.1 are shown on each plot.
- Diameter versus thrust ratio at forward propellant burning-rate exponents of 0.6, 0.8, and 0.9 (Figures B-60, B-61, and B-62, respectively). Curves for constant aft propellant burning-rate exponents of 0.8, 1.0, and 1.1 are shown on each plot.
- Mass fraction versus minimum thrust (Figure B-63). Curves for constant theta values of 2, 3, and 4 are shown.
- Delta velocity versus minimum thrust (Figure B-64). Curves for constant theta values of 2, 3, and 4 are shown.
- Length versus minimum thrust (Figure B-65). Curves for constant theta values of 2, 3, and 4 are shown.
- Diameter versus minimum thrust (Figure B-66). Curves for constant theta values of 2, 3, and 4 are shown.

(Confidential)

CONFIDENTIAL

CONFIDENTIAL

AFRPL-TR-65-209, Vol II

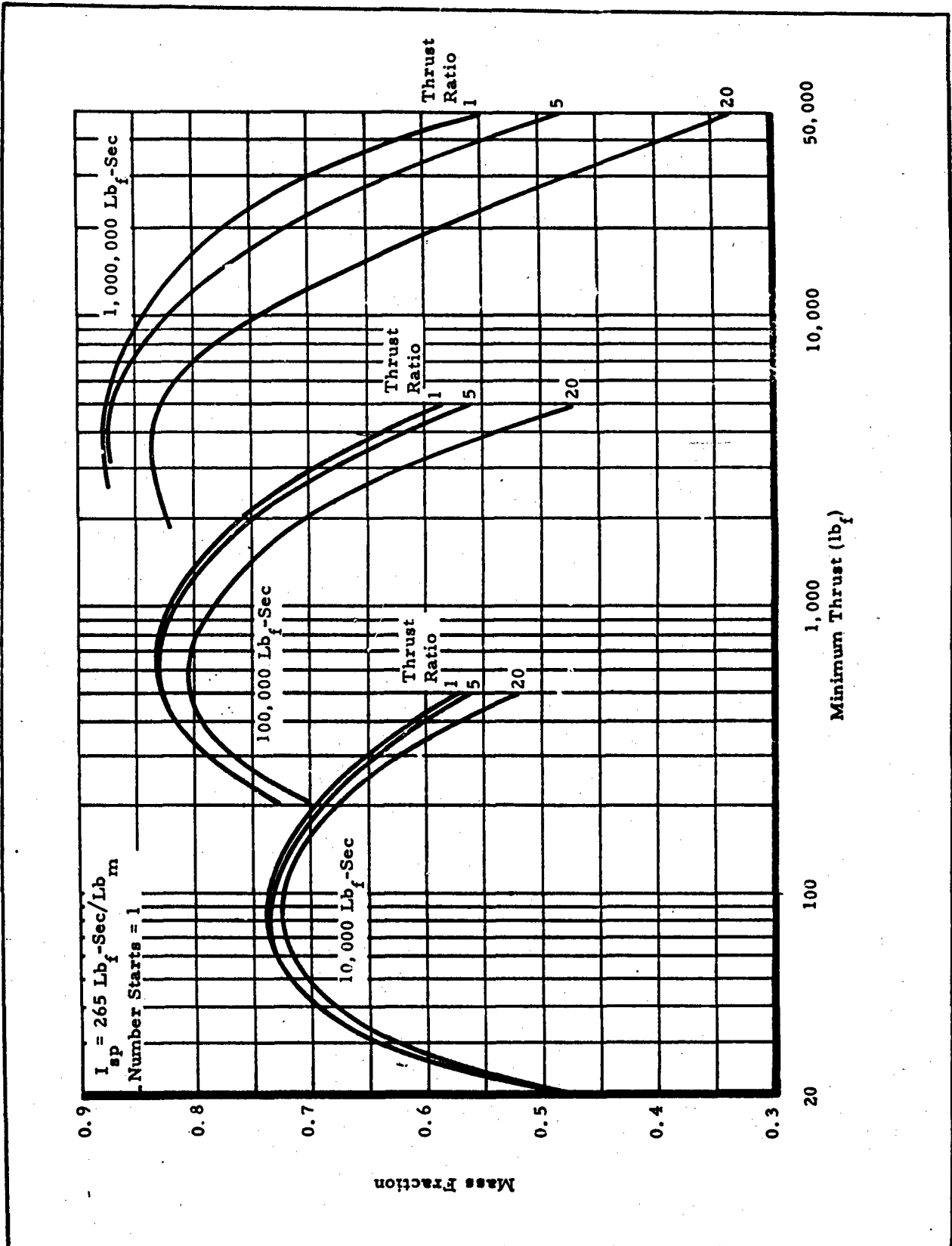


Figure P. 1 - Mass Fraction versus Minimum Thrust for $I_{sp} = 265 \text{ Lb}_f\text{-Sec/Lb}_m$ and 1 Start

CONFIDENTIAL

CONFIDENTIAL

AFRPL-TR-65-209, Vol II

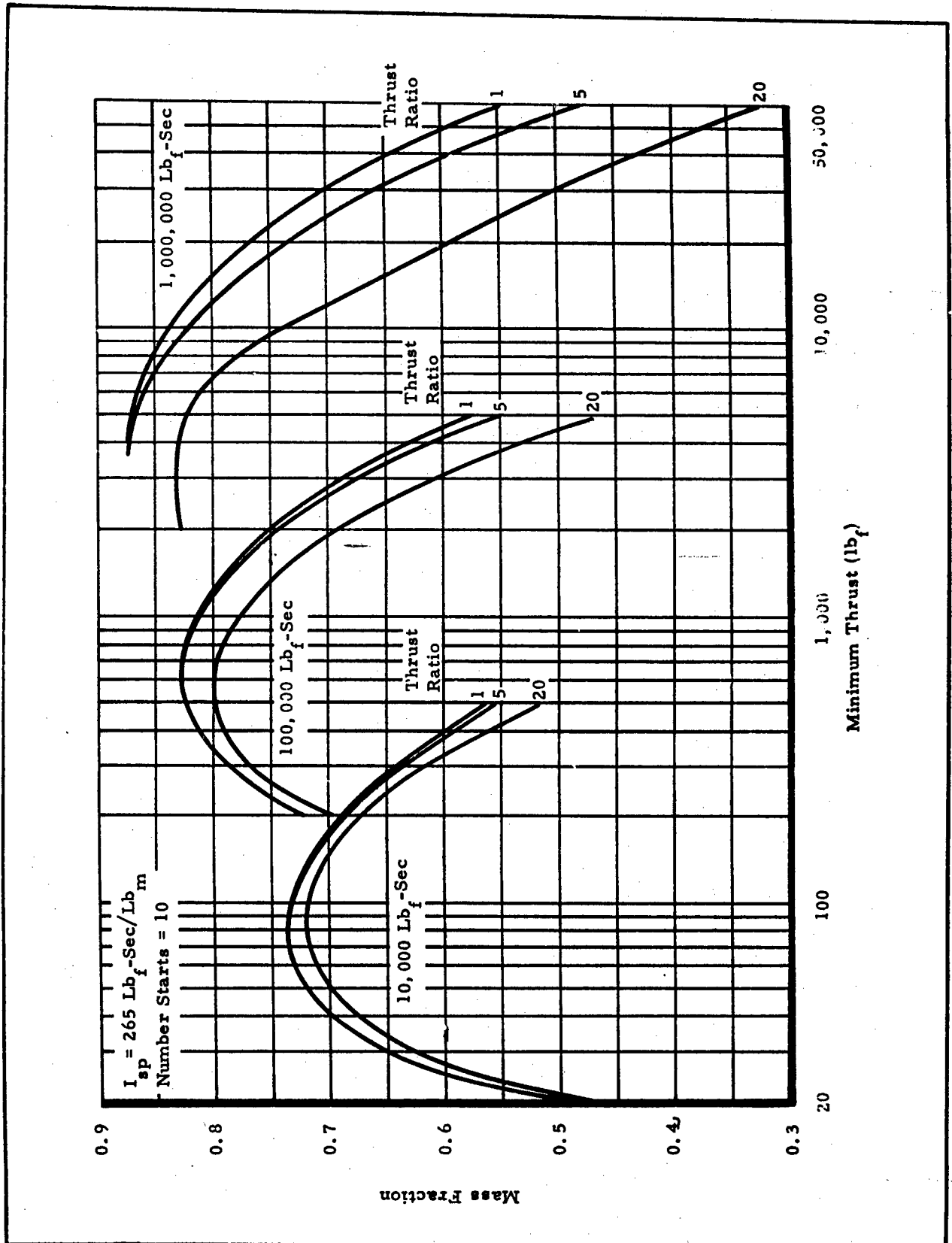


Figure B-2 - Mass Fraction versus Minimum Thrust for $I_{sp} = 265 \text{ Lb}_f\text{-Sec/Lb}_m$ and 10 Starts

CONFIDENTIAL

CONFIDENTIAL

AFRPL-TR-65-209, Vol II

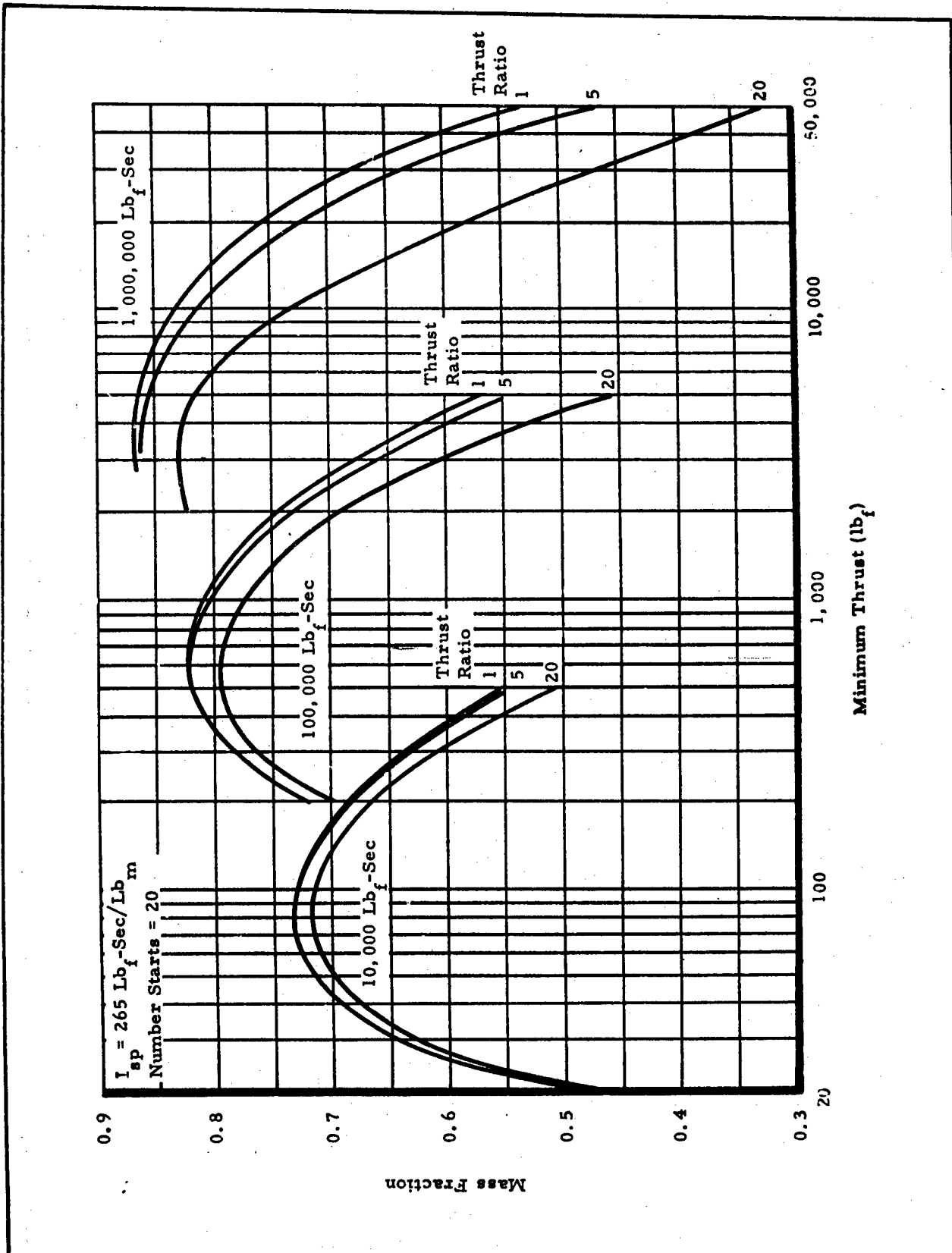


Figure B-3 - Mass Fraction versus Minimum Thrust for
 $I_{sp} = 265 \text{ lb}_f\text{-Sec/Lb}_m$ and 20 Starts

B-6

CONFIDENTIAL

CONFIDENTIAL

AFRPL-TR-65-209, Vol II

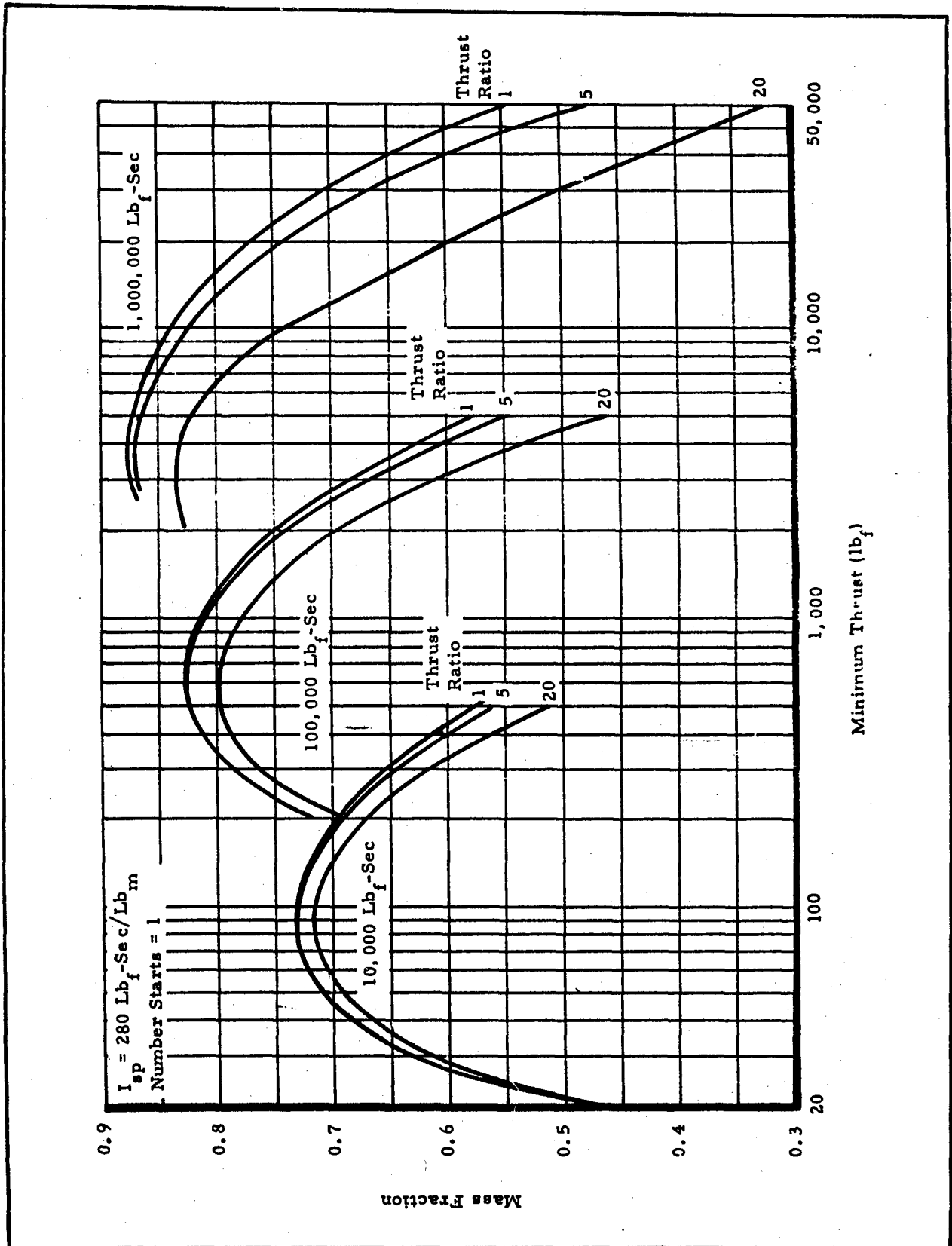


Figure B-4 - Mass Fraction versus Minimum Thrust for $I_{sp} = 280 \text{ Lb}_f\text{-Sec/Lb}_m$ and 1 Start

CONFIDENTIAL

CONFIDENTIAL

AFRPL-TR-65-209, Vol II

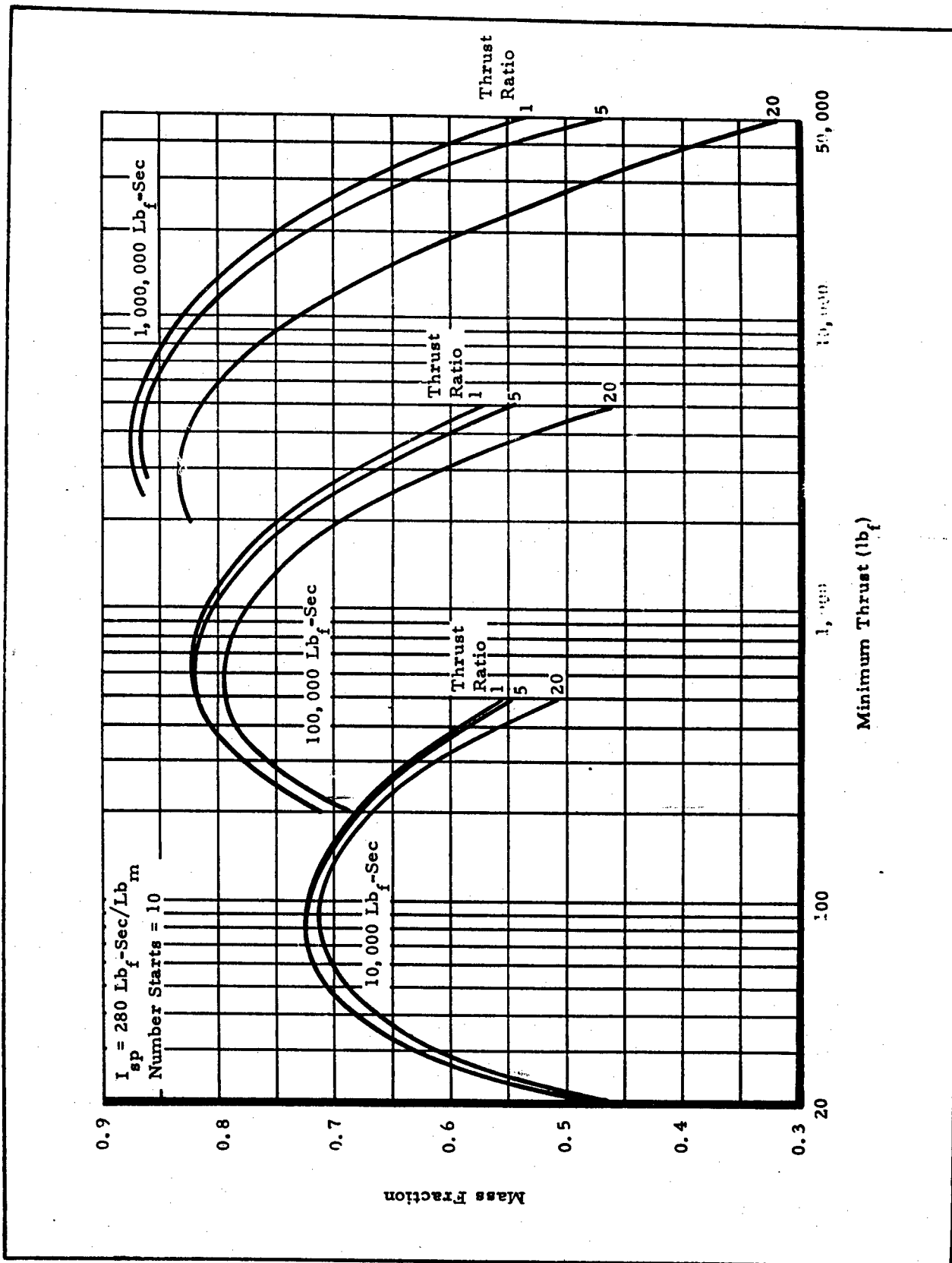


Figure B-5 - Mass Fraction versus Minimum Thrust for $I_{sp} = 280 \text{ Lb}_f\text{-Sec/Lb}_m$ and 10 Starts

B-8

CONFIDENTIAL

CONFIDENTIAL

AFRPL-TR-65-209, Vol II

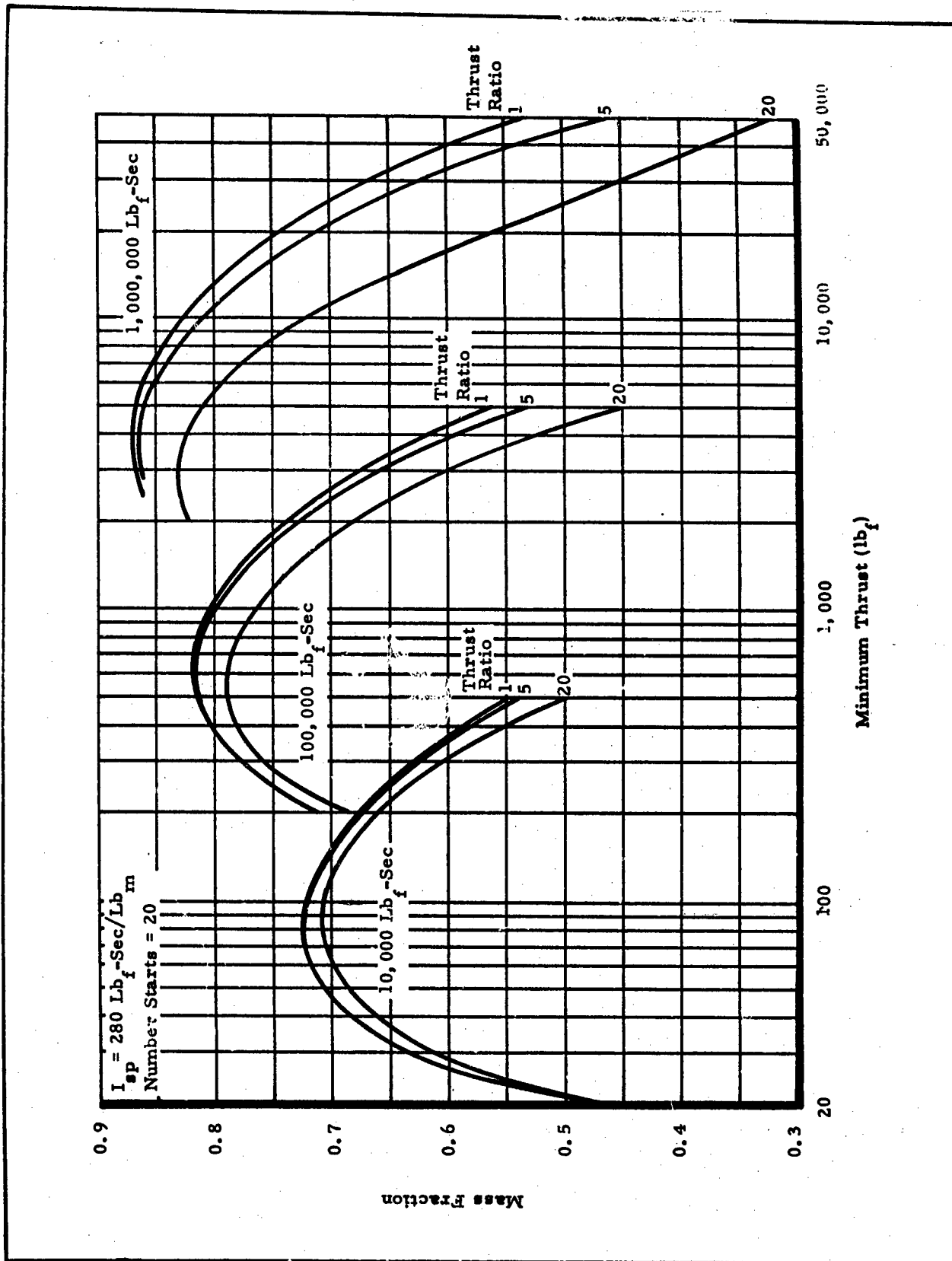


Figure B-6 - Mass Fraction versus Minimum Thrust for $I_{sp} = 280 \text{ Lb}_f\text{-Sec/Lb}_m$ and 20 Starts

CONFIDENTIAL

CONFIDENTIAL

AFRPL-TR-65-209, Vol II

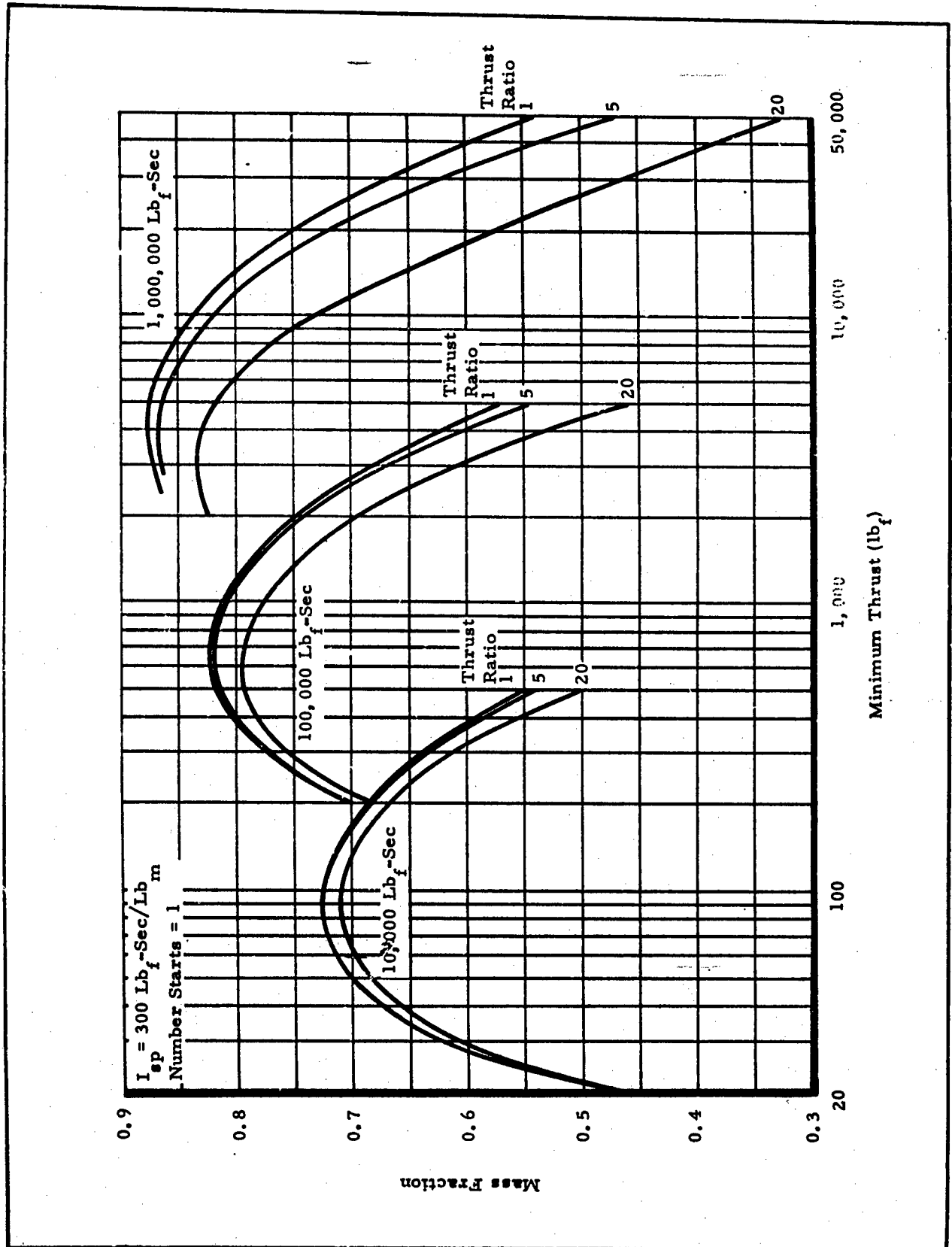


Figure B-7 - Mass Fraction versus Minimum Thrust for $I_{sp} = 300 \text{ lb}_f\text{-Sec/Lb}_m$ and 1 Start

CONFIDENTIAL

CONFIDENTIAL

AFRPL-TR-65-209, Vol II

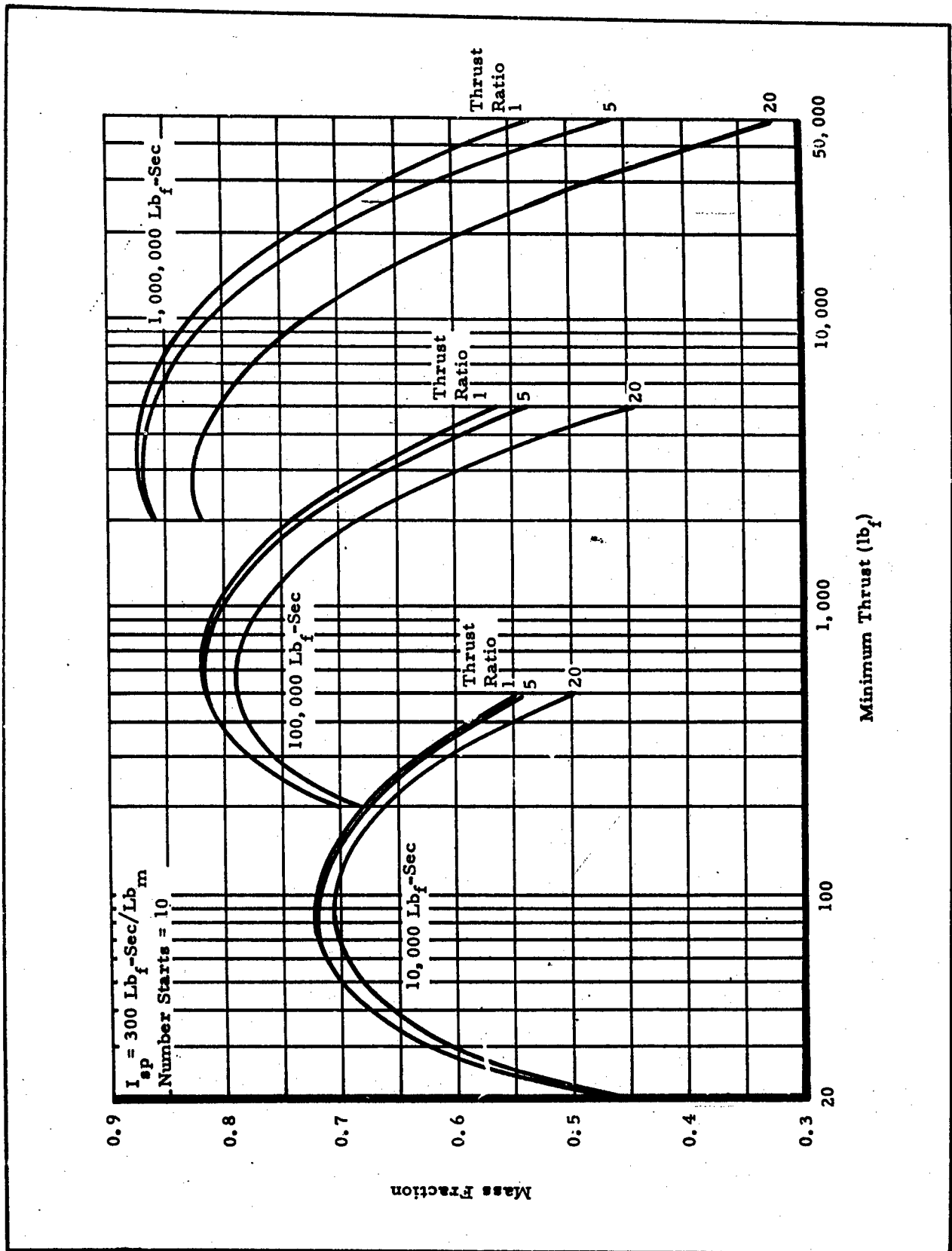


Figure B-8 - Mass Fraction versus Minimum Thrust for

$I_{sp} = 300 \text{ Lb}_f\text{-Sec/Lb}_m$ and 10 Starts

CONFIDENTIAL

CONFIDENTIAL

AFRPL-TR-65-209, Vol II

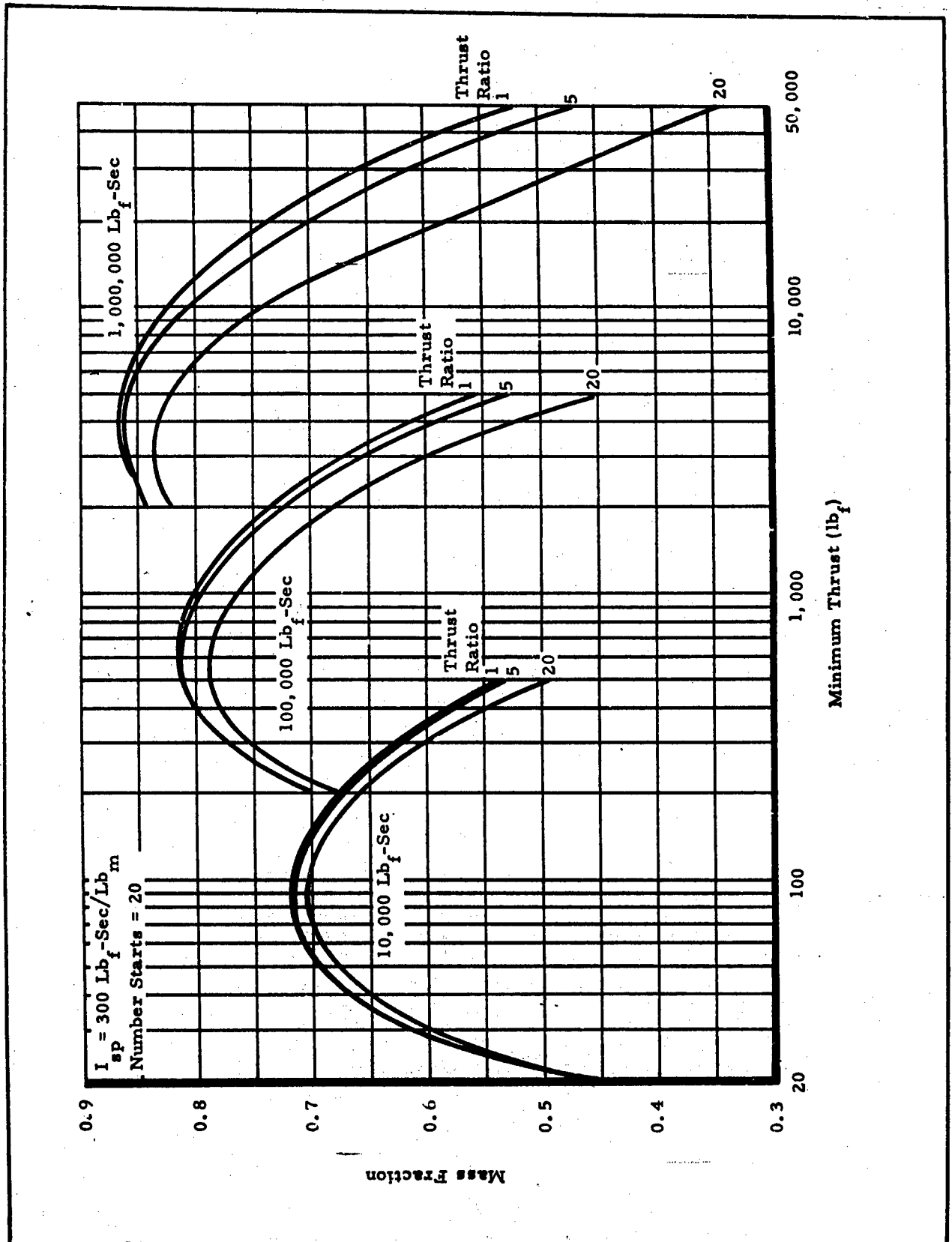


Figure B-9 - Mass Fraction versus Minimum Thrust for $I_{sp} = 300 \text{ Lb}_f\text{-Sec/Lb}_m$ and 20 Starts

CONFIDENTIAL

CONFIDENTIAL

AFRPL-TR-65-209, Vol II

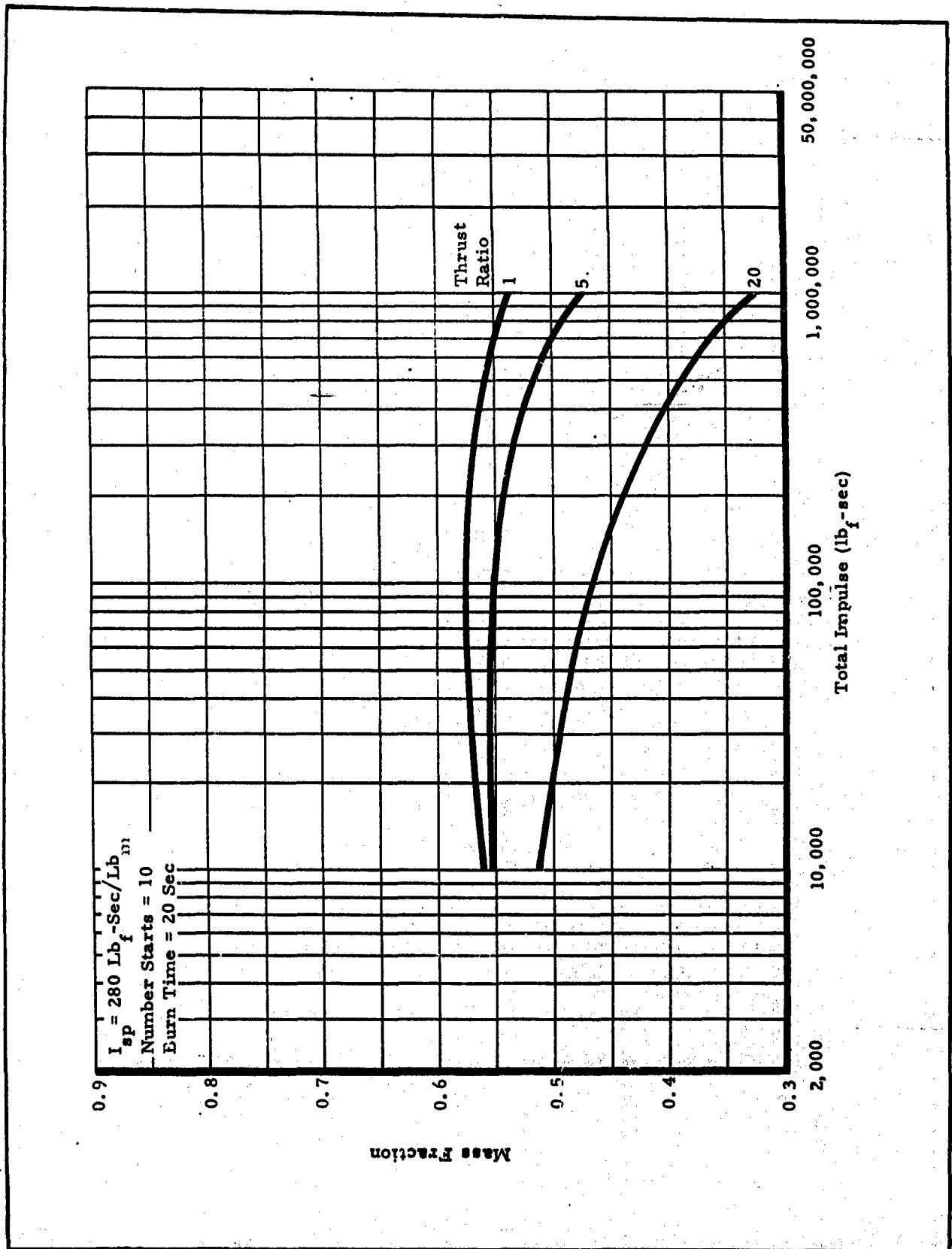


Figure B-10 - Mass Fraction versus Total Impulse for
20-Sec Burn Time

CONFIDENTIAL

CONFIDENTIAL

AFRPL-TR-65-209, Vol II

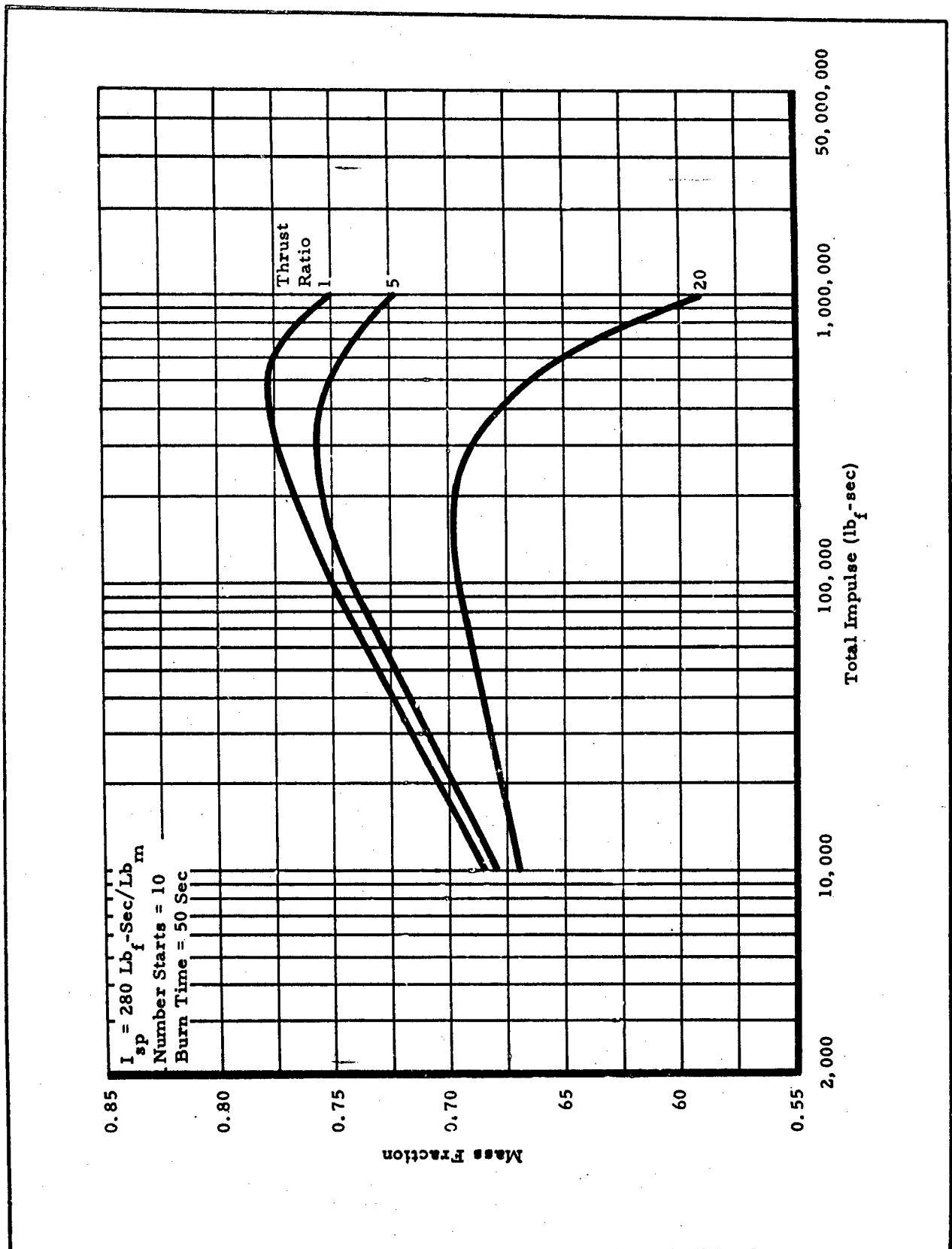


Figure B-11 - Mass Fraction versus Total Impulse for 50-Sec Burn Time

B-14

CONFIDENTIAL

CONFIDENTIAL

AFRPL-TR-65-209, Vol II

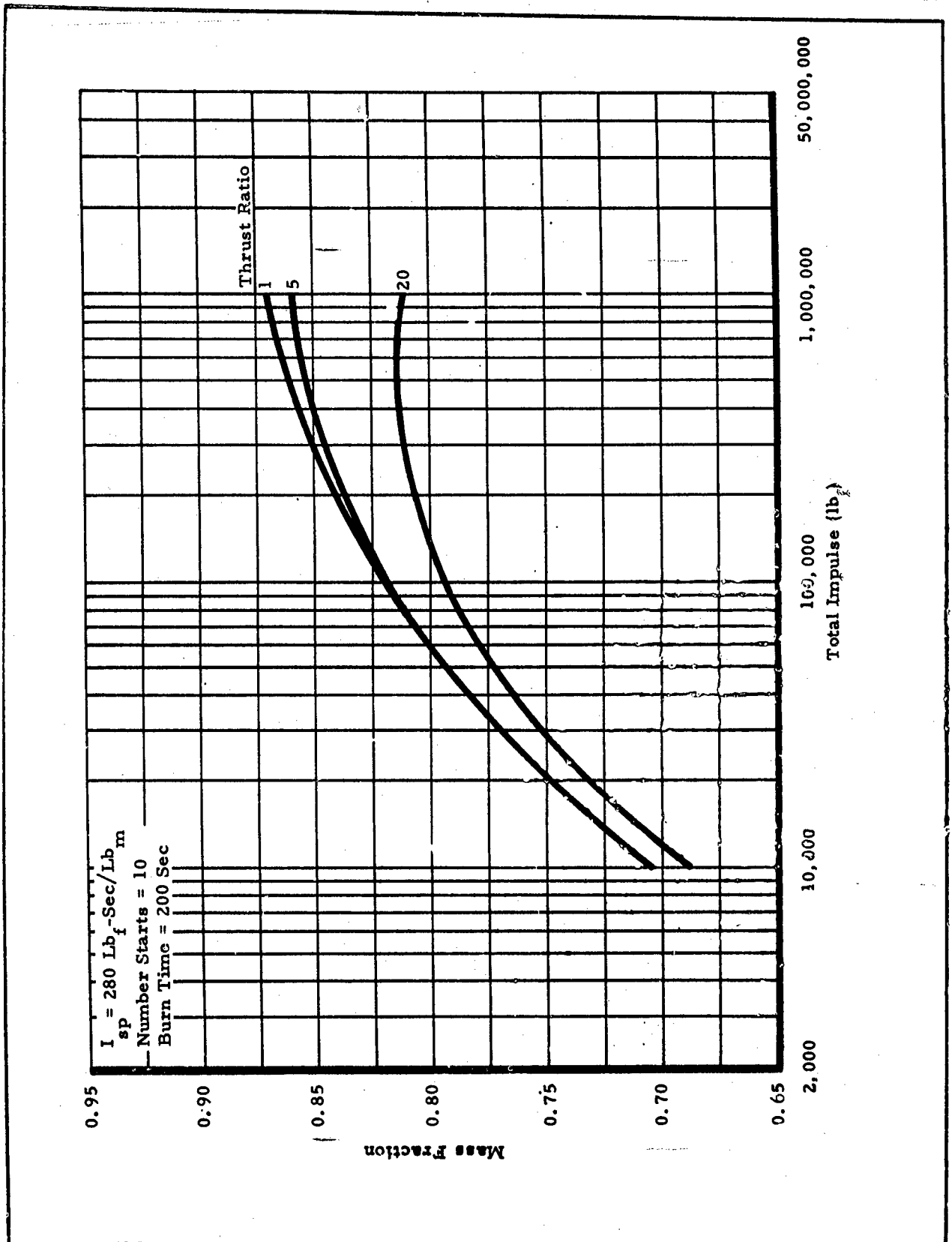


Figure B-12 - Mass Fraction versus Total Impulse for 200-Sec Burn Time

CONFIDENTIAL

CONFIDENTIAL

AFRPL-TR-65-209, Vol II

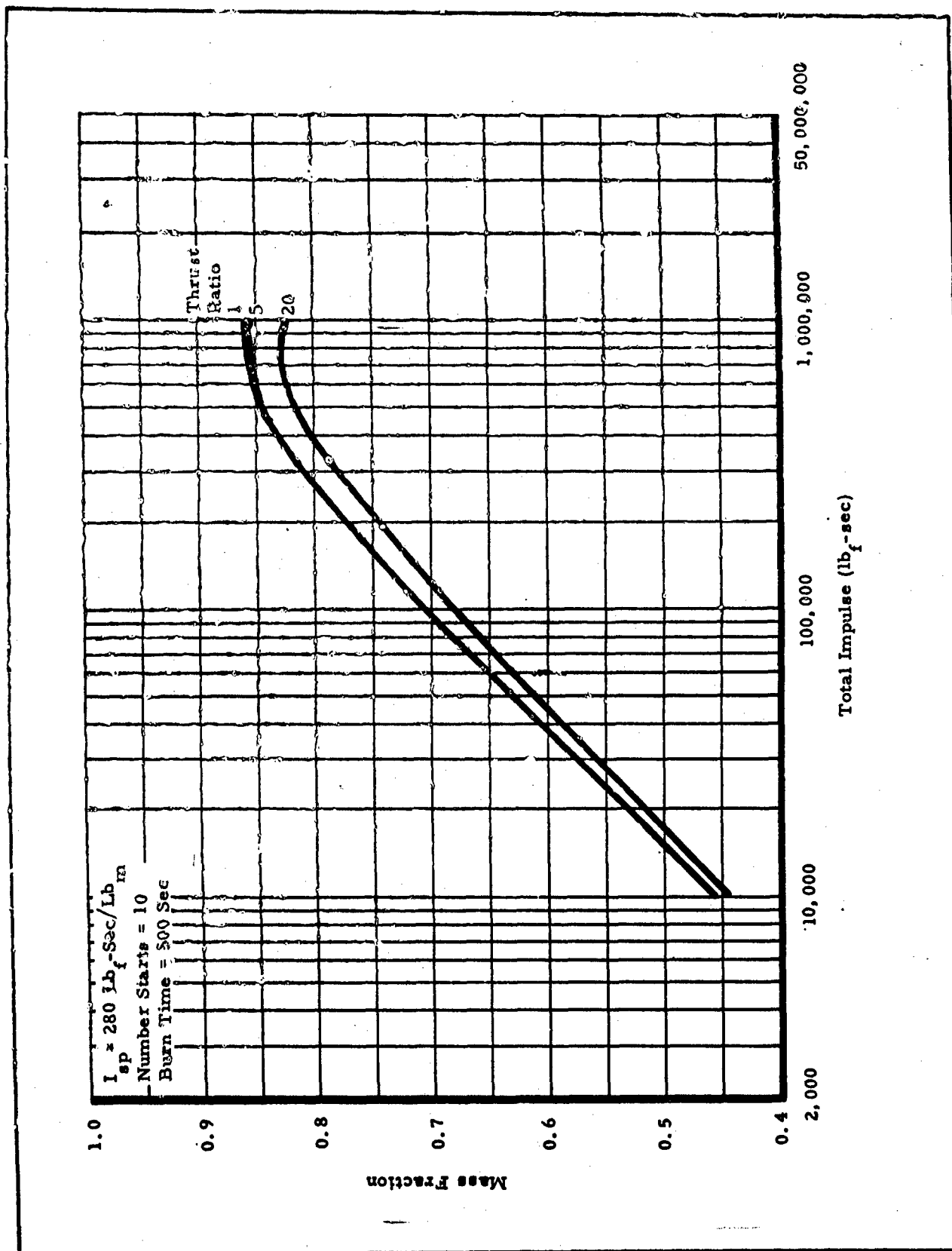


Figure B-13 - Mass Fraction versus Total Impulse for
500-Sec Burn Time

B-16

CONFIDENTIAL

CONFIDENTIAL

AFRPL-TR-65-209, Vol II

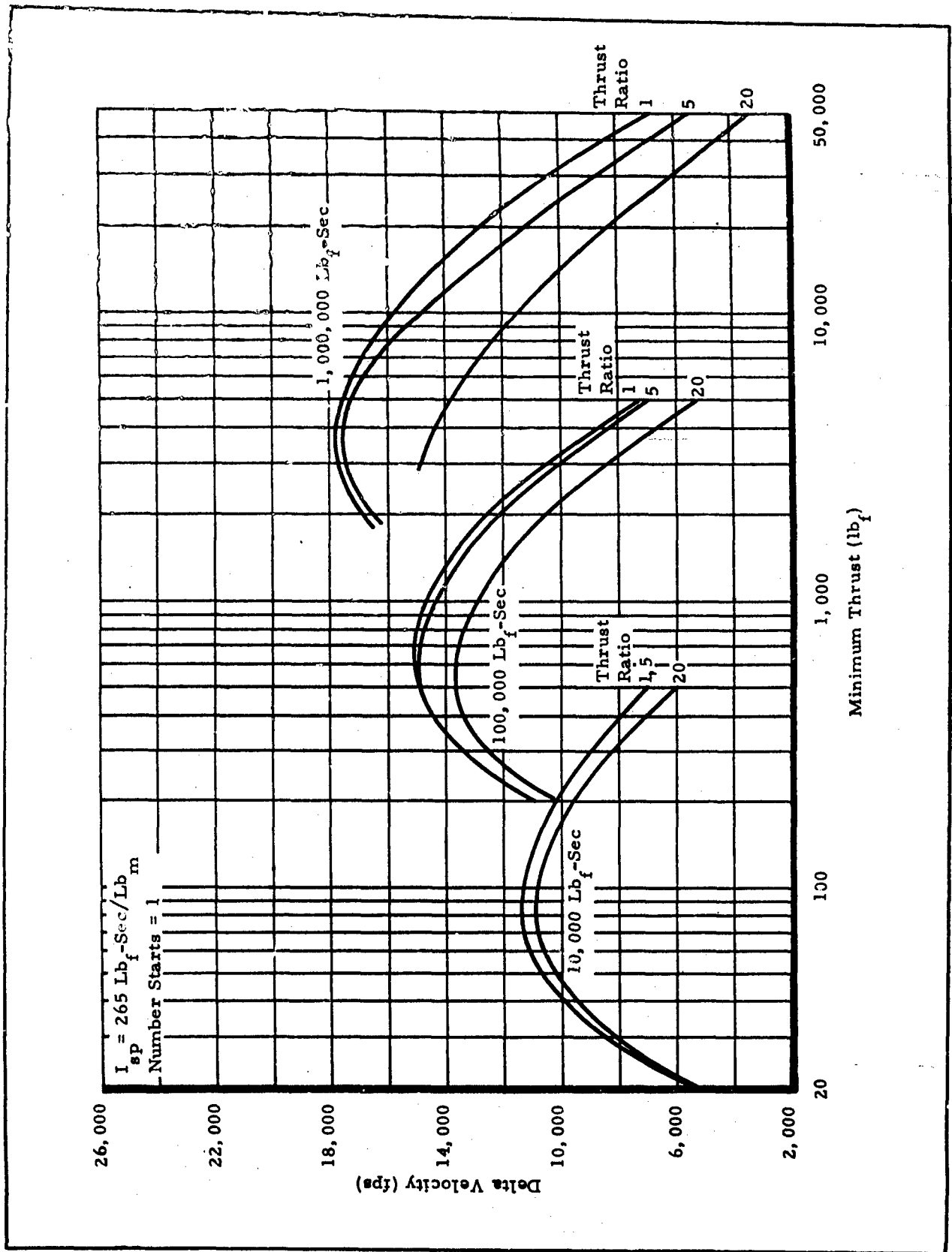


Figure B-14 - Delta Velocity versus Minimum Thrust for

$I_{sp} = 265 \text{ Lb}_f\text{-Sec/Lb}_m$ and 1 Start

CONFIDENTIAL

CONFIDENTIAL

AFRPL-TR-65-209, Vol II

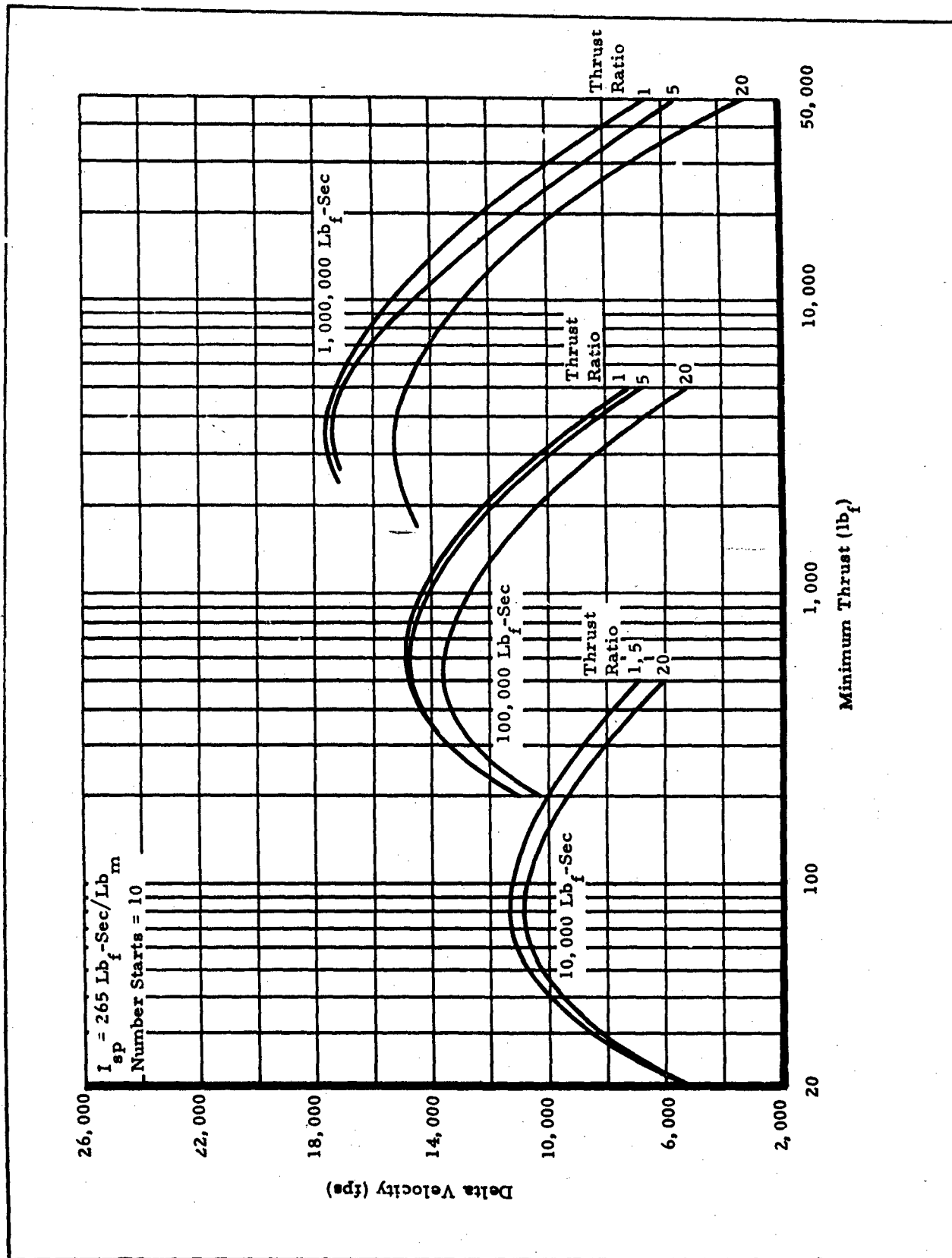


Figure B-15 - Delta Velocity versus Minimum Thrust for

$I_{sp} = 265 \text{ Lb}_f\text{-Sec/Lb}_m$ and 10 Starts

B-18

CONFIDENTIAL

CONFIDENTIAL

AFRPL-TR-65-209, Vol II

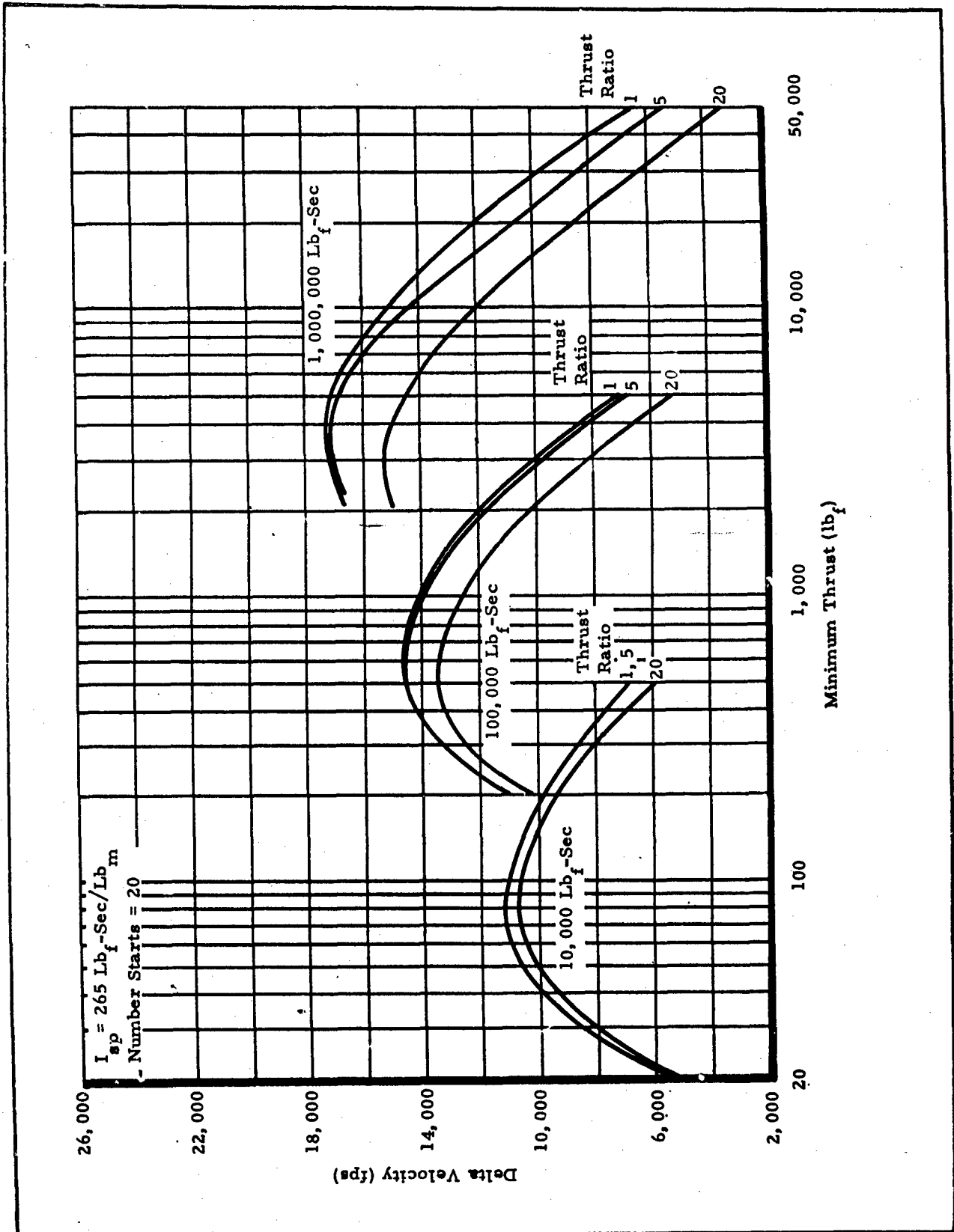


Figure B-16 - Delta Velocity versus Minimum Thrust for $I_{sp} = 265 \text{ Lb}_f\text{-Sec/Lb}_m$ and 20 Starts

CONFIDENTIAL

CONFIDENTIAL

AFRPL-TR-65-209, Vol II

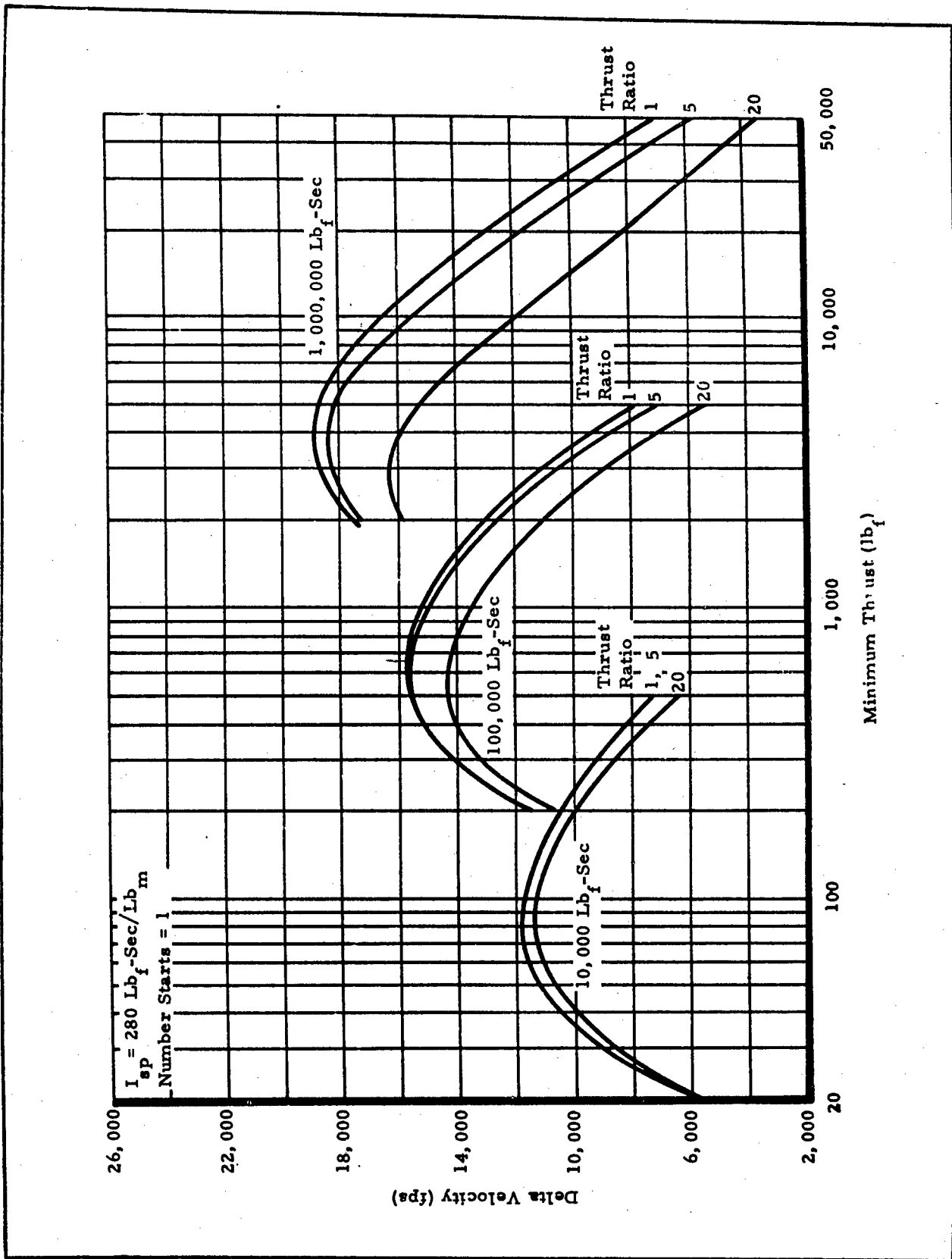


Figure B-17 - Delta Velocity versus Minimum Thrust for

$I_{sp} = 280 \text{ Lb}_f\text{-Sec/Lb}_m$ and 1 Start

CONFIDENTIAL

CONFIDENTIAL

AFRPL-TR-65-209, Vol II

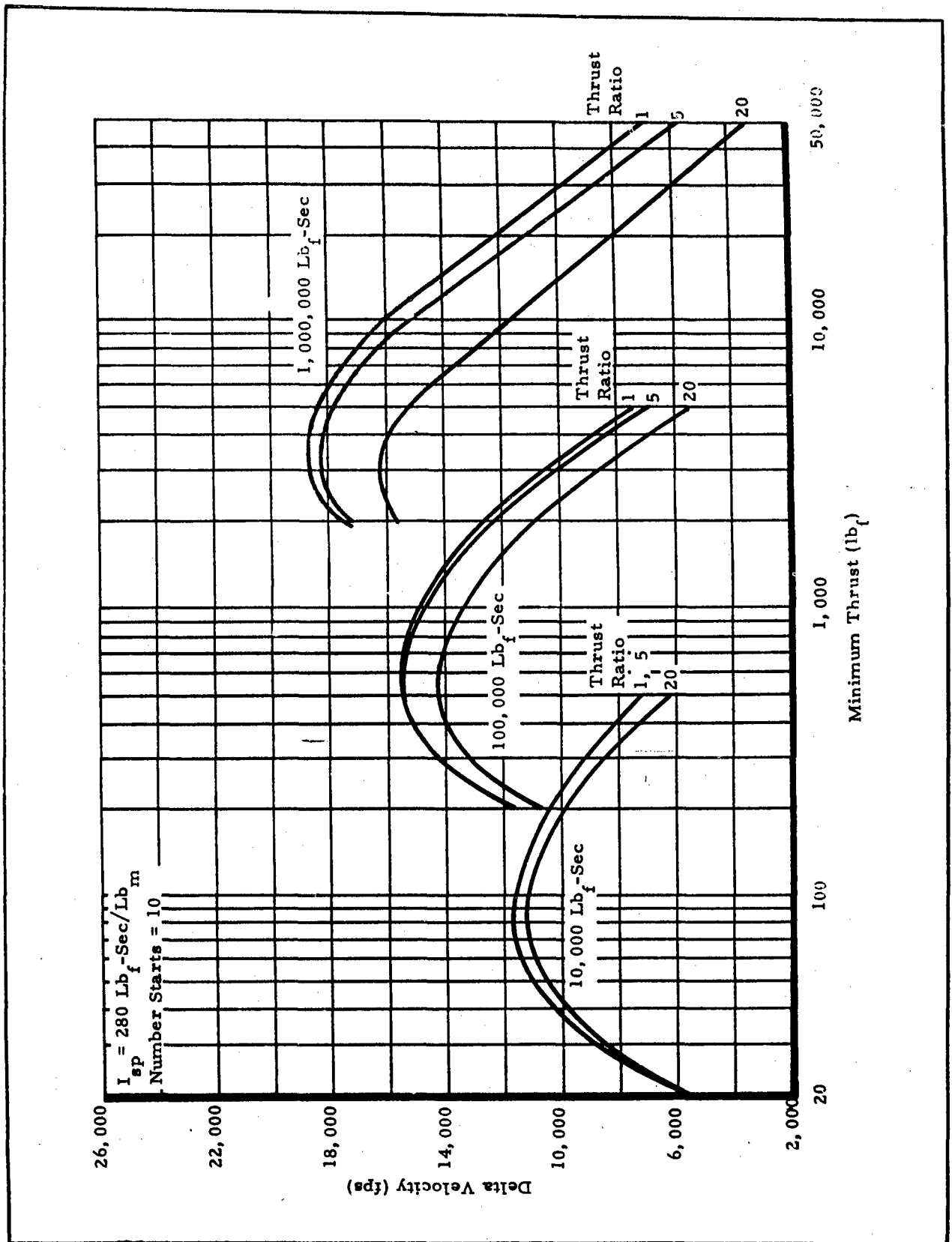


Figure B-18 - Delta Velocity versus Minimum Thrust for $I_{sp} = 280 \text{ Lb}_f\text{-Sec/Lb}_m$ and 10 Starts

CONFIDENTIAL

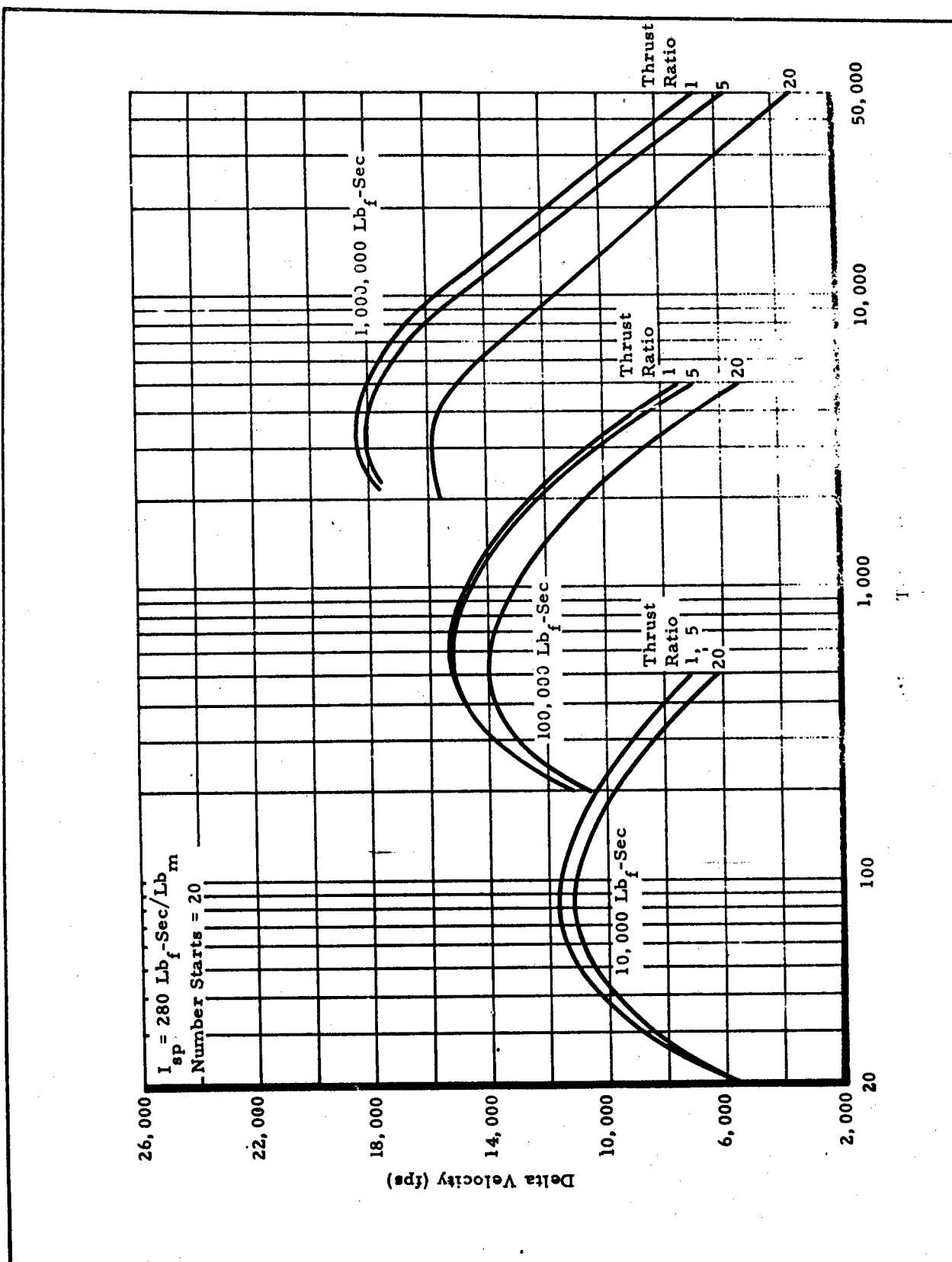


Figure B-19 - Delta Velocity versus Minimum Thrust for $I_{sp} = 280 \text{ Lb}_f\text{-Sec/Lb}_m$ and 20 Starts

CONFIDENTIAL

AFRPL-TR-65-209, Vol II

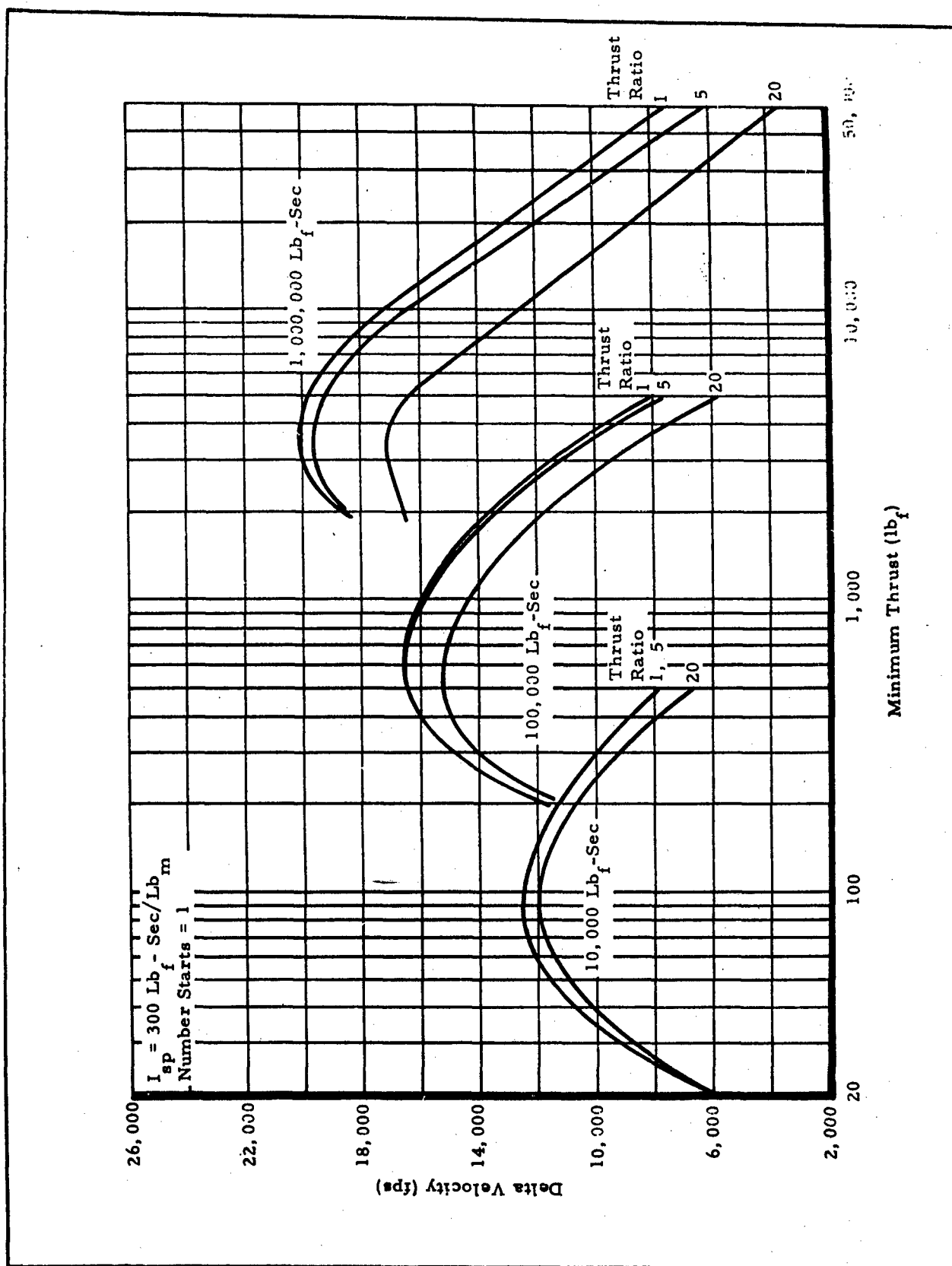


Figure B-20 - Delta Velocity versus Minimum Thrust for $I_{sp} = 300 \text{ Lb}_f\text{-Sec/Lb}_m$ and 1 Start

CONFIDENTIAL

CONFIDENTIAL

AFRPL-TR-65-209, Vol II

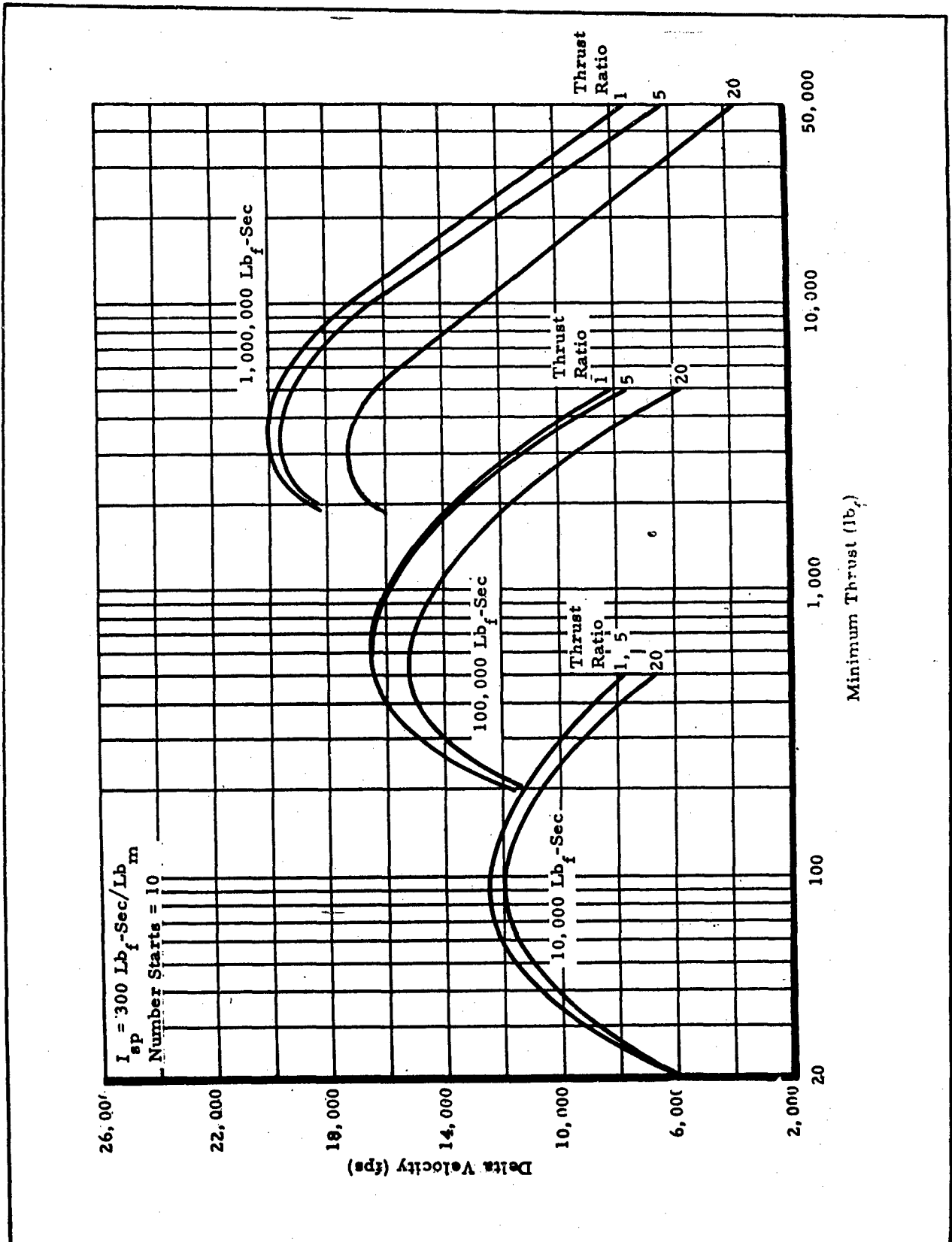


Figure B-21 - Delta Velocity versus Minimum Thrust for $I_{sp} = 300 \text{ Lb}_f\text{-Sec/Lb}_m$ and 10 Starts

CONFIDENTIAL

CONFIDENTIAL

AFRPL-TR-65-209, Vol II

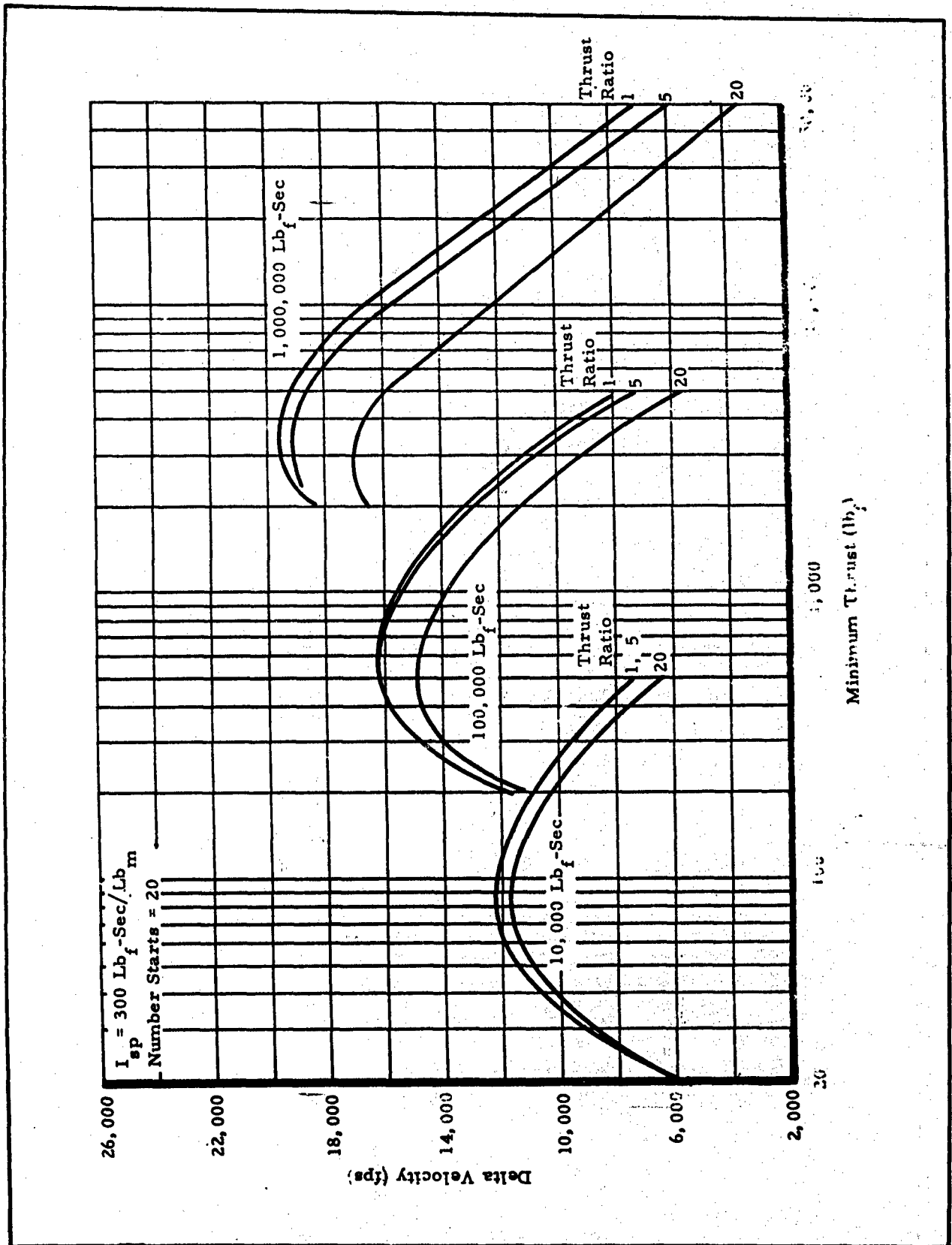


Figure B-22 - Delta Velocity versus Minimum Thrust for $I_{sp} = 300 \text{ Lb}_f\text{-Sec/Lb}_m$ and 20 Starts

CONFIDENTIAL

CONFIDENTIAL

AFRPL-TR-65-209, Vol II

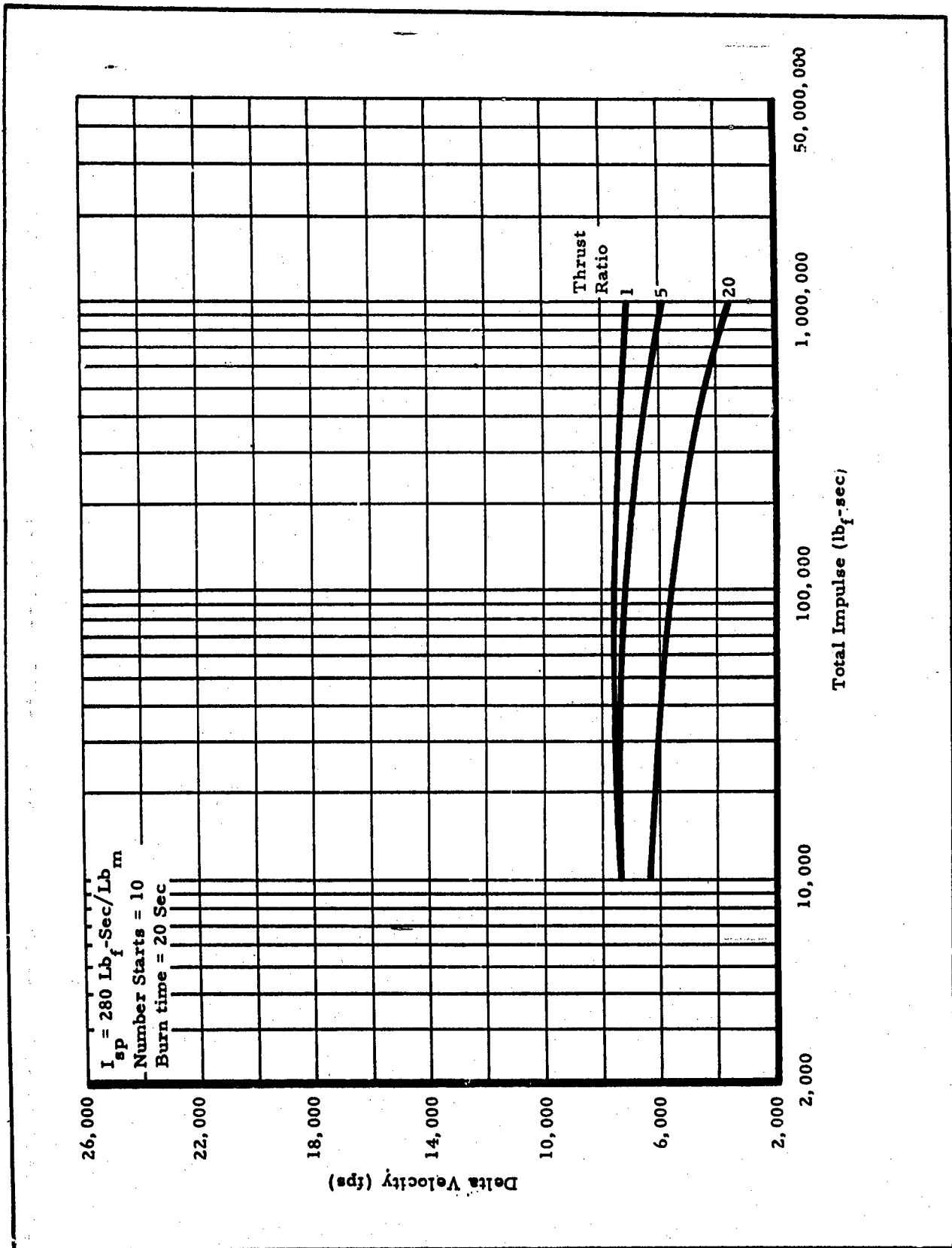


Figure B-23 - Delta Velocity versus Total Impulse
for 20-Sec Burn Time

B-26

CONFIDENTIAL

CONFIDENTIAL

AFRPL-TR-65-209, Vol II

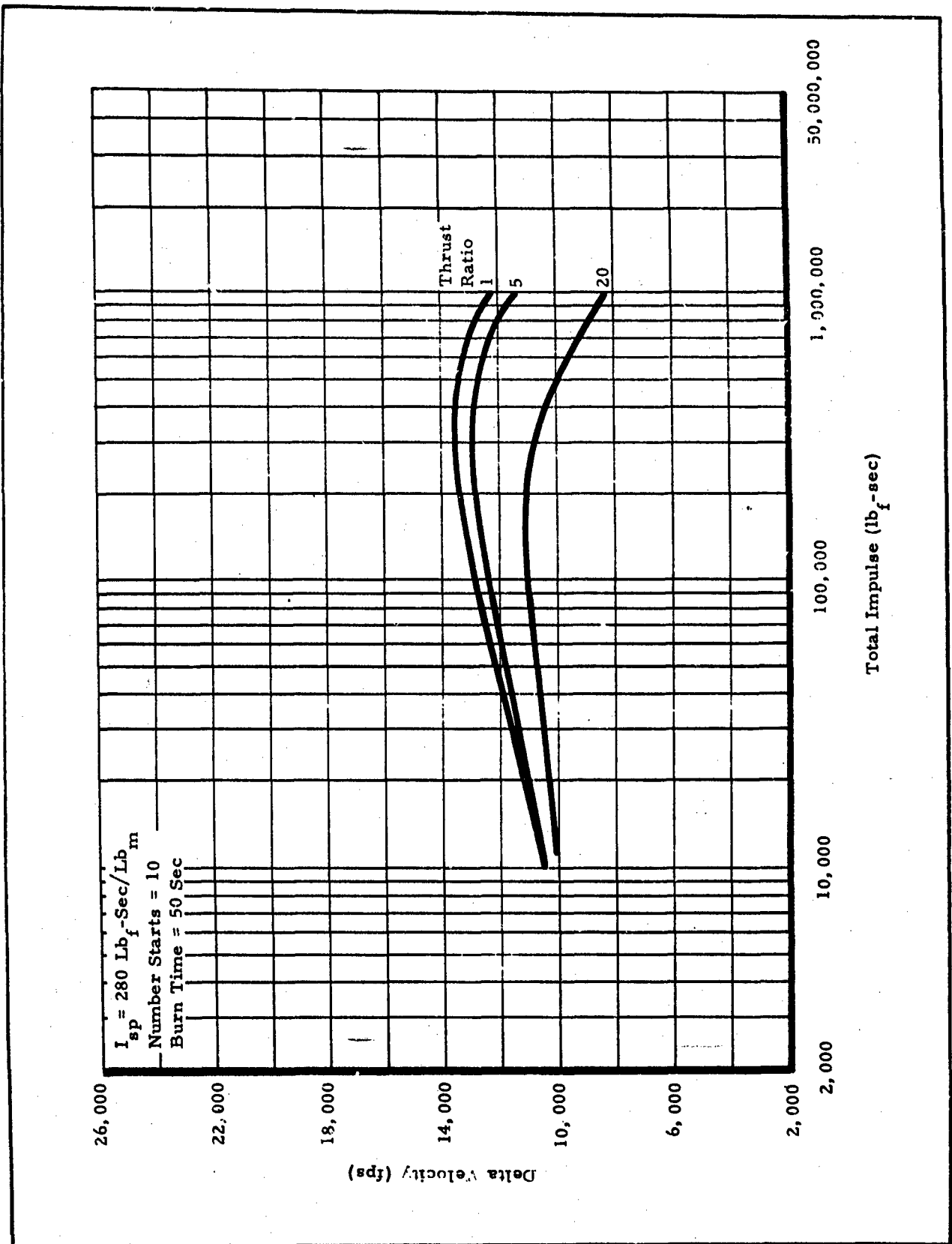


Figure B-24 - Delta Velocity versus Total Impulse
for 50-Sec Burn Time

CONFIDENTIAL

B-27

CONFIDENTIAL

AFRPL-TR-65-209, Vol II

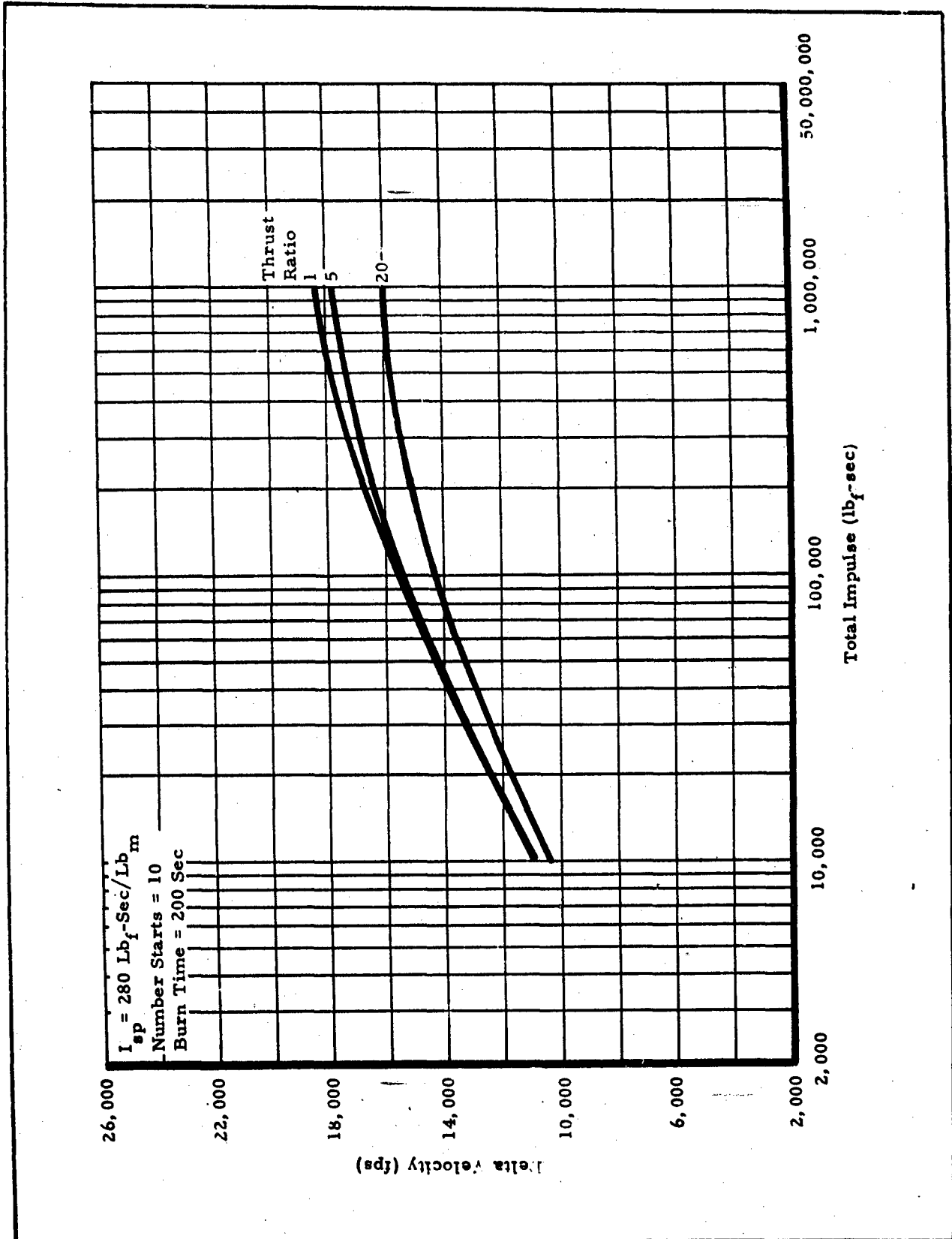


Figure R-25 - Delta Velocity versus Total Impulse
for 200-Sec Burn Time

B-28

CONFIDENTIAL

CONFIDENTIAL

AFRPL-TR-65-209, Vol II

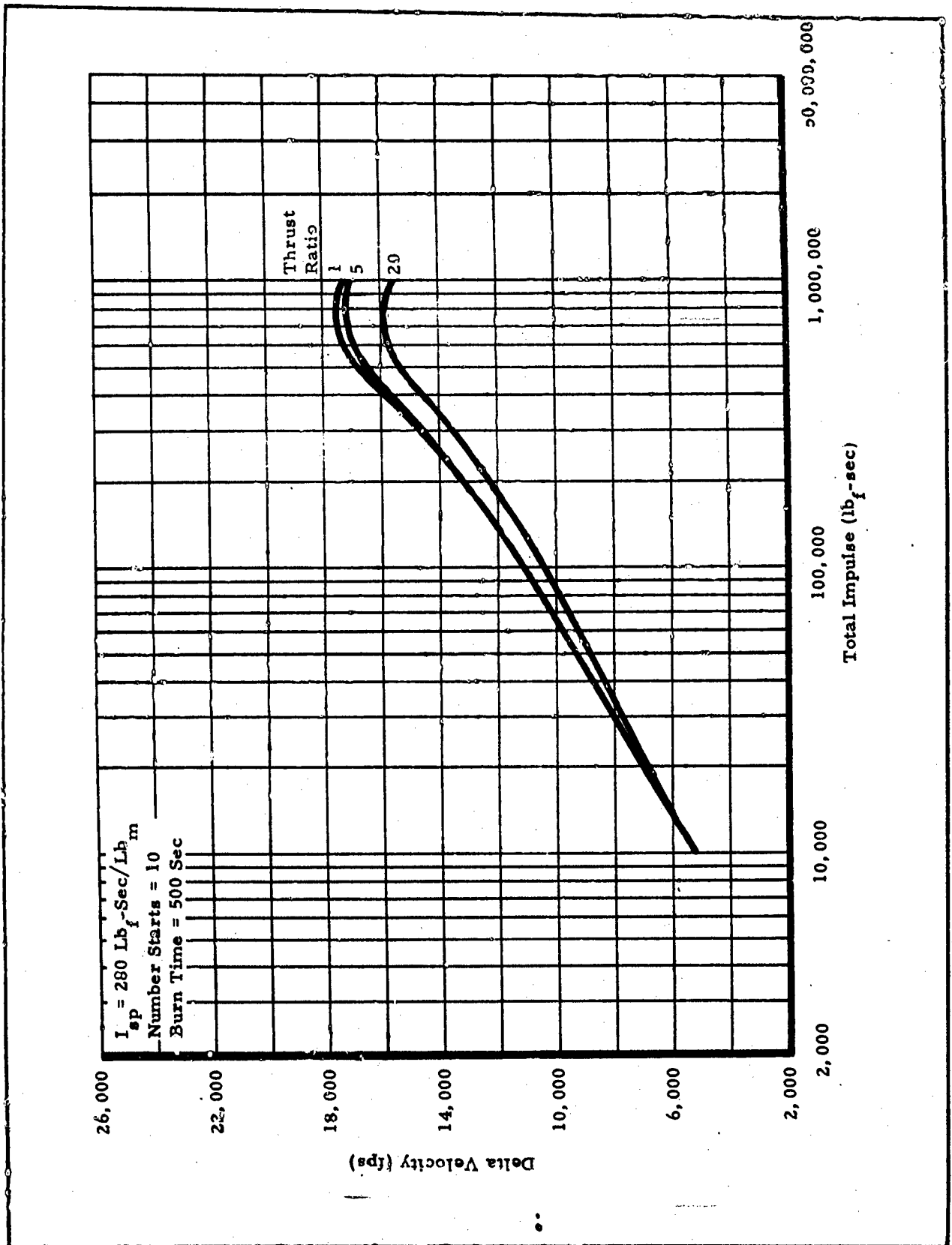


Figure B-26 - Delta Velocity versus Total Impulse
for 500-Sec Burn Time

CONFIDENTIAL

CONFIDENTIAL

AFRPL-TR-65-209, Vol II

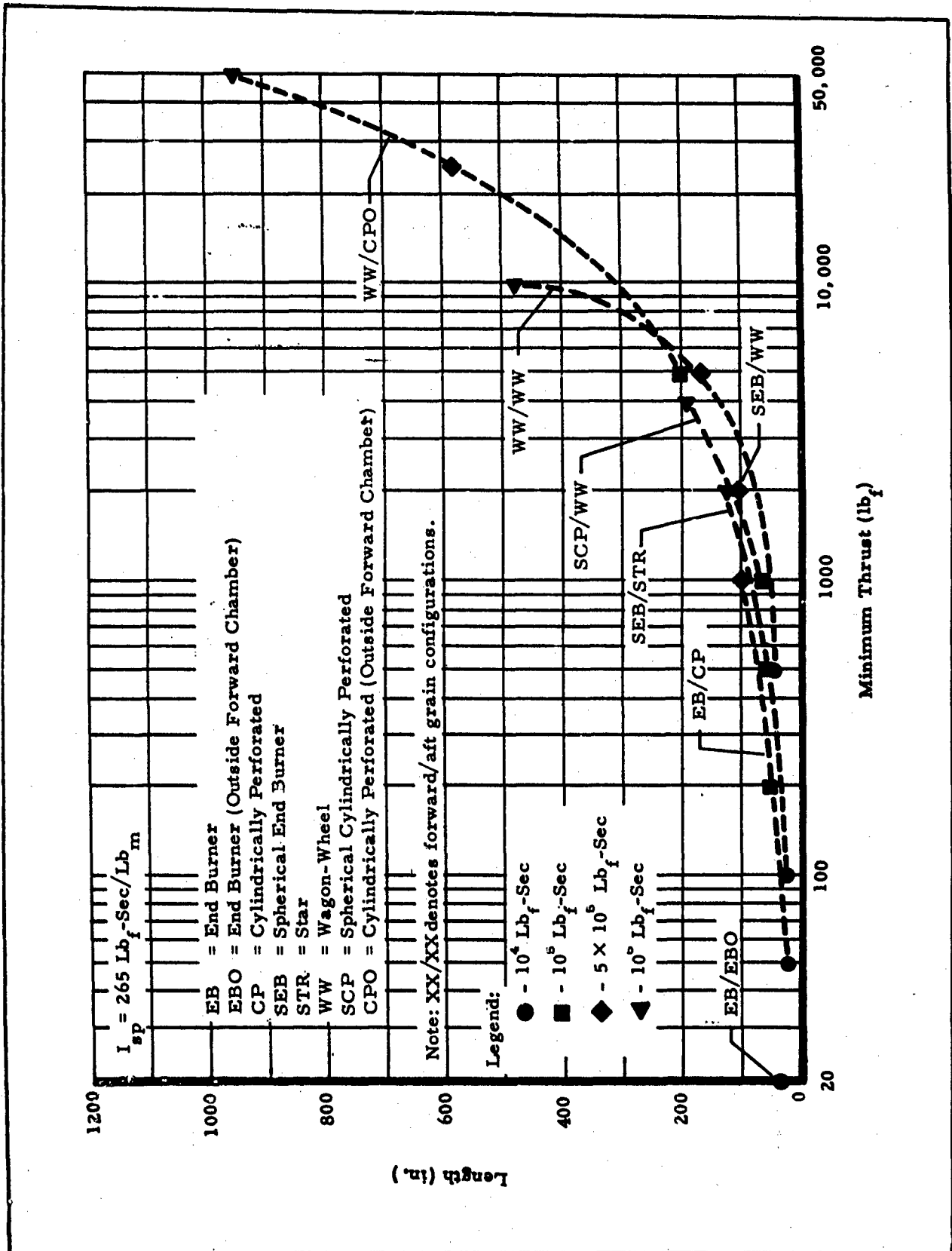


Figure B-27 - Length versus Minimum Thrust for

$I_{sp} = 265 \text{ Lb}_f\text{-Sec/Lb}_m$

B-30

CONFIDENTIAL

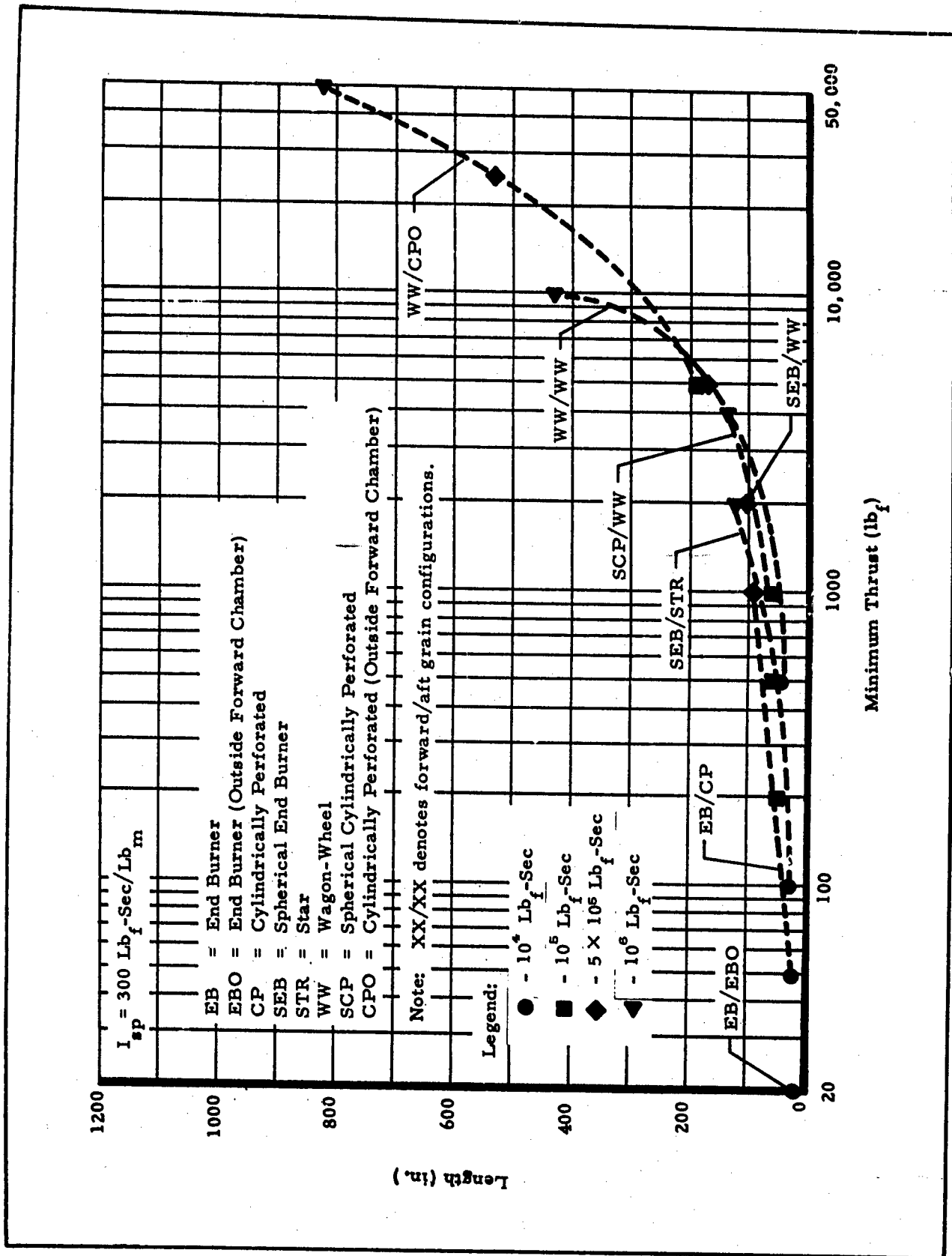


Figure B-28 - Length versus Minimum Thrust for

$I_{sp} = 300 \text{ Lb}_f\text{-Sec/Lb}_m$

CONFIDENTIAL

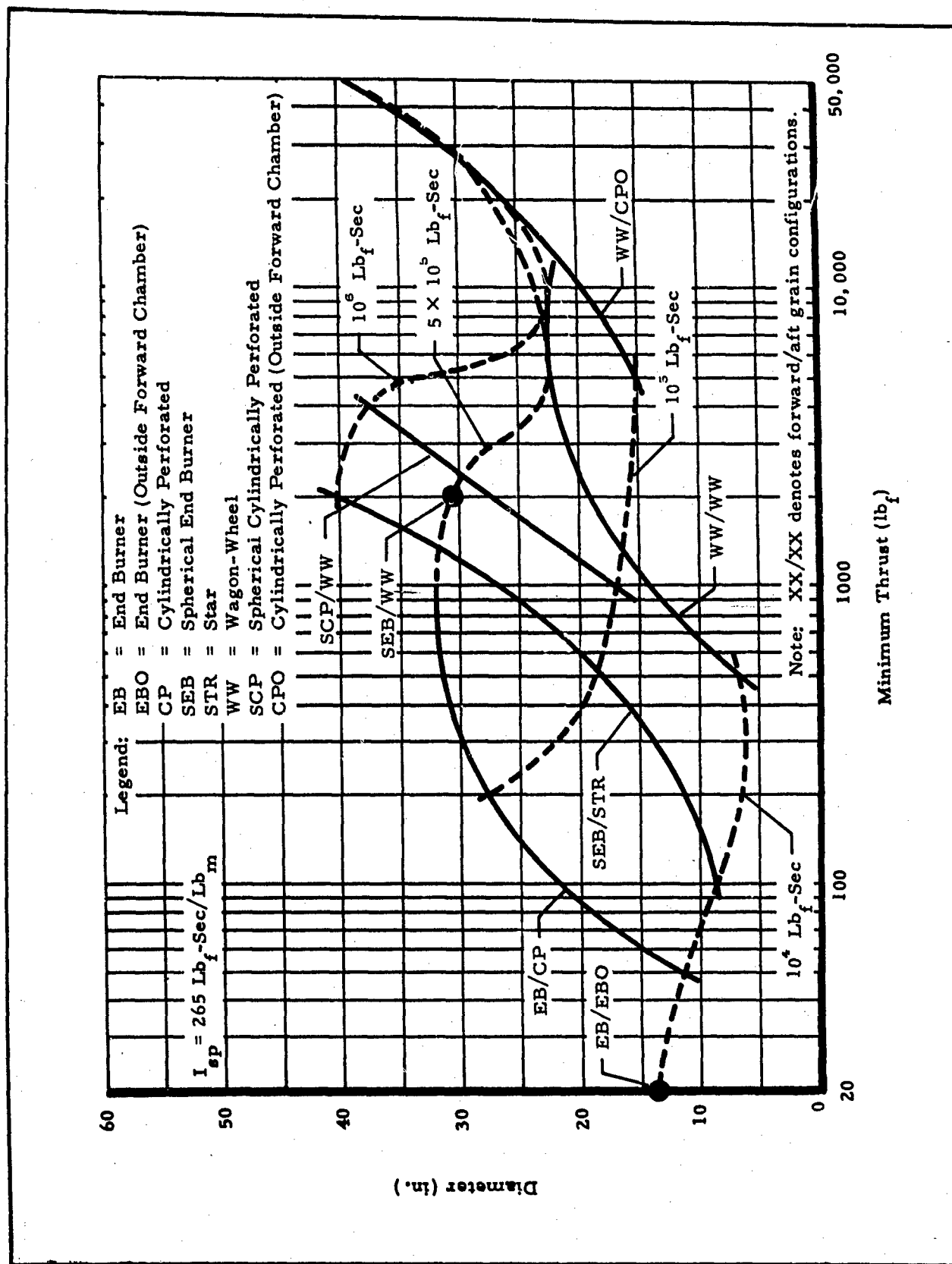


Figure B-29 - Diameter versus Minimum Thrust
for $I_{sp} = 265 \text{ Lb}_f\text{-Sec/Lb}_m$

B-32

CONFIDENTIAL

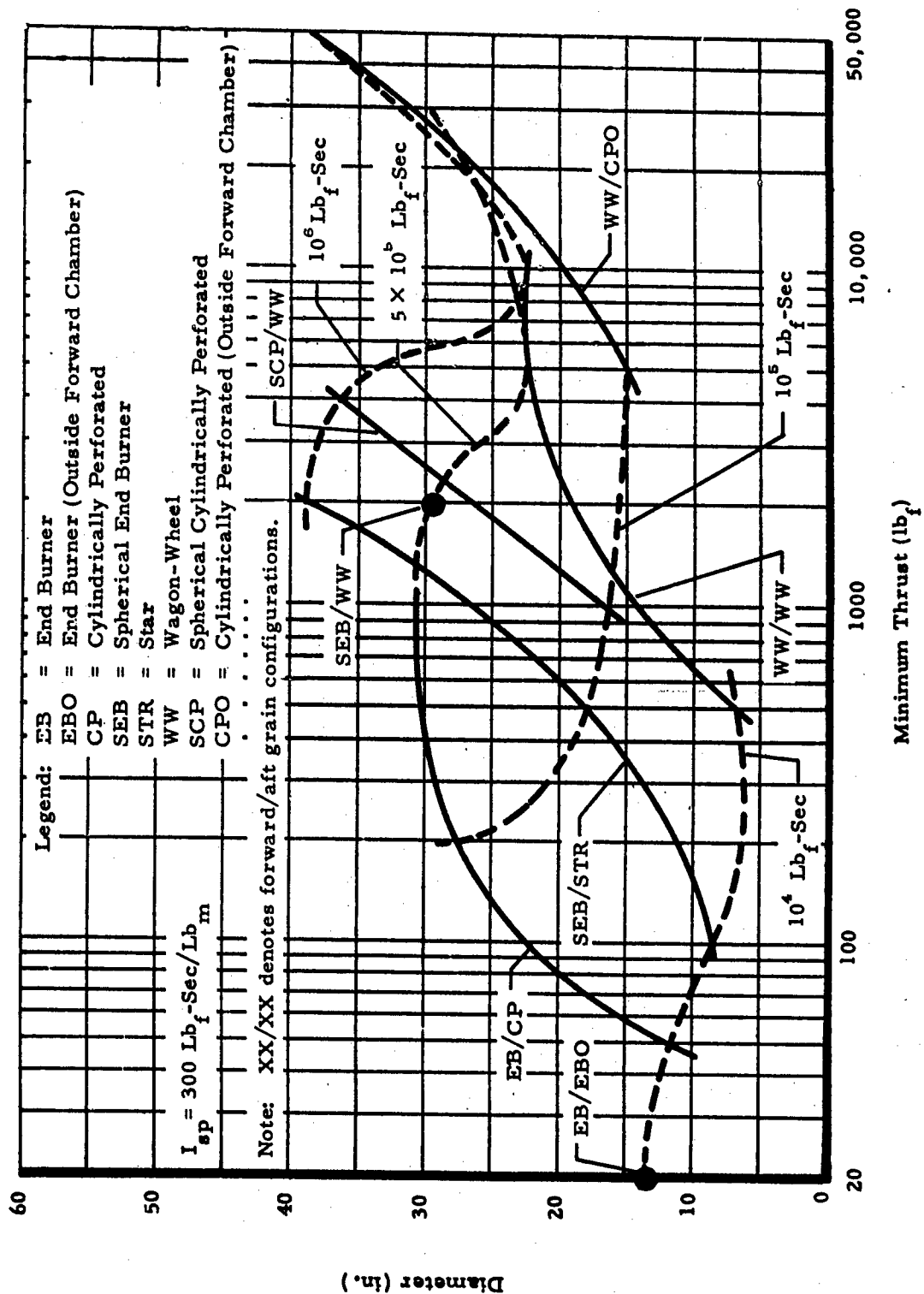


Figure B-30 - Diameter versus Minimum Thrust
for $I_{sp} = 300 \text{ Lb}_f\text{-Sec/Lb}_m$

CONFIDENTIAL

CONFIDENTIAL

AFRPL-TR-65-209, Vol II

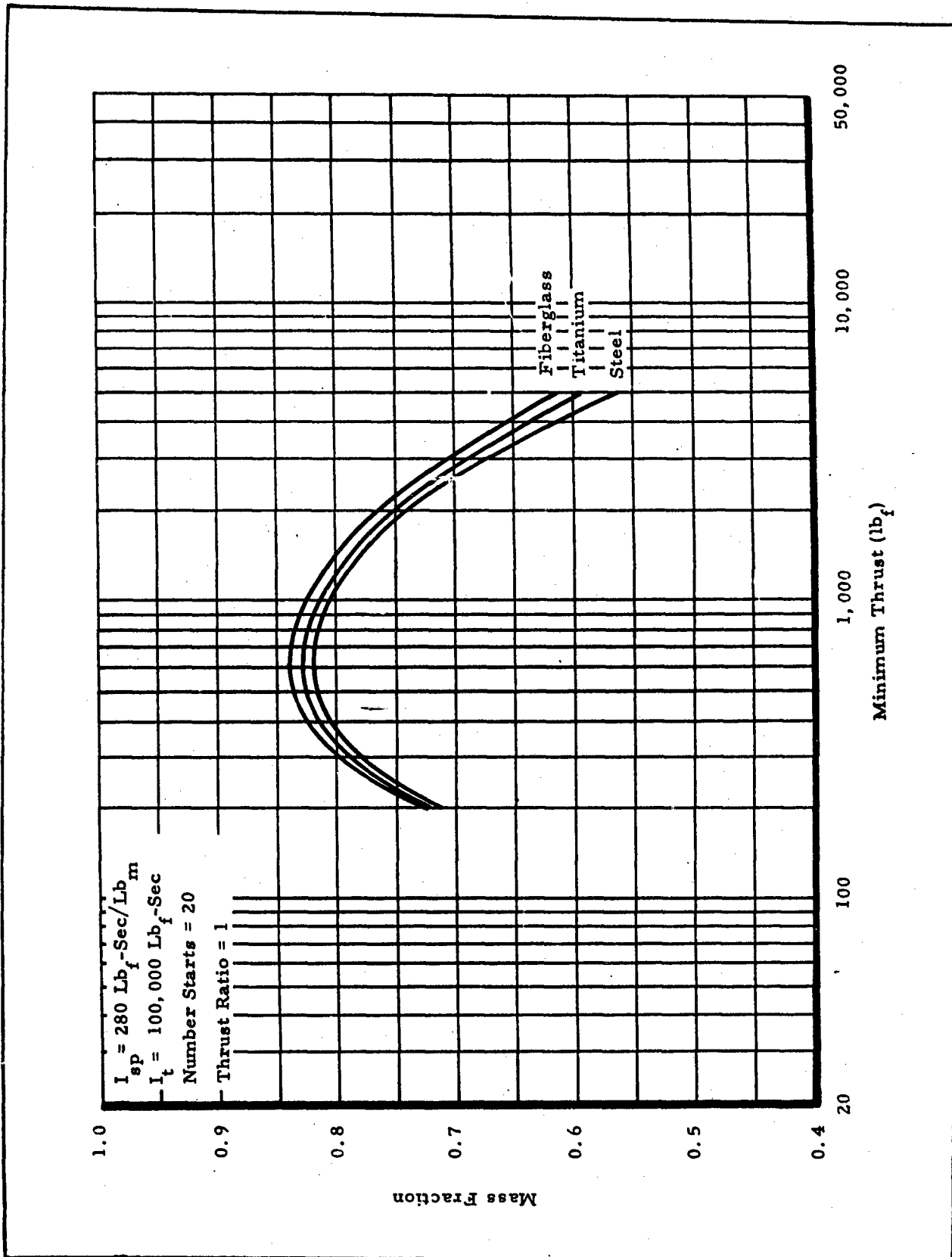


Figure B-31 - Mass Fraction versus Minimum Thrust at Thrust Ratio of 1

B-34

CONFIDENTIAL

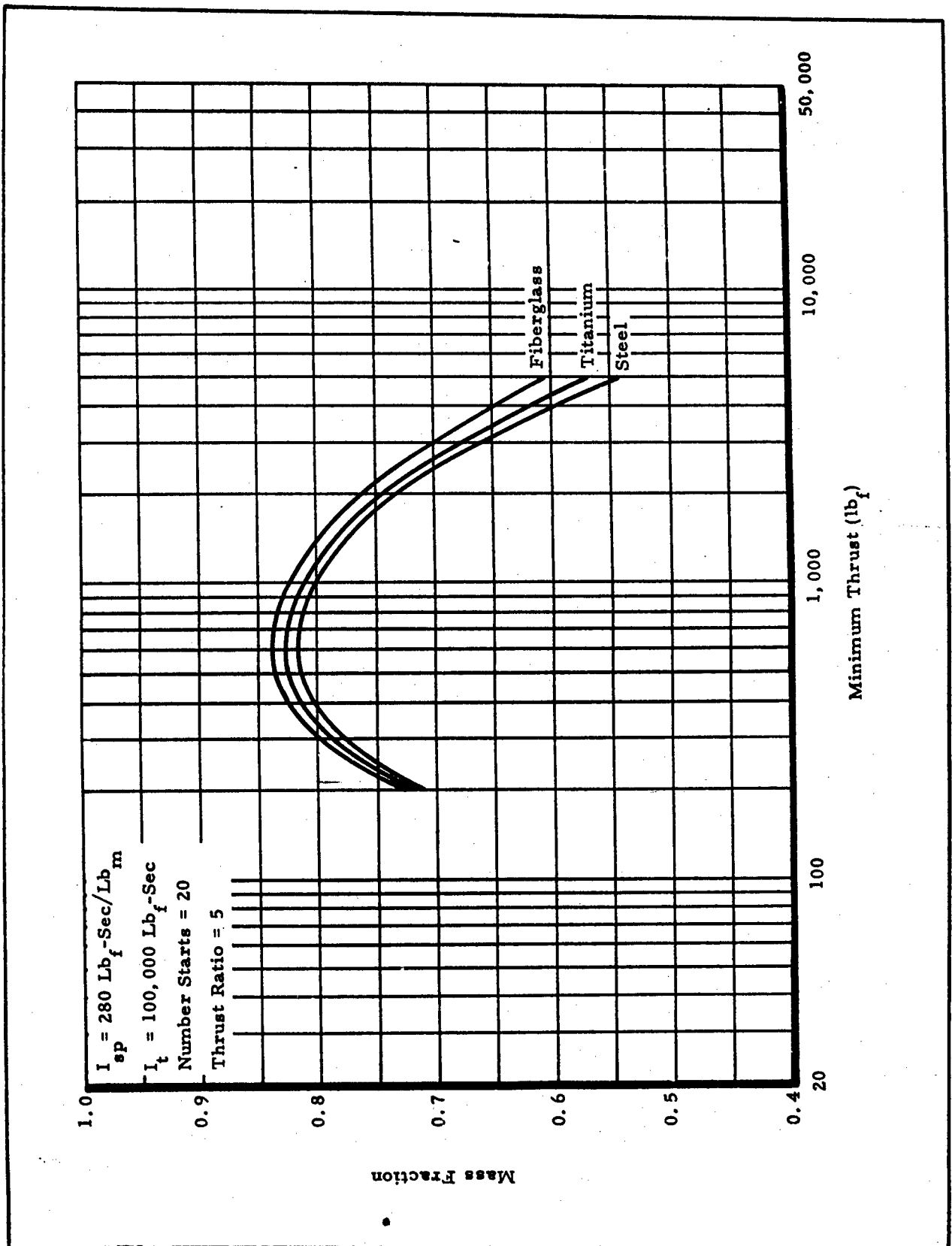


Figure B-32 - Mass Fraction versus Minimum Thrust at Thrust Ratio of 5

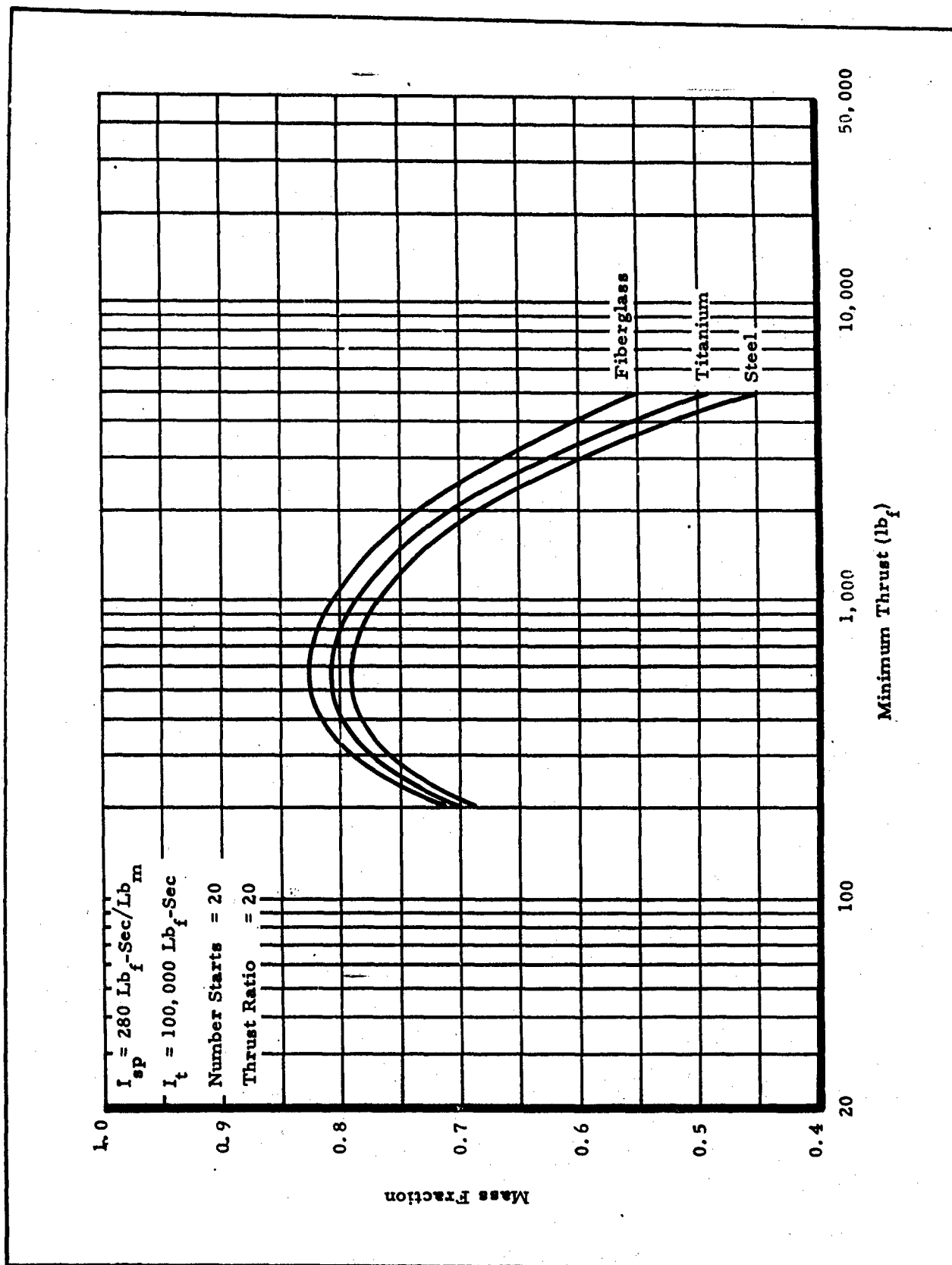


Figure B-33 - Mass Fraction versus Minimum Thrust at Thrust Ratio of 20

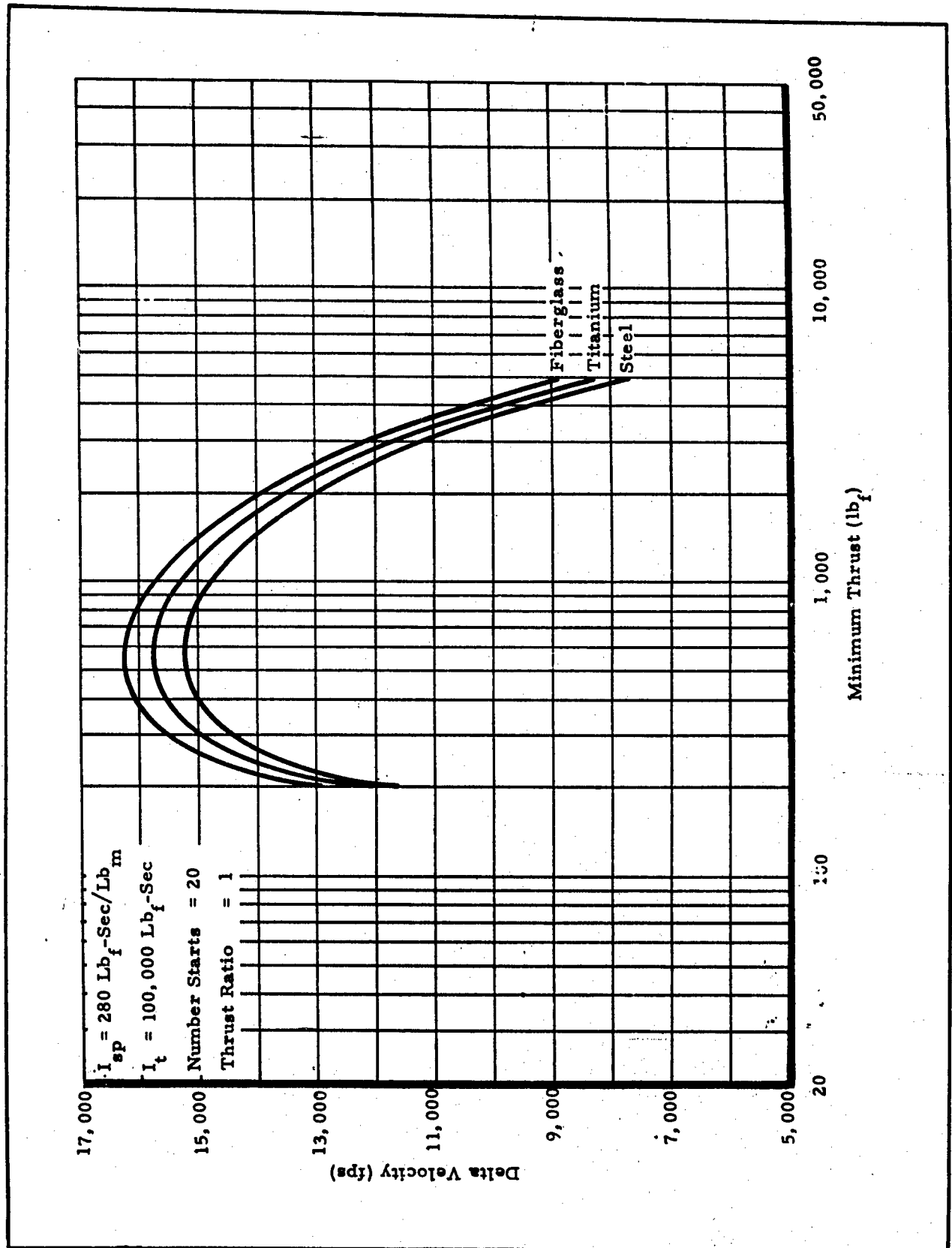


Figure B-34 - Delta Velocity versus Minimum Thrust at Thrust Ratio of 1

CONFIDENTIAL

AFRPL-TR-65-209, Vol II

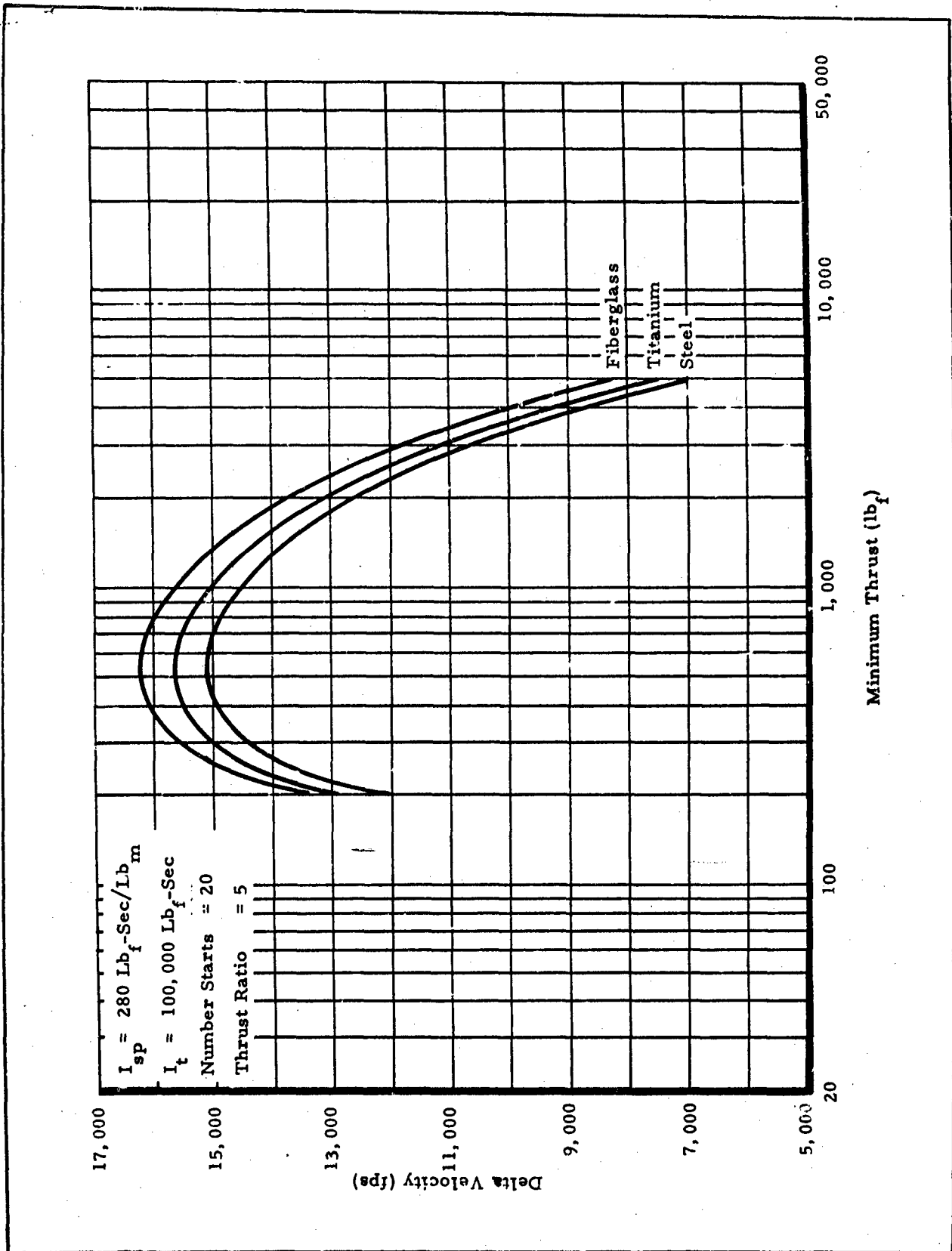


Figure B-35 - Delta Velocity versus Minimum Thrust at Thrust Ratio of 5

B-38

CONFIDENTIAL

CONFIDENTIAL

AFRPL-TR-65-209, Vol II

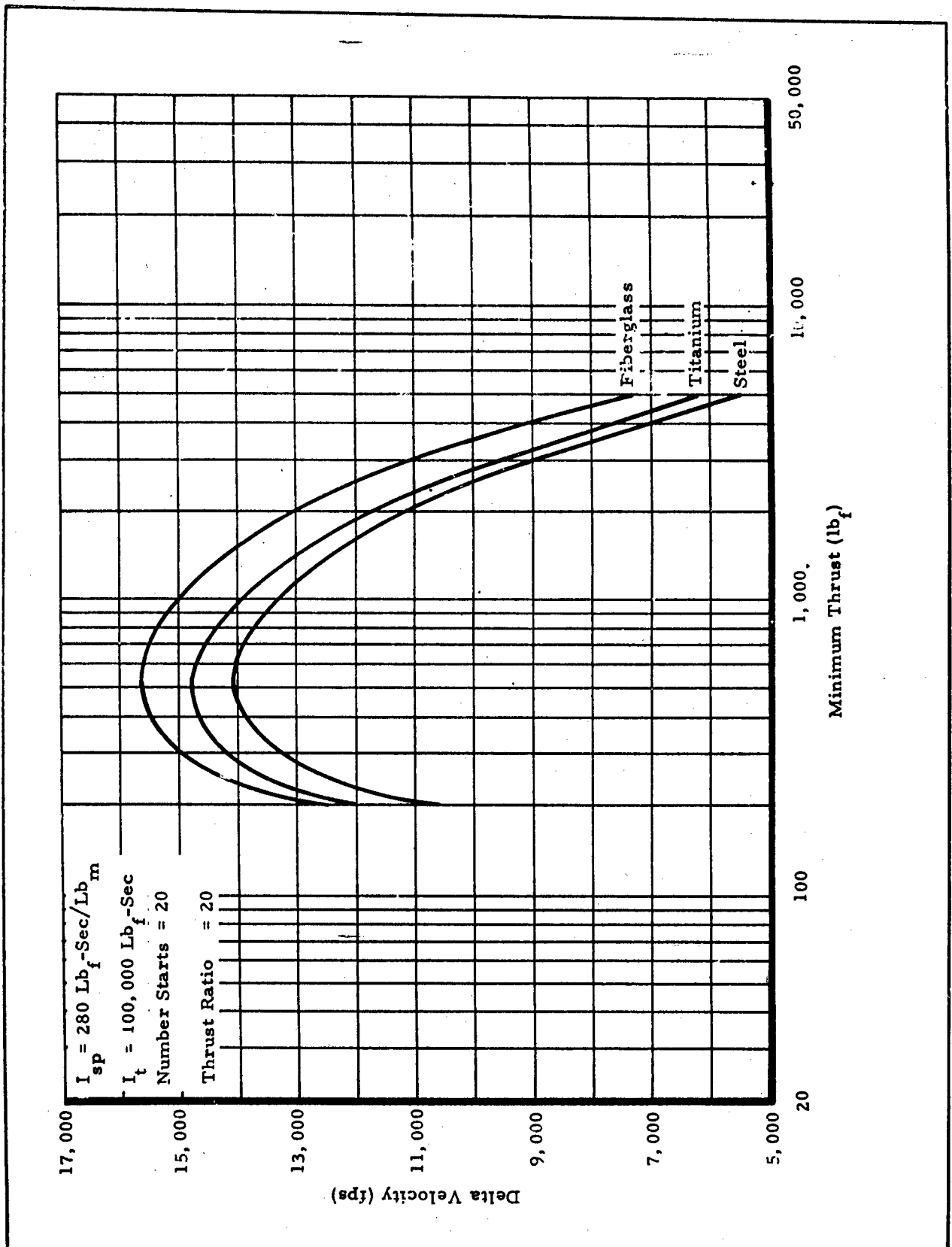


Figure B-36 - Delta Velocity versus Minimum Thrust at Thrust Ratio of 20

CONFIDENTIAL

CONFIDENTIAL

AFRPL-TR-65-209, Vol II

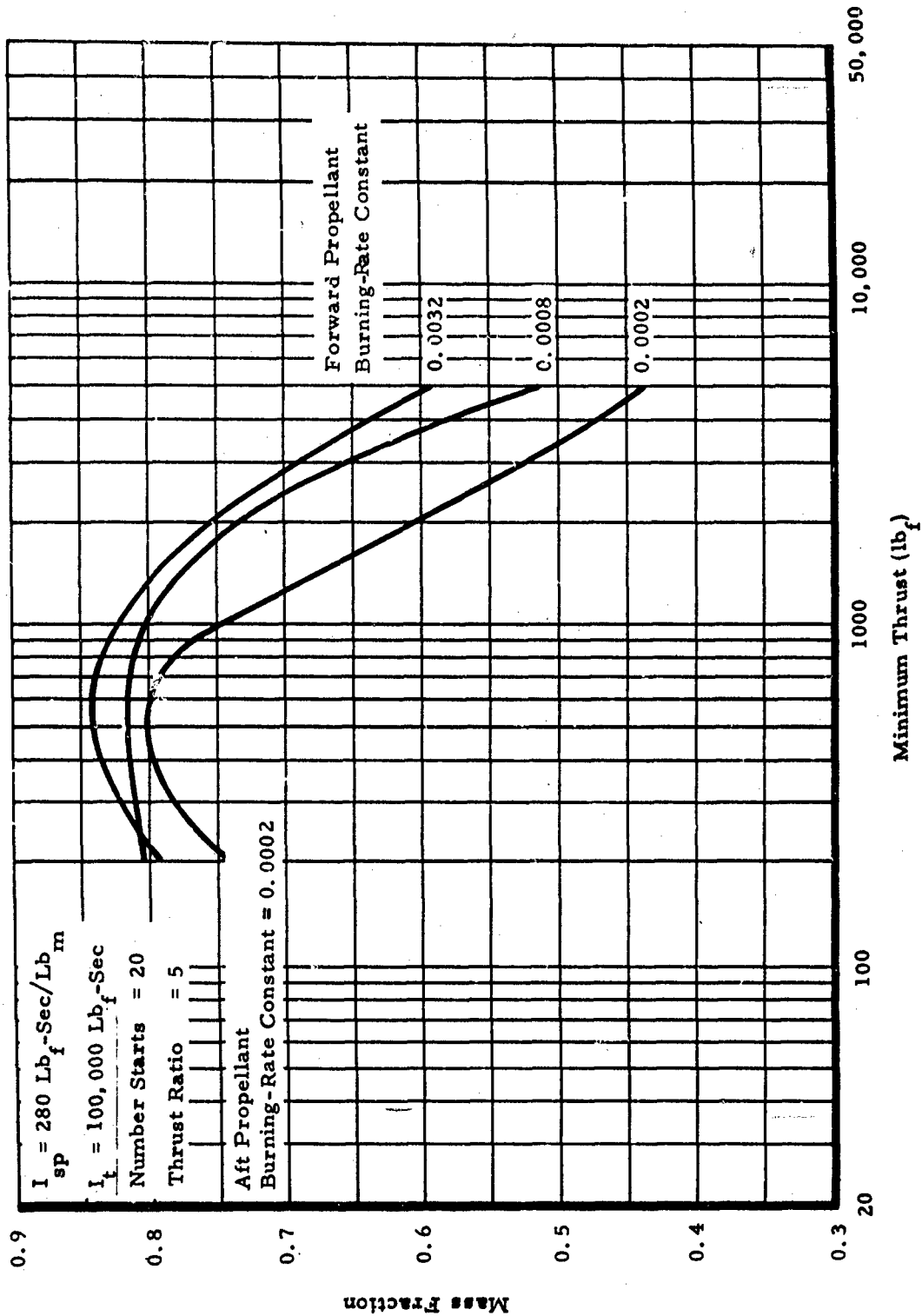


Figure B-37 - Mass Fraction versus Minimum Thrust for Aft Propellant Burning-Rate Constant of 0.0002

B-40

CONFIDENTIAL

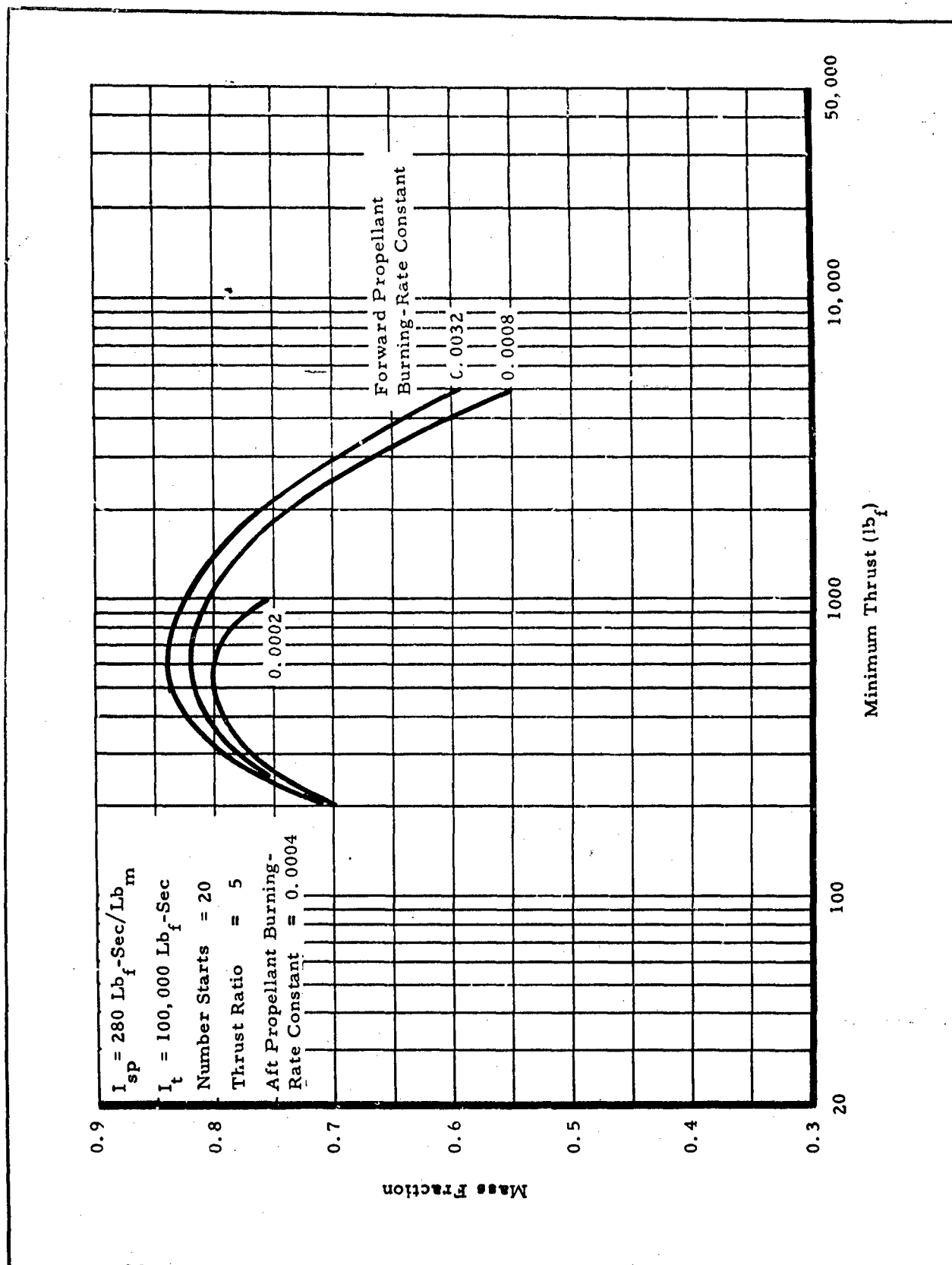


Figure B-38 - Mass Fraction versus Minimum Thrust for Aft Propellant Burning-Rate Constant of 0.0004

CONFIDENTIAL

CONFIDENTIAL

AFRPL-TR-65-209, Vol II

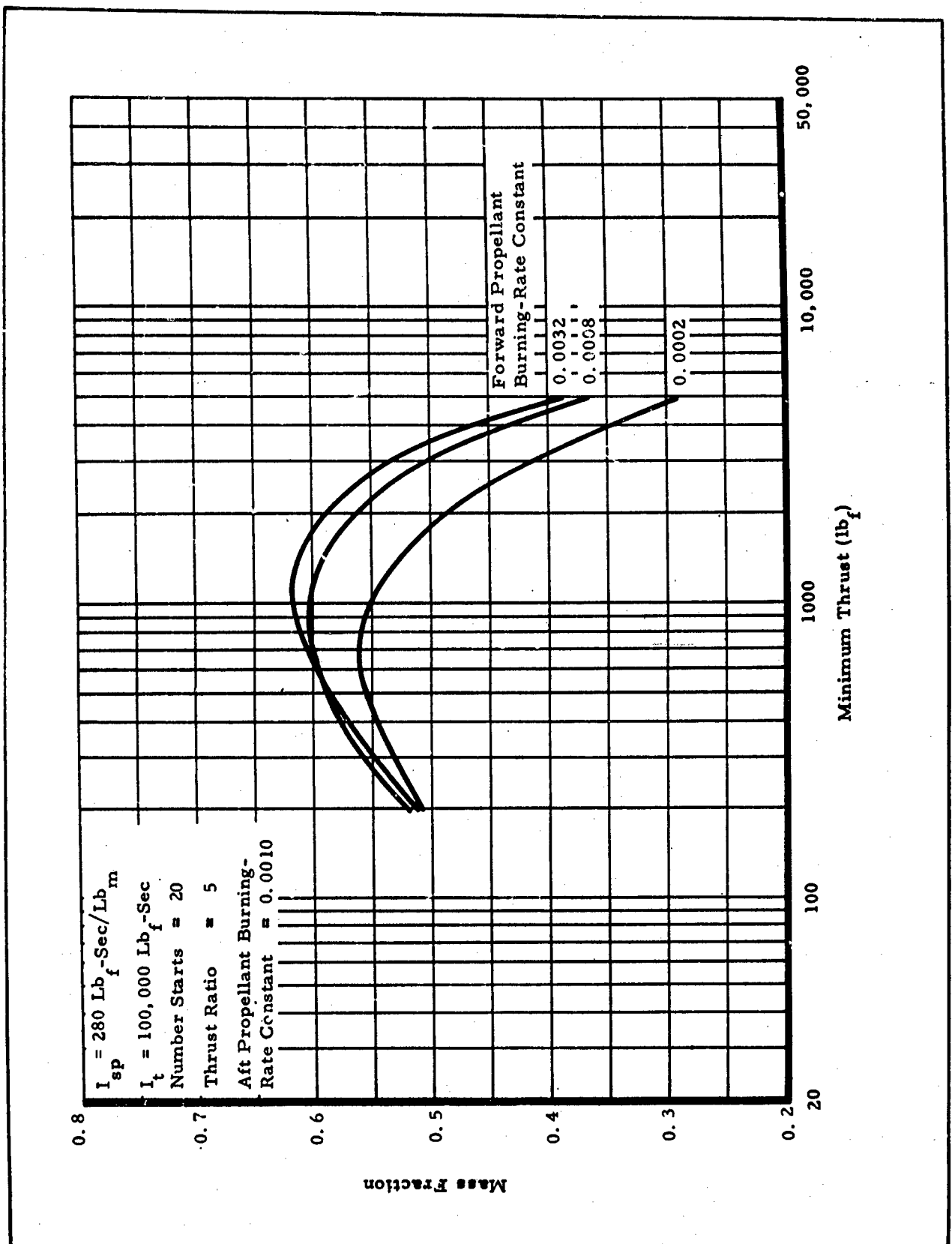


Figure B-39 - Mass Fraction versus Minimum Thrust for Aft Propellant Burning-Rate Constant of 0.0010

B-42

CONFIDENTIAL

CONFIDENTIAL

AFRPL-TR-65-209, Vol II

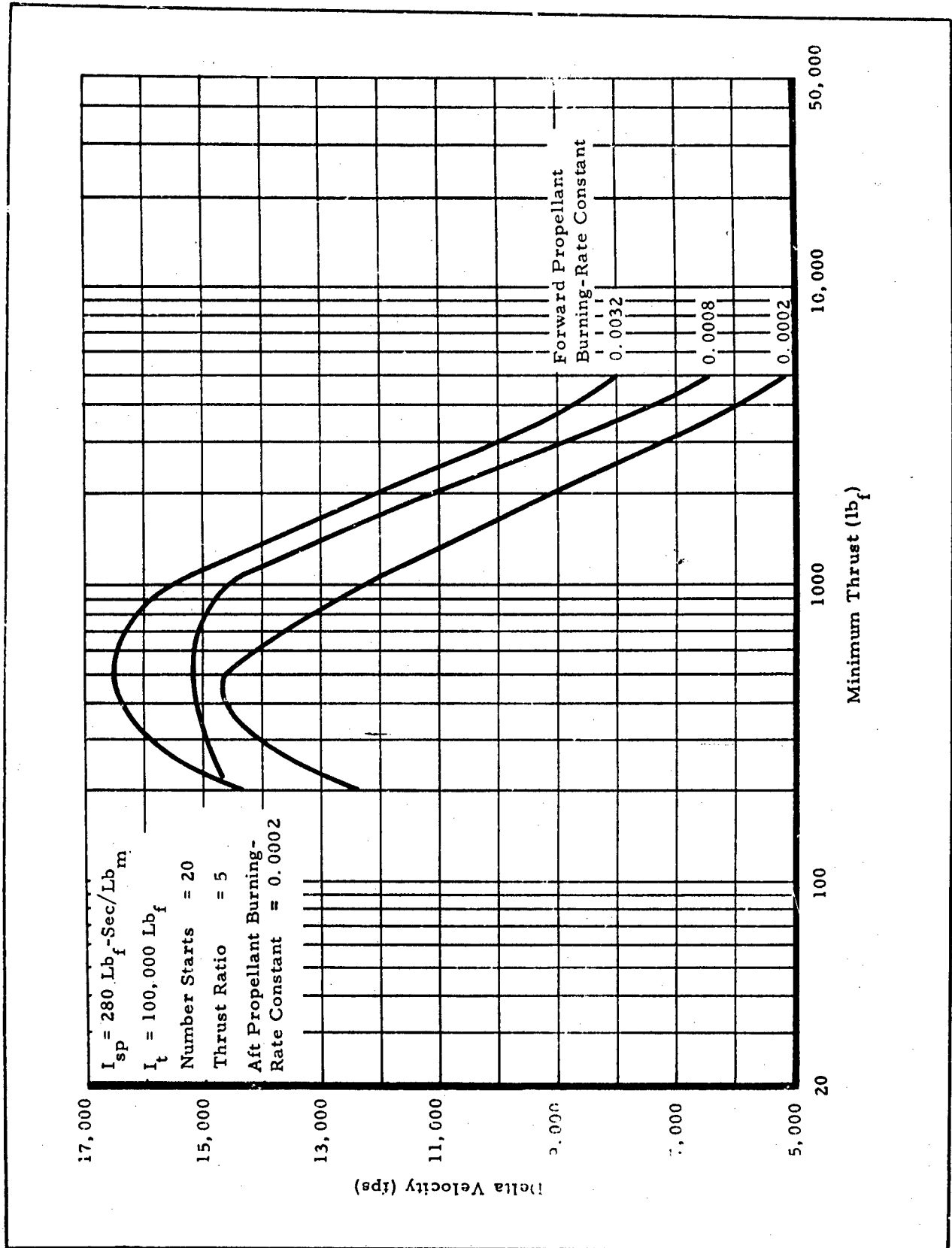


Figure B-40 - Delta Velocity versus Minimum Thrust for Aft Propellant Burning-Rate Constant of 0.0002

E-43

CONFIDENTIAL

CONFIDENTIAL

AFRPL-TR-65-209, Vol II

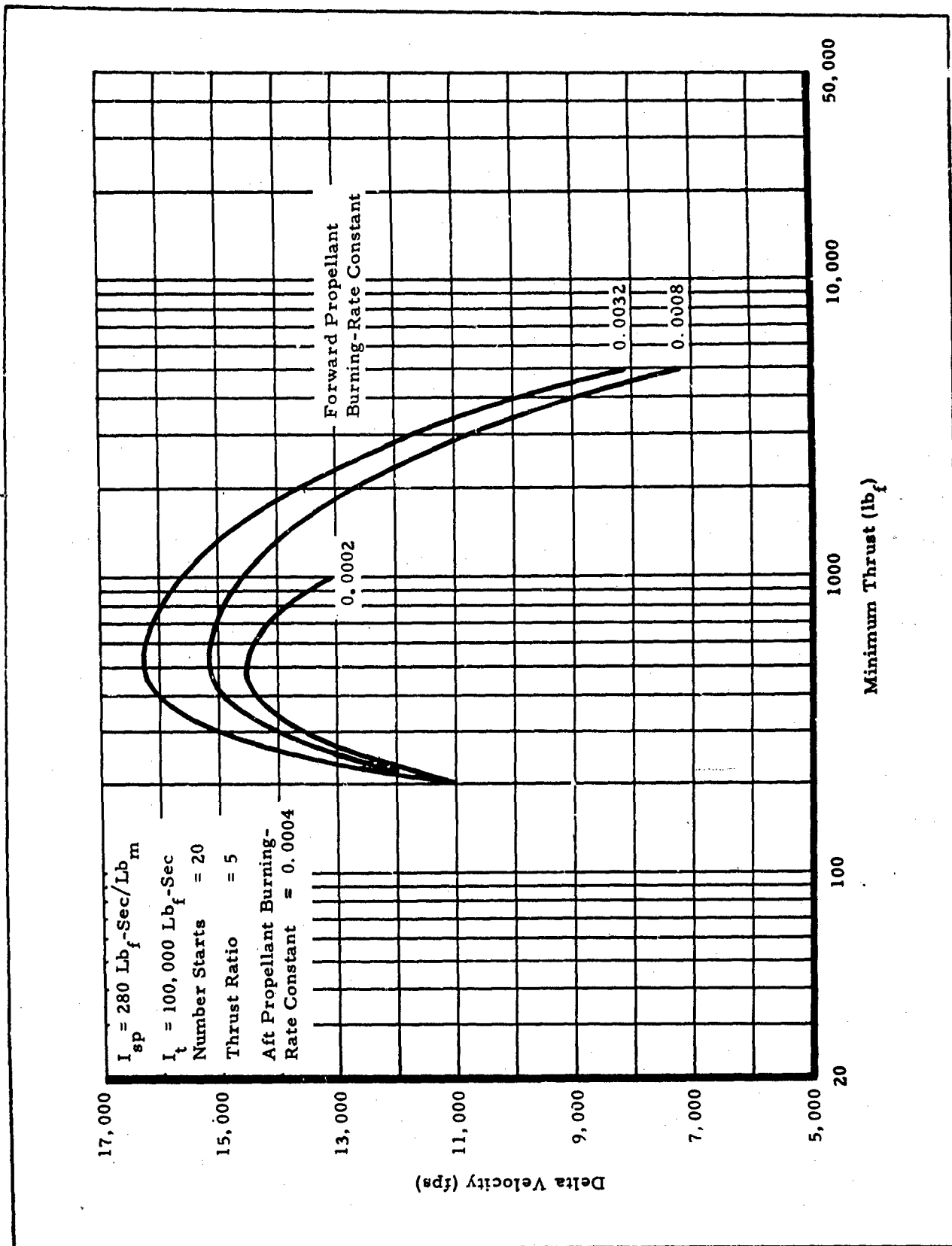


Figure B-41 - Delta Velocity versus Minimum Thrust for Aft Propellant Burning-Rate Constant of 0.0004

B-44

CONFIDENTIAL

CONFIDENTIAL

AFRPL-TR-65-209, Vol II

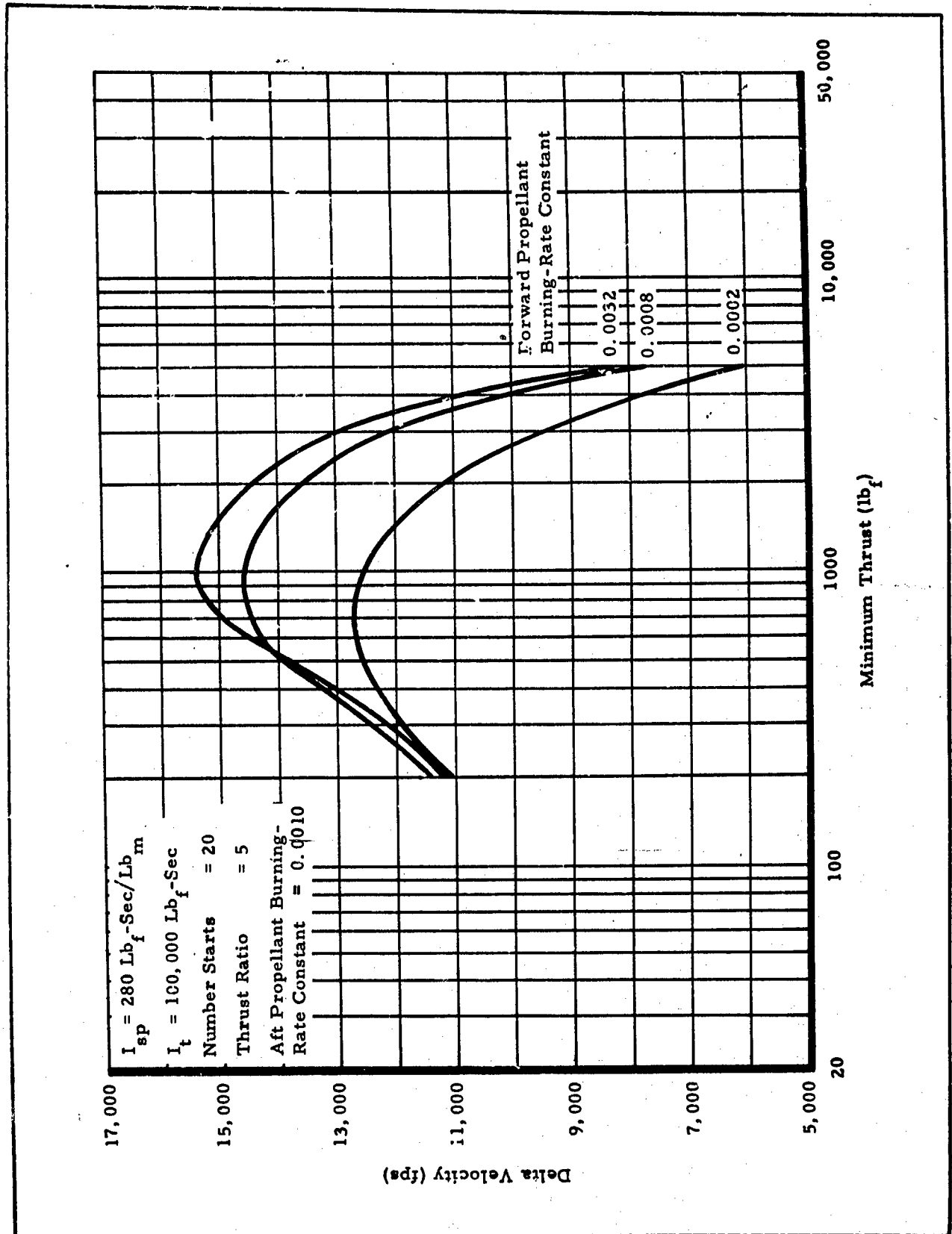


Figure B-42 - Delta Velocity versus Minimum Thrust for Aft Propellant Burning-Rate Constant of 0.0010

CONFIDENTIAL

CONFIDENTIAL

AFRPL-TR-65-209, Vol II

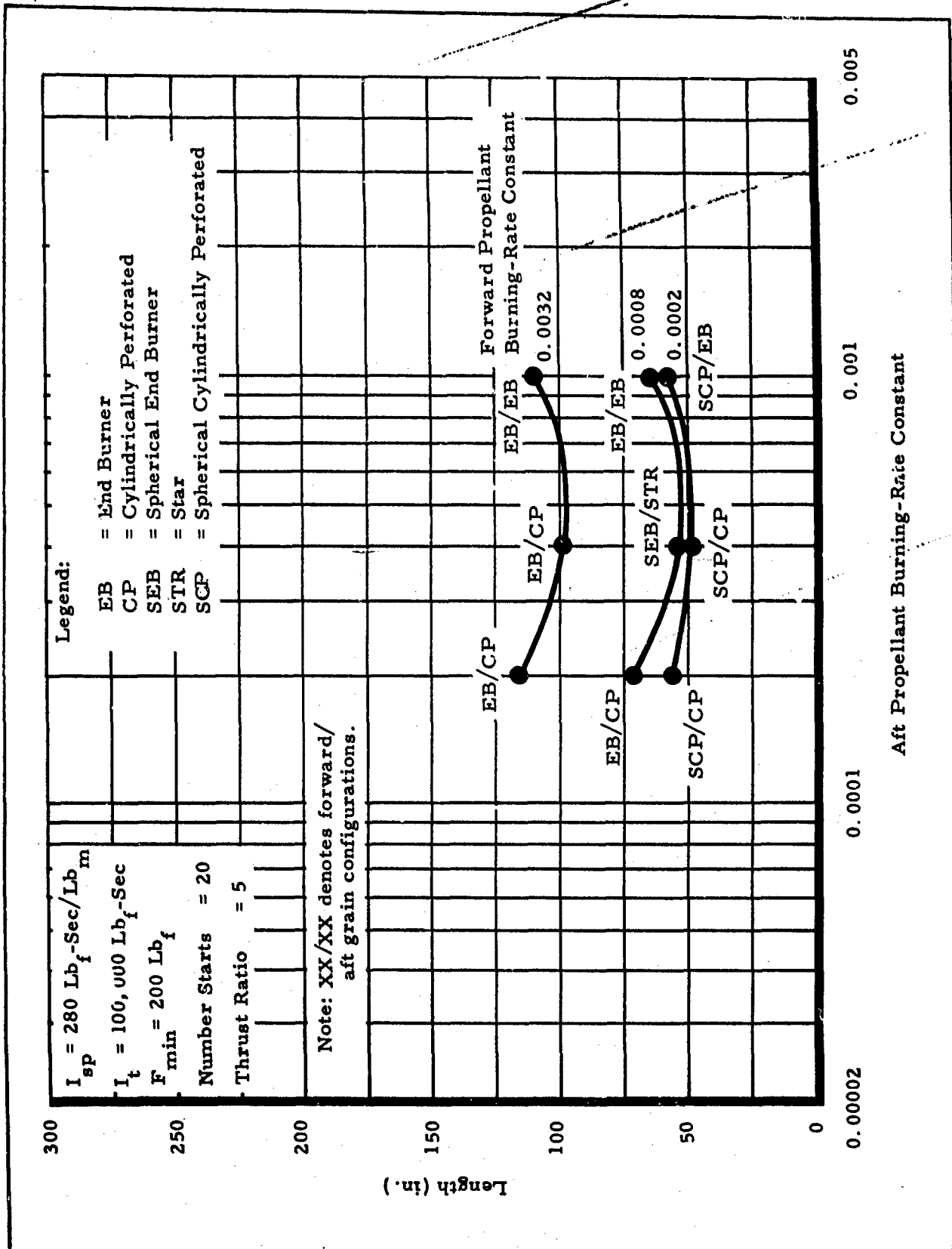


Figure B-43 - Length versus Aft Propellant Burning-Rate

Constant for $F_{min} = 200 \text{ Lb}_f$

B-46

CONFIDENTIAL

CONFIDENTIAL

AFRPL-TR-65-209, Vol II

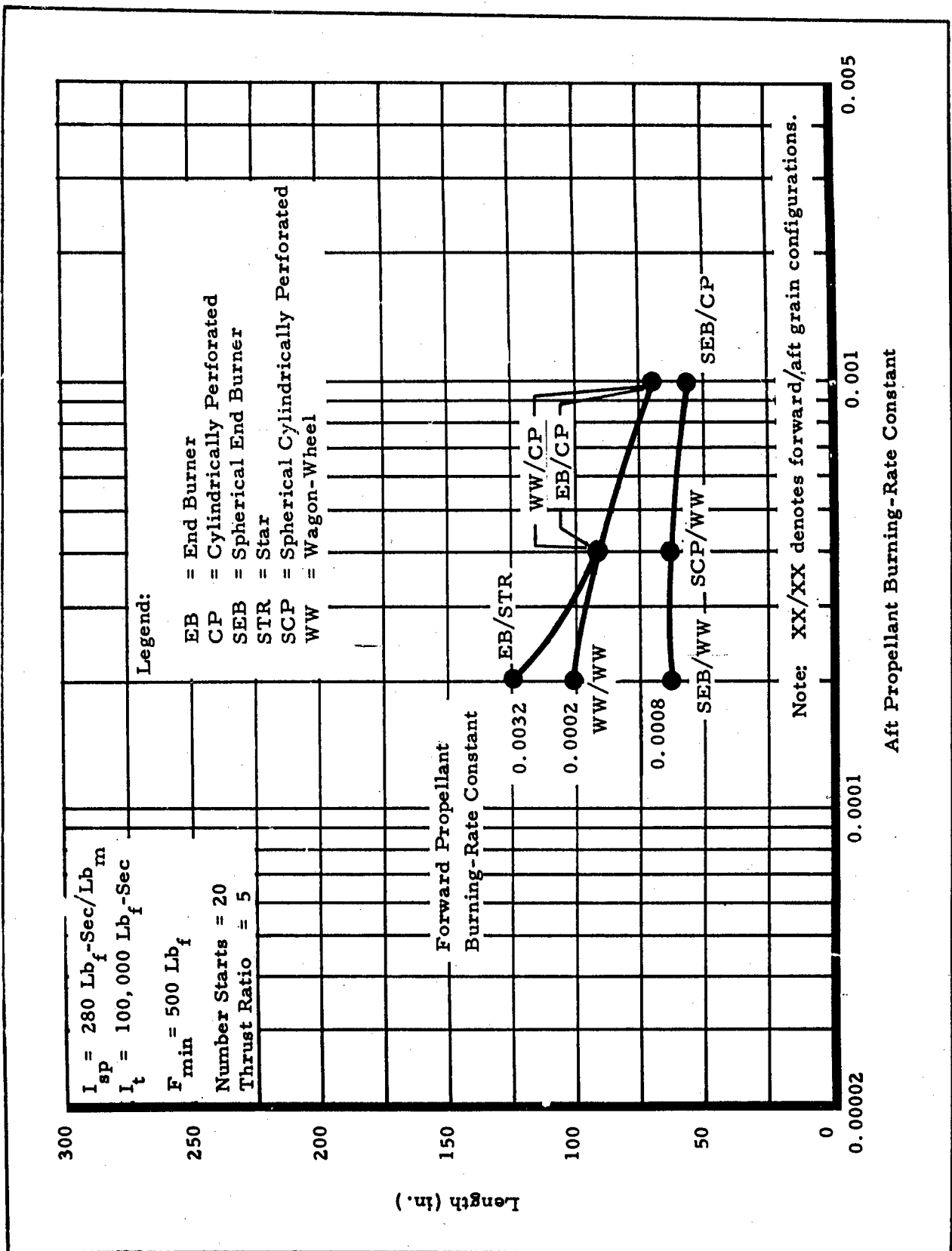


Figure B-44 - Length versus Aft Propellant Burning-Rate Constant for $F_{min} = 500 \text{ Lb}_f$

CONFIDENTIAL

CONFIDENTIAL

AFRPL-TR-65-209, Vol II

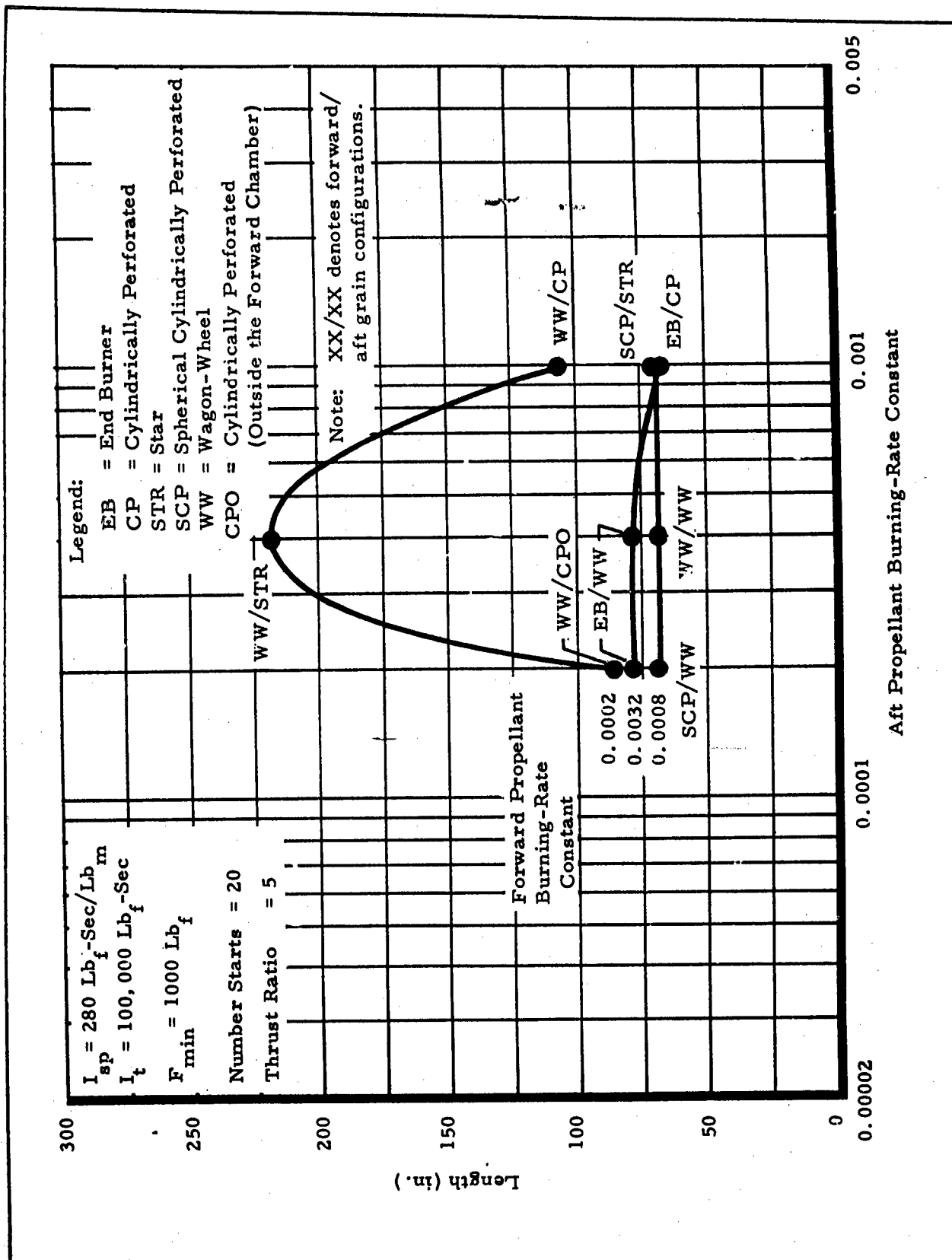


Figure B-45 - Length versus Aft Propellant Burning-Rate Constant for $F_{min} = 1000 \text{ Lb}_f$

CONFIDENTIAL

CONFIDENTIAL

AFRPL-TR-65-209, Vol II

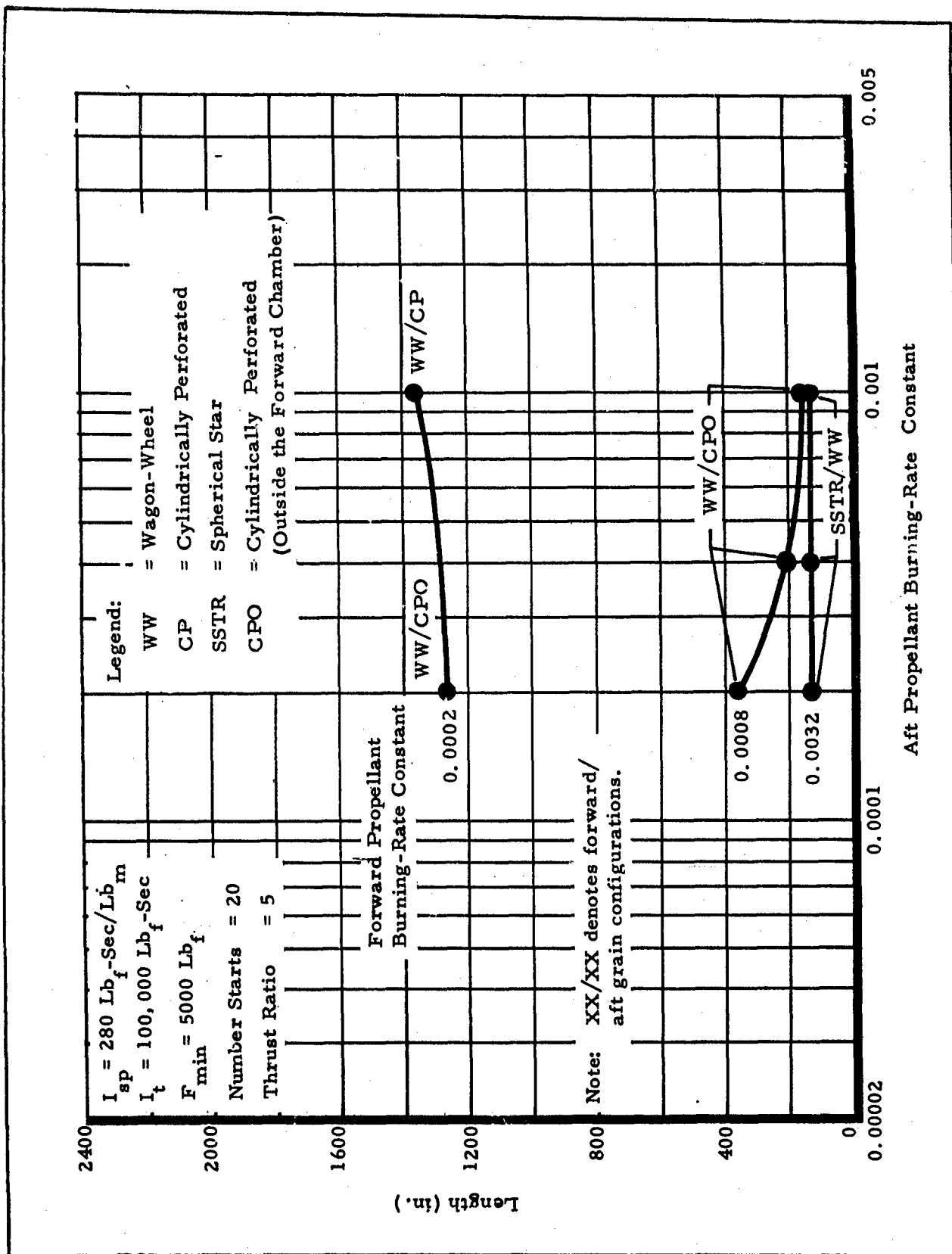


Figure B-46 - Length versus Aft Propellant Burning-Rate Constant for $F_{min} = 5000 \text{ Lb}_f$

CONFIDENTIAL

CONFIDENTIAL

AFRPL-TR-65-209, Vol II

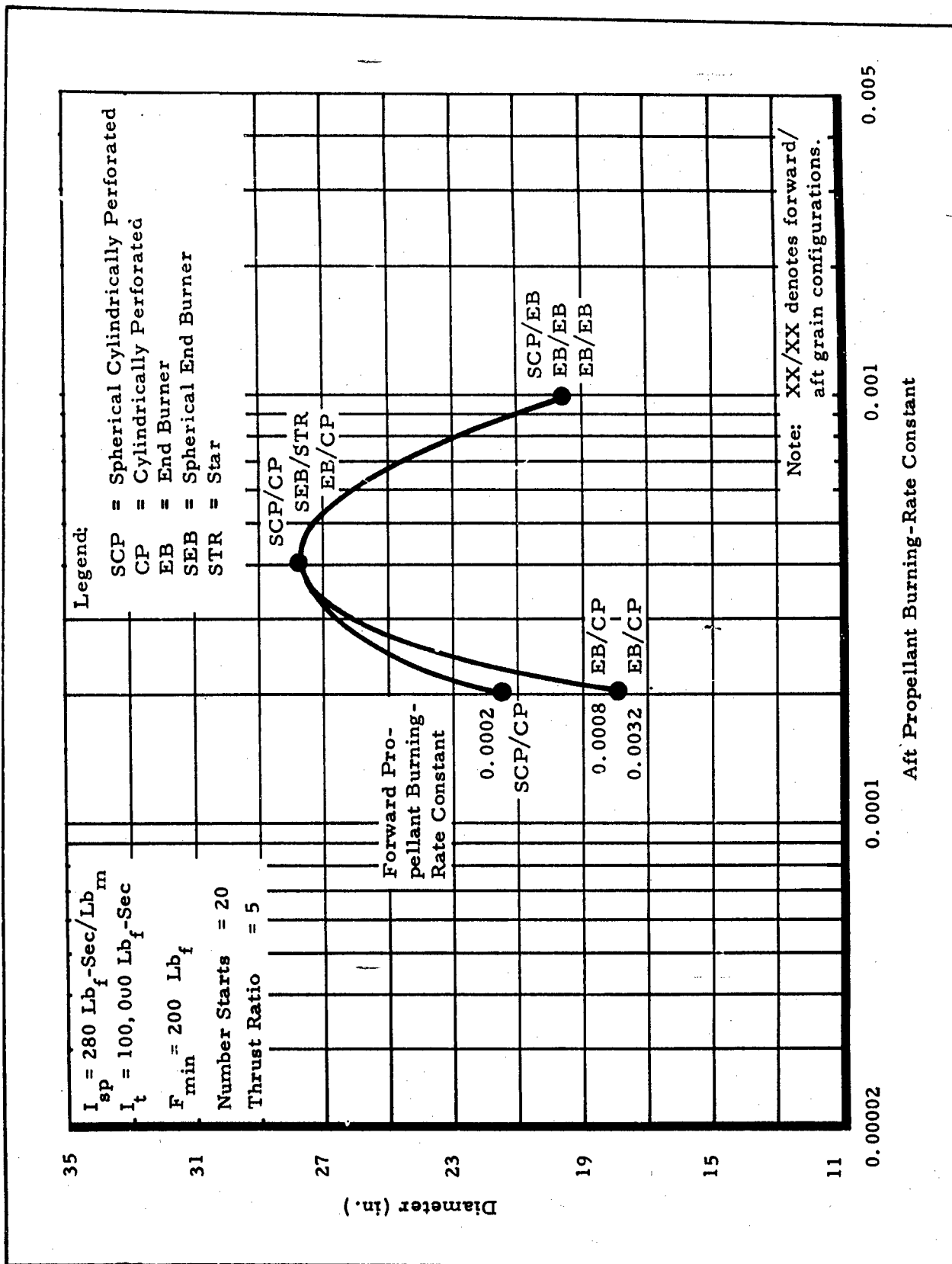


Figure B-47 - Diameter versus Aft Propellant Burning-Rate Constant for $F_{min} = 200 \text{ Lb}_f$

B-50

CONFIDENTIAL

CONFIDENTIAL

AFRPL-TR-65-209, Vol II

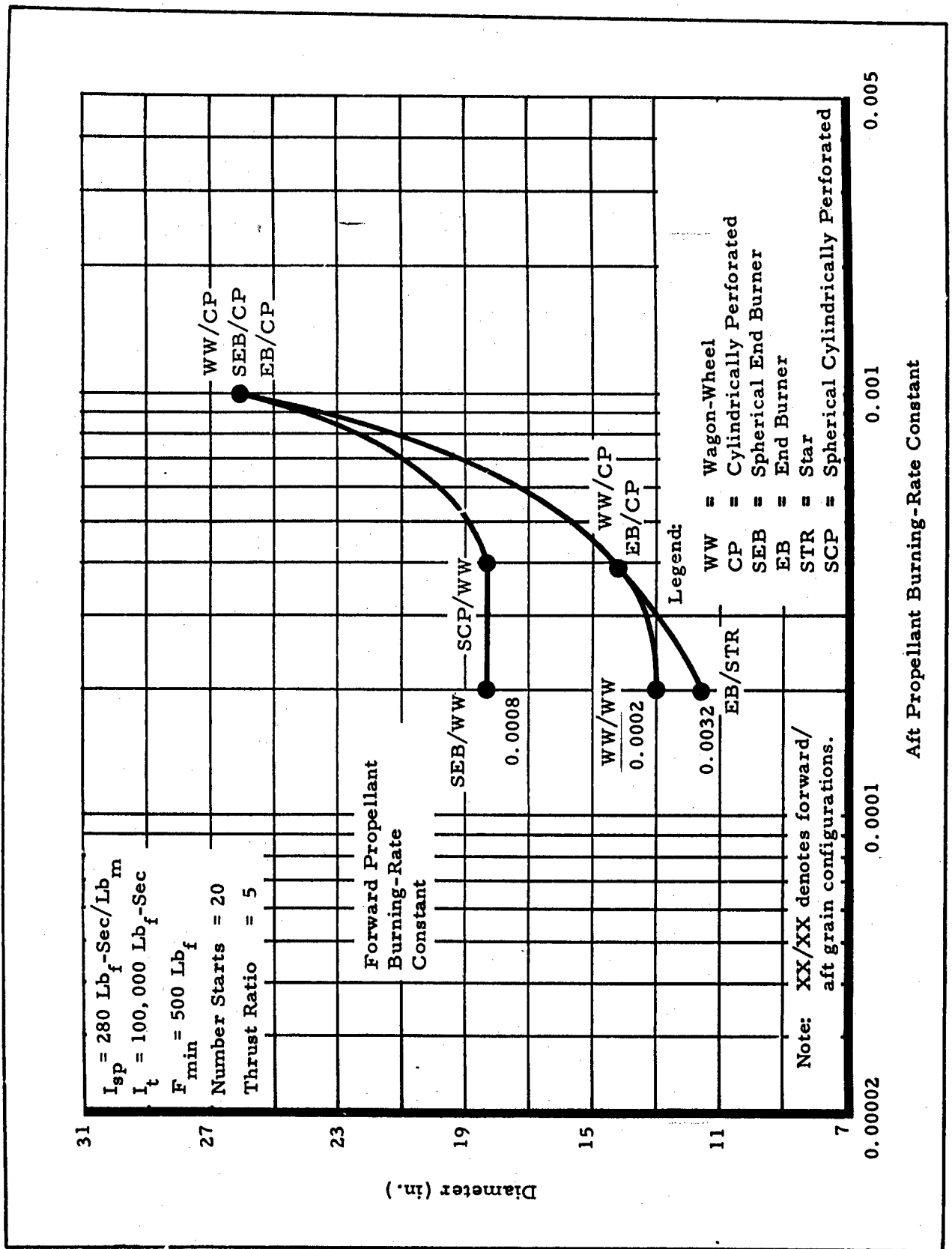


Figure B-48 - Diameter versus Aft Propellant Burning-Rate Constant for $F_{min} = 500 \text{ Lb}_f$

CONFIDENTIAL

CONFIDENTIAL

AFRPL-TR-65-209, Vol II

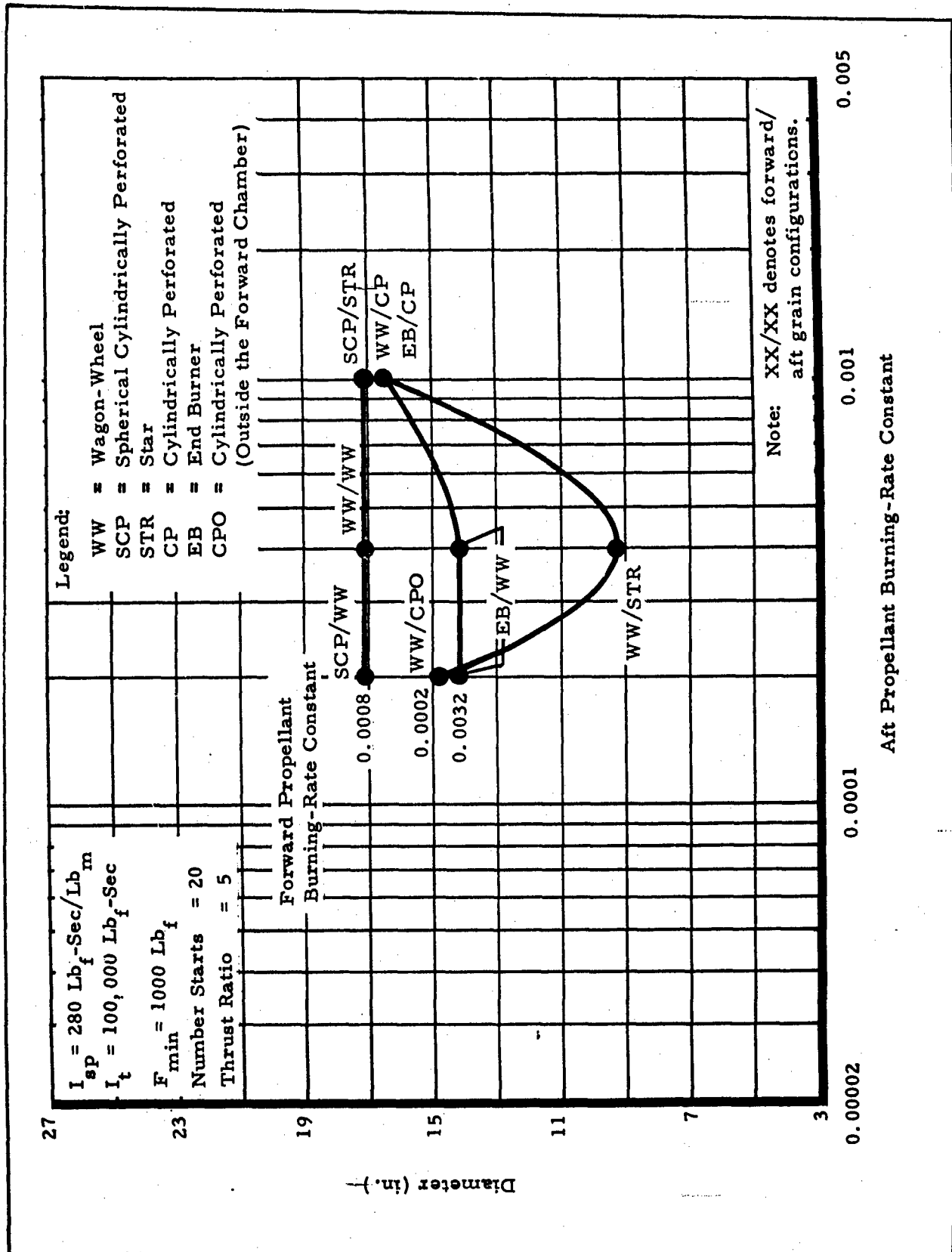


Figure B-49 - Diameter versus Aft Propellant Burning-Rate Constant for $F_{min} = 1000 \text{ Lb}_f$

B-52

CONFIDENTIAL

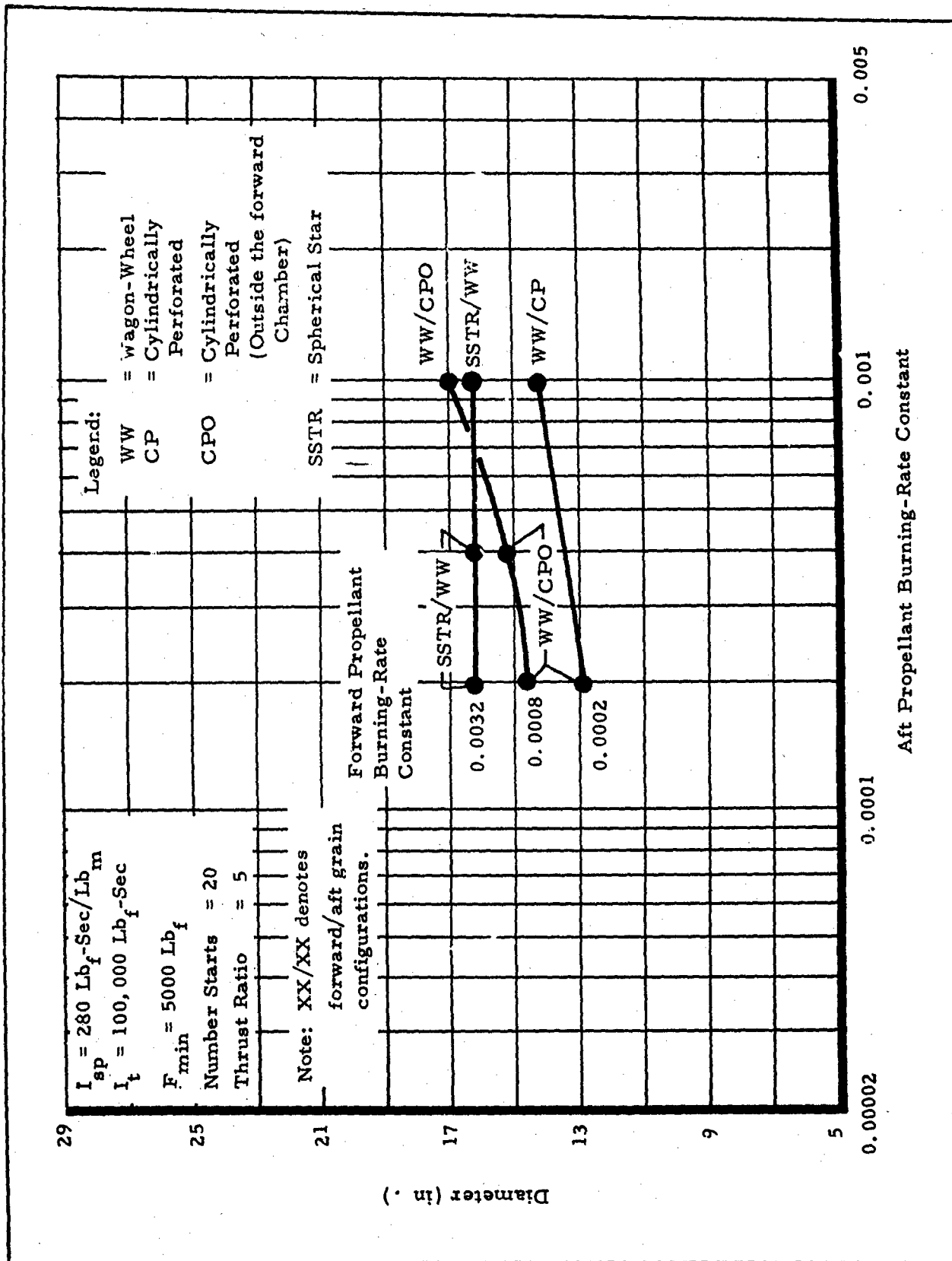


Figure B-50 - Diameter versus Aft Propellant Burning-Rate Constant for $F_{min} = 5000 \text{ Lb}_f$

CONFIDENTIAL

AFRPL-TR-65-209, Vol II

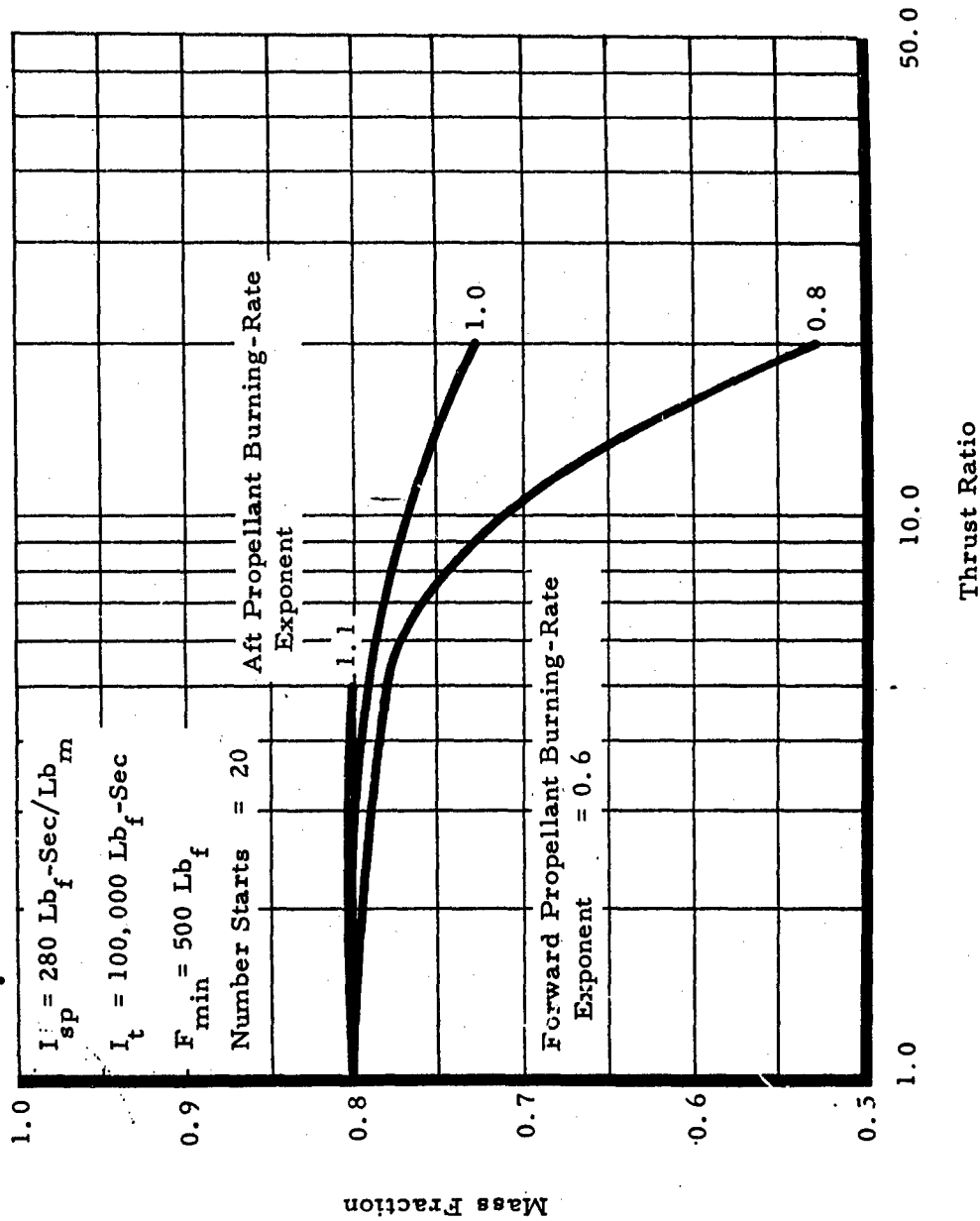


Figure B-51 - Mass Fraction versus Thrust Ratio for Forward Propellant Burning-Rate Exponent of 0.6

B-54

CONFIDENTIAL

CONFIDENTIAL

AFRPL-TR-65-209, Vol II

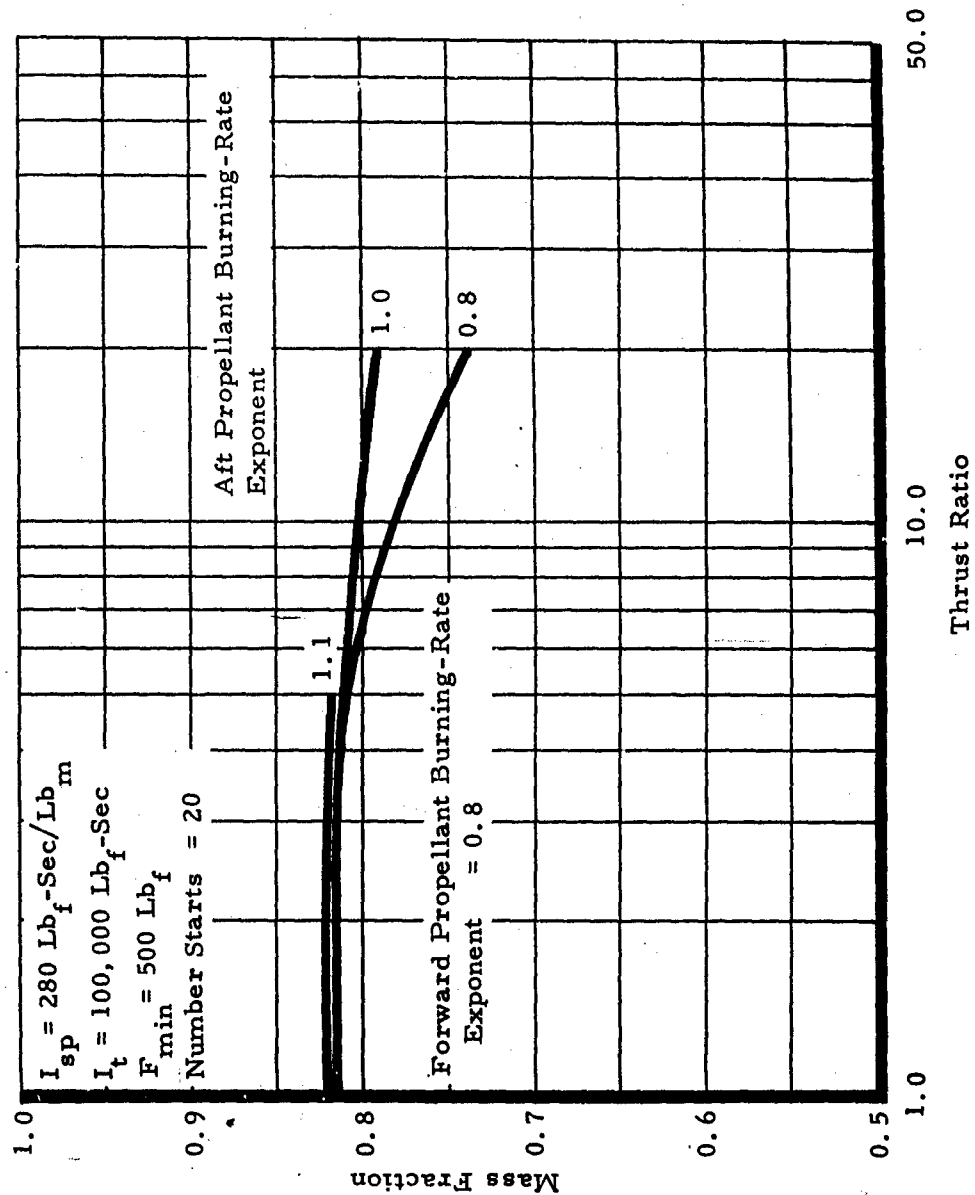


Figure B-52 - Mass Fraction versus Thrust Ratio for Forward Propellant Burning-Rate Exponent of 0.8

CONFIDENTIAL

CONFIDENTIAL

AFRPL-TR-65-209, Vol II

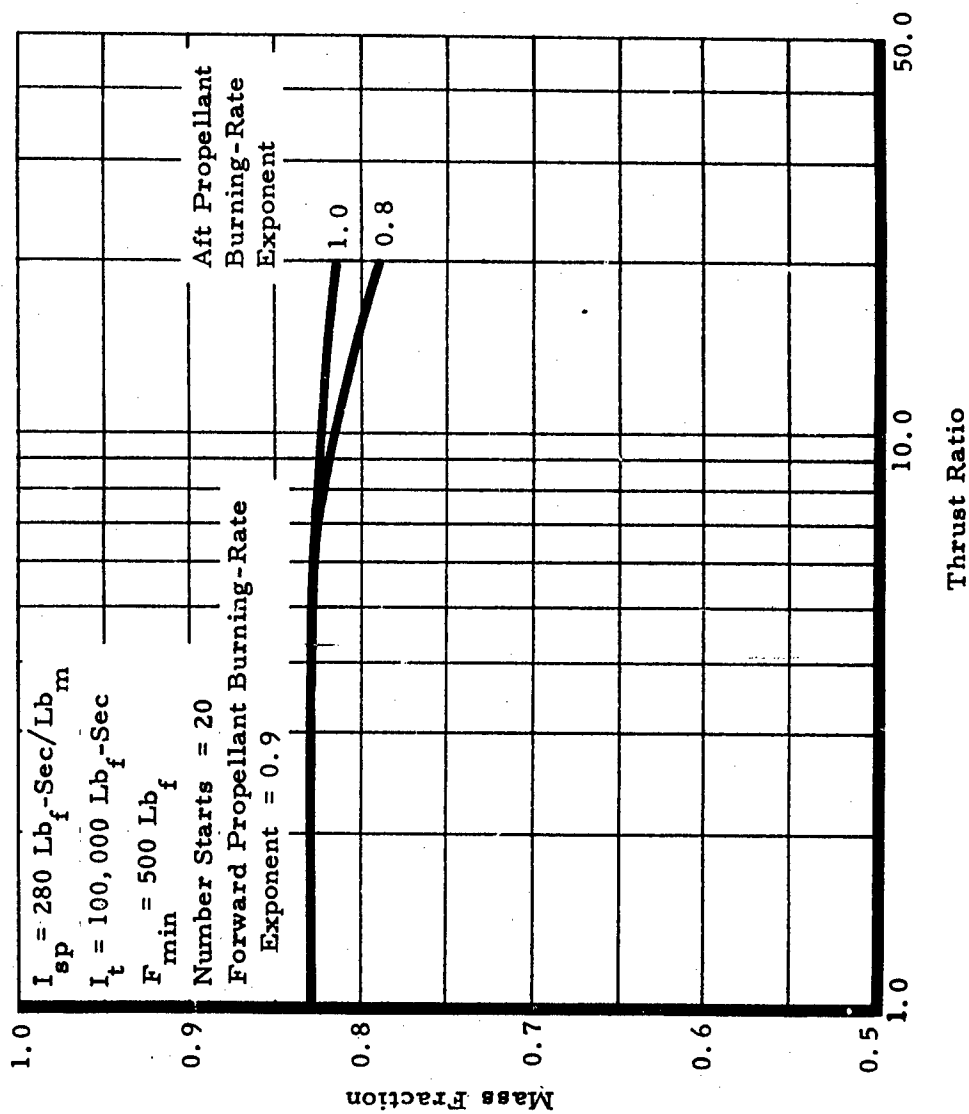


Figure B-53 - Mass Fraction versus Thrust Ratio for Forward Propellant Burning-Rate Exponent of 0.9

B-56

CONFIDENTIAL

CONFIDENTIAL

AFRPL-TR-65-209, Vol II

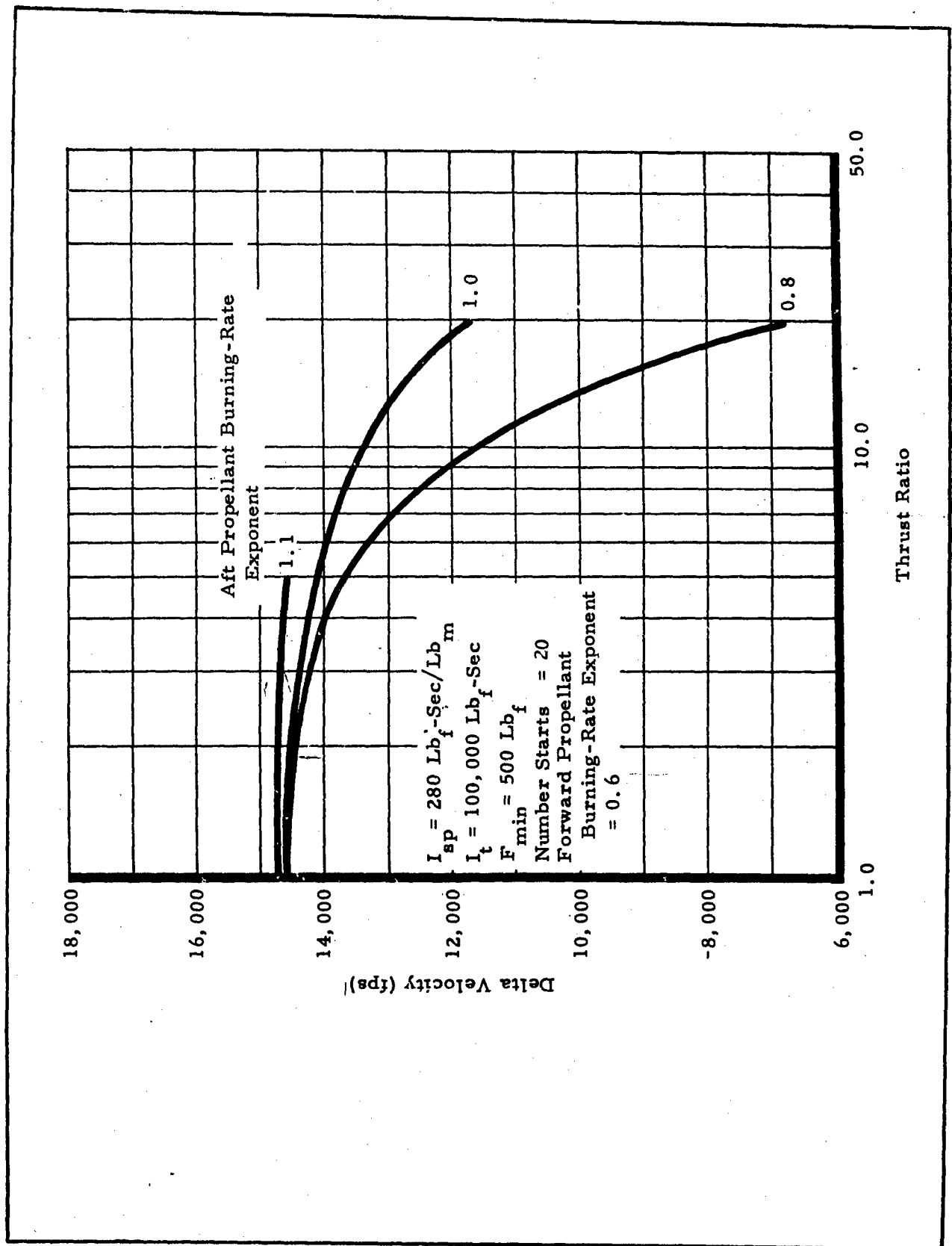


Figure B-54 - Delta Velocity versus Thrust Ratio for Forward Propellant Burning-Rate Exponent of 0.6

CONFIDENTIAL

CONFIDENTIAL

AFRPL-TR-65-209, Vol II

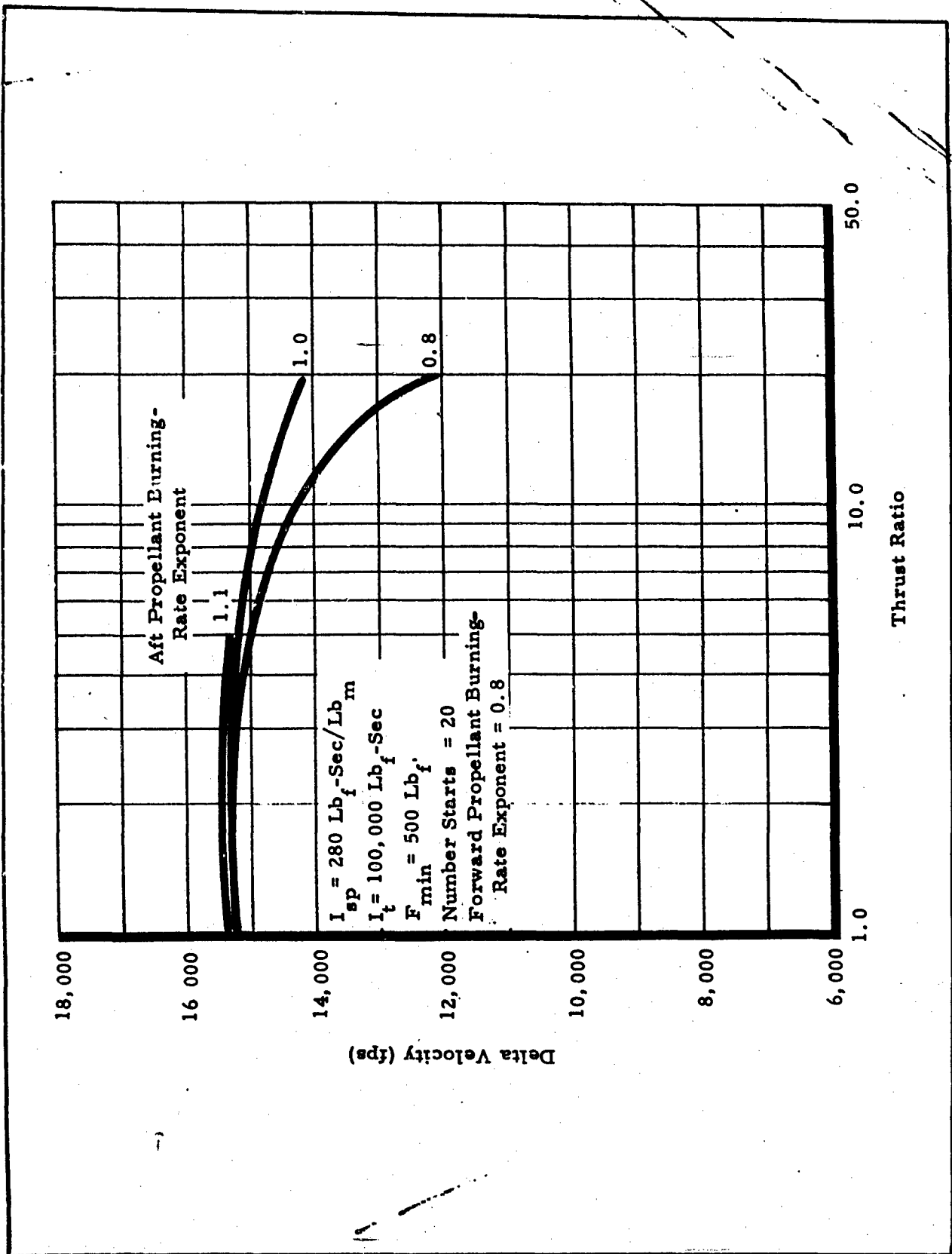


Figure B-55 - Delta Velocity versus Thrust Ratio for Forward Propellant Burning-Rate Exponent of 0.8

B-58

CONFIDENTIAL

CONFIDENTIAL

AFRPL-TR-65-209, Vol II

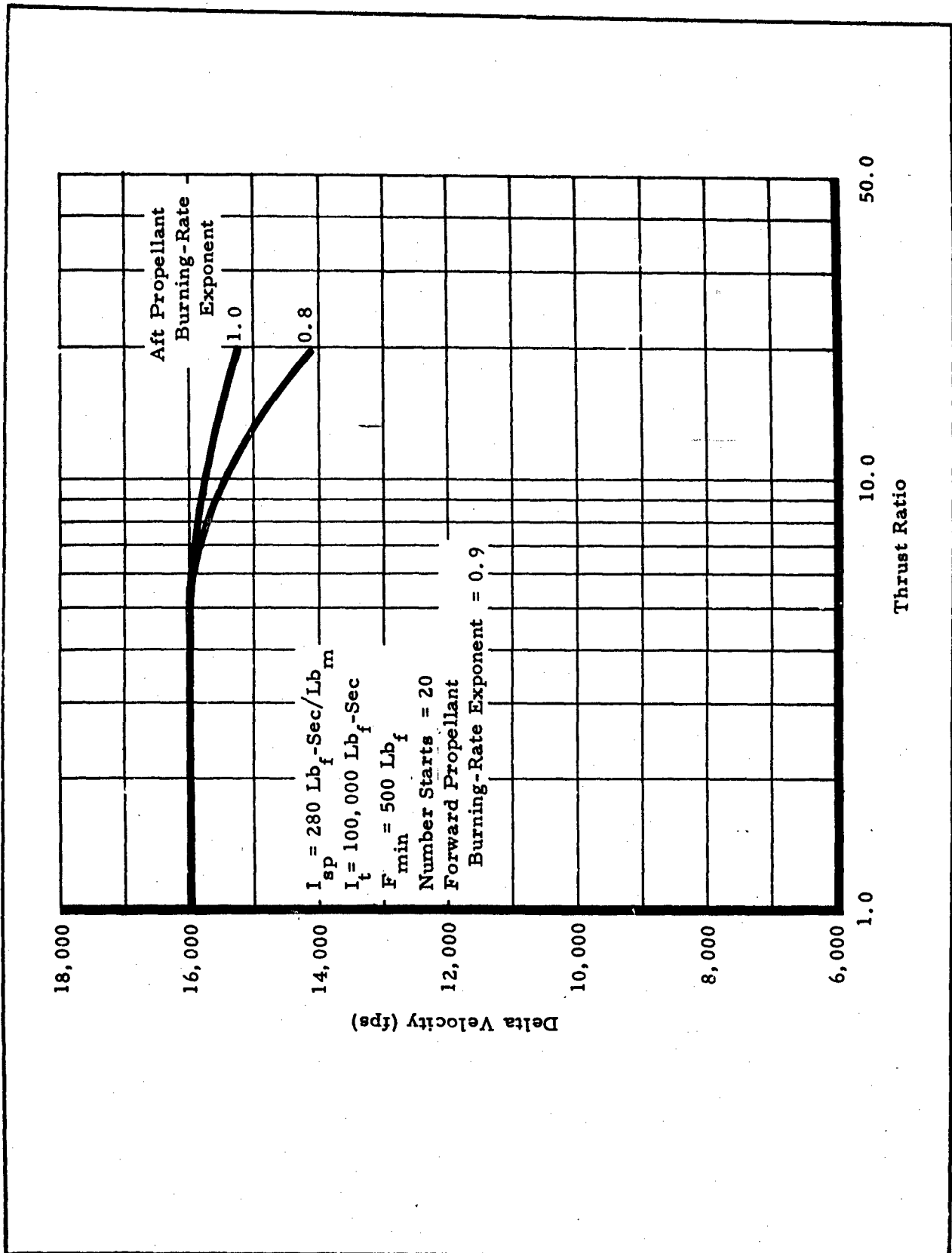


Figure B-56 - Delta Velocity versus Thrust Ratio for Forward Propellant Burning-Rate Exponent of 0.9

B-59

CONFIDENTIAL

CONFIDENTIAL

AFRPL-TR-65-209, Vol II

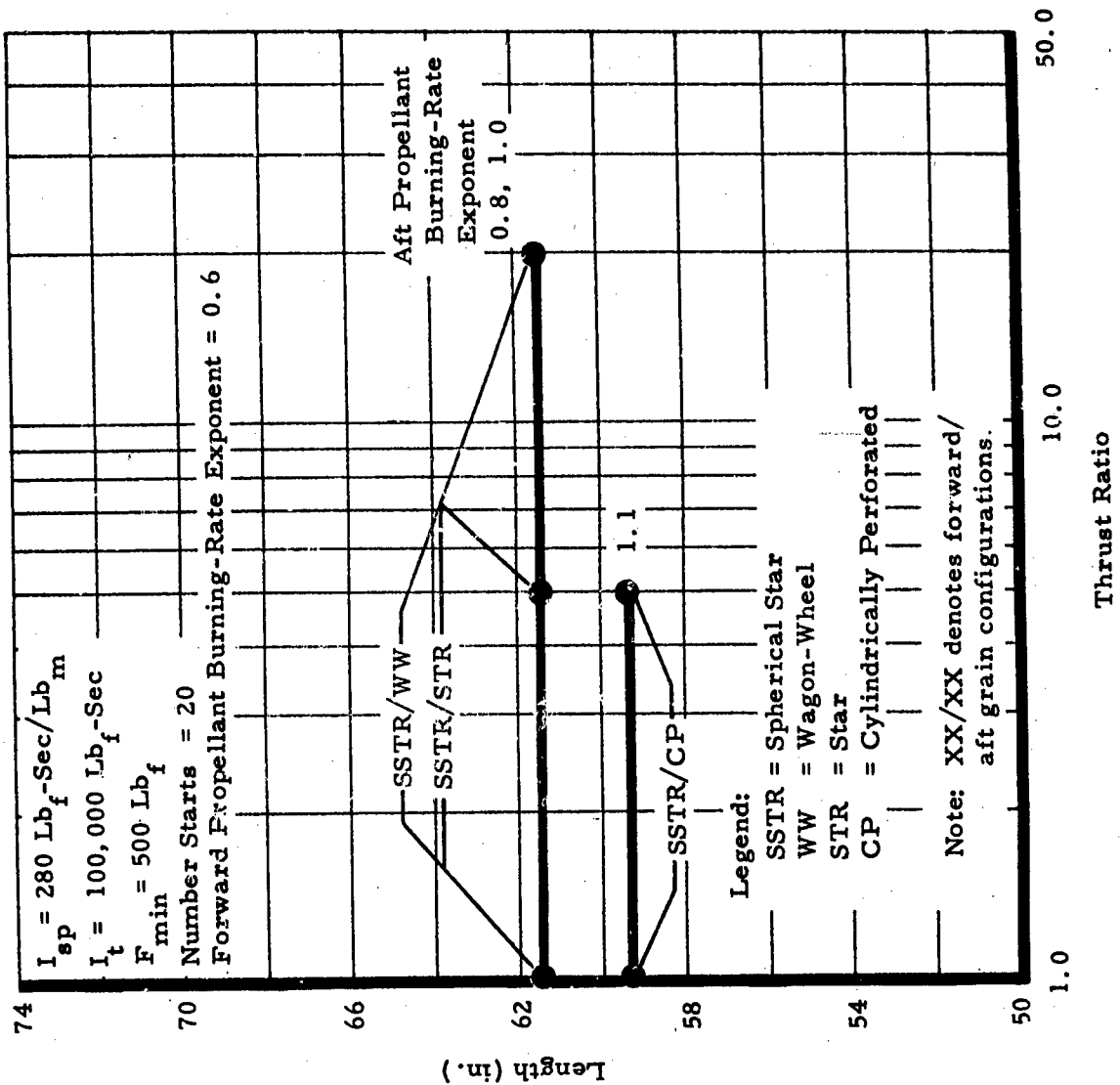


Figure B-57 - Length versus Thrust Ratio for Forward Propellant
Burning-Rate Exponent of 0.6

B-60

CONFIDENTIAL

CONFIDENTIAL

AFRPL-TR-65-209, Vol II

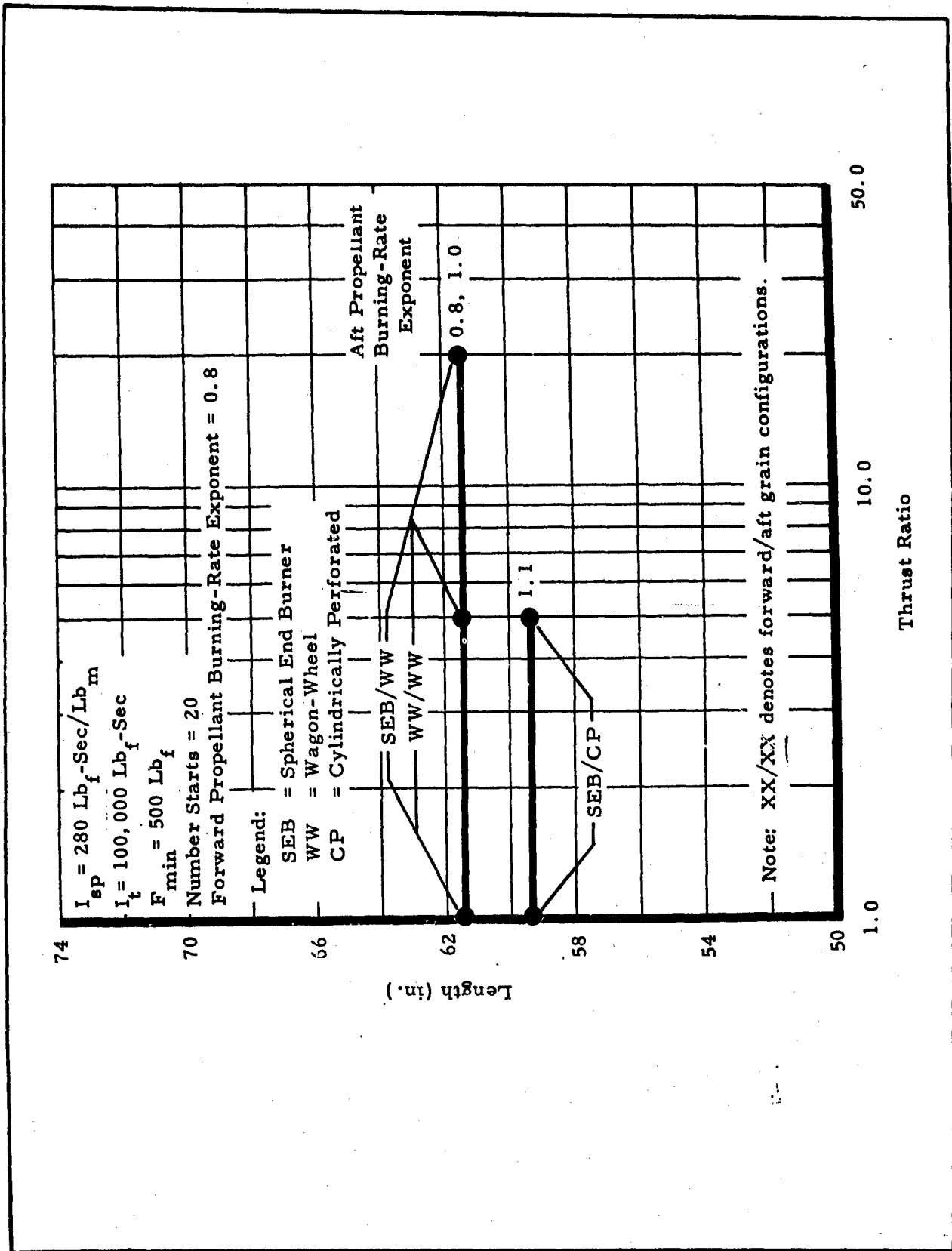


Figure B-58 - Length versus Thrust Ratio for Forward Propellant Burning-Rate Exponent of 0.8

B-61

CONFIDENTIAL

CONFIDENTIAL

AFRPL-TR-65-209, Vol II

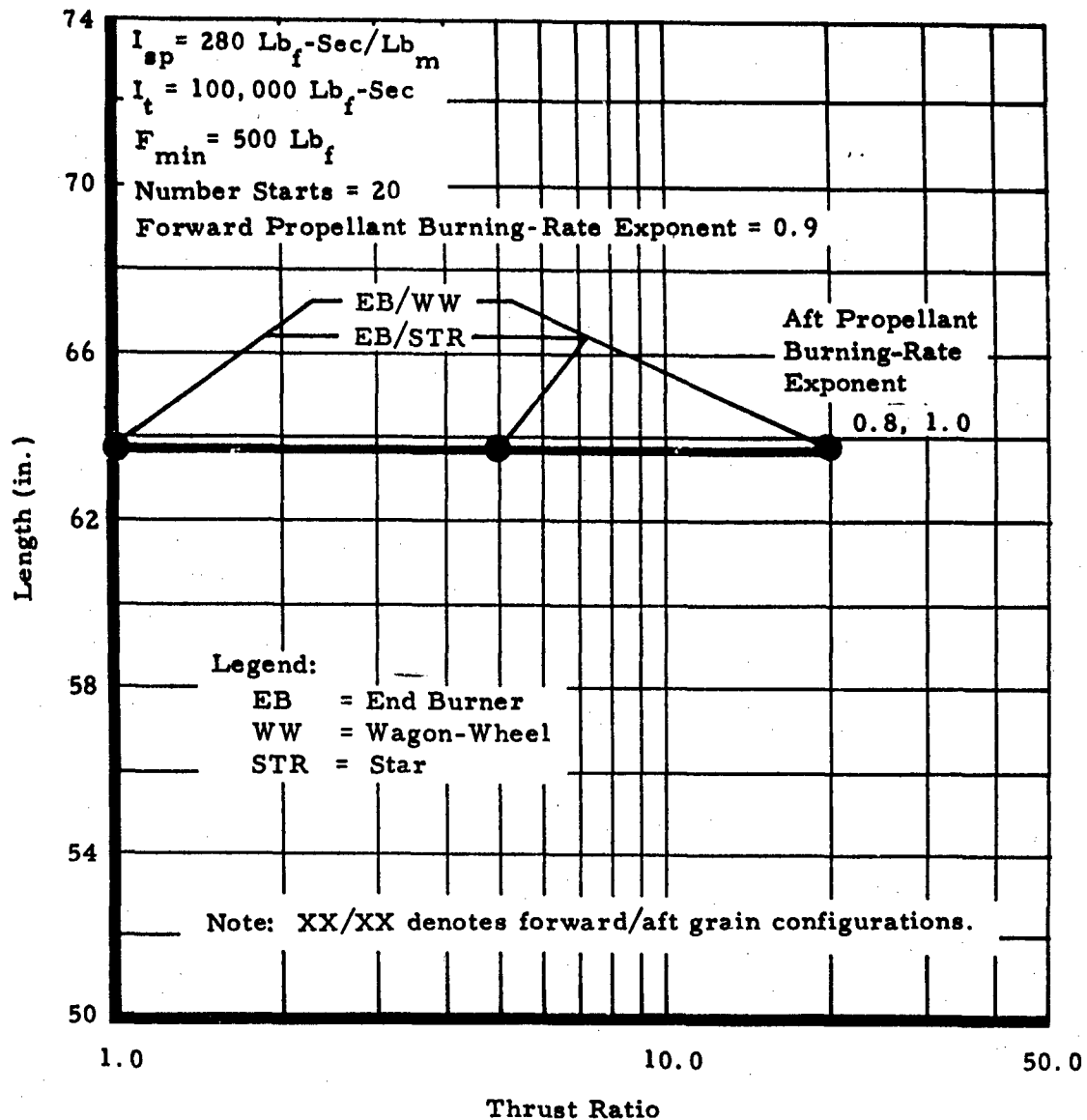


Figure B-59 - Length versus Thrust Ratio for Forward Propellant
Burning-Rate Exponent of 0.9

B-62

CONFIDENTIAL

CONFIDENTIAL

AFRPL-TR-65-209, Vol II

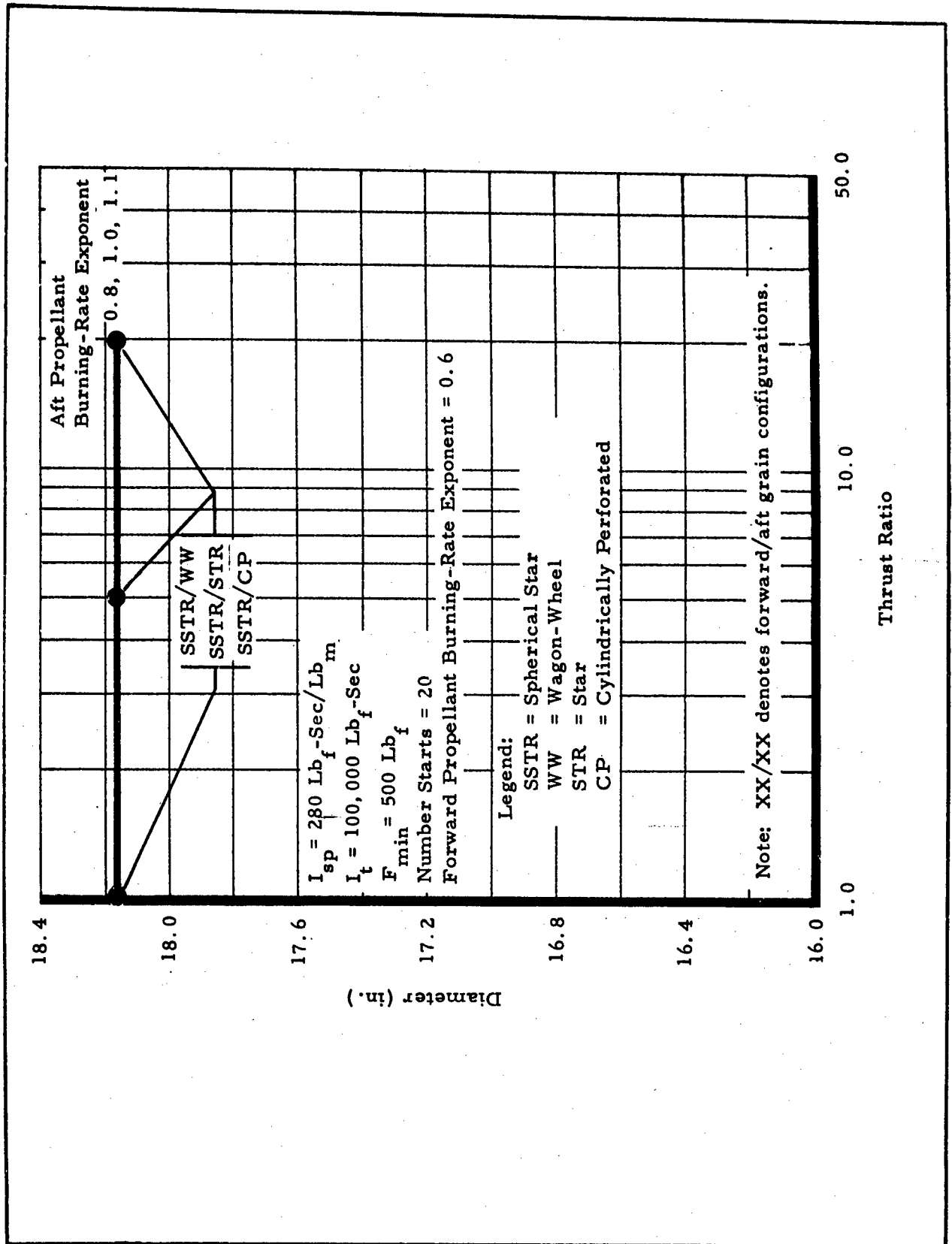


Figure B-60 - Diameter versus Thrust Ratio for Forward Propellant Burning-Rate Exponent of 0.6

CONFIDENTIAL

CONFIDENTIAL

AFRPL-TR-65-209, Vol II

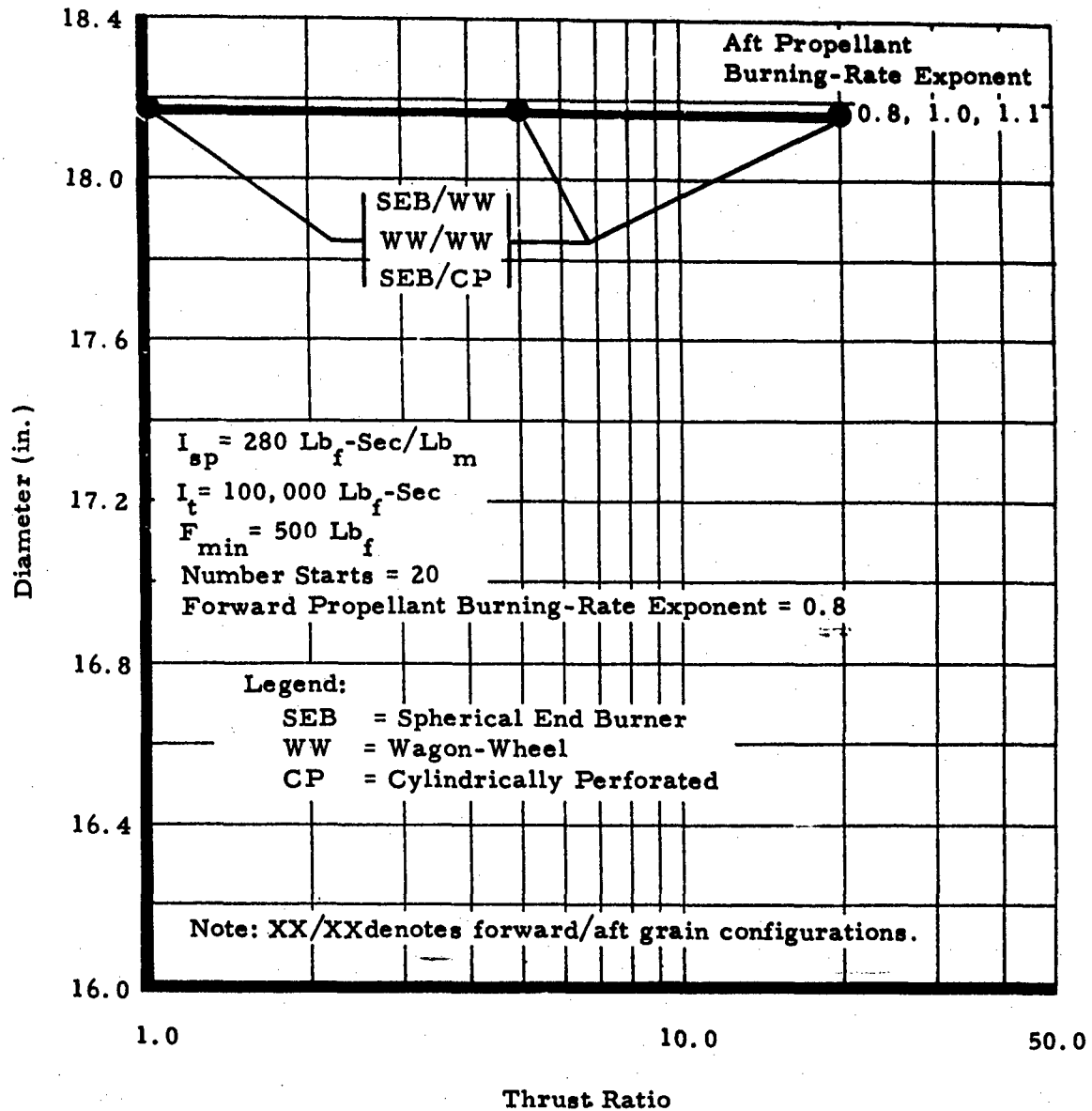


Figure B-61 - Diameter versus Thrust Ratio for Forward Propellant Burning-Rate Exponent of 0.8

B-64

CONFIDENTIAL

CONFIDENTIAL

AFRPL-TR-65-209, Vol II

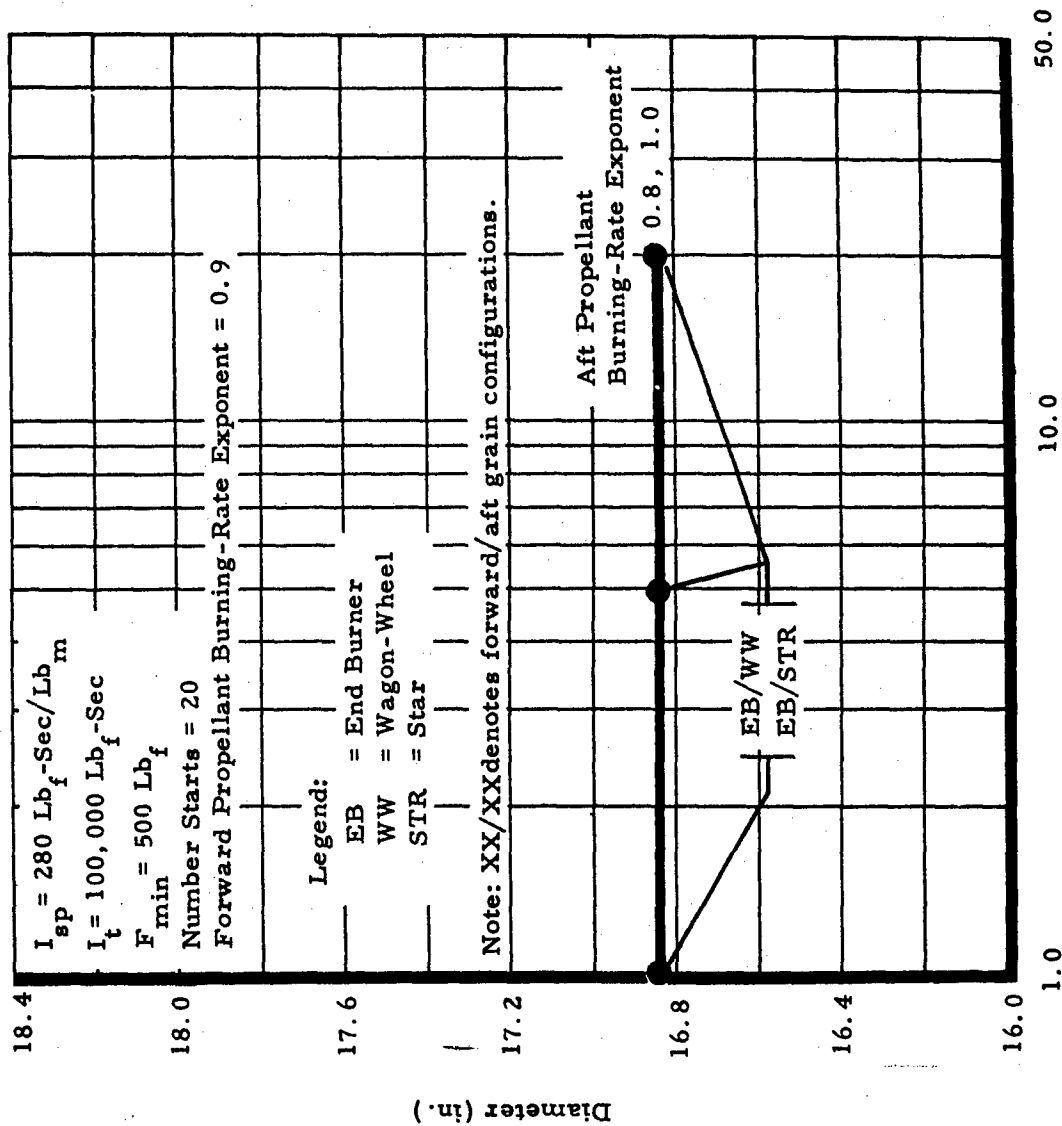


Figure B-62 - Diameter versus Thrust Ratio for Forward Propellant Burning-Rate Exponent of 0.9

B-65

CONFIDENTIAL

CONFIDENTIAL

AFRPL-TR-65-209, Vol II

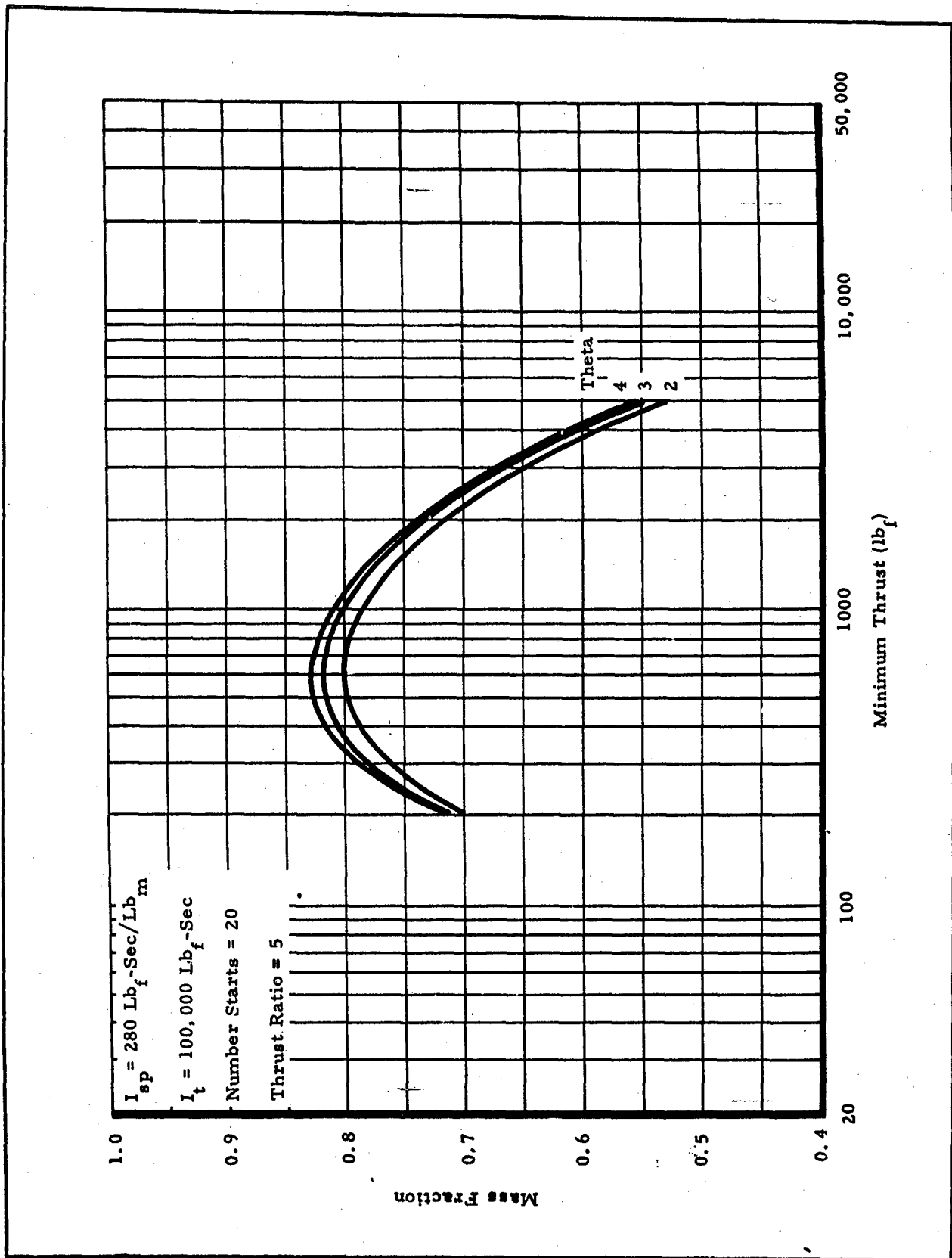


Figure B-63 - Mass Fraction versus Minimum Thrust for Theta Values of 2, 3, and 4

P-66

CONFIDENTIAL

CONFIDENTIAL

AFRPL-TR-65-209, Vol II

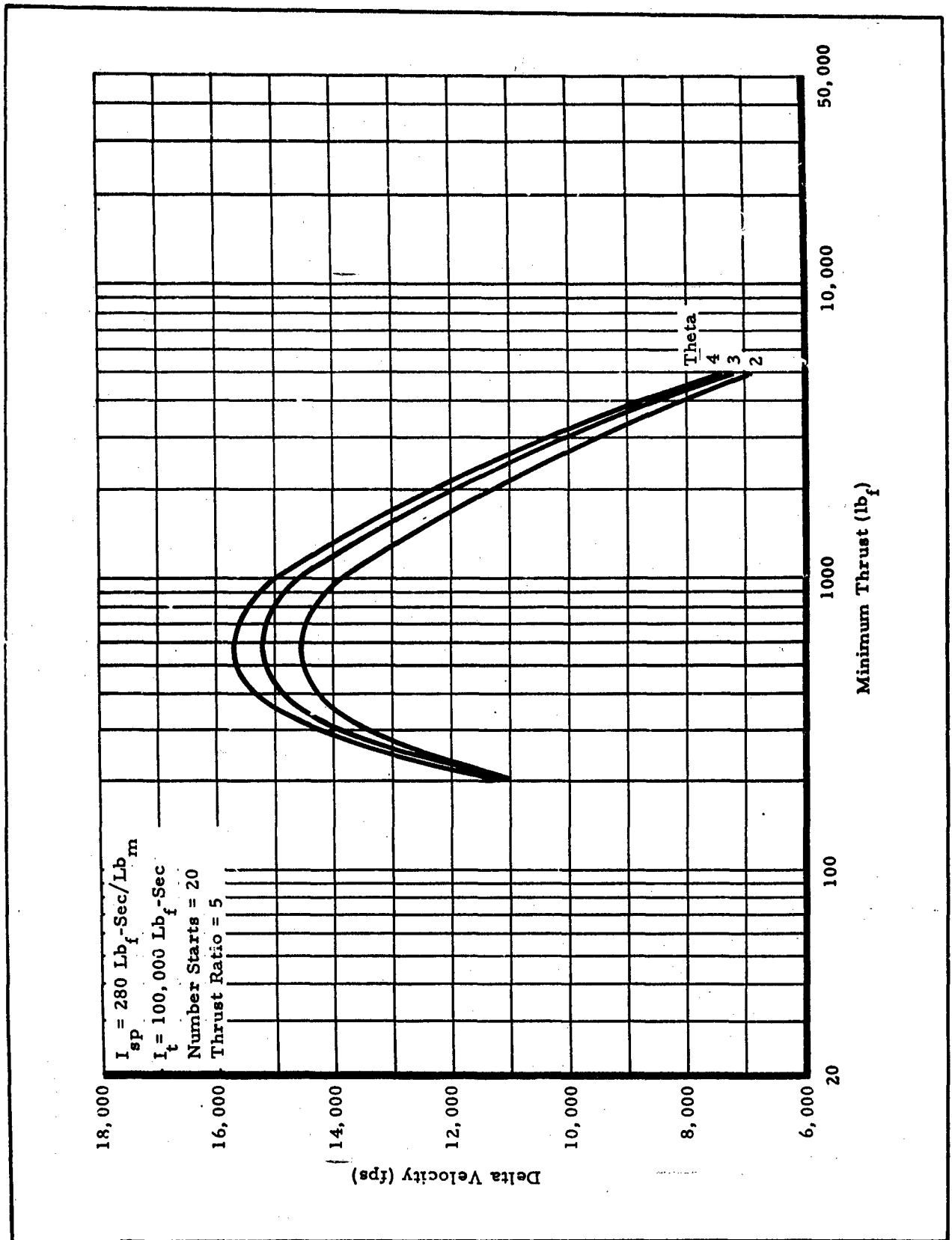


Figure B-64 - Delta Velocity versus Minimum Thrust for Theta Values of 2, 3, and 4

CONFIDENTIAL

CONFIDENTIAL

AFRPL-TR-65-209, Vol II

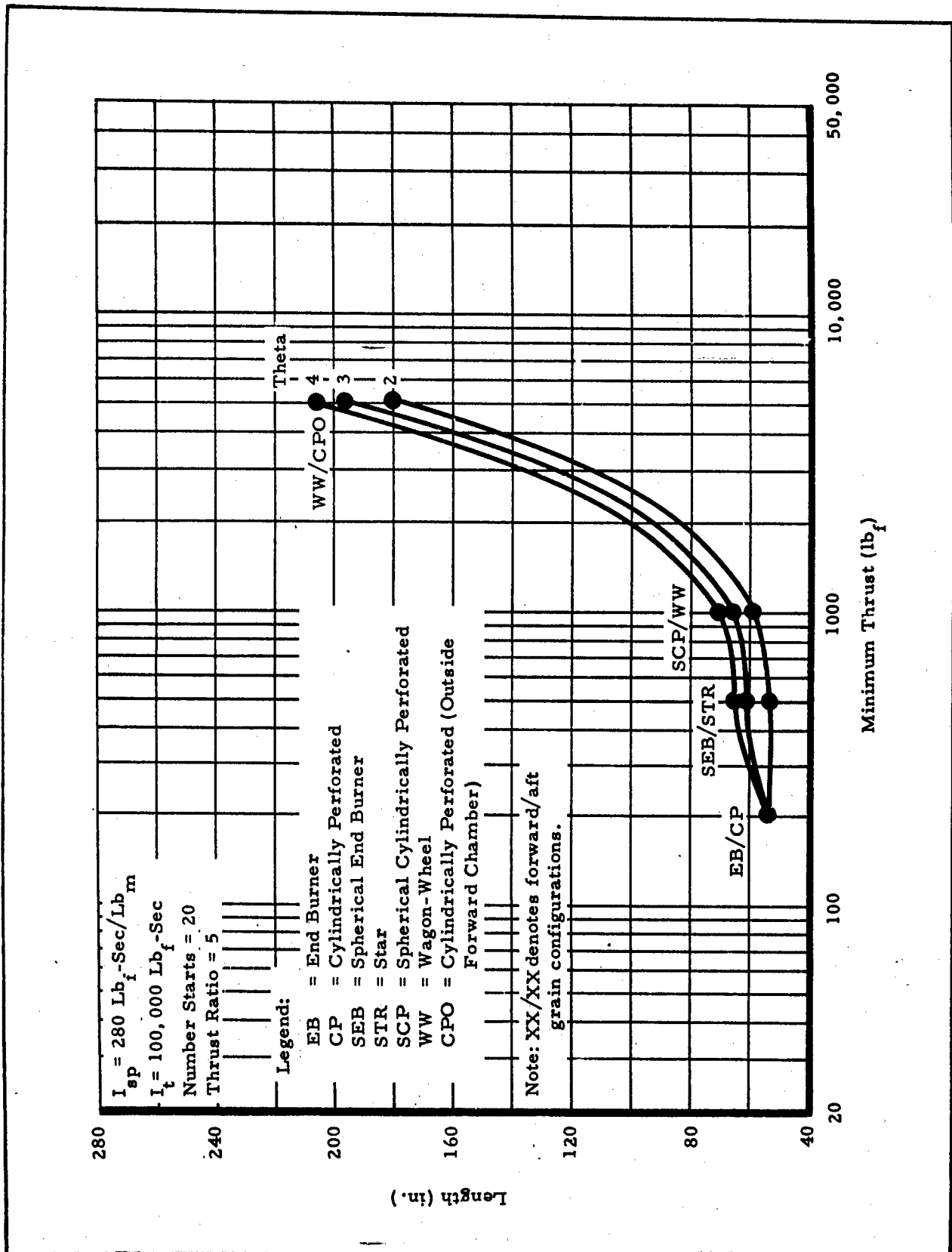


Figure B-65 - Length versus Minimum Thrust for Theta Values of 2, 3, and 4

B-68

CONFIDENTIAL

CONFIDENTIAL

AFRPL-TR-65-209, Vol II

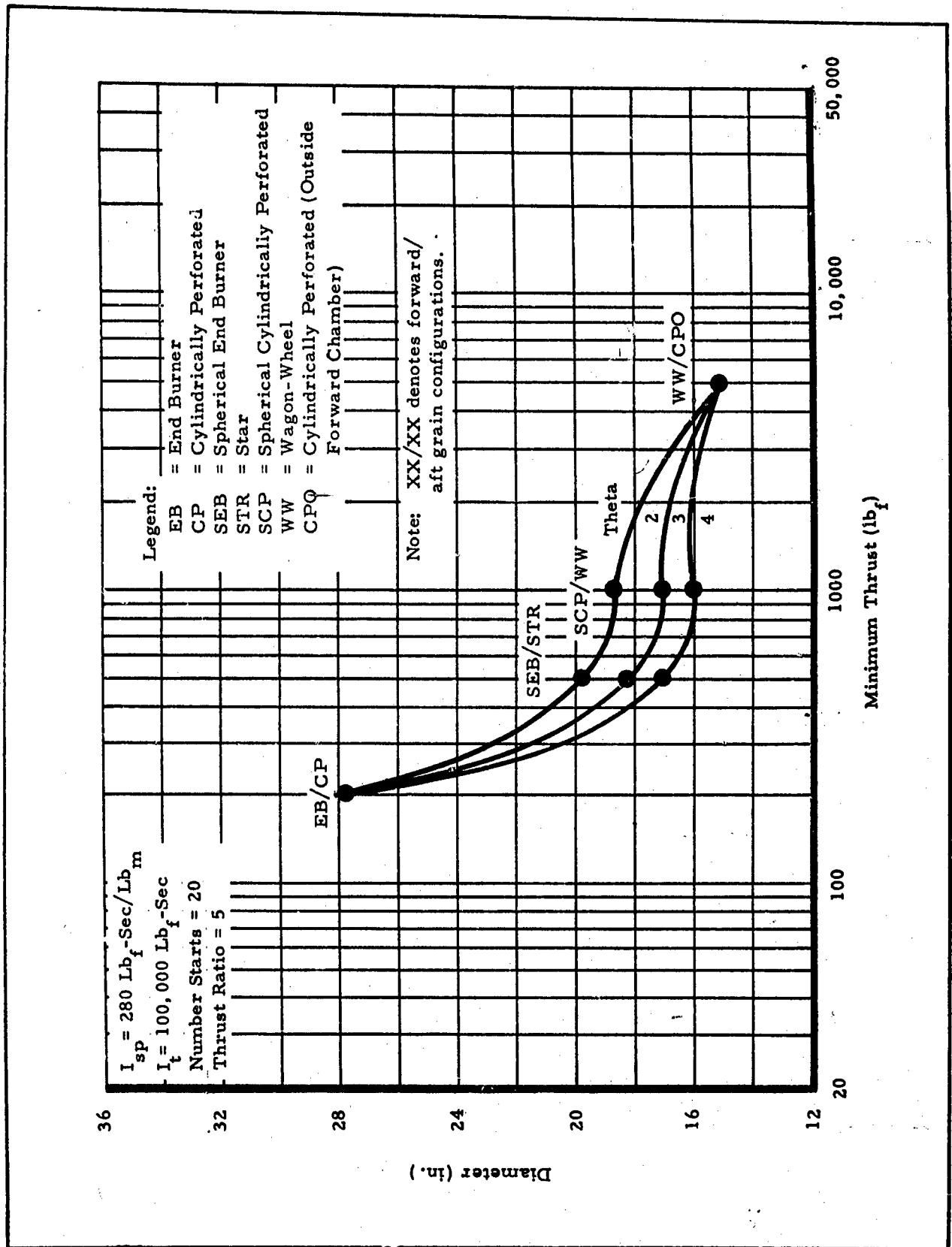


Figure B-66 - Diameter versus Minimum Thrust for Theta Values of 2, 3, and 4

CONFIDENTIAL